THE UNIVERSITY
of EDINBURGH

The role of the innate immune system in the regeneration of the zebrafish larvae spinal cord

Themistoklis Tsarouchas

Doctor of Philosophy

The University of Edinburgh

2018

Statement of original contribution

Unless stated otherwise, the work in this thesis has been performed by the candidate, Themistoklis M. Tsarouchas.

Neither this dissertation nor part thereof has been submitted for academic merit at another educational institution. Data within this thesis have been submitted for the following publications:

Tsarouchas, T. M., D. Wehner, L. Cavone, T. Munir, M. Keatinge, M. Lambertus, A. Underhill, T. Barrett, E. Kassapis, N. Ogryzko, Y. Feng, T. J. van Ham, T. Becker and C. G. Becker (2018). **Dynamic control of proinflammatory cytokines Il-1beta and Tnf-alpha by macrophages in zebrafish spinal cord regeneration**. Nat Commun 9(1): 4670.

Wehner, D., **Tsarouchas, T. M**., Michael, A., Haase, C., Weidinger, G., Reimer, M. M., Becker,T., Becker, C. G. **Wnt signaling controls pro-regenerative Collagen XII in functional spinal cord regeneration in zebrafish** (2017). Nat Commun. 2017 Jul 25;8(1):126. doi: 10.1038/s41467-017-00143-0.

Ohnmacht, J., Yang, Y., Maurer, G. W., Barreiro-Iglesias, A., **Tsarouchas, T. M**., Wehner, D., Sieger, D., Becker, C. G., Becker, T. (2016). **Spinal motor neurons are regenerated after mechanical lesion and genetic ablation in larval zebrafish**. Development. 2016 May 1;143(9):1464-74. doi: 10.1242/dev.129155.

29/10/2018

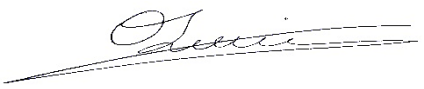

Abstract

Spinal cord injury leads to an increased response of innate immune cells (microglia, macrophages, neutrophils) in non-regenerating mammals and in successfully regenerating zebrafish. Here I characterize the axonal regrowth of the severed axons after complete spinal cord transection and define the role of the innate immune reaction in successful spinal cord regeneration in larval zebrafish.

I found that axons start to regenerate at 18 hours post injury and by 48 hours 80% of the injured larvae show axonal growth across the injury site. The use of reporter lines to visualize the neuronal and glial elements of the spinal cord combined with immunostaining and live imaging allowed me to find that the axons and the glial processes are able to regenerate independently, following different kinetics.

Inhibiting inflammation reduces and promoting it accelerates axon regrowth. Mutant analysis shows that peripheral macrophages, but not neutrophils or microglia, are crucial for axonal regeneration and functional recovery. Macrophage-deficient *irf8* mutants, characterized also by increased numbers of neutrophils, fail to down-regulate pro-inflammatory cytokines TNF-α and Il-1β and to up-regulate anti-inflammatory cytokines, indicating prolonged inflammation.

Because sustained inflammation is considered to be detrimental to regeneration in mammals, I determined the role of increased expression of *TNF-α* and *Il-1β* in axonal regeneration. Inhibition of TNF-α does not rescue the mutant but impairs axonal growth in wildtype larvae. Furthermore, CRISPR/Cas9-mediated disruption of TNF-α led to increased expression of the pro-inflammatory cytokine *Il-1β*. Taken together these findings indicate an unexpected pro-regenerative and anti-inflammatory role of TNF-α.

In contrast, inhibition of Il-1β using pharmacological and genetic approaches rescues axonal regeneration and functional recovery in *irf8* mutants, indicating that Il-1β is a major determinant during successful spinal cord regeneration. In order to determine

the relative importance of the neutrophils for the regenerative failure in *irf8* mutants, we used morpholino injections to reduce their numbers. The treatment prevented the formation of the neutrophils and decreased the expression levels of *Il-1β*, indicating that neutrophils act as a source for Il-1β in the *irf8* mutants. In wildtype animals, early, but not late axon regrowth is attenuated by Il-1β inhibition, indicating dynamic changes in Il-1β function during regeneration.

However, the regenerative potential of adult and larval zebrafish is not restricted only to their ability to re-grow severed axons, since they can make lost neurons as well after injury. In order to assess the role of the innate immune response during neuronal regeneration, I used dexamethasone to inhibit the inflammation that occurs after injury. I found that the treatment leads to a decreased number of new-born motor neurons in the injury site, indicating the importance of the inflammatory response for axonal, as well as, neuronal regeneration of the spinal cord after injury. Furthermore, I used the macrophage deficient *irf8* mutants in order to assess how lost motor neurons are regenerated in an environment with no macrophages/microglia. I found that motor neurons fail to regenerate properly after injury in the mutants, indicating the importance of macrophages/microglia, during neuronal regeneration.

Taken together, these results demonstrate the complex inflammatory response that occurs after spinal cord injury and provide insight into the role of macrophages that tightly control it, by expressing *TNF-α* and preventing prolonged expression of *Il-1β*, to promote successful spinal cord regeneration in zebrafish.

Lay Summary

Mammals are unable to regenerate their injured nervous system after injury, leading to permanent behavioural deficits. In contrast to mammals, zebrafish larvae and adults exhibit regenerative capacity of their nervous system after injury. Their nervous system shares similarities with the mammalian. This feature combined with their regenerative potential, make it an ideal model for studying the regenerative events that occur after injury and the contribution of the inflammatory response to this process. The immune system is a complex part of each organism. It consists of a variety of specialised cells that defend our body against pathogens and produce inflammatory signals (like Il-1β and TNF-α) to do so.

Because of its complexity and the limited capacity for regeneration that characterizes the mammalian nervous system, it is very difficult to accurately assess the role of the immune reaction after an injury. For this reason, I used the larval zebrafish model. They exhibit a high regenerative capacity and their immune system shares common cellular and molecular processes with the one in mammals . Furthermore, the larval model allowed me to focus my analysis on each individual immune cell type and assess its role during regeneration independently of the other cell populations during the regeneration of the injured nervous system. This is because there are suitable tools, like different animal lines where the different cell populations are tagged with different colours or are manipulated using genetic techniques, and their response can be monitored live. Furthermore, their innate and adaptive immunity mature during different stages of development allowing their clear separation during the analysis.

Here I characterized the immune response that occurs after spinal cord injury in zebrafish larvae, with a special focus on the role of three main immune cell types which are the macrophages, the neutrophils and the microglial cells. The hypothesis was that each cell type is important for functional spinal cord regeneration. In order to test this hypothesis, I used a variety of tools. The first thing to do was to perform spinal cord injuries and then characterize the cellular and molecular immune

response that occurs, which showed that neutrophils are the first cells that respond and accumulate in the injury site initiating the inflammatory response, whereas the other cell populations including macrophages and microglia respond much later. In addition, I assessed the levels of molecules produced by the immune cells during the same time points that were used for the analysis of the cellular response after injury.

Next, after the injury, I manipulated the immune system with genetic and pharmacological approaches to highlight the importance of each cell type during regeneration of the injured spinal cord. In order to assess regeneration, I used the ability of the axons to cross the injury site within 24 and 48 hours post injury and quantified the number of animals that showed axonal continuity during these time points.

I found that inhibiting inflammation reduces and promoting it accelerates regeneration after injury. Furthermore, I show that macrophages are the most important immune cell population that contribute to successful axonal regeneration and functional recovery after injury by reducing the levels of inflammation by regulating the levels of the inflammatory and anti-inflammatory proteins. My results highlighted two immune molecules that appear to have differential roles during regeneration, TNF-α and Il-1β. TNF-α has a pro-regenerative role whereas Il-1β appears to be detrimental for regeneration.

Taken together, these results show the importance of the inflammatory response during the regenerative events after injury of the nervous system. Also, they demonstrate the different roles of each immune cell type suggesting that the knowledge obtained might contribute to the development of therapeutic strategies in humans using manipulations of the immune system or specific parts of it.

Acknowledgements

First and foremost, I would like to thank my PhD supervisors Prof. Catherina G. Becker and Dr Thomas Becker, for the opportunity to be part of their lab and for their useful comments, suggestions and support all these years and my thesis committee members Prof. Dies Meijer, Dr. Dirk Sieger and Dr. Yi Feng.

I would like to thank Drs Leonardo Cavone, Daniel Wehner, Marcos Cardozo, Yujie Yang, Karolina Mysiak and Ana Maria Oprisoreanu for their invaluable support, comments and help during these 4 years of my PhD.

A big thank you to past and present members of the Becker lab and especially Andria Michael and my fellow PhD students in the Becker lab Hannah Smith, Lindsey Caldwell and Tess McCann, for your support, amusement and for being the best colleagues that someone could have.

Thank you to the Kelda Chia, Julie Mazzolini and Katy Astell from the Sieger lab for allowing me to use their fish-lines and for their useful suggestions and discussions and for being such good friends.

Thank you to Jason Early from the Lyons lab for his help during imaging and image analysis and to all the Lyons lab for allowing me to use some of their fish-lines and reagents.

A big thank you to Marcus Keatinge for his great help and expertise regarding the CRISPR/Cas system and for designing the TNF-α gRNA.

Thank you to all the co-authors of my paper for your hard work, and determination. It's been a pleasure to work with you guys and we achieved this together.

Special thanks to Sofia Anagianni for all these years, for her support and for always being there during the good and the bad times.

Special thanks to my parents and my brother for the undivided support they provided me with all these years and for their understanding especially during the last months of my PhD.

Contents

Abbreviations

5--Ethynyl--2´--deoxyuridine (EdU)

Adenosine triphosphate (ATP)

Antigen presenting cell (APC)

Central Nervous System (CNS)

Clustered regularly interspaced short palindromic repeats (CRISPR)

Collagen XII (ColXII)

Common lymphoid progenitor (CLP)

Common myeloid progenitor (CMP)

Connective tissue growth factor (ctgfa)

Days post fertilization (dpf)

Days post lesion (dpl)

Death domain (DD)

Dendritic cell (DC)

Dimethyl sulphoxide (DMSO)

Discosoma sp. red fluorescent protein (dsRed)

Ependymo--radial glial cells (ERGs)

Extracellular matrix (ECM)

Fibroblast growth factor (Fgf)

Fluorescence-activated cell sorting (FACS)

Glial fibrillary acidic protein (GFAP)

Glutamate receptor 2 (GluR2)

Green fluorescent protein (GFP)

Guide-RNA (gRNA)

Helper T cells (TH cells)

Hematopoietic stem cell (HSC)

Hydrogen peroxide (H_2O_2)

Hypoclorous acid (HClO)

Inteleukin 1β protein (Il-1β)

Inteleukin 1β mRNA (*Il-1β*)

Janus kinase/signal transducers and activators of transcription (JAK/STAT)

Leukemia inducing factor (LIF)

Lipopolysaccharides (LPS)

Metronidazole (MTZ)

Mitogen-activated protein (MAP)

Morpholino (MO)

Motor neuron progenitor domain (pMN) (pMN)

Myelin associated glycoprotein (MAG)

Natural killer (NK)

Neutrophil extracellular traps (NETs)

Nicotinamide adenine dinucleotide phosphate (NADPH)

Nitric oxide synthetase (iNOS)

Nitroreductase (NTR)

Pathogen associated molecular patterns (PAMPs)

Pattern recognition receptors (PRRs)

Peripheral Nervous System (PNS)

Reactive nitrogen species (RNS)

Reactive oxygen species (ROS)

Restriction fragment length polymorphism (RFLP)

Reverse transcription polymerase chain reaction (RT-PCR)

Schwann Cells (Scs)

Spinal Cord Injury (SCI)

Spinal Muscular Atrophy (SMA)

Terminal deoxynucleotidyl transferase dUTP nick end labelling assay (TUNEL)

Toll like receptor (TLR)

Transforming growth factor (Tgf)

Traumatic brain injury (TBI)

Tumour necrosis factor receptor I, II (TNFRI, TNFRII)

Tumour necrosis factor α protein (TNF-α)

Tumour necrosis factor α, mRNA (*TNF-α*)

Zebrafish information network (ZFIN)

α-amino-3-hydroxy-5-methyl-4-isoxazolepropionic acid (AMPA)

Chapter 1: General Introduction

1.1 Nervous system regeneration

The nervous system is a complex organization of nerves and neurons that are responsible for the transmission of information between different parts of the body. Structurally, it is divided into two components: the central nervous system (CNS) and the peripheral nervous system (PNS). Their function is to relay signals from and to all other parts of the body. This is achieved through a complex network of neurons and supporting glial cells. An injury can cause axons to be partially or completely severed, crushed, compressed, or stretched. When an axon is severed, its distal part undergoes Wallerian degeneration. The injury also induces responses of glial cells, including oligodendrocytes, astrocytes, and microglia in the CNS, Schwann cells (SCs) in the PNS, and blood-derived macrophages and neutrophils. The responses of these cells cover a broad spectrum of events including cell death, proliferation, migration, and production of inflammatory mediators and growth factors, thus influencing processes of axonal degeneration and regeneration. Regeneration of the nervous system can be divided into two aspects: the neuronal regeneration which includes the replacement of lost neurons and glia, and the axonal regeneration which includes the regrowth of neuronal and/or glial processes. Neural regeneration differs between the PNS and the CNS due to the different environments that the regenerating axons and cells encounter.

The PNS consists of motor neuron axons and sensory axons, which originate from the CNS and innervate tissues and send signals to sensory neurons, which reside in ganglia and transmit information to the CNS. After injury, when a peripheral axon is severed, the tip of the proximal segment develops a growth cone, which then navigates through its environment following growth signals derived from its target cells and extends toward them (Hu et al. 2010).

On the other side of the spectrum, injured CNS neurons fail to regenerate their severed axons across the injury site. It has been shown that there are phylogenetic differences in the regeneration capacity of various species (Zhang et al. 2012).

Whereas axons in the CNS of mammals do not regenerate, those in many other vertebrates such as, zebrafish (Becker et al. 1997, Becker and Becker 2014, Wehner et al. 2017), salamander (McHedlishvili et al. 2012) and newts (Oudkhir et al. 1992) can regenerate after injury. However, young mammals are also capable of substantial CNS neural regeneration (Terman et al. 2000) indicating that the lack of CNS regeneration in warm-blooded vertebrates may be due to evolutionary changes. In order to explain this difference across vertebrates, the neuron's intrinsic growth state (Kumamaru et al. 2018), the glial (Cregg et al. 2014, Liddelow and Barres 2016) and fibrotic scar (Soderblom et al. 2013, Fernandez-Klett and Priller 2014), myelin inhibitors (Filbin 2003, McKerracher and Rosen 2015), and invading cells from the periphery have been studied regarding their role in CNS regeneration.

The severity of CNS injuries has been described many centuries ago. Very characteristic is the following statement which was written on an ancient papyrus: "A medical condition that cannot be healed". This is how the spinal injuries have been described in the Edwin Smith papyrus, the oldest known surviving trauma text in history, dating from the seventeenth century B.C. (Moore 2011). Although therapeutic and research techniques have advanced considerably over the years, spinal cord injury (SCI) remains a devastating condition that leads to permanent deficits and functional impairment affecting millions of people worldwide (Anand and Mondal 2018).

The reason for these long-term impairments is the inability of the CNS to repair itself compared to other tissues of the human body where injuries are usually resolved within a few days. The main reason for this inability is the complex environment after the injury. SCI leads to cascade of events which include infiltration of immune cells to the injury site (Kasinathan et al. 2015), axonal transection, neuronal death (Ahuja et al. 2017) and the formation of a glial scar (Yuan and He 2013) and fibrotic scar (Kawano et al. 2012). Furthermore, there are inhibitory factors present like components of the extracellular matrix (ECM) that prevent the anatomical and functional restoration of the CNS (James et al. 2015).

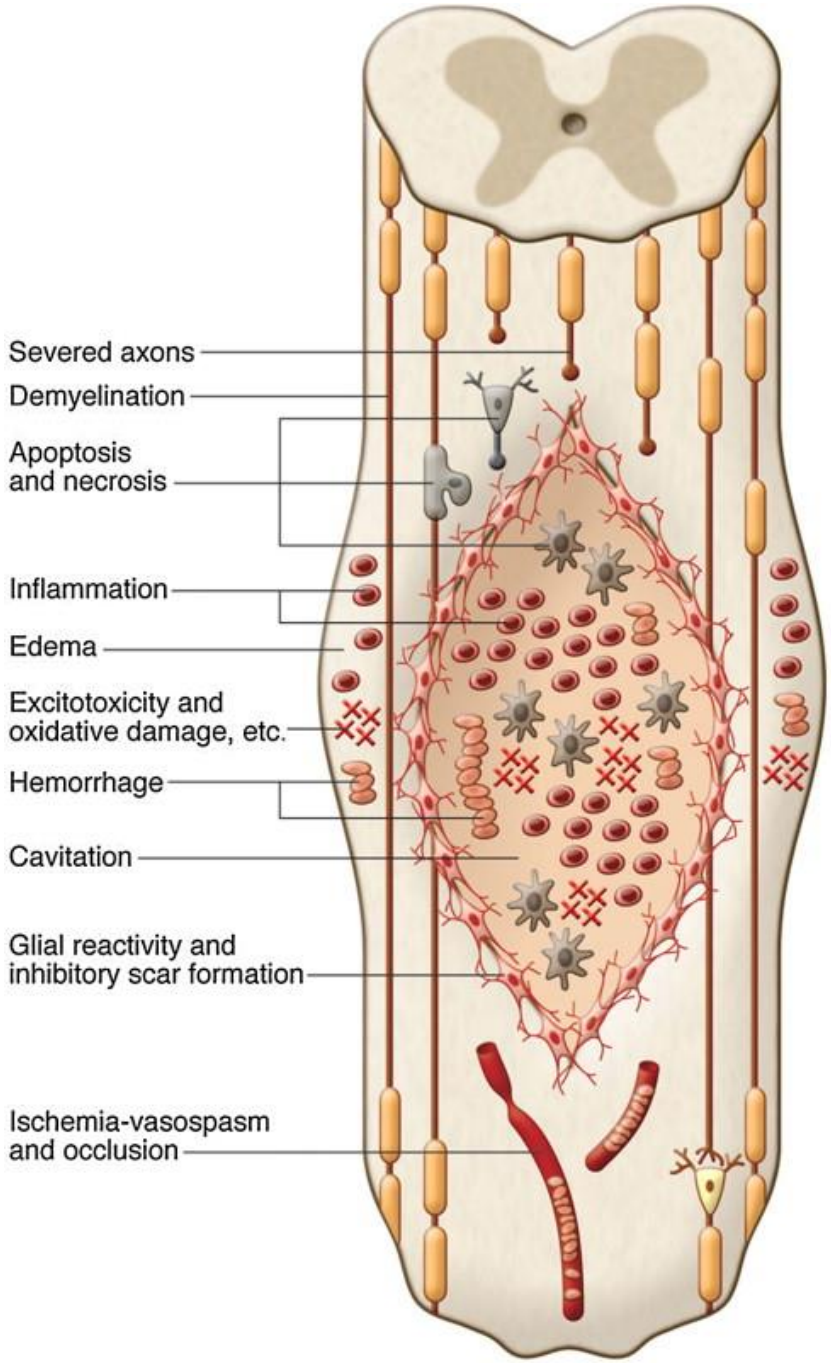

Figure 1.1. Pathophysiology of SCI showing the different events that occur after spinal cord injury (adapted from (Mothe and Tator 2013)).

In many neurodegenerative disorders specific cell populations die, leading to specific deficits. For example, in Multiple Sclerosis (MS) there is loss of myelin (Love 2006), in Spinal Muscular Atrophy (SMA) where there is degeneration of motor neurons (Tu et al. 2017) and in Parkinson's disease there is loss of dopaminergic neurons (Naoi and

Maruyama 1999). Similarly to the rest of the CNS, the mammalian spinal cord is characterized by the inability to replace the lost neurons (Hilton and Bradke 2017) and to re-establish functional connections of the severed axons (Hilton and Bradke 2017). Like in all mammals, the regenerative capacity of the human CNS is low. However, previous studies have shown that although the mammalian CNS axons are not able to regenerate after an injury, they still possess an intrinsic capacity for axonal growth when given a permissive environment as shown by previous in vivo studies. More specifically, (Richardson et al. 1980) using adult rats, showed that CNS neurons can regenerate axons into peripheral nerve segments transplanted into the transected spinal cord when a 5-mm segment of the midthoracic spinal cord was removed and an autologous sciatic nerve graft was inserted sub-pially between rostral and caudal spinal cord stumps. Additionally, David and Aguayo demonstrated that after SCI the severed axons of adult rats exhibit regenerative capacity when the glial environment is replaced by peripheral nerve bridges (David and Aguayo 1981). These pioneering studies changed the thinking in the field, providing evidence that mammalian CNS exhibits regenerative potential after injury. Work from (Canty et al. 2013) showed that depending on cell type some axons can exhibit spontaneous growth and at speed comparable to peripheral nerve regeneration. Although never reconnecting to the original targets, axons consistently form new boutons at comparable prelesion synaptic densities, implying the existence of intrinsic homeostatic programmes, which regulate synaptic numbers on regenerating axons. CNS axons can be guided using the peripheral nerve graft towards their target, but they are not able to extend beyond the distal part of the graft due to of the inhibitory environment at the site of SCI (Côté et al. 2011). In order to overcome this, several studies have used PNS grafts combined with digestion of the chondroitin sulphate proteoglycans that are associated with a glial scar, which showed promising results in acute SCI models (Côté et al. 2011). Based on this observation, that the mammalian neurons under specific conditions are able to extend axonal processes, it is important to study and understand the principles that control regeneration in other species that exhibit high regenerative potential in the CNS.

1.2 Overview of the immune system

In all CNS insults across the literature, inflammation is always mentioned among others as one of the key regulators of the degenerative and/or regenerative events that occur. Inflammation is the orchestrated response of the immune system after an infection or injury. In other words, our body's defence mechanism against diseases and pathogens. It is highly adaptable to defend our body against the wide spectrum of invaders that can be found in the environment that surrounds us. It can be divided into the innate and the adaptive immune system (Chaplin 2010). These two systems work together to protect the body against foreign invaders.

The innate immune response includes built-in molecular and cellular mechanisms that aim at preventing infection or quickly eliminating common invaders after injury. This includes physical (Gallo and Nizet 2008) and chemical (Gallo and Nizet 2008) barriers to infection, as well as receptors recognizing common chemical structures of many pathogens (Thompson et al. 2011) . Innate immunity also includes a plethora of proteins that bind common pathogen associated structures and initiate a cascade of events. This highly effective first line of defence eliminates infectious agents within hours.

A second form of immunity, known as adaptive immunity, is much more specialised to subtle molecular differences. This part of the system, relies on B and T lymphocytes (Vitetta et al. 1991), takes longer to occur, but is much more antigen specific. Adaptive immunity is slower because fewer cells possess the perfect receptor that is antigen specific. Activation of the adaptive immune response is a multistep process. The number of epitopes which the T-cells and B-cells must recognize is extremely high.

When an antigen enters the body, a B or T cell with specificity for this particular antigen has to encounter it while the cells circulate via blood and lymph. This process takes time, occurring in scale of hours (Valitutti et al. 2010). Furthermore, T cell cells require considerable amount of time after the antigen has been presented by the

antigen presenting cells (APCs). After antigen encounter, T and B lymphocytes undergo selection and proliferation (Pennock et al. 2013, Hoffman et al. 2016). Once these cells have been selected, they can typically resolve the infection. The adaptive immune response evolves in real time in response to injury or infection and adapts to better recognize, eliminate, and remember the invading pathogen.

Although for simplicity the immune system is typically divided into these two kinds of the response, there is considerable communication of the cells and mechanisms involved in each of these two systems (Clark and Kupper 2005). This communication is achieved by both cell-cell contact and by soluble messengers. Most of these soluble proteins are molecules known as cytokines (Ito et al. 2013). Cytokines and cell surface ligands can bind to receptors found on responding cells and signal these cells to initiate functions, such as synthesis of other soluble factors or differentiation (Zhang and An 2007). A subset of these soluble signals is called chemokines because of their chemotactic activity.

In contrast to the adaptive immune response, which takes days to occur, the cellular innate immune responses after an injury or infection are rapid, typically beginning within minutes. These responses are triggered by cell surface or intracellular receptors that recognize conserved molecular components of pathogens (Colaco and Moita 2016) and molecules produced by injured tissues cells like Adenosine triphosphate ATP and other danger signals (Rock and Kono 2008). During this macrophages and neutrophils are activated to rapidly engulf and destroy extracellular microbes through the process of phagocytosis (Schnyder and Baggiolini 1978). Other receptors initiate the production of proteins and other substances that have a variety of beneficial effects, including the recruitment of cells, and accumulation of molecules to sites of infection. Such local innate responses usually are essential for eliminating pathogens and damaged or dead cells and promoting healing (MacLeod and Mansbridge 2016). For example, increased levels of antimicrobial substances and phagocytic cells help to eliminate the pathogens, and dendritic cells take up pathogens for presentation to lymphocytes, activating adaptive immune responses (den Haan et al. 2014). However, in some situations

these innate inflammatory responses can be harmful, leading to local or systemic consequences that can cause chronic inflammation and tissue damage (Xiao 2017, Chen et al. 2018).

Macrophages, neutrophils, and dendritic cells in tissues and monocytes in the blood are the main cell types that carry out phagocytosis (Silva and Correia-Neves 2012). Élie Metchnikoff initially described the process of phagocytosis in the 1880s using cells from starfish similar to vertebrate white blood cells (Metchnikoff 1892). Phagocytes express on their surfaces a variety of receptors, some of which directly recognize specific conserved molecular components on the surfaces of microbes, such as cell wall components of bacteria and fungi. These conserved motifs are called pathogen-associated molecular patterns (PAMPs) (Emlet et al. 2019). The receptors that recognize PAMPs are called pattern recognition receptors (PRRs) (Emlet et al. 2019). Most PAMPs that induce phagocytosis are cell wall components, including complex carbohydrates, lipopolysaccharides (LPS), other lipid-containing molecules, peptidoglycans, and surface proteins (Mogensen 2009).

The binding of microbes to phagocytes via pattern recognition receptors activates signaling pathways. These signaling pathways trigger actin polymerization, resulting in membrane extensions around the microbe particles and their internalization, forming phagosomes (Pauwels et al. 2017). The phagosomes then fuse with lysosomes and, in neutrophils, with preformed primary and secondary granules. The resulting phagolysosomes contain an arsenal of antimicrobial agents that then kill and degrade the internalized microbes. These agents include antimicrobial proteins and peptides (including defensins and cathelicidins) (Jeschke and Haas 2016), low pH, acid-activated hydrolytic enzymes (including lysozyme and proteases) (Jeschke and Haas 2016), and specialized molecules that mediate oxidative attack (Libardo et al. 2018). Oxidative attack on the phagocytosed microbes, performed by neutrophils, macrophages, and dendritic cells, employs reactive oxygen species (ROS) and reactive nitrogen species (RNS), which damage intracellular components. Stimulated neutrophils activate their NADPH oxidase (NOX2) to generate large amounts of superoxide, which acts as a precursor of hydrogen peroxide and other reactive

oxygen species that are generated by their heme enzyme myeloperoxidase. When neutrophils engulf bacteria, they enclose them in small vesicles (phagosomes) into which superoxide is released by activated NOX2 on the internalized neutrophil membrane (Winterbourn et al. 2016). ROS and RNS can also be released from activated neutrophils and macrophages and kill extracellular pathogens (Fialkow et al. 2007).

1.2.1 Cells of the immune system

All mature blood cells (red blood cells, granulocytes, macrophages, dendritic cells, and lymphocytes) arise from a single cell type, the hematopoietic stem cell (HSC) (Moore 2014). The process by which HSCs differentiate into mature blood cells is called hematopoiesis. An HSC after differentiation, loses its self-renewal capacity and makes one of two broad lineage commitment choices (Moore 2014). It can become a common myeloid-erythroid progenitor (CMP), which gives rise to all red blood cells (the erythroid lineage), granulocytes, monocytes, and macrophages (the myeloid lineage), or it can become a common lymphoid progenitor (CLP), which gives rise to B lymphocytes, T lymphocytes, and NK cells (Moore 2014). Myeloid cells and NK cells are members of the innate immune system and are the first cells to respond to infection or an injury (Porcelli 2017). Lymphocytes are members of the adaptive immune response and generate a refined antigen-specific immune response that also gives rise to immune memory (Bonilla and Oettgen 2010). Cells that arise from a CMP include red blood cells (erythroid cells) as well as various types of white blood cells (myeloid cells such as granulocytes, monocytes, macrophages, and some dendritic cells) (Figure 1.2). Myeloid cells are the first to respond to the invasion of a pathogen or injury and transmit the information regarding the presence of an insult to cells of the lymphoid lineage.

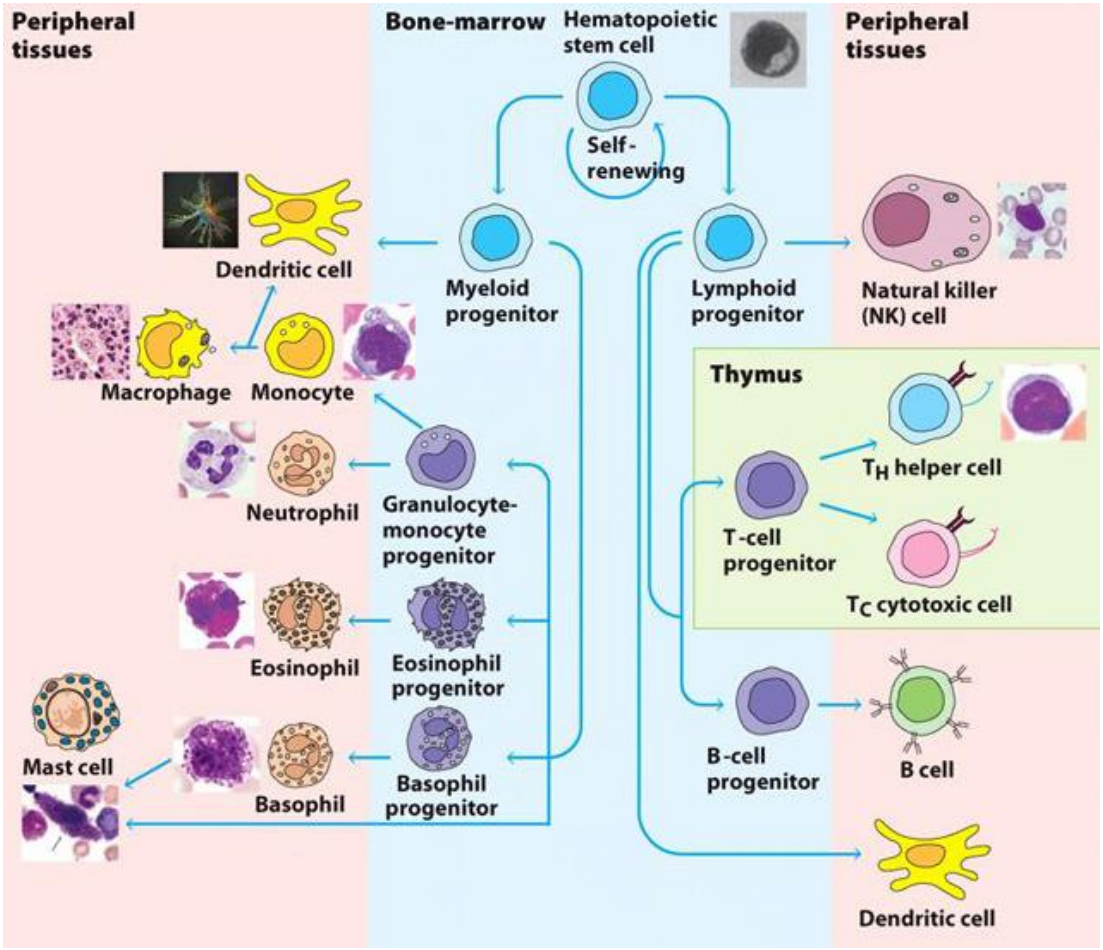

Figure 1.2. Hematopoiesis. Hematopoietic stem cells give rise to lymphoid and myeloid progenitors which differentiate into innate and adaptive immune cell types. (Modified from Kuby immunology 7th edition)

Granulocytes

Granulocytes are white blood cells (leukocytes) that are classified as neutrophils, basophils, mast cells, or eosinophils based on differences in cellular morphology and the staining of their characteristic cytoplasmic granules (Bosch and Ramos-Casals 2014). All granulocytes have multilobed nuclei that make them visually distinctive and easily distinguishable from lymphocytes, whose nuclei are round. Their cytoplasm is full of granules that are released in response to contact with pathogens (Bosch and Ramos-Casals 2014). These granules contain a variety of proteins with distinct functions: Some damage pathogens directly some regulate trafficking (Bosch and

Ramos-Casals 2014) and activity of other white blood cells, including lymphocytes; and some contribute to the remodelling of tissues at the site of infection.

Neutrophils constitute the majority (50% to 70%) of circulating leukocytes (Bosch and Ramos-Casals 2014). After differentiation in the bone marrow, neutrophils are released into the peripheral blood and migrate into the tissues, where they have a life span of only a few days (Simon and Kim 2010). In response to many types of infections or insults, the number of circulating neutrophils increases, and more are recruited to tissues (Kolaczkowska and Kubes 2013). Neutrophils are recruited to the site of infection in response to inflammatory molecules (e.g., chemokines) generated by innate cells (including other neutrophils) that have engaged a pathogen. In tissues, neutrophils phagocytose bacteria very effectively, and also secrete a range of proteins that have antimicrobial effects and tissue remodelling potential. Although once considered a simple cell, the neutrophil has recently been connected with regulation of the adaptive immune response (Rosales et al. 2017).

Basophils are nonphagocytic granulocytes that contain large granules filled with basophilic proteins. Basophils are relatively rare in the circulation but can be very potent. In response to an insult, basophils release the contents of their granules (Bosch and Ramos-Casals 2014).

Eosinophils, like neutrophils, are motile phagocytic cells that can migrate from the blood into the tissues (Kolaczkowska and Kubes 2013). Their phagocytic role is significantly less important than that of neutrophils, and it is thought that they play their most important role in the defence against parasitic organisms (O'Connell and Nutman 2015). Like neutrophils and basophils, eosinophils may also secrete cytokines that regulate B and T lymphocytes, thereby influencing the adaptive immune response (Long et al. 2016).

Mast cells are released from the bone marrow into the blood and can be found in a wide variety of tissues, including the skin, connective tissues of various organs, and mucosal epithelial tissue of the respiratory, genitourinary, and digestive tracts (St John and Abraham 2013). They possess cytoplasmic granules that contain histamine

and other active substances and play therefore an important role in the development of allergies and in the initiation and resolution of acute inflammation (St John and Abraham 2013).

Antigen-Presenting-Cells

Myeloid progenitors give rise to monocytes, macrophages, and dendritic cells that act as antigen-presenting cells (APC) (Flaherty 2012). Each can ingest pathogens via phagocytosis, and then present these peptide antigens on their membrane surfaces. Macrophages and neutrophils are efficient in removing pathogens and damaged cells and provide a first line of defence. Activated, APCs are more effective than resting ones in eliminating potential pathogens. They exhibit greater phagocytic activity, an increased ability to kill ingested microbes, increased secretion of inflammatory and cytotoxic mediators, and the ability to activate T cells. Activated macrophages also function more effectively as antigen-presenting cells for helper T cells (TH cells), which, in turn regulate and enhance macrophage activity (Flaherty 2012).

1.2.2 Phagocytosis

The components of dead/dying cells and damaged tissues that are recognized by PRRs leading to their clearance are sometimes referred to as damage-associated molecular patterns (DAMPs) (Emlet et al. 2019). Phagocytosis is the major way of clearance of cells that have undergone apoptosis as part of developmental remodelling of tissues, normal cell turnover, killing of infected cells by innate and adaptive immune responses or after injury. Apoptotic cells attract phagocytes by expressing on their surfaces an array of molecules such as phosphatidyl serine (Segawa and Nagata 2015), annexin I (Weyd et al. 2013), and specific carbohydrates (Eda et al. 2004). These are recognized directly by phagocytic receptors such as the phosphatidyl serine receptor and scavenger receptor SR-A1 (Labonte et al. 2017).

Healthy cells avoid being phagocytosed by not expressing signals, such as phosphatidyl serine, and also by expressing the protein CD47 (Schürch et al. 2018). CD47, expressed on many cell types throughout the body, is recognized by the SIRP-receptor on macrophages, which transmits signals that inhibit phagocytosis (Métayer et al. 2017).

1.2.3 Cytokines and chemokines

One key aspect of the immune system is the ability of its various components to communicate quickly and efficiently with one another, so that the right cells can move to the appropriate locations and take the necessary measures to destroy invading pathogens. Molecules that communicate among cells of the immune system are called cytokines (Chung 2009) (Figure 1.2). In general, cytokines are soluble molecules (Lewko and Oldham 2009), although some also exist in membrane-bound forms (Lewko and Oldham 2009). The interaction of a cytokine with its receptor on a target cell can cause changes in the expression of adhesion molecules and chemokine receptors on the target membrane, thus allowing it to move from one location to another (Spangler et al. 2015). Cytokines can also signal an immune cell to increase or decrease the activity of particular enzymes or to change its transcriptional program, thereby altering and enhancing its effector functions (Wojdasiewicz et al. 2014). Finally, they can regulate the cell cycle of epithelial cells (Tanaka et al. 2009). Although the term cytokine refers to all molecules that communicate among immune cells, the name chemokine is used specifically to describe that subpopulation of cytokines that share the specific purpose of mobilizing immune cells from one organ, or indeed, from one part of an organ, to another. Chemokines belong to the class of molecules called chemo-attractants, molecules that attract cells by influencing the assembly, and disassembly of cytoskeleton proteins and the expression of cell-surface adhesion molecules (Ambriz-Peña et al. 2014). Chemokines attract cells with the appropriate chemokine receptors to regions where the chemokine concentration is highest. For example, chemokines are important in attracting cells of the innate

immune system to the site of infection (Esche et al. 2005) and inducing T cells to move toward antigen-presenting cells in the secondary lymphoid tissues (Esche et al. 2005).

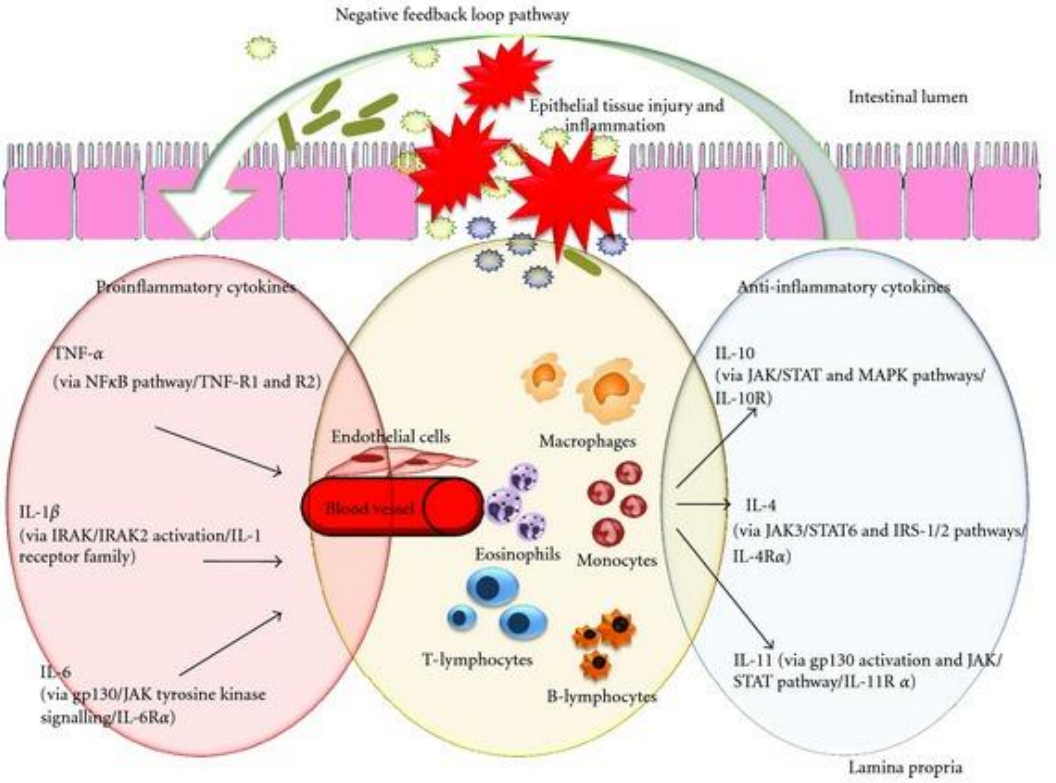

Figure 1.2. Interaction between pro and anti-inflammatory cytokine signaling. (adapted from (Sultani et al. 2012))

1.3 Immune system and spinal cord regeneration

Spinal cord injury results in often permanent motor and sensory impairment due to the inability of the adult Central Nervous System (CNS) to regenerate the severed axons, to establish new functional connections, and to replace the neurons lost. The lack of regeneration is caused by a variety of factors within the CNS environment and within the neurons themselves. However, the initial injury is followed by a cascade of

events that spreads the tissue damage throughout the spinal cord leading to additional neuronal loss, axonal damage, demyelination and cell death. These events are caused by injury induced factors released within the injury site such as adenosine triphosphate (ATP) (Davalos et al. 2005), damage-associated molecular patterns (DAMPs) (Piccinini and Midwood 2010), and cytokines (Pineau and Lacroix 2007). These factors trigger the inflammatory response that is one of the main events occurring after spinal cord injury and involves mainly infiltrating macrophages, neutrophils, and the resident microglia. This response occurs normally as the system tries to prevent infection because of the injury, clear the injury environment and eventually repair the wound. Several studies have shown the importance of the inflammatory response after injury highlighting that the balance during the different phases and the resolution of the immune reaction are crucial for successful regeneration. Absence or delay of the resolution lead to chronic inflammatory phenotypes which can exacerbate tissue damage after injury (Pruss et al. 2011).

1.3.1 Cellular response to SCI

Resident cells within the spinal cord, including microglia, neurons, oligodendrocytes, and astrocytes, respond rapidly to SCI by expressing cytokines and chemokines, which leads to a cascade of responses that culminate in the influx and activation of various immune cells from the periphery, as well as the activation of microglia and astrocytes. After injury neutrophils are the first cell type to enter the injury site followed by monocytes and macrophages (Kigerl et al. 2006, Donnelly and Popovich 2008).

Neutrophils

Neutrophils are the first cells that enter the spinal cord within minutes after the injury. In mammalian models their numbers peak at 24 hours post lesion (hpl) and return to basal levels within 3 days post injury (dpl) (Yang et al. 2005, Donnelly and

Popovich 2008). This early influx of neutrophils after injury is similar to what has been reported in CNS (Allan and Rothwell 2003) and non-CNS injury models (Yang and Hu 2018). Neutrophils can remove pathogens by releasing factors such as lysozyme and collagenase (Odeberg and Olsson 1976), by phagocytosis (Lee et al. 2003), and by realising neutrophil extracellular traps (NETs) which trap and kill the pathogens (Shah et al. 2017).

There is a debate regarding the role of the neutrophils after SCI. Several interventions that lead to a reduction in neutrophils and improved locomotor recovery and tissue protection after SCI have been interpreted as showing a detrimental effect of neutrophils (Taoka et al. 1997, Naruo et al. 2003, Bao et al. 2004, Gris et al. 2004, Bao et al. 2008, Geremia et al. 2012). A large number of neutrophils at 24 h after SCI express inducible nitric oxide synthase (iNOS), and there is evidence that blocking iNOS with antisense oligonucleotides improves outcome after SCI (Pearse et al. 2003, Maggio et al. 2012). Additionally, some of the products of NETs (antimicrobial peptide LL-37, DNA, and HMGB1) are DAMPs that trigger TLR signalling (Makuloluwa et al. 2014). Depletion of neutrophils after SCI using the Ly6G/Gr-1 monoclonal antibody in mice led to impairment of functional recovery and tissue damage (Stirling et al. 2009). However, a study using the same antibody did not find any effect on neutrophil recruitment and locomotor recovery after SCI (Lee et al. 2011). Depletion of both neutrophils and macrophages led to improvement in locomotor recovery and reduction in secondary damage (Lee et al. 2011). Conversely, neutrophils that enter the eye after optic nerve lesion produce oncomodulin, a neuroprotective and axon-growth-promoting molecule (Kurimoto et al. 2013). The role of neutrophils in the CNS still remains unclear, however most studies indicate that these cells are detrimental to regeneration.

Macrophages/Microglia

Microglia respond rapidly to injury and are the first cell type to respond within minutes in traumatic brain injury (TBI) models (Donat et al. 2017). They extend processes toward the injury site and obtain an activated phenotype by retracting

their processes and phagocytosing cellular debris. It has been shown that after injury, the nearby astrocytes and resident microglia are activated and migrate towards the injury site. Activated astrocytes and other glial cells form the glia scar. Microglial cells are mainly present in the marginal and uninjured areas, whereas peripheral macrophages accumulate in the centre of injured spinal cord (Zhou et al. 2014). Whereas in TBI models, microglia are the key regulators of the inflammation and the regenerative outcome, in zebrafish, it has been shown that the activation and presence of peripheral macrophages in the injury site is essential for the regeneration of motor neurons and axons after SCI (Tsarouchas et al. 2018) by regulating the levels of pro-inflammatory cytokines and the number of neutrophils.

1.3.2 Cytokines in SCI

The other potent regulators of the lesion environment are pro- and anti-inflammatory cytokines, which include interleukins, TNF-α, transforming growth factor-β, and others. Increase in proinflammatory cytokine expression after SCI occurs within minutes after injury and peaks in the first 24 h (Bartholdi and Schwab 1997, Yang et al. 2004, Yang et al. 2005, Kigerl et al. 2006, Pineau and Lacroix 2007).

Interestingly, it has been reported that expression of cytokines is starting before the influx of peripheral immune cells (Kigerl et al. 2006), suggesting that CNS cells and other cell types respond to the insult by producing cytokines before the specialised immune cells I'll focus here on two pro-inflammatory cytokines, Il-1β and TNF-α. These are the most common pro-inflammatory cytokines that respond rapidly after injury and I found that they are key mediators of axonal regeneration after spinal cord injury in zebrafish larvae (Tsarouchas et al. 2018).

Interleukin-1β

The interleukin-1 (Il-1) family consists of 11 proteins (Il-1F1 to Il1F11) encoded by 11 distinct genes in mammals. These molecules are major mediators of innate immune reactions, and blockade of the founding members Il-1α or Il-1β by the interleukin-1 receptor antagonist (Il-1RA) has demonstrated a central role of Il-1 in a number of human autoinflammatory diseases (Dinarello 1996, Farasat et al. 2008, Martinon et al. 2009). These cytokines rapidly increase mRNA expression of hundreds of genes in multiple different cell types. The potent proinflammatory activities of Il-1α and Il-1β are restricted at three major levels: (i) synthesis and release (Farasat et al. 2008), (ii) membrane receptors(Dinarello 2005), and (iii) intracellular signal transduction(Weber et al. 2010).

In response to ligand binding of the receptor, a complex sequence of phosphorylation and ubiquitination events results in activation of nuclear factor κB signaling and the JNK and p38 mitogen-activated protein kinase pathways, which, induce the expression of canonical Il-1 target genes (such as Il-6, Il-8, MCP-1, COX-2, IκBα , Il-1α , Il-1β , MKP-1) by transcriptional and post-transcriptional mechanisms (Weber et al. 2010) (Fig 1.3.1). Functional studies of the type I Il-1R demonstrated that the cytoplasmic segments, possessing a sequence similarity with the Drosophila Toll gene product or Il-6R β chain, gpl30, are important for transmitting activity that induces cytokine genes (Kuno and Matsushima 1994). Furthermore, several groups reported that Il-1 and tumor necrosis factor (TNF) rapidly induce sphingomyelin turnover in various types of cells, producing ceramide, which may act as a second messenger molecule in an intracellular signaling cascade(Kuno and Matsushima 1994).

For the rest of the thesis I focus on Il-1β because there is no zebrafish orthologue for the mammalian Il-1α.

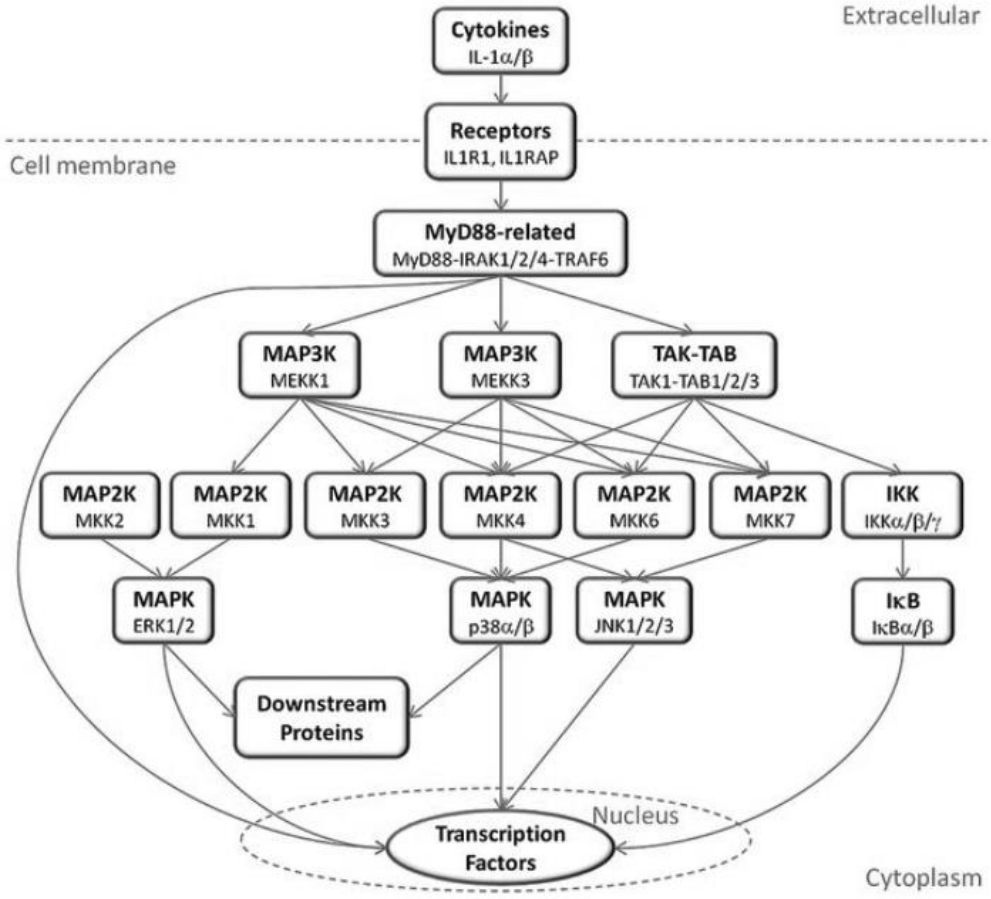

Figure 1.3.1 Il-1 signaling pathway (modified from(Acuner Ozbabacan et al. 2014))

Expression studies have shown that Il-1β expression peaks 12 h after injury by microglia, astrocytes, and some infiltrating neutrophils (Pineau and Lacroix 2007). Signaling via Il-1R1 is required for the influx of neutrophils and monocytes after SCI (Pineau et al. 2010). Rodent studies have shown that administration of Il-1β into the mouse spinal cord white matter undergoing Wallerian degeneration led to a rapid macrophage/microglial activation and myelin clearance (Perrin et al. 2005). On the other hand the infusion of function-blocking antibody against Il-1β suppressed macrophage responses and myelin clearance, indicating that Il-1β can regulate the recruitment of macrophages from the circulation and their activation to remove cellular debris (Perrin et al. 2005). The endogenous antagonist of Il-1α (Il-1 receptor antagonist, Il-1ra) is also upregulated after SCI (Liu et al. 2008), that regulates the

effects of Il-1β. Administration of IL-1ra mediates a reduction in neuronal apoptosis and caspase-3 expression via p38 MAP kinase (Wang et al. 2005) and improvement in functional recovery (Zong et al. 2012) after SCI. It also reduces neuronal death after brain ischemia (Loddick and Rothwell 1996, Relton et al. 1996), whereas treatment with exogenous Il-1β worsens brain injury in ischemic and excitotoxic models (Loddick and Rothwell 1996, Lawrence et al. 1998). Furthermore, administration of caspase-1 inhibitor leads to successful axonal regeneration and functional recovery in zebrafish (Tsarouchas et al. 2018). These and other studies indicate strongly that the expression of Il-1β increases after spinal cord and other CNS insults and that this proinflammatory cytokine mediates detrimental effects via multiple mechanisms.

Tumour Necrosis Factor-α

Tumor necrosis factor alpha (TNF-α) is a proinflammatory cytokine involved in various biological processes including regulation of cell proliferation, differentiation, apoptosis and immune response. TNF-α is mainly produced by macrophages, also by other tissues including lymphoid cells, mast cells, endothelial cells, fibroblasts and neuronal tissues. TNF was identified as a soluble cytokine produced upon the activation by the immune system and able to exert cytotoxicity on tumor cell lines and cause tumor necrosis in animal models. TNF is primarily produced as a type II transmembrane protein arranged as stable homotrimers.

The members of TNF-α family exert their cellular effect through two distinct surface receptors of the TNF receptor family, TNFRSF1A (TNF-R1) and TNFRSF1B (TNF-R2). TNF-R1 is ubiquitously expressed, whereas TNF-R2 is found typically on cells of the immune system and is highly regulated. TNF-R1 and TNF-R2 binds membrane-integrated TNF (memTNF) as well as soluble TNF (sTNF) TNF-R1 contains a protein-protein interaction domain, called death domain (DD). This domain interacts with other DD-containing proteins and couples the death receptors to caspase activation and apoptosis. TNF-R2 induces gene expression by a TRAF-2 dependent signaling mechanism and also crosstalk's with TNF-R1. The pleiotropic biological effects of TNF

can be attributed to its ability to simultaneously activate multiple signaling pathways in cells. Binding of TNFα to TNF-R1 on the cell surface triggers trimerization of the receptor and exposes intracellular domain of TNF-R1 following the release of an inhibitory protein. This intracellular domain recruits a death-domain containing adaptor protein, TRADD by homophilic interactions. TRADD, which acts as a scaffold protein, recruits TRAF2 and RIPK1 to form a complex, referred to as complex 1. Complex 1 is believed to be important in NF-κB activation and JNK activation (Fig 1.3.2).

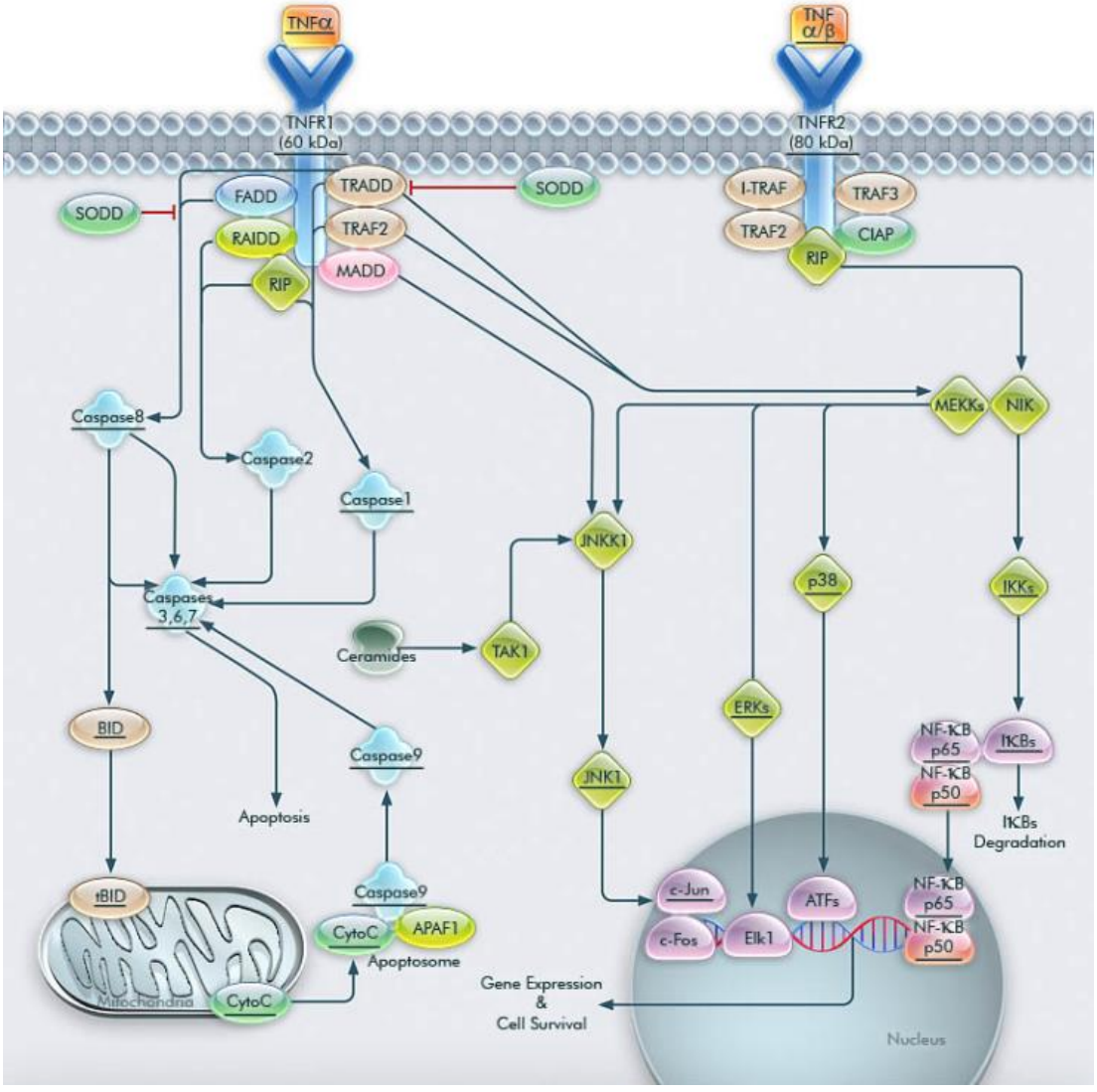

Figure 1.3.2 TNF-α signaling pathway (adapted from Thermo-Fisher Scientific)

Tumour necrosis factor acts as an acute-phase cytokine in regulating immune cell responses, inflammatory cascades, and cell death. TNF-α mediates its effects by binding to two receptors, TNFRI (Tseng et al. 2018) and TNFRII (Tseng et al. 2018). The expression of this cytokine is upregulated after SCI in mice (Pineau and Lacroix 2007), zebrafish (Tsarouchas et al. 2018) and in human TBI and ischemia models (Tuttolomondo et al. 2014). In situ hybridization has shown that after injury, TNF-α is expressed firstly by all CNS cell types (Pineau and Lacroix 2007), whereas during later stages of inflammation, it is expressed mainly by activated microglia/macrophages (Pineau and Lacroix 2007), indicating that it mediates different effects during early and later periods after injury. In humans, TNF-α protein is expressed early after injury in neurons and in microglial cells (Yang et al. 2005), followed later by immune cells from the periphery that are recruited to the site of injury. In experimental models of SCI, pharmacological manipulations of TNF signaling (Genovese et al. 2006, Genovese et al. 2008) or TNFR1-knockout (Genovese et al. 2008) improved locomotor recovery in mice. However, another study showed that TNFR2-null mice exhibit poor locomotor recovery after SCI (Kim et al. 2001). There is also evidence that TNF-α increases cell death in the spinal cord by trafficking of GluR2 deficient AMPA receptors to the cell surface of neurons (Ferguson et al. 2008). Furthermore, in this thesis I show that pharmacological blocking of the release of TNF-α and CRISPR/Cas mediated genome editing in zebrafish led to impaired axonal regeneration after injury (Tsarouchas et al. 2018), showing that TNF-α has a pro-regenerative role after injury.

These seemingly contradictory findings show that is very difficult to highlight the exact role of innate immune cells and cytokine signaling during spinal cord injury. It is even more difficult to address these questions in adult mammalian models, in which both adaptive and innate immune system are present due to interactions between the two. For these reasons it is important to study and understand the principles that regulate the role of the inflammatory response during regeneration of the CNS in other species that exhibit a high regenerative potential in the CNS and their immune response can be studied separately. This is the case in larval zebrafish

where innate and adaptive immune system mature during different stages of development.

1.4 The zebrafish as an animal model

Zebrafish (*Danio rerio*) is a teleost freshwater fish that belongs to the *Cyprinidae* family, first described by Francis Hamilton in 1822 (Hamilton 1822). George Streisinger used them in medical research as he was looking for a model that could easily be genetically manipulated (Streisinger et al. 1981). Over the years, zebrafish have become more popular and this is reflected in the information that is available and in the increasing number of studies that use zebrafish as an animal model. More specifically, according to Zebrafish Information Network (ZFIN) the number of publications with zebrafish as an animal model on 1998 was 1938, whereas 20 years later, on 2018, this number is 17 times higher reaching 32267 publications. There are many features that make zebrafish a good animal model. It develops rapidly, and the maintenance cost is low compared to other vertebrate models. 70% of human genes have zebrafish orthologues (Howe et al. 2013). They breed and can produce as many as 300 eggs at a time. Eggs are fertilized externally, which allows them to be manipulated easily by injecting DNA or RNA into the zygote in order to modify gene expression. Furthermore, zebrafish larvae are transparent which allows the visualization of fluorescent tissues under the microscope in vivo (Fetcho 2003). However, there are also some downsides like the long generation time. In order to have a breeding colony the fish need to be at least 3 months old. Furthermore, some conserved genes between mammals and zebrafish have multiple orthologues in zebrafish due to its genome duplication which makes them sometimes difficult to study. They are also greatly influenced by their environment, which means that parameters like water quality and temperature must be tightly controlled.

Figure 1.4 The zebrafish during different developmental stages (modified from (Saleem and Kannan 2018))

1.5 Spinal cord regeneration in the zebrafish model

Zebrafish, in contrast to mammals, are capable of functional CNS regeneration after injury during the larval but also during the adult stages. In the adult spinal cord, neurogenesis is rare across species, including primates, rodents, birds and fish (Alunni and Bally-Cuif 2016). A consequence of the spinal cord injury is the sudden loss of motor neurons and disconnection of axons. As part of the repair process, replenishing new motor neurons and a re-connection of axons may be necessary. This requires endogenous progenitors to exit from their quiescent stage to undergo active neurogenesis and cell proliferation. In the lesioned spinal cord of adult zebrafish, newly regenerated motor neurons are derived from the olig2-expressing ependymal radial glial cells (ERGs) that line in the central canal of the spinal cord (Reimer et al. 2008, Reimer et al. 2009). Transcription factors that define the progenitor zones in the neural tube of embryos, such as Olig2, Shh, Pax6 and Nkx6.1, were expressed in the ventrolateral ERGs around the central canal, indicating that these ERGs are equivalent to pMN progenitor cells in the neural tube that give rise to motor neurons during the development (Reimer et al. 2009). Ependymal cell activation was also observed in mammals following the spinal cord injury; however, the newly generated ependymal cells mainly give rise to astrocytes that migrate to the lesion site to form the glia scar and prevent axon regeneration (Panayiotou and Malas 2013). Similar to the adult zebrafish, neuronal replacement, axonal outgrowth and functional recovery also occurred in larval zebrafish. Many developmental signals, such as Notch, Hedgehog (Hh), Bone Morphogenetic Protein (BMP), Wnt, Fibroblast Growth Factor (FGF), Retinoic Acid (RA) and neurotransmitters are redeployed during regeneration in the larval model and activate resident spinal progenitor

cells in the fully patterned adult spinal cord. Furthermore, the neural and axonal repair is quicker in the larval model as it happened within 48 hours as opposed to 6 weeks in adults.

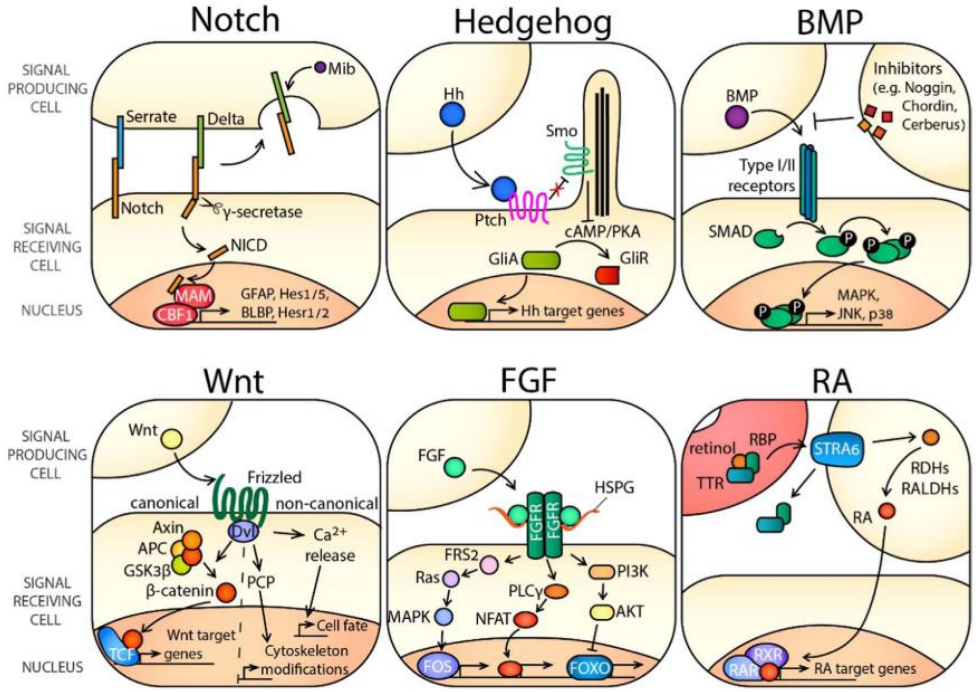

Figure 1.3.3 Molecular basics of signalling pathways involved in zebrafish adult and larval spinal cord regeneration and development (adapted from (Cardozo et al. 2017))

In mammals, including humans, damage to spinal cord after injury leads to permanent functional deficits. This is mainly due to the fact that adult axons cannot regenerate after transection in mammals. The main reason for this is an environment containing inhibitors of axon regeneration, such as the myelin-associated inhibitors nogo-A (Otero-Ortega et al. 2017), myelin-associated glycoprotein (MAG) (McKerracher and Rosen 2015), and oligodendrocyte myelin glycoprotein (Geoffroy and Zheng 2014). Another group of inhibitors are components of the ECM that are found in the glial scar formed at the injury site such as chondroitin sulfate proteoglycans. Other molecules, like ColXII (Wehner et al. 2017), Semaphorin 3D (Wolman et al. 2007), Tenascin-C (Schweitzer et al. 2005), have been shown to have pivotal roles in axonal growth. ColXII has been shown to be essential for axonal regeneration after injury (Wehner et al. 2017) whereas Semaphorin 3D is involved in

axon-axon interactions and promotes fasciculation (Wolman et al. 2007) and Tenascin-C is involved in motor axon out-growth (Schweitzer et al. 2005).

However, re-growth of injured axons in the mammalian CNS exhibits variability, depending on cell type. Whereas many cell types in the mammalian CNS show some axon re-growth when a permissive environment is provided, some neuronal cell types, such as Purkinje cells, are still unable to extend their axons (Rossi et al. 1995). The intrinsic capacity of neurons to extend their axons has been extensively studied over the years. (He and Jin 2016, Mahar and Cavalli 2018) and others have reviewed the intracellular communication mechanisms required to change the genetic and epigenetic programme of injured neurons in order to allow axon regeneration to occur and also the roles of the cellular environment, axon–soma signalling and growth cone formation and dynamics during regeneration.

The zebrafish has many features in common with non-regenerating mammals such as the brainstem organization (Moens and Prince 2002) and the genes activated during axon re-growth (Bernhardt 1999). They exhibit functional recovery after a different types of injuries, like spinal cord injuries (Becker et al. 1997, Wehner et al. 2018), injury in the telecephalon (Kyritsis et al. 2012), and the retina (Rao et al. 2017) or optic nerve transection (Diekmann et al. 2015, Van houcke et al. 2017). Zebrafish have the capability of robust axonal regeneration following spinal cord and optic nerve injuries. Transected axons can regrow and functional restoration can take place. After injury, zebrafish are paralyzed caudal to the lesion site but regain their normal swimming behaviour within 6 weeks (Becker et al. 2004, Dias et al. 2012). They have the ability to replace lost neurons (Becker and Becker 2008, Reimer et al. 2008, Ohnmacht et al. 2016) upon injury and also to establish new functional axonal connections (Becker et al. 1997, Becker and Becker 2014, Wehner et al. 2017).

Over the years many different signalling molecules have been found to play a crucial role during regeneration after injury or ablation in the zebrafish CNS, like dopamine (Reimer et al. 2013), serotonin (Barreiro-Iglesias et al. 2015) and sonic hedgehog (Reimer et al. 2009) Fig. 1.3.4. Additionally, it has been shown that upregulation of Nogo-A homologue, which has inhibitory role in axonal growth in mammals

(Grandpre and Strittmatter 2001), is required for the success of axon regeneration in the zebrafish visual system, and its downregulation caused severe defects in the retinotectal projection (Welte et al. 2015). The main source of inhibitors of regeneration is the glial scar formed at the injury site in mammals (Sofroniew 2009, Yuan and He 2013). There is no evidence of major astrocytic scar formation in fish. Studies in the spinal cord of goldfish (Nona and Stafford 1995), have shown the lesion site is devoid of glial fibrillary acidic protein-positive (GFAP) processes when axons cross the lesion site. This indicates the lack of an astroglial scar. Chondroitin sulfate proteoglycans are another hallmark of a glial scar, and mostly inhibit axonal regeneration (Bradbury et al. 2002). In contrast to mammals (Selles-Navarro et al. 2001), there is also no increased immunoreactivity to chondroitin sulfates in the optic nerve of zebrafish at the lesion site (Becker and Becker 2002). This again indicates that if there is a glial scar, it is not prominent in the lesioned CNS of adult teleosts.

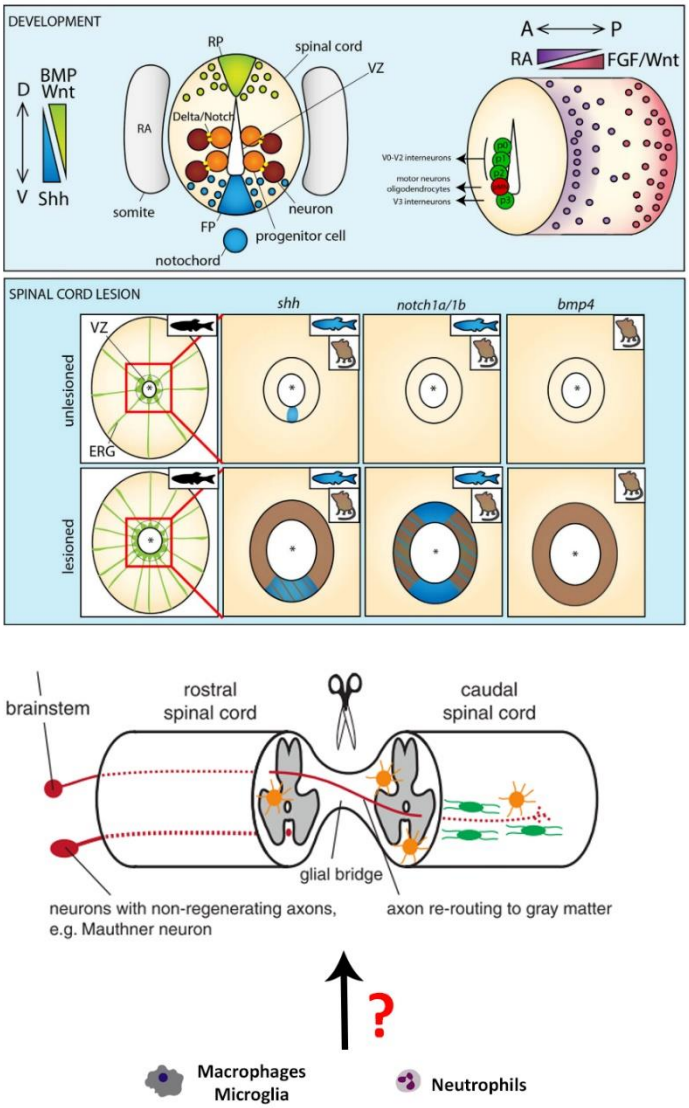

Figure 1.3.5 Events occurring in the zebrafish spinal cord during regeneration after SCI and development. After an injury the neural progenitors upregulate the expression of genes present during spinal cord development, such as wnt, shh, notch1a/1b and bmp4 that are also upregulated in mammalian models after SCI. Furthermore, glial bridges are contributing to axonal regeneration after injury whereas the role of the innate immune system during this process remains unclear (modified from (Becker and Becker 2014, Cardozo et al. 2017)).

Another important characteristic of the zebrafish that makes them ideal CNS regeneration model is the fact that they are able to re-establish functional axonal connections. Recovery of swimming function critically depends on regeneration of axonal connections across the complex non-neural injury site (Becker et al. 1997, Wehner et al. 2018). In order to set the scene for functional regeneration five criteria

were proposed in 1980 which should be met in order to demonstrate functional recovery after SCI (Guth et al. 1980). According to Guth et al., 1980 these criteria are the following:

1. The experimental lesion must cause disconnection of nerve processes.
2. Processes of CNS neurons must bridge the level of injury.
3. The regenerated fibers must make junctional contacts.
4. The regenerated fibers must generate postjunctional responses.
5. Changes in function must derive from regenerated connections

Zebrafish manage to meet these criteria after SCI and can regenerate functionally. Understanding the mechanisms that allow this regenerative capacity will allow comparison with organisms in which regeneration is not as pronounced, such as humans. Given that there are many examples of gene conservation between the zebrafish and other vertebrate species, their study may eventually lead to the increased success of clinical regenerative methods.

1.6 Zebrafish immune system

The tools for identifying danger signals derived from either injury or infection are conserved within species. Several studies have identified that innate and adaptive immunity are present in fish and more specifically in zebrafish (Renshaw and Trede 2012). Innate immunity includes autonomous mechanisms that are active not only in immune cells but also in cells with epithelial origin (Iversen et al. 2015, Ross and Herzberg 2016). Several hundreds of proteins are involved in autonomous immune protection which are present in zebrafish. They include receptors that recognize molecules specific for pathogens, called pattern recognition receptors (PRRs) and various effectors that restrict the spread of pathogen or induce cell death. In addition, infected cells produce cytokines such as interferons that activate autonomous immune mechanisms in neighbouring cells. Interferons regulate a large fraction of autonomous immune genes (Schneider et al. 2014). IFN type I and III are induced when PRRs bind products from pathogens activating IFN regulatory factors (IRF) 3, 5,

and 7, c-Jun, and NFkB. This leads to the formation of a signaling complex that contains STAT1 and 2 and interferon regulatory factor 9 (IRF9). This complex drives the expression of IFN-stimulated genes (ISGs). Another innate immune mechanism is the inflammation, which is associated with the recruitment of immune cells to the site of infection or injury. It translates autonomous response at the cellular level to the response on the level of organism. Many cells respond to infection, stress and other homeostasis-altering processes by assembly of inflammasomes (Liston and Masters 2017). Recently it has been characterized by (Li et al. 2018) that zebrafish exhibit a unique activation mechanism for the NLRP1 inflamamsome, which is one of the best-characterized inflammasomes in humans and in other mammalian models.

Innate and adaptive immunity must coordinate for successful defence against pathogens, and for immunological memory to protect against future infections. Macrophages and Dendritic cells (DCs) are professional antigen presenting cells (APCs) that are endowed with both phagocytic functions and cell-surface receptors that allow them to orchestrate the activation of T and B cells. DCs were originally distinguished in mammals as cells with a distinct stellate morphology and later functionally defined as the most potent initiators of the adaptive immune response (Nussenzweig and Steinman 1980). Upon encounter with antigen, DCs migrate to the T cell areas of local lymph nodes and other lymphatic tissues. A hallmark feature of DCs that distinguishes them from other MPs is the interaction of DCs with T cells in these organized lymphatic areas, which results in highly efficient priming of T cells. Many different types of DCs have been identified in mammals based on divergent functional characteristics. DCs have been historically subdivided into two subsets: CD8− (CD11b+) DCs, which engage in conventional antigen presentation of external antigen upon MHC class II molecules and internal antigen upon MHC class I receptors, and CD8+ DCs, which are thought to specialize in cross-presentation, or the presentation of processed external antigen on MHC class I molecules rather than MHC class II molecules (Edelson et al. 2010).

Cells that morphologically resemble classical DCs have been identified in several teleost species, including rainbow trout (Bassity and Clark 2012), medaka (Aghaallaei

et al. 2010), and Atlantic salmon (Haugland et al. 2012). In zebrafish, the work from (Lugo-Villarino et al. 2010) showed that cells with dendritic morphology have been isolated from kidney marrow, a hematopoietic site akin to the mammalian bone marrow. Similarly, the pivotal receptors CD40-CD40 ligand (Gong et al. 2009) and the adaptor molecule TRAF6, which is required for DC maturation (Kobayashi et al. 2003), have been identified in zebrafish and other jawed vertebrates. Additionally, the works from (Liu et al. 2017) and (Zhang and Wiest 2016) have provided evidence regarding the development and maturation of B and T cells in zebrafish. Hence, zebrafish resembles a good tool for the study of innate and adaptive immunity.Teleosts, like mammals, have a similar arsenal of defence mechanisms against infections. Like in other vertebrate models, these mechanisms include specialised immune cell types (macrophages, neutrophils, microglia, B-cells, T-cells) similar to mammals in terms of structure and cytochemistry, and phagocytic and secretory abilities (Traver et al. 2003) cytokine and interferon release. The cellular elements of the teleosts immune response have been described (Traver et al. 2003). Zebrafish leukocytes, even in embryos are fully functional and participate in host defence. Neutrophils are the first to respond to an injury; macrophages are subsequently recruited to inflamed tissues to phagocytose pathogens and tissue debris. In the first line of zebrafish defence,Toll-like receptors (TLRs) (Li et al. 2017) are expressed on the surface of dendritic cells and macrophages and recognize (PAMPs) derived from injury. Following PAMP binding, TLRs transduce signals to the nucleus, which leads to activation of MAP kinase family members, translocation of NFκB to the nucleus, that leads to gene expression (Akira and Hemmi 2003). In all of the aforementioned regeneration paradigms the common feature is the inflammatory response that occurs after injury. There are several studies that address the role of inflammation during regeneration of the zebrafish CNS after injury (Kyritsis et al. 2012, Carrillo et al. 2016, Bollaerts et al. 2017, Wang et al. 2017). The immune reaction to injury may be a determining factor for regenerative success (Kroner et al. 2014, Chassot et al. 2016). In mammals, a prolonged and non-resolving immune response, consisting of pro-inflammatory macrophages (Kigerl et al. 2009), microglia

cells (Norden et al. 2015) and neutrophils (Taoka et al. 1997) together with cytokines released from other cell types, such as endothelial cells, oligodendrocytes or fibroblasts (Tran et al. 2018) contribute to an inflammatory environment that is hostile to axonal regeneration. However, activated macrophages can also promote axonal regeneration (Gensel et al. 2009), suggesting complex roles of the immune response after spinal injury.

In zebrafish, the roles of all of these cell types can be distinguished in a system that shows a high capacity for axonal regeneration and functional spinal cord repair (Becker and Becker 2014). Similar to mammals (Renshaw and Trede 2012), zebrafish possess an innate immune system from early larval stages and develop an adaptive immune system at juvenile stages (Meijer and Spaink 2011). CNS injury models in zebrafish have shown that there is an activation of the microglia as response to injury (Kyritsis et al. 2012). Stimulation of acute inflammatory response after optic nerve injury in zebrafish activates microglia and leads to recruitment of neutrophils and peripheral macrophages, similar to what is observed in mammalian models (Bollaerts et al. 2017). Although several factors and pathways like LIF (Ogai et al. 2014) and the JAK/STAT3 (Elsaeidi et al. 2014) and mTOR (Huang et al. 2017) signaling pathways are implicated in CNS regeneration in zebrafish, the exact mechanism of how the positive effects of acute inflammation is mediated remains unclear. Retina studies show that immunomodulation can enhance or impair regeneration of photoreceptors after ablation (White et al. 2017). After a SCI in zebrafish, microglia are activated (Becker and Becker 2001, Ghosh and Hui 2018) and neutrophils and blood-borne macrophages infiltrate the lesion site, although their precise contribution to axonal regeneration is still unknown. Despite the similarities between zebrafish and mammals the contribution of inflammation to the regenerative process after SCI is still unclear.

Zebrafish larvae exhibit temporal separation of innate immunity from adaptive responses. This makes zebrafish larvae particularly useful for dissecting the innate host factors involved in pathology without any implications derived from the interaction between innate and adaptive immune response. For this reason, I decided

to use the larval model in order to assess the role of the innate immune system (macrophages, neutrophils, microglial cells) during the regeneration of the zebrafish spinal cord. I find that innate immune response is essential for regeneration after spinal cord injury. Peripheral macrophages are necessary in order to tightly control the levels of inflammation by regulating the expression of Il-1β and preventing other cells like neutrophils and keratinocyte form increasing its levels. Furthermore, macrophages are the main source of TNF-α which has a pro-regenerative role after injury and an anti-inflammatory role during inflammation as CRISPR mediated disruption of TNF-α led to increased numbers of neutrophils and increased expression of Il-1β after injury. However, the potential beneficial role of the adaptive immunity cannot be excluded and in order to assess it, experiments in adult zebrafish should be carried out.

1.7 Conclusions and statement of aims

In this thesis I investigated the contribution of the innate immune system to the regeneration of the motor neurons and axons in zebrafish larvae. In order to achieve this, I addressed the following aims:

- To characterize the cellular and molecular immune response that occurs after injury
- To investigate the neuronal regeneration after genetic and pharmacological inhibition of the immune response
- To investigate and characterize the axonal regeneration that occurs after injury
- To characterize the axonal regeneration after genetic and pharmacological manipulation of the immune response
- To determine which innate immune cell types are the most important during spinal cord regeneration in zebrafish larvae

Chapter 2: Materials and methods

2.1 Zebrafish techniques

2.1.1 Fish husbandry

All zebrafish lines that were used for the purpose of this study were kept and raised under standard conditions (Westerfield 2000), at the temperature of 26.5°C and a 14 hour-light and 10 hour-dark cycle. Larvae were kept at 28.5°C in conditioned aquarium water containing methylene blue (2ml of 0.1% methylene blue, to 1 liter of fish water). The following lines were used: wild type (*wik*), *Tg(Xla.Tubb:DsRed)*, abbreviated as nbt:DsRed where neuronal elements of the spinal cord fluoresce red (Peri and Nusslein-Volhard 2008); *Tg(mpeg1:EGFP),* abbreviated as mpeg:GFP where macrophages/microglial cells fluoresce green (Ellett et al. 2011), and *Tg(mpx:GFP),* abbreviated as mpx:GFP where neutrophils fluoresce green (Renshaw et al. 2006), *Tg(fli1:EGFP),* abbreviated as fli:GFP where blood vessels fluoresce green (Lawson and Weinstein 2002), *irf8*$^{st95/st95}$ (Shiau et al. 2015), these animals do not have macrophages/microglial cells during the larval stage of development, *Tg(gfap:GFP)*^{mi2001}, abbreviated as GFAP:GFP where glial elements fluoresce green, (Bernardos and Raymond 2006), *TgBAC(pdgfrb:Gal4FF);Tg(UAS:GFP*), abbreviated as pdgfrb:GFP where pericytes and epithelial cells fluoresce green (Ando et al. 2016), *Tg(her4.3:GFP*) where the glial elements of the spinal cord fluoresce green (Yeo et al. 2007), *Tg(gfap:Gal4ffs995;UAS:NTR-mCherry)* where the glial cells express the enzyme nitroreductase under the gfap promoter which allows to selectively ablate the glial population after addition of metronidazole which is the substrate for nitroreductase (Matsuoka et al. 2016), *Tg(her4.3:irtTAM2(3F)-p2a-AmCyan*^{ulm6}*),* abbreviated as her4.3:TetA AmCyan where the glial elements of the spinal cord fluoresce cyan (Geurtzen et al. 2014), *Tg(her4.1:Tet-GBD-p2A-mCherrytud6)* abbreviated as her4.3:mCherry where the glial elements of the spinal cord fluoresce red (Knopf et al. 2010), *Tg(claudin k:Gal4)*^{ue101}; *Tg(14xUAS:GFP)* abbreviated as cldnK:GFP where the myelin associated protein claudin K fluoresces

green (Munzel et al. 2012), *Tg(TNFTNFa:eGFPF)*^{sa43296}, abbreviated as TNFTNFTNF-α:GFP where the TNF-α expressing cells fluoresce green(Nguyen-Chi et al. 2015) , *Tg(Il-1β:eGFP)*^{sh445}, abbreviated as Il-1β:GFP where the il-1β expressing cells fluoresce green (Ogryzko et al. 2018), *csf1ra*$^{-/-}$*; csf1rb*$^{-/-}$ abbreviated as csf1ra/b. These animals carry double mutation on the *csf1ra* and *csf1rb* genes which regulate the density and the distribution of microglial cells leading to microglia loss (Oosterhof et al. 2018).

2.1.2 Drug treatment

Dexamethasone (Sigma) was dissolved in DMSO to a stock concentration of 5mM. The working concentration was 100µM prepared by dilution from stock solution.
Ac-YVAD-cmk (Sigma) was dissolved in DMSO to a stock concentration of 10mM. The working concentration was 50µM prepared by dilution from the stock solution.
Q-VD-OPh (Sigma) was dissolved in DMSO to a stock concentration of 10mM. The working concentration was 50µM prepared by dilution from stock solution.
IWR-1 (Sigma) was dissolved in DMSO to a stock concentration of 6mM. The working concentration was 15µM prepared by dilution from the stock solution.
O-Phospho-L-serine (Sigma) was dissolved in PBS to a stock concentration of 10mM. The working concentration was 10µM prepared by dilution from stock solution.
Lipopolysaccharides from Escherichia coli O55:B5 (LPS, Sigma) was dissolved in PBS to a stock concentration of 1mg/ml. The working dilution was 50µg/ml prepared by dilution from stock solution.
Pomalidomide (Cayman Chemicals) was diluted in DMSO at a stock concentration of 10mg/ml. The working concentration for the experiments was 170 µM.
Larvae were collected from the breeding tanks and divided into Petri dishes at a density of maximum 30 larvae per dish. For the Dexamethasone experiment the larvae were treated from 6 hours post fertilization until 5 days post fertilization (dpf). For the pomalidomide treatment, larvae were pre-treated for 2 hours before the injury and were incubated for 24 and 48 hpl. For the rest of the drug

treatments, larvae were incubated with the drug from 3 days post fertilization until 5 days post fertilization. The larvae were divided into groups of 20 into 6 well-plates for every drug treatment. For all the experiments the drugs were tested using treatment after injury and pre-treatment and the effects were compared. For all the experiments in this thesis I used the pre-treatment in order to maximise the effect which could be less profound, due to pharmacokinetics, when the animals were treated after injury.

2.1.3 EdU administration

Zebrafish larvae at 3 dpf were anesthetized in PBS containing 0.02% aminobenzoic acid-ethyl-methyl-ester (MS222, Sigma) and were placed in a lateral position on an agar plate and injected into the yolk with ∼5 nl 5 mM EdU in 0.1 M sterile KCl and 7.5% DMSO. After washing, larvae were allowed to develop under standard conditions.

2.1.4 Spinal cord lesions and behavioral recovery

Zebrafish larvae at 3 dpf were anesthetized in PBS containing 0.02% aminobenzoic-acid-ethyl methyl-ester (MS222, Sigma). Larvae were transferred to a plastic Petri dish coated with agarose. Following removal of excess water, the larvae were placed in lateral position, and the tip of a sharp 30G $^{1/2}$ syringe needle was used to inflict a lesion in the dorsal part of the trunk at the level of the end of the yolk extension.

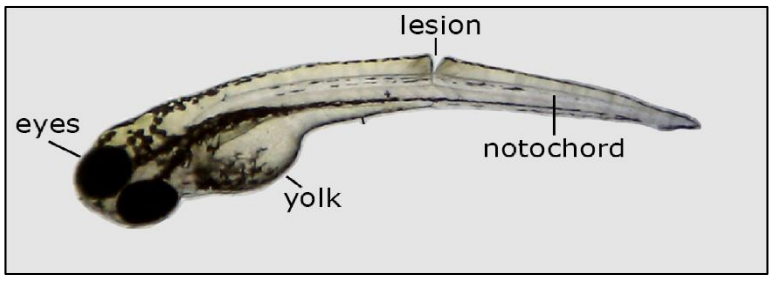

Figure 2.1.4. Picture showing the injury site in a 3 dpf zebrafish larva (adapted from (Ohnmacht et al. 2016)

In order to assess behavioral recovery, lesioned and unlesioned control larvae were touched with a glass capillary on the median fin fold caudal to the lesion site. The swim path of their escape response was recorded and analysed using a Noldus behavior analysis set-up and EthoVision software (v. 7). Data are shown as distance travelled during the first 15 s after touch, averaged from triplicate measures per larva.

2.2 Molecular biology

2.2.1 Primer design

Primers were designed using Primer3web and Primer Blast tool available at (https://www.ncbi.nlm.nih.gov/tools/primer-blast). The primers were selected based on their length, melting temp and %GC content to achieve high specificity of amplification and checked for self-complementarity using the Oligo-Calc: Oligo-Calc: Oligonucleotide Properties Calculator (http://biotools.nubic.northwestern.edu/OligoCalc.html). Primer oligonucleotides were ordered from Integrated DNA Technologies, BVBA; Leuven, Belgium.
The list of designed primers is given below:

Primer name	Orientation	Sequence
irf8	Forward	5'-ACATAAGGCGTAGAGATTGGACG-3'
	Reverse	5'-GAAACATAGTGCGGTCCTCATCC-3'
col1a1a	Forward	5'-AACACGTCTGGTTCGGAGAG-3'
	Reverse	5'-AAATCCTGACCTGGTGTTGG-3'
col1a1b	Forward	5'-TACACAGACCGGACCCTACG-3'
	Reverse	5'-TCACTGCCATAAGCCATCTG-3'
col5a1	Forward	5'-CTGTAACTTCACAGCAGGTGGA-3'

	Reverse	5’-GGGTTATTATCGTATGACATCTC-3’
col5a2a	Forward	5’-AGCTGAGGGAAATAACCGCTTTA-3’
	Reverse	5’-AGGTAGCTTGCACTGTTCTGTAA-3’
col5a2b	Forward	5’-TGATTATTGGATAGACCCGAATG-3’
	Reverse	5’-TGCTGTACGAAGTGCAAGTTAAA-3’
col5a3b	Forward	5’-AAATGGCTTCATGGAGCAAAGAG-3’
	Reverse	5’-CTATACACCCTTACTGACGCCTC-3’
col12a1a	Forward	5’-TCCAGCTCCAGATGTTTGATATT-3’
	Reverse	5’-AGGTCCAGGTAATCCTCTCTGTC-3’
col12a1b	Forward	5’-CATTGATCCCACATTCACAACCC-3’
	Reverse	5’-CCGTATTTGGTTGCAGGTTTCTT-3’
fn1b	Forward	5’-CAACCTCCAATTCACCTCCCTAA-3’
	Reverse	5’-ATAAGAGTGGCAGTTGTGGATGT-3’
beta actin qPCR	Forward	5’-CACTGAGGCTCCCCTGAATCCC-3’
	Reverse	5’-CGTACAGAGAGAGCACAGCCTGG-3’
tgfb-1a qPCR	Forward	5’-GCTGTATGCGCAAGCTTTACA-3’
	Reverse	5’-GGACAATTGCTCCACCTTGTG-3’
Il-1β qPCR	Forward	5’-ATGGCGAACGTCATCCAAGA-3’
	Reverse	5’-GAGACCCGCTGATCTCCTTG-3’
tgfb3 qPCR	Forward	5’-AAAACGCCAGCAACCTGTTC-3’
	Reverse	5’-CCTCAACGTCCATCCCTCTG-3’
TNF-α qPCR	Forward	5’-TCACGCTCCATAAGACCCAG-3’
	Reverse	5’-GATGTGCAAAGACACCTGGC-3’
mpeg1 ISH(Ellett et al. 2011)	Forward	5’-GGATCCATCATGAAGTCAAG-3’’
	Reverse	5’-CTCGAGTACTTGAACCCGTG-3’’
tgfb1a probe	Forward	5’-AAAGAGCCTGAATCCGGAGC-3’
	Reverse	5’-ACTTGCAGTTCCTCACCACC-3’

Il-1β gRNA	Forward	5’-GAGATCAGCGGGTCTCTGG-3’
	Reverse	5’-GATGCGCACTTTATCCTGCAG-3’
TNF-α gRNA	Forward	5’-ACCAGGCCTTTTCTTCAGGT-3’
	Reverse	5’-AGCGGATTGCACTGAAAAGT-3’
Il-1β MO (Nguyen-Chi et al. 2014)	Forward	5’-TGCCGGTCTCCTTCCTGA-3’
	Reverse	5’-GCAGAGGAACTTAACCAGCT-3’
mmp2	Forward	5’-TGGCCGAAATGAACATGGTG-3’
	Reverse	5’-GGAACCCATCATCTCGACCC-3’
mmp9	Forward	5’-TACGGTAATGCTGAGGGTGC-3’
	Reverse	5’-GCCGTATCTCTGTTAGGGCA-3’
mmp11a	Forward	5’-CGCGAGATGCTTGCCTTTAC-3’
	Reverse	5’-AGCGCTGGATTTTGTAGGTGA-3’
mmp11b	Forward	5’-GCAGAGAGACGACCCACATT-3’
	Reverse	5’-ACCCAGTAATTCTGGCCTTGG-3’
mmp13a	Forward	5’-GCCAACAACCAGGTTTACAGTTAT-3’
	Reverse	5-TCTTCAGGCGGTAAGTATTAAAGAA-3’
mmp13b	Forward	5’-GCTCACGAGTTTGGTCATGC-3’
	Reverse	5’-CAGCCTCCAGTAAAACCTGTCT-3’
mmp14a	Forward	5’-TGAGTGAGGATGGAGCCAATG-3’
	Reverse	5’-GCGGTGACAGTAGAGTAGGC-3’
mmp14b	Forward	5’-AACGTCTGTATTCTCCCGCT-3’
	Reverse	5’-AGCCATGCCTCAGGTTTCAT-3’
mmp15a	Forward	5’-TTCAATGCGGAGTCTTGGCT-3’
	Reverse	5’-CTTTGGGCGAGTGGTTTTGG-3’
mmp15b	Forward	5’-AAAATCAGACTGGAGGTGGCA-3’
	Reverse	5’-TTGTTAGCAGATGACGGCGA-3’
mmp16a	Forward	5’-TGGACAACGAAACCAGCACT-3’
	Reverse	5’-AGAGCATAAACGCACCCCTC-3’

mmp16b	Forward	5’-GTGAGAGAACGGCAGGTAATG-3’
	Reverse	5’-GAATCCTCCGTCGCAGATGT-3’
mmp17a	Forward	5’-ATCTTTCCTGGAGGGTGAGGA-3’
	Reverse	5’-TGCAAACAGGTCCATCCCAT-3’
mmp17b	Forward	5’-CGGTCTGTAATGCGTCCGTA-3’
	Reverse	5’-ACATGCTCTGGCCTTTGAAGA-3’
mmp19	Forward	5’-TGTCGCACAACTAGGGTTTCA-3’
	Reverse	5’-AGCAGTGCCGAAGTGAATCT-3’
mmp20a	Forward	5’-CGCAACGAGTGGCATATGTT-3’
	Reverse	5’-TGAACGCGTCCATTGAGTTC-3’
mmp20b	Forward	5’-’ATTCCCATCAGGCGGACATC-3’
	Reverse	5’-GTCTCTTGGCCCGTAGAGC-3’
mmp23bb	Forward	5’-GCTCATGAAATCGGTCACGC-3’
	Reverse	5’-CTGCATCCAGAGGCTCGTAG-3’
mmp24	Forward	5’-CATGACGGCAATGACCTGTTC-3’
	Reverse	5’-GAGACTGACGCTCGTGTTTG-3’
mmp28	Forward	5’-TGCTATCAGAGAGTTTCAGTGGTT-3’
	Reverse	5’-CCTGACTGGTAGAAAGGCTCC-3’
mmp30	Forward	5’-GGTGTTCTGGCTCATGCAAA-3’
	Reverse	5’-TCGAACACCGTACAAAGCCT-3’

2.2.2 RNA preparation

RNA from the desired tissue (lesion site of larvae), was extracted using the RNeasy Mini Kit (Qiagen), according to manufacturer’s protocol.

Procedure

1. Disrupt the tissue and homogenize the lysate in 350 µl of Buffer RLT. Centrifuge the lysate for 3 min at maximum speed.

Carefully remove the supernatant by pipetting and use it in step 2.

2. Add 1 volume of 70% ethanol to the lysate and mix well by pipetting. Do not centrifuge. Proceed immediately to step 3.
3. Transfer up to 700 µl of the sample, including any precipitate, to an RNeasy Mini spin column placed in a 2 ml collection tube. Close the lid, and centrifuge for 15 sec at ≥8000 x g. Discard the flow-through.
4. Add 700 µl Buffer RW1 to the RNeasy spin column. Close the lid, and centrifuge for 15 sec at ≥8000 x g. Discard the flow-through.
5. Add 500 µl Buffer RPE to the RNeasy spin column. Close the lid, and centrifuge for 15 sec at ≥8000 x g. Discard the flow-through.
6. Add 500 µl Buffer RPE to the RNeasy spin column. Close the lid, and centrifuge for 2 min at ≥8000 x g.
7. Place the RNeasy spin column in a new 1.5 ml collection tube (supplied). Add 30 µl RNase-free water directly to the spin column membrane. Close the lid, and centrifuge for 1 min at ≥8000 x g to elute the RNA.
8. Check the quality by running a small amount on a gel. Intact total RNA run on a denaturing gel will have sharp, clear 28S and 18S rRNA bands.
9. The RNA was stored at-80°C.

2.2.3 cDNA preparation

cDNA was prepared using the iScript^{TM} cDNA synthesis kit (BIO-RAD). 500 ng of RNA was mixed with 4 µl 5xiScript Reaction Mix and 1µl of iScript Reverse Transcriptase. Total volume up to 20µl was filled with Nuclease-free water. The samples were placed in thermal cycler and incubated using the following protocol: Priming – 5min at 25^{o}C, Reverse transcription – 20 min at 46^{o}C, RT inactivation -1 min at 95^{o}C. The cDNA was stored at -20°C.

2.2.4 Polymerase Chain Reaction (PCR)

TAG DNA Polymerase (NEB) was used for PCR. Master mix was made according to the manufacturer's instructions. The annealing temperature was calculated based on the melting temperature (Tm) of the primer. The cycler was set to the following values:

- Initial denaturation: 3 min
- Denaturation: 30 sec, 95 ^{O}C
- Annealing: 30 sec, 58 ^{O}C
- 35 cycles
- Extension: 15 - 40 sec, 72 ^{O}C
- Final extension: 10 min, 72 ^{O}C
- Hold: forever, 4 ^{O}C

2.2.5 Reverse transcriptase PCR and quantitative RT-PCR

Standard RT-PCR was performed using 10mM of each dNTP and each primer. qRT-PCR was performed at 58 °C using Roche Light Cycler 96 and relative mRNA levels determined using the Roche Light Cycler 96 SW1 software. Samples were run in duplicates and expression levels were normalized to β-actin control.

2.2.6 Gel electrophoresis and purification

The PCR products were run on 2% agarose gel in TAE buffer with 0.005% GelRed. For the *in situ* probe generation, the bands of appropriate size were cut out of the gel under UV light and subsequently extracted using the QIAquick® Gel Extraction Kit (Qiagen) according to manufacturer's instructions.

2.2.7 Ligation into vector and transformation into bacteria

The ligation into pGEM-T Easy vectors (Promega) was performed according to the manufacturer's protocol (Promega). The vectors were transformed into NEB5'-'alpha competent cells (NEB). The cells were initially pre-incubated with the vectors for 20 min on ice, heat-shocked at 42^{O}C for 50s, and incubated on ice for further 5 min. After adding 950µl SOC medium, the cells were incubated for 1 hour on orbital shaker at 37^{O}C and 250rpm. 100µl bacterial colonies were plated on restrictive LB Agar plates containing 100µg/ml ampicillin and grown overnight at 37^{O}C. Before plating the bacteria, the plates were freshly coated with 20ul 50mg/ml (X-Gal, Sigma) allowing the selection of colonies based on the blue/white selection cassette within the pGEM-T Easy vectors. Bacteria transfected with empty vectors contained a functional lacZ gene, which mediated the conversion of X-Gal into a blue product. The successfully ligated PCR product disrupted the lacZ sequence present within the blue/white selection cassette making the colonies appear white. Single, circular, white colonies were picked using a sterile pipette tip. The selected cultures were grown overnight at 37^{O}C on orbital shaker in 15ml blue cap tubes containing 2ml of the restrictive 2-YT medium containing 100µg/ml ampicillin.

2.2.8 Plasmid isolation and sequencing

The 2ml cultures were used for plasmid purification using QIAGEN Mini-preparation kit (QIAprep Spin Miniprep Kit) according to manufacturer's instructions. All sequencing was performed by Source Bioscience UK. The plasmids containing the inserts of correct sequences were used for the generation of the *in-situ* probes.

Procedure

1. Resuspend pelleted bacterial cells in 250 µl Buffer P1 and transfer to a microcentrifuge tube.
2. Add 250 µl Buffer P2 and mix thoroughly by inverting the tube 4–6 times.
Mix gently by inverting the tube.
3. Add 350 µl Buffer N3. Mix immediately and thoroughly by inverting the tube 4–6 times.
4. Centrifuge for 10 min at 13,000 rpm (~17,900 x g) in a table-top microcentrifuge.
5. Apply 800 µl of the supernatant from step 4 to the QIAprep 2.0 spin column by pipetting.
6. Centrifuge for 30–60 s. Discard the flow-through.
7. Wash QIAprep 2.0 spin column by adding 0.75 ml Buffer PE and centrifuging for 30–60 s.
8. Discard the flow-through, and centrifuge at full speed for an additional 1 min to remove residual wash buffer.
9. Place the QIAprep 2.0 column in a clean 1.5 ml microcentrifuge tube. To elute DNA, add 50 µl Buffer EB (10 mM Tris·Cl, pH 8.5) or water to the center of each QIAprep 2.0 spin column, let stand for 1 min and centrifuge for 1 min.

2.2.9 Restriction and probe synthesis

The plasmid was cut upstream of the insert using appropriate NEB enzymes and buffers and a polymerase downstream was used for the transcription reaction to prepare the anti-sense probe. The success of the digestion was assessed using agarose gel. The linearized DNA was precipitated overnight at -20°C with 0.3M Sodium Acetate, and two volumes of 100% ethanol. The *in vitro* transcription of the RNA probe was done using MAXIScript® Kit (Ambion), according to manufacturer's instructions. 1µg of linearized plasmid DNA was used for the reaction setup. For the generation of labelled *in situ* probes, the DIG RNA Labeling

Mix (Roche) was used. The probes were purified by precipitation with 2.5 volumes of 100% ethanol and 0.1 volumes of 8M Lithium Chloride for at least 1 hour. The reactions were centrifuged at 13000 rpm at 4°C for 45 min, washed with 70% ethanol, centrifuged again for 15 min (13000 rpm, 4°C), air dried and resuspended in 20µl RNase-free water. In order to verify the probe synthesis and test the integrity, 1µl of the transcription reaction was loaded on an agarose gel.

2.2.10 CRISPR-mediated genome editing

CRISPR gRNA for *il-1beta* was designed using CRISPR Design (http://crispr.mit.edu) and ZiFit (http://zifit.partners.org/ZiFiT) webtools. Vectors were made by ligating the annealed oligonucleotides into pT7-gRNA expression vector as previously described (Wehner et al. 2018) ENREF 36. The gRNA was transcribed using the mMESSAGE mMACHINE T7 kit (Ambion) and assessed for size and quality on an electrophoresis gel.

The injection mix consisted of 75 pg *il-1beta* gRNA (target sequence: 5'-TGTGGAGCGGAGCCTTCGGCGGG-3') and 150pg Cas9 RNA and was injected into single cell stage larvae. The gRNA for the *TNF-αlpha* (target sequence: 5'-CCCGATGATGGCATTTATTTTGT-3') and the generic crRNAs/tracrRNA were ordered from (Merck KGaA, Darmstadt). The injection mix included 1µl Tracer 250 ng /µl, 1 µl gRNA, 1µl Cas9 protein, 1µl RNAse free H20, 1µl fluorescent dextran. Larvae injected with GFP gRNA (target sequence: 5'GGCGAGGGCGATGCCACCTA-3') and uninjected larvae were used as controls. The efficiency of the mutagenesis was assessed by Restriction Fragment Length Polymorphism (RFLP) analysis. The basic technique for the detection of RFLPs involves fragmenting a sample of DNA with the application of a restriction enzyme, which can selectively cleave a DNA molecule wherever a short, specific sequence is recognized in a process known as a restriction digest. The DNA fragments produced by the digest are then separated by length through a process known as agarose gel electrophoresis and transferred to a membrane via the Southern blot procedure. Hybridization of the membrane

to a labeled DNA probe then determines the length of the fragments which are complementary to the probe. A restriction fragment length polymorphism is said to occur when the length of a detected fragment varies between individuals, indicating non-identical sequence homologies. Each fragment length is considered an allele, whether it actually contains a coding region or not, and can be used in subsequent genetic analysis.

2.2.11 Morpholino injection

All morpholinos were injected into single cell stage larvae in total volume of 2 nl. Knockdown of *Il-1β* was carried out using the antisense morpholino *Il-1β* (5'-CCCACAAACTGCAAAATATCAGCTT-3') targeting the splice site between intron 2 and exon 3 according to (Nguyen-Chi et al. 2014). In order to block neutrophil development, we used the previously described MO combination (Feng et al. 2012) of *pu.1* (5'-GATATACTGATACTCCATTGGTGGT-3')(Rhodes et al. 2005) which targets the translational start (ATG) of the pu.1 and the splice blocking MO against *gcsfr* (5'- TTTGTCTTTACAGATCCGCCAGTTC-3') (Halloum et al. 2016) . All morpholinos and standard control (5'-CCTCTTACCTCAGTTACAATTTATA-3') were obtained from Gene Tools, LLC.

2.2.12 Fluorescence-activated cell sorting

Macrophages and microglia were isolated from 4 dpf transgenic mpeg1:eGFP embryos by FACS. For this purpose, about 500 fish were lesioned by transecting the spinal cord. Trunk-containing lesion site were dissected and collected at 24 hpl and used for cell dissociation. Cells purified after FACS were used for qRT-PCR.

2.3 Histology

2.3.1 In situ hybridisation (ISH) on whole mount larvae

The larvae were fixed overnight at 4 °C in 4% PFA-PBS. On the following day, larvae were washed twice in PBT (0.1% Tween-20 in PBS) and incubated for 30 min in PBT containing 40 µg/ml Proteinase K (Invitrogen). Thereafter, larvae were washed briefly in PBT and were refixed for 20 min in 4% PFA-PBS followed by five washes in PBT for 5 min each. After washes, larvae were incubated at 67 °C for 2h in pre-warmed hybridization buffer (5x SSC, 500 µg/ml type VI Torula yeast RNA, 50 µg/ml Heparin, 0.1% Tween 20, 9mM citric acid, 50% formamide, pH 6.0). Hybridization buffer was replaced with digoxigenin (DIG) labelled ISH probes diluted in hybridization buffer and incubated at 67 °C overnight. The next day, larvae were washed at 67 °C twice in hybridization buffer, three times in 50% 2×SSCT/50% deionized formamide, and three times in 2xSSCT for 20 min each, followed by four washes at 67 °C in 0.2x SSCT (20x SSC: 300mM NaCl, 200mM Na-Citrate, pH 7; SSCT: 0.1 % Tween 20 in 1xSSC) for 30 min each. Larvae were then washed in PBT and incubated for 1 h in blocking buffer (5% heat-inactivated sheep serum, 10 mg/ml BSA in PBT) under slow agitation. Thereafter, larvae were incubated overnight at 4 °C in blocking buffer containing pre-absorbed anti-DIG antibody coupled to alkaline phosphatase (1:3000–4000). The next day, larvae were washed five times in PBT for 20 min each, followed by three washes in staining buffer (50mMMgCl_2, 100mMNaCl, 100mM Tris-HCl, 0.1% Tween 20, pH 9.5) for 5 min each. Color reaction was performed by incubating larvae in staining buffer supplemented with NBT/BCIP (Sigma-Aldrich) substrate. The staining reaction was terminated by washing larvae in PBT. For chromogenic ISH, background staining was cleared by incubating larvae two times in 100% EtOH for 15 min each, followed by five washes in PBT for 5 min each.

2.3.2 Immunohistochemistry (IHC) on whole mount larvae

All incubations were performed at room temperature unless stated otherwise. For most immunolabelling experiments, the larvae were fixed in 4% PFA-PBS containing 1% DMSO at 4°C overnight. After washes in PBS, larvae were washed in PBTx. After permeabilization by incubation in PBS containing 2 mg/ml Collagenase (Sigma) for 25 min larvae were washed in PBTx. They were then incubated in blocking buffer for 2 h and incubated with primary antibody (1:50–1:500) diluted in blocking buffer at 4°C overnight. On the following day, larvae were washed times in PBTx, followed by incubation with secondary antibody diluted in blocking buffer (1:300) at 4°C overnight. The next day, larvae were washed three times in PBTx and once in PBS for 15 min each, before mounting in glycerol.

For whole mount immunostaining using primary antibodies from the same host species (rabbit anti-Il-1b, rabbit anti-Mpx, rabbit anti-Tp63) after fixation the samples were initially incubated with the first primary antibody at 4^{o}C overnight. After washes with PBTx the samples were incubated with the conjugated first secondary antibody overnight at 4^{o}C. Subsequently samples were incubated with blocking buffer for 1 h at RT in order to saturate open binding sites of the first primary antibody. Next, the samples were incubated with unconjugated Fab antibody against the host species of the primary antibody in order to cover the IgG sites of the first primary antibody, so that the second secondary antibody will not bind to it. After this, samples were incubated with the second primary antibody overnight at 4oC and subsequently with the second conjugated secondary antibody overnight at 4oC before mounting in glycerol. No signal was detected when the second primary antibody was omitted, indicating specificity of the consecutive immunolabeling protocol.

For whole mount immunostaining of acetylated tubulin, the protocol was performed as previously described 1. Briefly, larvae were fixed in 4% PFA for 1 h and then were dehydrated and transferred to 100% MeOH and then stored at 20°C

overnight. The next day head and tail were removed, and the samples were incubated in pre-chilled Acetone. Thereafter larvae were washed and digested with Proteinase K and re-fixed in 4% PFA. After washes the larvae were incubated with BSA in PBTx for 1 h. Subsequently the larvae were incubated for 2 overnights with primary antibody (acetylated tubulin). After washes and incubation with the secondary antibody the samples were washed in PBS for 15 min each, before mounting in glycerol.

2.3.3 Evaluation of cell death using Acridine orange

In order to assess the levels of cell death after injury I used the acridine orange live staining. At 1day and two days post lesion the larvae were incubated in 2.5µg/ml solution of dye diluted into conditioned water for 20 minutes. After the staining, the larvae were washed by changing the water and live mounted for imaging.

2.3.4 Identification of dying cells after injury

In order to assess the levels of cell death after injury and identify the type of cells that are dying after the injury whole mount larvae and cross sections of larvae were used. Larvae were fixed in 4% PFA overnight at 4oC. After washes with PBSTx 0,5%, the larvae were transferred to 100% Methanol and incubated for 10 min at room temperature. After rehydration, the larvae were washed with PBSTx 0,5%. The larvae were then permeabilized using 14µg/ml diluted in 0,5%PBSTx. After brief wash with PBSTx the larvae were postfixed for 20min in 4%PFA. Excess of PFA was washed out and the larvae were incubated with the TUNEL reaction mix according to In Situ Cell Death Detection Kit TMR red protocol. Following this the larvae were processed for Immunofluorescence. After washes, larvae were then incubated in blocking buffer (0.7% PBTx, 1% DMSO, 1% normal donkey serum, 1% BSA) for 2 h,

and incubated with primary antibody (1:50–1:300) diluted in blocking buffer at 4 °C overnight. On the following day, larvae were washed 5 times in PBTx, followed by incubation with secondary antibody diluted in blocking buffer (1:300) at 4 °C overnight. The next day, larvae were washed three times in PBTx and once in PBS for 15 min each, before mounting in 70% Glycerol-PBS.

2.3.5 EdU detection

For the detection of EdU in larvae, the IHC protocol was modified as follows: After washing the tissue with PBSTx and PBS washes, the larvae were permeabilized by incubation in PBS containing 2 mg/ml Collagenase (Sigma) for 25 min after washes with PBSTx larvae were incubated for 2.5 hours in the Click-iT™ reaction cocktail (Invitrogen) at room temperature with gentle agitation, protected from light. The reaction cocktail was removed with several PBS washes, and the larvae cleared with 70% glycerol in PBS. The components of the reaction cocktail, previously optimized for the use in either larvae or the adult tissue, are listed in the table below:

Reaction components	**Whole-mount embryo**
10 x Click-iT™ reaction buffer	10.75 µl
H_2O	233 µl
$CuSO_4$	5 µl
Alexa Fluor azide 647	0.25 µl
Reaction buffer additive	1.25 µl
Total volume	**250 µl**

2.3.6 EdU detection/HB9 IHC

For the detection of newborn motor neurons the larvae were washed with PBSTx and PBS washes followed by permeabilization by incubation in PBS containing 2 mg/ml Collagenase (Sigma) for 25 min. After washes with PBSTx larvae were incubated for 2.5 hours in the Click-iT™ reaction cocktail (Invitrogen) at room temperature with gentle agitation, protected from light. The reaction cocktail was removed with several PBS washes, and the larvae were washed with PBStx 0.5%, 3x 10 min each.

After this, the larvae were incubated into 10mM citric acid, pH=6 at 110 ^{o}C 10min using a pressure cooker for antigen retrieval. Samples were then washed once with PBStx and transferred to blocking buffer (1% NDS, 1% DMSO, 1% BSA, 0.7% Triton X-100) for 1 hour at room temperature under slow agitation. After this the larvae were incubated with mouse anti-HB9 1:200 at 4 ^{o}C for 2 nights. The primary antibody was removed by washing the samples with PBStx and then they were incubated with secondary antibody overnight at 4^{o}C. Following this the larvae were washed with PBStx once in PBS for 15 min each, before mounting in 70% Glycerol-PBS.

2.4 Quantification and data analysis

2.4.1 Live imaging of zebrafish larvae and time-lapse imaging

For the acquisition of all fluorescent images, LSM 710 and LSM 880 confocal microscopes were used. For live confocal imaging, zebrafish larvae were anesthetized in PBS containing 0.02% MS222 and mounted in 1.5% low melting point agarose (Ultra-PureTM, Invitrogen). During imaging, the larvae were covered with 0.01% MS222-containing fish water to keep preparations from drying out. For time-lapse imaging, agarose covering the lesion site was gently removed after gelation. Time-lapse imaging

was performed for 19 h starting at 6 hpl. Acquired time-lapse images were denoised using the ImageJ plugin CANDLE-J algorithm, which allows to remove the noise compartment while preserving the structural information with high fidelity (Coupe et al. 2012). Comparison of raw movies with CANDLE-J-processed movies, showed that edges of features remained conserved after denoising.

2.4.2 Assessment of spinal cord bridging

Re-established axonal or glial connections (bridges) were scored in static preparations (fixed immunolabelled samples, live transgenic animals) or in still images of time-lapse movies at time points of interest. Larvae were directly visually evaluated using confocal imaging (Zeiss LSM 710, 880). A larva was scored as having a bridged lesion site when continuity of the neuronal or glial labeling between the rostral and caudal part of the spinal cord was observed. Continuity of labeling was defined as at least one fascicle being continuous between rostral and caudal spinal cord ends irrespective of the fascicle thickness. Larvae in which the lesion site was obscured by melanocytes were excluded from analysis. Quantification of axonal and glial fascicle composition in static preparations at 1 dpl it was performed after confocal imaging (Zeiss LSM 880) of immunolabeled or live animals. Fascicles were identified as fluorescent protrusions from the severed spinal cord that projected into the injury site for at least 20 µm or had crossed it completely. This was done by inspecting single optical sections and 3D renderings of the lesion site. If more than half of the length of a fascicle contained fluorescence for both glial and neuronal markers it was scored as “mixed”, otherwise it was scored as purely “axonal” or “glial” depending on the markers used. The threshold of half the length was used to exclude situations in which one type of process followed the other long after that one was established. For quantification of axonal and glial fascicle composition in time-lapse movies we included only fascicles that grew during the observation period. Fascicles were classified as purely “axonal” or “glial” when the distal part of a given fascicle was labelled by the respective marker throughout the entire observation period. In “mixed” fascicles, both markers were present in the distal portion

of the fascicle. In some cases, the thickness of the axonal bridge was measured in collapsed confocal image stacks, by determining the length of (a) vertical line(s) that covers the width of crossing fascicles at the center of the injury site. For all quantifications, I was blinded to the experimental treatments. Before starting the experiment, a member of the lab was blinding the groups for me by remaining them using numbers and after I was done with the quantifications the groups were unblinded.

2.4.3 3D cell counting

A volume of interest was defined centered on the lesion site from confocal images. The dimensions were: width = 200 µm, height = 75 µm (above the notochord), depth = 50 µm. Images were analysed using the Imaris (Bitplane, Belfast, UK) or the ImageJ software. The number of cells was quantified manually in 3D view, blinded to the experimental condition on at least three independent clutches of larvae.

2.4.4 Quantification of diffused signal in whole mount larvae

For most quantifications of diffuse signal, image stacks, centered in the lesion site (height: 50 µm) were collapsed and an area of interest defined: width = 100 µm, height = 50 µm (above the notochord). The image was thresholded and the ''Analyze Particles'' tool in Fiji (Schindelin et al. 2012) with default settings was used to calculate the percentage of area taken up by signal. To quantify Col I in the injury site we used a previously published protocol (Wehner et al. 2017). All analyses were performed blinded to the experimental condition on at least three independent clutches of larvae.

2.4.5 Image acquisition and analysis

For the acquisition of all fluorescent images, Zeiss LSM 710 and Zeiss LSM 880 confocal microscopes operated by Zeiss Zen 2011 software were used. Image analysis was performed using ImageJ (http://imagej.nih.gov/ij). Power analysis using G*Power (Faul et al. 2009), was used to calculate power (aim > 0.8) for the experiments and determine the group sizes accordingly. Statistical power was > 0.8 for all experiments. All quantitative data were tested for normality and analyzed with parametric and non-parametric tests as appropriate. The statistical analysis was performed using IBM SPSS Statistics 23.0. Shapiro-Wilk's W-test was used in order to assess the normality of the data. Quantitative RT-PCR data were analyzed as previously described (Livak and Schmittgen 2001, Ganger et al. 2017). Kruskal-Wallis test followed by Dunn's multiple comparisons, One-way ANOVA followed by Bonferroni multiple comparisons test, two-way ANOVA, followed by Bonferroni multiple comparisons, t-test, Mann–Whitney U test or Fischer's exact test were used, as indicated in the Figure legends. *P< 0.05, **P< 0.01, ***P< 0.001, n.s. indicates no significance. Error bars indicate the standard error of the mean (SEM). The Figures were prepared with Adobe Photoshop CC and Adobe Illustrator CC. Graphs were generated using GraphPad Prism 7.

Chapter 3: Regeneration of zebrafish motor neurons

Ohnmacht, J., Yang, Y., Maurer, G. W., Barreiro-Iglesias, A., **Tsarouchas, T. M**., Wehner, D., Sieger, D., Becker, C. G., Becker, T. (2016). **Spinal motor neurons are regenerated after mechanical lesion and genetic ablation in larval zebrafish**. Development. 2016 May 1;143(9):1464-74. doi: 10.1242/dev.129155.

Contribution: Assessing the role of the immune system during regeneration of the motor neurons after spinal cord injury using dexamethasone (Figure 5).

3.1 INTRODUCTION

In this chapter I assessed the role of the innate immune response to the regeneration of the motor neurons after injury. This part of my thesis has already been published with me as a contributing author (Ohnmacht et al., 2016). The purpose of this study was to establish a larval regeneration paradigm and assess the plasticity of the spinal progenitors after injury and whether these cells react to signals from the environment similar to those during regeneration in the adult model. It has been shown from (Kyritsis et al. 2012) that the microglial response is essential for neuronal regeneration after stab injury of the adult zebrafish telencephalon. Furthermore, the inflammatory response is one of the key events that occur after injury in different models and it's diverse role in each case has been mentioned by different studies. Therefore, I wanted to assess the role of the immune response in the larval SCI injury context and used pharmacological and genetic approaches. What I found is that motor neuron regeneration is inhibited after manipulation of the immune response, suggesting that direct or indirect signalling from the innate immune cells to the progenitor cells occurs and is important for regeneration after injury.

3.1.1 Zebrafish as a model to study neuroregeneration.

In contrast to mammals, fish and amphibians are characterized by high regenerative potential of their CNS after injury. In the lesioned spinal cord of salamander, ependymal cells migrate to the lesion site and contribute to the production of new neurons. These animals can also regenerate their severed axons and establish new functional connections which contributes to successful spinal cord repair (Tazaki et al. 2017). Amphibians such as frogs are also capable of regenerating their injured spinal cord, however, this regenerative capacity lasts only until the metamorphosis stage (Beattie et al. 1990). Regeneration of spinal cord has also been described in birds but their regenerative ability declines during development (Shimizu et al. 1990).

Until recently there has been a dogma that adult neurogenesis occurs in distinct proliferative zone in the mammalian brain. It has been demonstrated that there are some populations of neural stem cells that have the ability to self-renew and differentiate in the adult mammalian brain (Reynolds and Weiss 1992). For example, in rodents it has been observed that new neurons are generated throughout adulthood (Lois and Alvarez-Buylla 1994). However, the regenerative capacity of mammals is limited (Gage and Temple 2013) and a recent study suggests that hippocampal neurogenesis drops to undetectable levels in humans after childhood (Sorrells et al. 2018).

In order to explain the difference in neurogenic capability between organisms such as mammals and teleosts, such as the zebrafish, it has been suggested that this difference is due to the number of proliferative zones present in the CNS (Grandel et al. 2006). The number of proliferative zones in mammals has been proposed to be reduced across evolution (Tanaka and Ferretti 2009). Another theory suggests that the reduction in neurogenic capacity in the mammalian CNS might also be because their brains stop growing in size during adult stages. In other animals, like zebrafish, which have a higher neurogenic capacity, growth of the brain is life-long and may therefore exhibit higher levels of proliferation (Grandel et al. 2006). Several studies have shown that zebrafish as well as other members of the teleost family have an extensive network of proliferative zones in the adult brain including in the olfactory bulb, telencephalon, diencephalon and mesencephalon (Grandel et al. 2006). It has also been shown that apart from adult neurogenesis there is also differentiation into different types of neurons as dopaminergic neurons and serotonergic neurons which are incorporated into areas such as the olfactory bulb and diencephalon in adult stages (Grandel et al. 2006). This evidence of constitutive neurogenesis makes the zebrafish an attractive model to study the mechanisms underlying adult neurogenesis which is very restricted in the mammalian models. The neurogenic regions of the mammalian CNS have been localised to the dentate gyrus of the hippocampus in the subgranular zone and the lateral ventricles of the forebrain in the subventicular zone (Gross 2000, Alvarez-Buylla and García-Verdugo 2002).

In zebrafish, after CNS injury, cells contained in proliferative zones are triggered and carry out neurogenesis (Ghosh and Hui 2016). However, there are different factors that affect the survival of the newly formed neurons, for example the lack of functional integration into the system. Other factors may also influence the survival of newly generated neurons such as the formation of glial scars and a non-favourable extracellular environment for growth of axons (Ming and Song 2005). In the mammalian brain, parenchymal astrocytes after activation following injury, are recruited to the injury site. These activated astrocytes then form a glial scar which is known to be impermeable to axon growth (Rolls et al. 2009).

Unlike mammals, zebrafish do not form glial scars following CNS injury. Instead they demonstrate recovery of tissue integrity without scarring, such as in the spinal cord and brain (Becker and Becker 2007, Reimer et al. 2008, Kizil et al. 2011). This suggests that the zebrafish brain maintains a more permissive environment following injury for the recovery of neurons and their axons to re-establish brain architecture. This regenerative quality is independent on the type of injury, as recovery is observed following a plethora of lesions such as spinal cord injuries (Becker et al. 1997, Wehner et al. 2018), injury in the telecephalon (Kyritsis et al. 2012), and the retina(Rao et al. 2017) or optic nerve transection (Diekmann et al. 2015, Van houcke et al. 2017). Assessment of regeneration and its functional results can be achieved in that model through genetic techniques including the use of reporter lines as well as established behavioural and electrophysiological testing (Becker et al. 2004, Ohnmacht et al. 2016, Moreno et al. 2017, Wehner et al. 2017). Although proliferative zones are more numerous in the zebrafish compared to mammals, the underlying processes of neurogenesis are believed to be similar. Neurogenesis within the zebrafish brain occurs in subventricular proliferative zones arising from radial glia-type progenitors and then the newly generated neurons migrate to their intended destinations (Kroehne et al. 2011). In the zebrafish these cells are referred to as ependymoradial glia cells (ERGs) due to their soma being located on the ependymal lining of the ventricle and their characteristic radial processes that contact the pial surface and believed to be the stem cells within the zebrafish CNS responsible for the

regenerative capacity of zebrafish (Becker and Becker 2015). Following an injury to the brain proliferation of ERGs could be activated in two ways; either directly due to the injury causing disruption to the radial processes of the ERGs, or indirectly via chemical signals such as glutamate and ATP leading to calcium release by surrounding tissues (Sieger et al. 2012, Franze et al. 2013).

CNS injuries also lead to the activation of the immune system which leads to the recruitment of CNS immune cells such as microglia. This immune response is believed to be a crucial component of regeneration as illustrated by studies in which this immune response is inhibited, leading to less neuronal regeneration (Kizil et al. 2012). (Kyritsis et al. 2012) showed that a microglia reaction following injury increases the amount of proliferation and tissue repair in the zebrafish. Therefore, factors released by microglia have been suggested as promotors of neurogenesis. Evidence for this hypothesis comes from experiments in which a signalling molecule, believed to be released by microglia - leukotriene C4, was shown to promote neurogenesis in a non-injured context (Kyritsis et al. 2012). However, the role of inflammation during CNS injury is still unclear.

One main reason for this relative lack of knowledge of the role of inflammation in CNS is the complexity of the system. The majority of injury models are characterised by an interaction between innate and adaptive immunity. Therefore, it is very difficult to characterise the contribution of either the innate or the adaptive immune response alone during injury. Several studies mention the role of innate immunity (Kyritsis et al. 2012, McMurran et al. 2016) and adaptive immunity (Kipnis 2016) during CNS regeneration. Zebrafish larvae offer the advantage that we can selectively study the contribution of the two arms of immunity due to the time difference between their development and maturation (Meijer and Spaink 2011). Additionally, it has been shown that motor neuron regeneration can be studied in larvae after CNS injury (Ohnmacht et al. 2016). Injury in the larval spinal cord leads to increased proliferation of larval progenitor cells in the neuron progenitor domain (pMN). This feature makes zebrafish larvae an excellent model to study the regenerative events that occur CNS after injury combined with the inflammatory response.

3.1.2 The Inflammatory response in zebrafish larvae

Teleosts, like mammals, are equipped with defence mechanisms against pathogens. These include production of molecules like cytokines and chemokines and specialised cells like neutrophils and macrophages that are responsible for maintaining homeostasis. The cellular machinery of the teleosts has been described by Traver et al.,2003 (Traver et al. 2003). Signaling pathways that are well studied in mammals and include activation of NF-κB, TLRs and TIR are conserved in fish (Oshiumi et al. 2003, Oshiumi et al. 2003) in general and more specifically in zebrafish (Jault et al. 2004). Adaptive immunity is also conserved in zebrafish. However, although the development of the thymus initiates early in zebrafish, with the thymic rudiment to be formed by 60 hours post fertilization (hpf), there is no clear distinction between cortex and medulla derived from the interaction between T cell precursors and thymic epithelial cells until 3-4 weeks of age (Lam et al. 2002). Conversely, in mice this process is completed shortly after birth (Ritter 1978). This allows a temporal separation of innate and adaptive immunity in zebrafish studies which is not possible in mammals.

Zebrafish transparency and the ease of manipulation of its genome has allowed the development of transgenic lines that can be used for in vivo monitoring of leukocyte recruitment towards the injury or infection site over time. The first cells responding to the insult are the neutrophils which migrate into the wound, initiating the inflammatory response. They phagocytose debris and produce molecules like cytokines, chemokines and ROS that attract other cells like macrophages to the injury site. Over time the number of neutrophils decreases, and macrophages become the main cell type at the insult site. They phagocytose larger debris, resolve the inflammatory response and regulate tissue repair. The inflammatory response in zebrafish recapitulates what is known in mammals regarding the progression of inflammatory response after injury.

In order to assess the role of the inflammatory response for the regeneration of motor neurons after injury I used the larval injury model that has been established in

the Becker group (Ohnmacht et al. 2016) and quantified the inflammatory response and the regeneration of motor neurons two days post injury with or without manipulation of the immune response. The tools that were used to manipulate the immune response were pharmacological inhibition using dexamethasone and the *irf8* mutant line that lacks macrophages and microglia during the early stages of development (Shiau et al. 2015) These animals have a TALEN-mediated mutation that leads to embryos null for the Interferon regulatory factor 8 (*Irf8*) which is critical for mammalian macrophage development and innate immunity. *Irf8* is required for formation of all macrophages during primitive and transient definitive hematopoiesis, but not during adult-phase definitive hematopoiesis. These experiments showed that after injury the number of newborn motor neurons is significantly decreased compared to lesioned age-matched control groups, indicating that inflammatory response is essential for neuronal regeneration similar to what has been previously described in adult zebrafish (Kyritsis et al. 2012).

Therefore, it is essential to understand the immune mediators involved and the mechanisms behind successful regeneration in fish to apply these findings to future therapeutic interventions and treatments in mammals.

3.2 RESULTS

3.2.1 Dexamethasone impairs the migration of immune cells after injury

Reactive immune cells promote neuronal regeneration (Kyritsis et al. 2012) and the larval spinal cord offers the opportunity to study the innate immune system in isolation from the adaptive immune response, which develops only later (Danilova and Steiner 2002, Lam et al. 2004). To determine whether the innate immune system promoted motor neuron generation after a larval lesion, we labelled microglial cells with a 4C4 antibody (Becker and Becker 2001), and all macrophages/microglia and neutrophils with an L-plastin antibody (Feng et al. 2010). At 48 h after the lesion,

labelling of both 4C4 and L-plastin was concentrated in the lesion site (Fig. 3.1.A,B,D). This response was suppressed by incubating the larvae in the immunosuppressant dexamethasone (Kyritsis et al. 2012). In order to find the optimum concentration I performed a dose response using 1 µM, 5 µM, 10 µM, 20 µM 100 µM and 200 µM and found that 100 µM is the optimum concentration that shows an effect in the number of immune cell in the lesion site without impacting the survival of larvae. I also searched the literature and found that the same concentration has also been used by other groups (Meijer et al. 2015, Wilson et al. 2016). This strongly dampened the microglia/macrophage response (Fig. 3.1.C,E,F). This treatment also led to a reduction in the number of newly generated Hb9:GFP+/EdU+ motor neurons by 60% within 48 h of the lesion (3-5 dpf; Fig. 3G-I), suggesting that macrophages/microglial cells exert a positive influence on motor neuron regeneration.

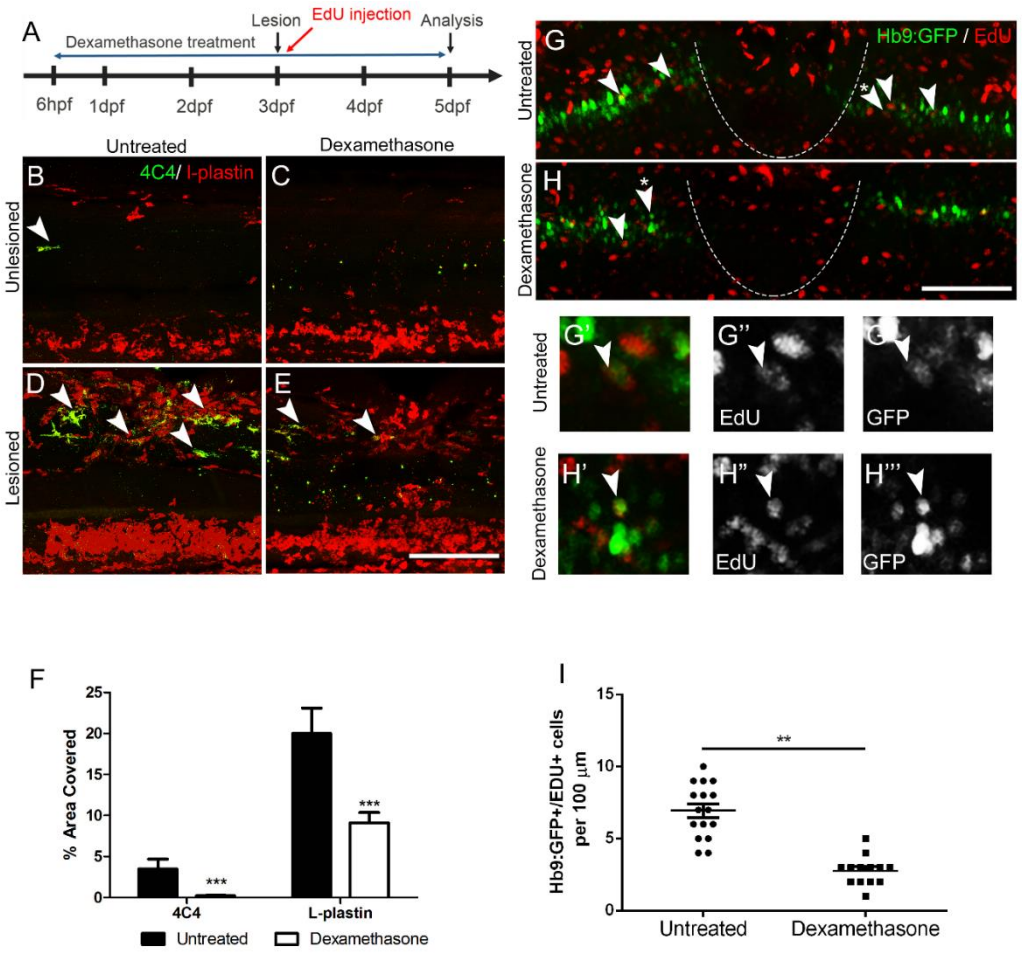

Figure 3.1. Suppression of the immune response inhibits motor neuron regeneration. (A) Time line for the experiments. (B-F) Incubation with dexamethasone does not lead to visible changes in unlesioned larvae (B,C), but strongly reduces the immune reaction at the lesion site (D,E) as indicated by reduced 4C4 (arrowheads indicate 4C4+ cells) and L-plastin immunoreactivity. Quantification of immunoreactivity is shown in F (Student's t-test, ***P<0.001; untreated, n=21; dexamethasone, n=25). (G-I) Dexamethasone treatment reduces the number EdU-labelled Hb9:GFP+ motor neurons (arrowheads). Higher magnifications of double-labelled neurons indicated by asterisks in G,H are shown in single optical sections in G'-H'''. (I) Quantification of the reduction in newly generated motor neurons (t-test; **P=0.0085; unlesioned, n=16; dexamethasone, n=13). Each point on figure relate to each larva used. Lateral views are shown; rostral is left, dorsal is up. The lesion site is indicated by a dashed line. Values are means±s.e.m. Scale bars: 100 µm in E for B-E; 100 µm in H for G,H; 50 µm in H''' for G'-H'''.

3.2.2 Absence of macrophages and microglia leads to decreased number of new-born motor neurons

The use of the *irf8* mutant model (Shiau et al. 2015) allowed to use an extra tool to study the regeneration of the motor neurons in the zebrafish larvae after injury. These animals are characterized by absence of macrophages and microglial cells and increased numbers of neutrophils (see Chapter 5) during the early stages of development. This allowed me to assess the role of the macrophages/microglia during regeneration of the spinal cord after injury. Hb9 immunostaining combined with EdU injections showed that the number of motor neurons after injury was significantly decreased compared to wildtype larvae. This showed that the absence of macrophages and microglia or increased presence of neutrophils in this model has a negative effect in the neuronal regeneration after injury (Figure 3.2).

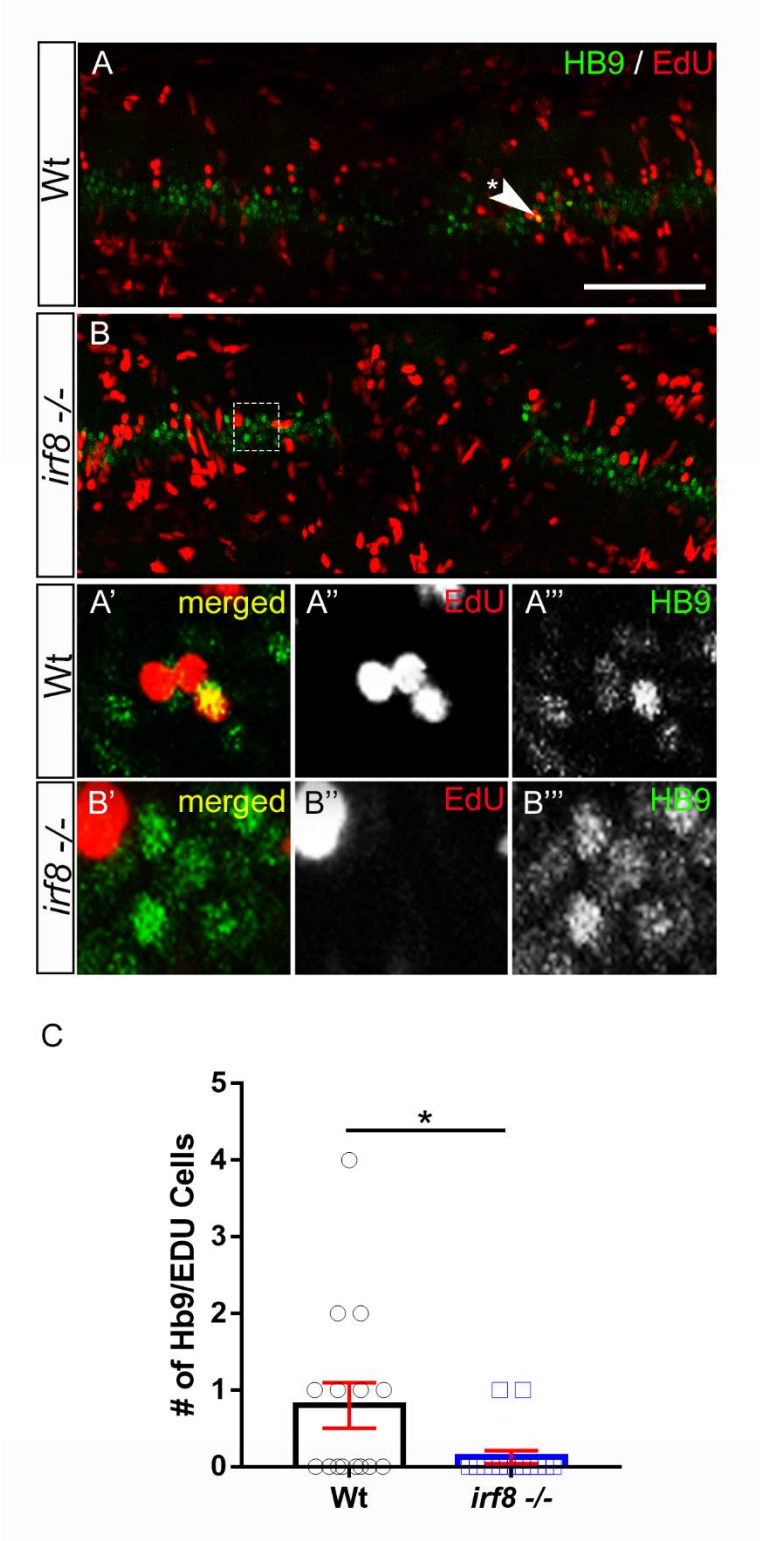

Figure 3.1. Absence of macrophages and microglia leads to decreased neuronal regeneration after spinal cord injury. (A) Wild type spinal cord after injury. (B) Spinal cord of the *irf8*-/- larvae. (A'-B''') Higher magnifications and single channels showing the the co-localization of the Hb9/EdU in wt and *irf8*-/- larvae. Each point on graph relates to each

zebrafish larva used. Quantification of immunoreactivity is shown in C (Student's t-test, *P<0.05). Values are means ±s.e.m. Scale bar: 100 µm.

3.3 Discussion

3.3.1 Microglia/macrophage signaling might contribute to regeneration

Activation of the immune system is one of the key features that is similar to what is happening to adult models after injury. It has been described in previous work of the Becker group that after injury in the adult CNS of the zebrafish there is an increase in the number of microglial cells in the injury site (Becker and Becker 2001). Furthermore, the importance of the microglial response during regeneration has been analysed by Kyritsis et al. (Kyritsis et al. 2012). Here is demonstrated that manipulation of the immune response either using pharmacology or mutant larvae lacking macrophages and microglia leads to impaired motor neuron regeneration after spinal cord injury.

Dexamethasone decreased the recruitment of immune cells to the injury site which subsequently led to decreased motor neuron regeneration. This is in agreement with previous studies, where inhibition of the inflammatory response led to decreased 4C4 and L-plastin immunoreactivity around the injury site, leading eventually to decreased neuronal regeneration (Kyritsis et al. 2012). This may be because immune cells produce molecules that have been shown to support neurogenesis from neural progenitor cells (Ziv and Schwartz 2008). Recruitment and induction of neural stem cells is crucial for the neuronal regeneration. Evidence regarding the involvement of the inflammatory response to neuronal regeneration mention that innate immune cell can act directly on neural progenitor cells or induce the production of growth factors from adjacent endothelial cells through cytokine production. Some of these factors, including TGF-β and SDF-1, induce neuronal progenitor cell proliferation and migration towards the injury site (Merino and Oset-Gasque 2013, Cheng et al. 2017).

Furthermore, neuronal and glial differentiation can be promoted by Notch and BDNF ligands that are produced by macrophages or microglia (Ziv and Schwartz 2008).

Another interesting aspect of the *irf8* mutants that exhibit decreased neuronal regeneration, is the fact that these animals exhibit also increased numbers of neutrophils under naïve conditions (Shiau et al. 2015)but also after injury.

Neutrophils have been shown to be detrimental for regeneration in different tissues. One example is a study from Li et al.,2012 where they highlight the different roles of macrophages and neutrophils during zebrafish tail fin regeneration. More specifically they have found that ablation of macrophages leads to delayed and impaired regeneration whereas ablation of neutrophils results in acceleration of the growth rate after injury (Li et al. 2012). Furthermore, neutrophils contribute to tissue injury by amplifying the inflammatory response by producing ROS and proteolytic enzymes and antimicrobial proteins (Wilgus et al. 2013). A possible explanation in our model for decreased neuronal regeneration could be that the increased number of neutrophils in the injury site creates a hostile environment by amplifying the immune response that occurs. It has been shown that there are multiple feedback amplification mechanisms, like tyrosine kinase signaling after injury which are involved in various neutrophil functions including cellular polarization, neutrophil recruitment, effector responses, and interactions with other immune and non-immune cells (Cheng et al. 2017). Furthermore, recent study on rats showed that inhibition of neutrophils elastase promoted upregulation of angiopoietin-1 which led to decreased glial scar and increased number of neurons after SCI (Kumar et al. 2018).

Questions to be answered in future research on this system: In order to get a better insight of how neuronal regeneration is mediated through inflammatory response the signal to the progenitors from the neutrophils and the macrophages needs to be found. For this, RNA sequencing could be a necessary experiment which will show what signals produced by neutrophils over time after injury. Taken together these

data combined with the results from Ohnmacht et al., 2016 can help to answer the question regarding which immune cell type is needed after injury.

Taken together these data show that after manipulation of the immune response using pharmacology or genetic manipulation, regeneration of the spinal cord is impaired indicating that inflammatory response is essential for regeneration after spinal cord injury, showing that there is a possible direct or indirect signaling from the immune system to the progenitors. Furthermore, this shows that the larval zebrafish SCI model resembles what is known in the adult system where activation of the innate immune response leads to neuronal regeneration (Kyritsis et al. 2012).

Chapter 4: Axonal regeneration in zebrafish larvae after spinal cord injury

Wehner, D., **Tsarouchas, T. M**., Michael, A., Haase, C., Weidinger, G., Reimer, M. M., Becker,T., Becker, C. G. **Wnt signaling controls pro-regenerative Collagen XII in functional spinal cord regeneration in zebrafish** (2017). Nat Commun. 2017 Jul 25;8(1):126. doi: 10.1038/s41467-017-00143-0.

Contribution: Characterization of the axonal regeneration after spinal cord injury and deciphering the role of the glial processes (Figure 1) using live imaging and immunohistochemical tools and the NTR/MTZ system to ablate the glia, behavioural testing to assess the role of Wnt/β-catenin during functional recovery after spinal cord lesion (Figure S5) which is not described in this chapter.

4.1 Introduction

In this chapter I assessed how axons regenerate after injury in zebrafish larvae and checked the hypothesis that the formation of glial scar is an essential substrate for the axons to grow on. This part of my thesis has already been published with me as a contributing author (Wehner et al. 2017). The purpose of this study was to characterise the substrate that the axons are growing on after injury and assess the role of the extracellular matrix (ECM) during axonal regeneration since very little is known about the regulation and composition of the growth promoting ECM in zebrafish. This study shows that the ECM is controlled by the Wnt signalling pathway and that the axons are able to navigate the lesion site without glial support. I used different reporter lines in order to visualize the glial and the neuronal elements of the spinal cord in combination with high resolution microscopy and immunohistochemical methods. I managed to show for the first time in zebrafish that axons are able to cross the injury site and establish new functional connections without the glial support. Furthermore, I used the MTZ/NTR system in order to selectively ablate the glial population. The treatment did not affect the ability of the axons to cross the injury site indicating that axons are able to navigate the ECM-rich lesion site and glial bridges do not appear to be an obligatory substrate during this process.

4.1.1 Axonal regeneration after injury

Following spinal cord transection, fish and amphibians have the ability to re-grow their severed axons across the injury site and establish functional connections, which leads to behavioural recovery. Severed axons can regrow following injury and therefore functional restoration can occur. However, not all the axons exhibit the same growth capacity. Regeneration of some axons after SCI is robust (Becker et al. 1997), but axonal regrowth to a large extent is variable, like in zebrafish where dorsal root axons and ascending axons of intraspinal neurons do not exhibit any significant

regrowth into the distal spinal cord stump (Becker et al. 1998, Becker et al. 2004), whereas aminergic axons regrow only a few micrometers.

Previous studies suggest that one of the reasons for failure of axonal regeneration after mammalian CNS injury is inefficient myelin clearance, whereas in the PNS myelin debris are efficiently cleared during Wallarian degeneration by Schwann cells and macrophages promotes regeneration (David and Lacroix 2003, Vargas and Barres 2007, Neumann et al. 2009) . In agreement with this concept, it has been observed that zebrafish macrophages are also involved in debris clearance, removal of apoptotic neurons, and engulfment of axonal fragments after SCI (Hui et al. 2010). After peripheral nerve injury in zebrafish, macrophages recruitment to the injured site occurs before axonal fragmentation, and is independent of Schwann cell derived signals as shown by (Rosenberg et al. 2012) where the use of sox10-/- mutants that lack Schwann cells, showed that after lesion, macrophages arrived at the lesion site with timing and morphology similar to those observed in wild-type larvae. Additionally, macrophages in these mutants were able to phagocytose axonal debris similarly to wild-type larvae.

A major determinant for successful axon regeneration of adult mammalian CNS is the poor intrinsic property of injured neurons. In order to promote regeneration a great deal of effort has been made to induce the intrinsic growth capacity of adult CNS neurons, and some studies involving peripheral conditioning lesions showed that several regeneration associated transcription factors such as c-Jun, CCAAT/enhancer binding protein, cAMP responsive element binding, STAT-3, ATF-3, SRY-box 1 and Smad 1 can enhance growth of the central process beyond the lesion (Filous and Schwab 2018).

Additionally, it has been reported that either suppression of inhibitory factors such as phosphatase and tensin homolog (PTEN), suppressor of cytokine signaling (Socs3) or overexpression of genes involved in PNS regeneration such as Klf7, CREB, and c-Jun could have a positive effect on axonal regrowth in adult CNS (Gao et al. 2004, Smith et al. 2009, Sun and He 2010, Smith et al. 2011, Blackmore et al. 2012, Lerch et

al. 2014). There are also several negative regulators axonal growth such as cAMP, PTEN and Socs3 in mammals. These are conserved and it has been shown that they exhibit similar roles in zebrafish (Smith et al. 2009, Liu et al. 2011, Elsaeidi et al. 2014, Diekmann et al. 2015). Similarly, mammalian target of rapamycin (mTOR) activation promotes axon regeneration. Activation of PI3K or inhibition of PTEN in DRG neurons increases neurite outgrowth. Blocking mTOR by rapamycin fails to inhibit neurite growth, suggesting that an mTOR independent mechanism may mediate the regeneration of peripheral sensory axons.

In order to understand whether active mTOR plays a role in zebrafish optic nerve regeneration, (Diekmann et al. 2015) studied mTOR signaling after injury and found that regulation of mTOR activity after optic nerve injury is different from that of mammals showing that inhibition with rapamycin only delays rather than abolishes axonal regeneration and functional recovery after optic nerve crush, whereas in mammals similar treatment led to impairment of optic nerve regeneration (Abe et al. 2010).

The most important aspect of axonal regeneration is that the regenerated axons reach the appropriate targets over long distances and re-establish functional connections, a phenomenon that does not happen in mammals. It has been hypothesized that regenerating axons could trace their original pathways along the degenerating tracts as happens in PNS (Graciarena et al. 2014). CSPG and other inhibitory molecules are known to play an important role during development by repelling axons from certain areas that are not meant to be innervated. The composition of the ECM in the CNS is different from that in the PNS. The dense glial scar that forms after injury and the ECM network act as a physical and molecular barrier to axon regeneration in the injured CNS. The major ECM molecules in the CNS include glycosaminoglycan hyaluronan and the glycoproteins tenascin-C and thrombospondin whereas the PNS ECM includes laminins, collagen, and heparin sulfate proteoglycan. (Wehner et al. 2017) have shown the importance of the ECM during axonal regeneration. Following injury, activation of Wnt/β-catenin signaling controls the composition of the spinal lesion ECM, which is crucial for functional

axonal regeneration in zebrafish. Upregulation of Wnt/β-catenin signaling in non-neural fibroblast-like cells leads to collagen deposition in the spinal lesion ECM which promotes axon growth and functional recovery in zebrafish.

In order to understand these findings, the relationship between axons and glia needed to be analysed. A major impediment to axonal growth in mammalian models is the formation of a glial scar. Astrocytes and oligodendrocyte progenitors are at the centre of reactive gliosis. In contrast to mammals, the adult zebrafish CNS is characterized by decreased expression of some glial and intermediate filament markers such as GFAP and vimentin following injury (Ghosh and Hui 2018). Unlike mammalian models, in which glial scar formation creates an obstacle to axon regrowth, in zebrafish there is an obvious lack of a permanent glial scar. Instead several studies mention the formation of a growth permissive glial bridge that may lead to axonal regeneration in adult zebrafish (Hui et al. 2010, Baumgart et al. 2012, Goldshmit et al. 2012, Mokalled et al. 2016). This glial bridging response is similar to Schwann cell behaviour in mammalian PNS. Upregulation of laminin triggers cytoskeletal rearrangements, which are essential for PNS regeneration (Chen et al. 2007).

Glial bridge formation appears to be conserved between mammals and fish. One example of this is the work from (Goldshmit et al. 2014) which suggests that fibroblast growth factor 2 (FGF2), given to a hemisection SCI model in mice, decreases infiltration of immune cells and gliosis, increases radial glia markers like Pax6 and promotes axonogenesis, and ultimately leads to improved functional recovery, through the formation of glial bridges, similar to what has been shown in zebrafish from the same group where Fgf-dependent glial cell bridges are essential for spinal cord regeneration after injury (Goldshmit et al. 2012). Another study from Mokalled et al.,2016 (Mokalled et al. 2016) identified connective tissue growth factor (ctgfa) as a major determinant for glial bridge formation and axonal regeneration. However, the role of the glial bridge for axonal regeneration after SCI is not clear as the data from these and other studies show that the manipulations influence both glia and

axons in the same way and but there is not a direct correlation between axonal re-growth and glial manipulation.

In order to address the question whether axons need a glial bridge as substrate to cross the injury site or whether glial and axonal processes cross the injury site independently, the following reporter lines were used: *Tg(Xla.Tubb:DsRed)*, abbreviated as nbt:DsRed where neuronal elements of the spinal cord fluoresce red (Peri and Nusslein-Volhard 2008); *Tg(gfap:GFP)*^{mi2001}, abbreviated as GFAP:GFP where glial elements fluoresce green, (Bernardos and Raymond 2006), *Tg(her4.3:GFP*) where the glial elements of the spinal cord fluoresce green (Yeo et al. 2007), *Tg(gfap:Gal4ffs995;UAS:NTR-mCherry)* where the glial cells express the enzyme nitroreductase under the gfap promoter which allows to selectively ablate the glial population after addition of metronidazole which is the substrate for nitroreductase (Matsuoka et al. 2016), *Tg(her4.3:irtTAM2(3F)-p2a-AmCyan*^{ulm6}*),* abbreviated as her4.3:TetA AmCyan where the glial elements of the spinal cord fluoresce cyan (Geurtzen et al. 2014), *Tg(her4.1:Tet-GBD-p2A-mCherrytud6)* abbreviated as her4.3:mCherry where the glial elements of the spinal cord fluoresce red (Knopf et al. 2010). This allowed me to visualise the neuronal and glial elements of the zebrafish spinal cord and also to selectively ablate the glial population. These lines combined with live imaging allowed me to characterise the relationship between axons and glial processes. This showed that axons are able to re-grow across the injury site without the glia support. Fascicles crossing the injury site are mostly neuronal at 1 day post injury whereas at 2 dpl the majority of the fascicles contain both neuronal and glial processes. Furthermore, after glial ablation the axons were still able to bridge the lesion site.

4.2 Results

4.2.1 There is no direct interaction between the regenerating axons and the glial processes

To determine how axons cross the lesion site, we analysed their relationship with astrocyte-like glial processes, as these have been shown to be supportive for axon regeneration in zebrafish (Goldshmit et al. 2012, Mokalled et al. 2016). We imaged axonal and glial processes in time-lapse video microscopy using double transgenic fish for Xla.Tubb:DsRED, to visualize neuronal processes, and either g*fap*:GFP (Bernardos and Raymond 2006) (n = 6 fish, 33 fasicles) or *her4.3*:EGFP (Yeo et al. 2007) (n=3 fish, 30 fasicles) to label astroglia-like processes. This revealed that the majority of fascicles that entered the lesion site were composed of axons without detectable glial processes (49–53%). Some fascicles contained both glial and axonal processes (20–21%) and some pure glial fascicles were observed (27–30%; Fig.4.1 see Methods section for scoring criteria). To confirm these findings, we used a range of combinations of immunohistochemical and transgenic markers for neuronal and glial processes in static images of live animals and histological preparations at 1 dpl. This showed that 63–77% of axon-containing fascicles (≙46–62% of all fascicles analysed) were devoid of detectable glial processes (Fig. 4.1b). Nineteen to 26% contained both axonal and glial processes and 19–28% of all analysed fascicles were only composed of glial processes. Moreover, double-immunohistochemistry for anti-acetylated Tubulin and anti-GFAP showed that at 1 dpl, only 36% of animals had glial processes bridging the lesion site, in contrast to 57% of the fish with an axonal bridge. At 2 dpl, glial processes had caught up (Fig. 4.1c). This suggests that axons cross the lesion site more rapidly than glial processes. In summary, these observations support that many axons rapidly extend into the lesion site and cross it independently of detectable glial processes.

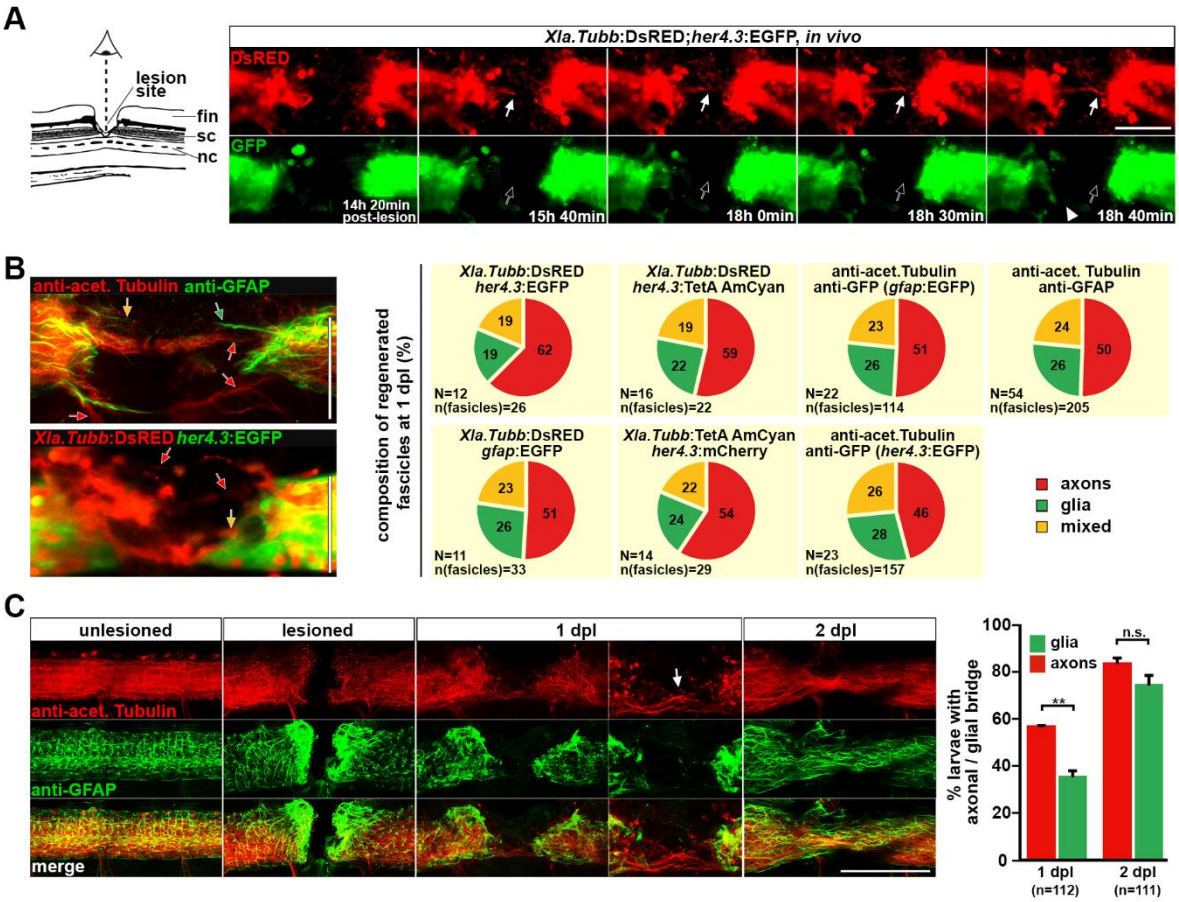

Figure 4.1. Regenerating axons navigate a non-neural lesion environment that is rich in ECM independently of astroglia-like processes. a Time-lapse video microscopy reveals that axonal growth cones (arrow, Xla.Tubb:DsRED) extend into the lesion site independently of astroglia-like processes (her4.3:EGFP, empty arrow points out lack of glial labelling). Arrowhead indicates glial process extending into the lesion site. Single frames are shown. Abbreviations: fin, dorsal fin fold; sc, spinal cord; nc, notochord. b Quantification of fascicle composition at 1 dpl using different combinations of immunohistochemical and transgenic markers for astroglia-like processes and axons indicates that the majority of fascicles are neuronal with no detectable glial component (46–62% of all fascicles analyzed). In the example scans on the left, yellow arrows indicate mixed fascicles, containing neurites and glial processes; green arrows indicate pure glial fascicles and red arrows indicate pure axonal fascicles. c Time course of re-growth of axons (anti-acetylated Tubulin+) and astroglia-like processes (anti-GFAP+) after spinal cord transection. Quantification of labelling continuity between rostral and caudal spinal cord stumps at 1 dpl and 2 dpl suggests faster bridging of the lesion site by neuronal rather than glial processes. Arrow points to axonal bridge with

very few glial processes in the lesion site at 1 dpl at higher magnification (Fischer's exact test: **P < 0.01; n.s. indicates not significant) N numbers on figure relate to number of larvae used.

4.2.2 Glial bridges are not an obligatory substrate for the axons to grow

To experimentally test a role of astroglia-like processes in supporting axonal regeneration, we ablated the majority of glial cells using *gfap*:Gal4ff;*UAS*:NTR-mCherry transgenic fish that express the enzyme nitroreductase under regulatory sequences of the *gfap* gene (Matsuoka et al. 2016) that uses the NTR/Mtz system (Curado et al. 2008). More specifically, bacterial Nitroreductase (NTR) is used to catalyze the reduction of the innocuous prodrug metrodinazole (Mtz), thereby producing a cytotoxic product that induces cell death. Based on this principle, NTR is expressed in transgenic zebrafish using the gfap promoter. Subsequent exposure to Mtz by adding it to the media induces cell death exclusively within NTR(+) glial cells. The treatment did not alter the viability of the larvae which did not exhibit any obvious deformities or functional impairment. The treatment almost completely eliminated transgene-expressing glial cells by 3 dpf (Fig. 4.2A). A dramatic depletion of astroglia-like processes in the lesion site was confirmed by anti-GFAP immunohistochemistry (Fig. 4.2 B). However, this treatment did not reduce the proportion of animals with axonal bridge (anti-acetylated Tubulin^{+}; Fig. 4.2 B). This further supports that glial processes do not have a major role in facilitating axonal regrowth across a spinal lesion site. However, we cannot rule out that glial processes that were not detected with our markers and were spared by the ablation still support axonal regeneration.

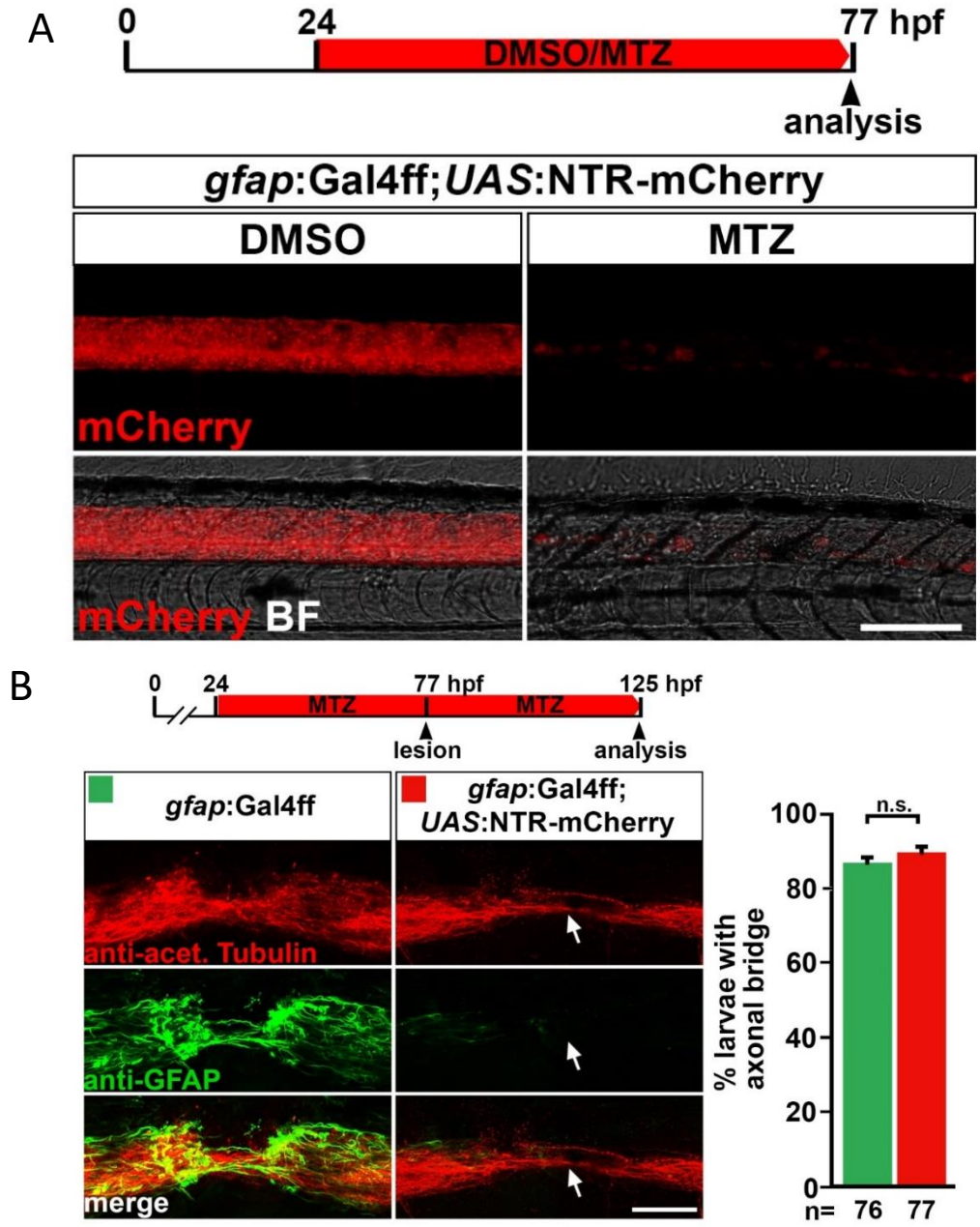

Figure 4.2. A. Treatment of gfap:Gal4ff;UAS:NTR-mCherry transgenic fish with the pro-drug Metronidozole (MTZ) almost completely ablates transgene-expressing glial cells by 3 dpf. B. Treatment of gfap:Gal4ff;UAS:NTRmCherry transgenic fish with MTZ dramatically reduces anti-GFAP+astroglia-like processes (t-test: ***P < 0.001) but does not reduce the proportion of larvae with axonal bridges at 2 dpl (Fischer's exact test: n.s indicates not significant). N numbers on figure relate to number of larvae used.

4.3 Discussion

4.3.1 Astro-glial bridges are not an obligatory substrate for axonal regeneration after SCI

The data presented in this chapter suggest that re-grown axons can navigate through the lesion environment and are not following the glial processes. In histological preparations this is difficult to assess, as axons and glial processes tend to fasciculate. Fasciculation is the ability of neuronal and glial processes to form bundles in order to ensure that they will reach their targets (Davis et al. 2017). In zebrafish larvae at 2 dpl almost all tissue bridges observed were composed of neuronal and glial processes. This makes it difficult to assess the dynamics of the neuronal and glial processes and how they interact while they navigate through the non-neural lesion site during the regeneration process. For this reason, time-lapse video imaging on double transgenic animals where both, their neuronal and glial elements are fluorescent, was performed. This showed that both axons and glia can grow independently across the injury site. Furthermore, live imaging during the first 24hours after injury showed that re-establishment of axonal continuity across the injury site precedes that of continuity and this was also verified with histological preparations in which 55% of the injured larvae exhibited axonal bridge at 1 dpl whereas, only 37% had glial processes that crossed the injury site. This is in agreement with previous studies in adult eel (Dervan and Roberts 2003) where after injury cells expressing GFAP do not appear in the injury site until 16 days post injury. Additionally, previous works studying the regeneration of the visual system of goldfish from Nona 2005 and also the spinal cord (Nona and Stafford 1995), have shown that the outgrowth of axons after injury does not appear to depend on direct association with glial cells. They found that glial processes are not observed among the axons that manage to cross the injury site indicating that glial processes follow rather than acting as a substrate for the axons to grow on.

In order to test the role of the glial processes during axonal regeneration of the zebrafish spinal cord I used the NTR/MTZ system which allowed me to selectively

ablate the glial population, by driving the expression of Nitroreductase under the GFAP promoter and assess the regenerative response of the axons in an environment devoid of GFAP+ glia. This treatment showed again that the axons are able to grow through the injury site without the glial support in contrast to what has previously been concluded from other studies which suggest that glial bridges are essential for functional axonal regeneration (Goldshmit et al. 2012, Goldshmit et al. 2014, Mokalled et al. 2016). While these observations support the hypothesis that glial substrates are not essential for axonal regeneration, we cannot exclude that fine glial processes that escaped detection and ablation still served as a substrate for axon regrowth. Every available reporter line to visualise the glial population, including gfap:Gal4ffs995;UAS:NTR-mCherry[31]);gfap:GFP[mi200129], her4.3:EGFP[y83]; her4.3:irtTAM2(3F)-p2a-AmCyan[ulm6]; her4.3:mCherry[41] was used and found that after injury neuronal axons where growing independently of the glial processes. Most of the glial fascicles quantified were purely neuronal. There were also cases where the glial processes were bridging the lesion site similarly to the axons, exhibiting the same time course but they were not in close proximity with the neuronal fascicles. However, we cannot exclude that maybe not all the glial populations have been expressing the fluorescent protein that allowed their detection. Additionally, I tried to perform immunostaining against nestin in order to visualise the young glial population that accumulate in the injury site very short after injury according to (Goldshmit et al. 2012) but never got it to work and therefore we cannot exclude the possibility that this cell population may act as a substrate for neuronal axons to grow across the lesion site.

Moreover, glial process are likely to support regeneration by physically aligning with regenerating fascicles (Goldshmit et al. 2012) and producing essential growth-factors (Mokalled et al. 2016). During this study I scored the number of animals that showed axonal continuity across the injury site after GFAP glia ablation. In both cases, with or without ablation, the fish exhibited similar bridging score after the injury. However, no formal assessment of the functionality of the axonal connections after the glial ablation was performed. Electrophysiological experiments or behavioural

experiments can be utilized in order to see if the treatment leads to any swimming defects already before the injury and if this ability of the axons to cross the injury site in the absence of glial support can lead to functional recovery. Furthermore, since ECM regulation by Wnt has been shown to be essential for axonal regeneration it would be good to see if the ECM composition was altered after the treatment. This would show if there are any other adverse effects and the crossing of the axons is not due to alteration of the ECM, for example due to possible increase in Collagen XII.

4.3.3 But what is the substrate for the axons to grow on and bridge the lesion site if not the glial processes?

It is still unknown the substrate that allows zebrafish axons to regenerate after spinal cord injury. What is that key element that makes their axons to grow through the lesion site? In order to answer this question more experiments need to be performed following up the data of this study. Axons can sense and follow signals from their environment through their growth cones. An EM study on the growth cones during different stages of axonal growth could provide more information regarding their composition and organization which may be different compared to mammals where the axons fail to regenerate after transection.

In addition, there also other cell populations that have been shown to be essential for axonal regeneration like fibroblasts (Wehner et al. 2017) or cells that respond rapidly and migrate into the injury site like immune cells (Ohnmacht et al. 2016, Tsarouchas et al. 2018) and pericytes (Wehner et al. 2017). Time lapse video microscopy could provide further information regarding the direct interaction of these cells with the axons during regeneration after spinal cord injury. Zebrafish larvae can be easily manipulated using pharmacological or genetic tools. In order to identify possible substrates for the axons the aforementioned cell populations can be easily manipulated generally or in a time dependent manner. It has been shown in this chapter that axons start to regenerate in the first 17 hours after injury. One possible experiment can be the use of vivo morpholino or the NTR/MTZ method in

order to ablate these cells during this early time window and assess the behaviour of the axons.

Very useful information for all the above will provide an unbiased approach to determine the composition of the injury site during different time points after injury. The use of zebrafish larvae allows the collection of hundreds of larvae relatively easy. The larvae can easily be injured, and their injury site can be collected and sent for RNA sequencing in bulk or specific populations can be isolated and sent for single cell RNA sequencing. The data obtained can be compared over different conditions and after different manipulations that have a positive or negative effect on axonal re-growth in order to identify molecules that act as key mediators of axonal growth.

Chapter 5: The role of the macrophages during axonal regeneration

Tsarouchas, T. M., D. Wehner, L. Cavone, T. Munir, M. Keatinge, M. Lambertus, A. Underhill, T. Barrett, E. Kassapis, N. Ogryzko, Y. Feng, T. J. van Ham, T. Becker and C. G. Becker (2018). "Dynamic control of proinflammatory cytokines Il-1beta and Tnf-alpha by macrophages in zebrafish spinal cord regeneration." Nat Commun 9(1): 4670.

According to the guidelines regarding inclusion of publications in Postgraduate research theses, for this chapter I wrote a new introduction and discussion. The results and figures have been taken from the paper which has been accepted in Nature Communications on the 12th of October 2018.

Contributions to this study: **TMT**: conceptualization, investigation, writing, Figure 1: A time points-(0.5h, 1h 48h)-I, Figure 2: A time points (0dpl-4dpl)-C, Figure 3, Figure 4, Figure 5, Figure 6: B,C, Figure 7: A,B,C, part of D, E, Figure 8, Figure 9:A time points-(0.5h, 1h 48h, part of B, D, Figure S1: together with TM, Figure S2: (Part of A,B), C,D, Figure S3, Figure S4: A, Part of B, C, D, Figure S5 part of A and B, Figure S6, Figure S7, Figure S8 A, Figure S9 A, Figure S10 A-J, Figure S11, Figure S12.

DW: Figure S4: E, Figure S10 designed gRNA for il1b with TB, Supervision, **LC**: Figure A,D, Figure S5: part of, Figure S8 B, Figure S9 B, Supervision, qPCR troubleshooting, **TM**: Figure 2: C (5dpl time point), Figure 9: Part of B, E, Figure S1, Figure S2 Part of A,B, **MK**: designed the gRNA for TNF-α, Table S1, **ML**: Figure 1 (A time points: 2h , 4h, 6h, 24h, 72h, 120h), **AU**: Figure 3 part of, **TBa**: Figure 7: part of D, Figure S10 designed gRNA for il-1b with DW, **EK**: Figure S4:part of B, **TJH**: Provided csf1ra/b mutant line, **NO**: F8: provided Il-1β probe, Il-1β:gfp tg line, **YF**: provided l-plastin antibody, supervision, **TB**: Figure 10, Conceptualization, supervision, funding acquisition, **CGB**: Conceptualization, supervision, funding acquisition.

5.1 INTRODUCTION

Trauma to the central nervous system (CNS) triggers inflammation and systemic immunity which regulates the mechanisms of tissue repair.

The inflammatory response that occurs after injury shows conserved features among vertebrates (Riera Romo et al. 2016). Neutrophils are the first cells that migrate to the injury site whereas microglia and peripheral macrophages migrate into the injury site later. It has been suggested that of these three cell types macrophages and neutrophils are crucial regulators of axonal regeneration after SCI by producing pro-and anti-inflammatory signals (Neirinckx et al. 2014, Wang et al. 2015) which regulate positively or negatively axonal regeneration after spinal cord injury. Both microglia and peripheral macrophages produce neuroprotective cytokines and growth factors like TGF-β which has beneficial effects on neurons (Kiefer et al. 1993). Other factors including CNTF, IGF, HGF, PDGF, NGF, BDNF, GDNF and NT-3 also are released by activated macrophages (Elkabes et al. 1996, Kerschensteiner et al. 1999, Nakajima et al. 2001, Nakajima and Kohsaka 2004, Hashimoto et al. 2005, Kim and de Vellis 2005) and have a neuroprotective role. However, the exact role of the immune system during CNS injuries is still unclear.

Zebrafish, in contrast to mammals, are capable of functional CNS regeneration after injury. Recovery of swimming behavior critically depends on regeneration of axons and the re-establishment of functional connections across the complex non-neural injury site (Becker et al. 1997, Wehner et al. 2017). Furthermore, several events and signaling cascades that follow injury in the CNS are conserved between mammals and zebrafish, although zebrafish regain motor function, whereas functional deficits in mammals are often permanent. It is therefore important to determine the factors that allow axons to cross the lesion site in zebrafish.

In mammals, a prolonged immune response, consisting of pro-inflammatory macrophages (Kigerl et al. 2009), microglia cells (Norden et al. 2015) and

neutrophils (Taoka et al. 1997) together with cytokines released from other cell types, such as endothelial cells, oligodendrocytes or fibroblasts (Tran et al. 2018) contribute to an inhibitory environment for axonal regeneration. Inflammatory responses and their role during injuries have been studied for many years. Interestingly there are several studies that mention that inflammation can be essential for regeneration but at the same time it can be detrimental, leading to chronic inflammatory phenotypes that result in exacerbation of the tissue damage. However, activated macrophages can also promote axonal regeneration (David et al. 1990, Yin et al. 2006, Gensel et al. 2009), suggesting complex roles of the immune response after spinal injury. The main difficulty in deciphering the exact role of the inflammatory cascades after injury is due to the complexity of the system and the plethora of cellular and molecular players. Compared to mammals, in zebrafish, we can dissect the roles of these cell types in successful functional spinal cord repair. Their main advantage from the inflammatory perspective is in zebrafish the innate immune system is fully functional during the early stages of development, whereas their adaptive immune system is fully functional after 4 weeks post fertilization (Renshaw and Trede 2012). This allows for the separate study of the innate or adaptive immune response contribution during axonal regeneration Furthermore, the cellular components of immunity in zebrafish are similar to mammals and show similar responses after injury. Indeed, microglia are activated after spinal cord injury in adult (Becker and Becker 2001, Hui et al. 2010) and larval zebrafish (Ohnmacht et al. 2016), suggesting functions of innate immune cells in repair. Adaptive immunity is also important for spinal cord regeneration (Hui et al. 2017). As with macrophages and neutrophils, the beneficial or detrimental nature of adaptive immune cells in CNS injury is becoming clearer. Studies from Pasare and Medzhitov on mice (Pasare and Medzhitov 2003, Pasare and Medzhitov 2004, Iwasaki and Medzhitov 2010) have identified the beneficial role of TLR signaling during T-cell-mediated neuroprotection, indicating the importance of adaptive immunity on top of the innate immunity for CNS regeneration. However, in case of neurodegenerative

disorders some studies have shown that TLR signaling exacerbates the pathology by amplifying the immune response (Hanke and Kielian 2011), whereas (Gesuete et al. 2014) mention that whether TLR activation is detrimental or neuroprotective depends on the timing and intensity of receptor stimulation.

In this chapter I focused only on the contribution of the innate immune response during regeneration of the zebrafish spinal cord. Zebrafish larvae regenerate more rapidly than adults. Their easiness in manipulating their genome combined with their transparency makes them an excellent tool to visualize in vivo the regenerative events that take place after injury at the same time with the inflammatory response. Previous work in the lab has shown that axons encounter Pdgfrb^{+} fibroblast-like cells that deposit regeneration-promoting Col XII in the lesion site in a Wnt-signalling dependent manner (Wehner et al. 2017). These cells and molecules are present also in the injury sites of adult zebrafish and mammals (Wehner et al. 2017, Tran et al. 2018). How immune cells contribute to this growth-conducive lesion site environment in zebrafish is unclear.

In this chapter I show that after spinal cord injury, peripheral macrophages are a major determinant of axonal regeneration. Macrophages promote axonal regeneration by producing pro-regenerative tumour necrosis factor alpha (TNF-α) and by reducing levels of interleukin-1 β (Il-1β). Early expression of *Il-1β* promotes axonal regeneration, whereas prolonged high levels of Il-1β in the macrophage-less *irf8* mutant has a negative effect on regeneration. Additionally, preventing formation of Il-1β producing neutrophils or inhibiting excess *Il-1β* directly, largely restored repair in *irf8* mutants.

5.2 RESULTS

5.2.1The immune response coincides with axonal regeneration

I analysed axonal regrowth in larval zebrafish that underwent complete spinal cord transection at 3 days post-fertilisation (dpf) in relation to invasion of the injury site by different cell types. Axons were present in the injury site by 1 day post- lesion (dpl). The thickness of the axonal bundle that connects the injured spinal cord increased up to 2 dpl and thereafter plateaued for up to at least 4 dpl (Fig. 1A).

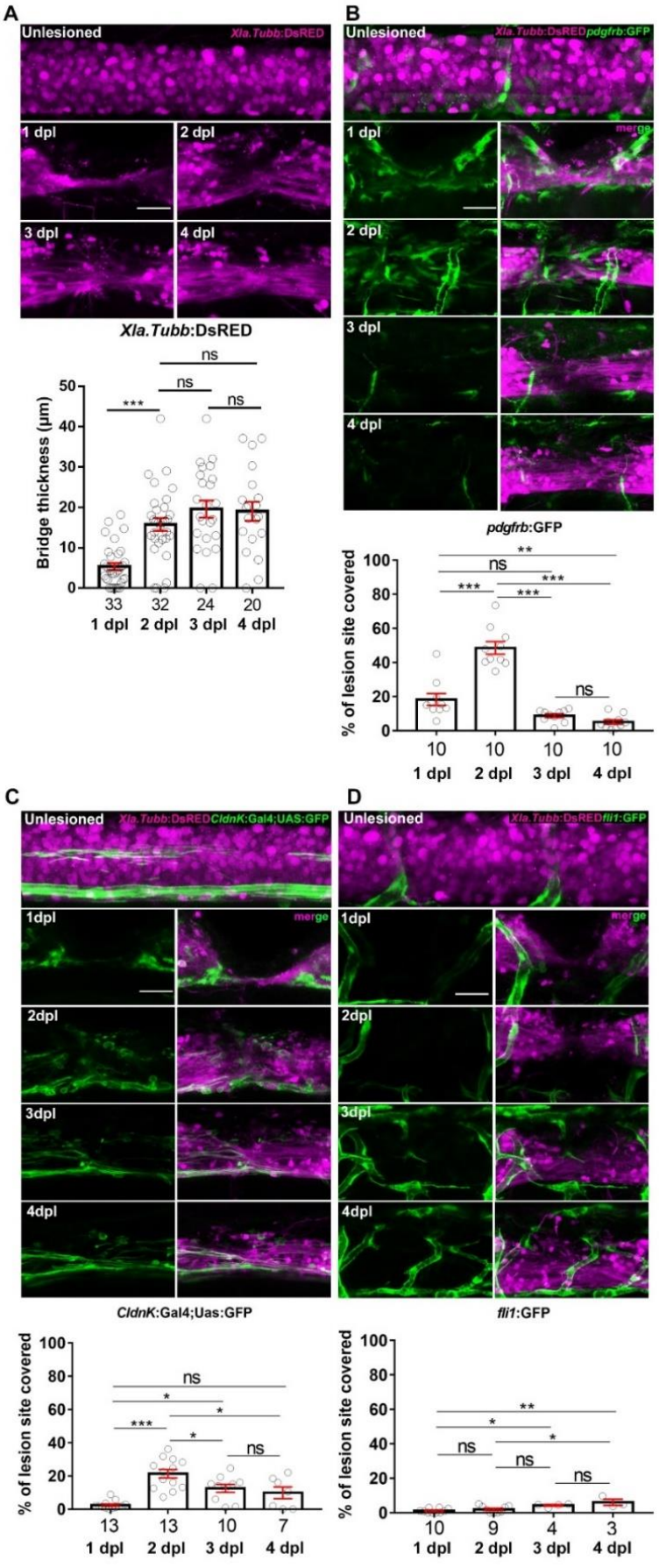
A
Unlesioned
Xla.Tubb:DsRED
1 dpl
2 dpl
3 dpl
4 dpl
Xla.Tubb:DsRED
Bridge thickness (µm)
ns
ns
ns
***
33
32
24
20
1 dpl
2 dpl
3 dpl
4 dpl
B
Unlesioned
Xla.Tubb:DsREDpdgfrb:GFP
merge
pdgfrb:GFP
% of lesion site covered
**
ns
***
***
***
ns
10
10
10
10
C
Unlesioned
Xla.Tubb:DsREDCldnK:Gal4;UAS:GFP
1dpl
2dpl
3dpl
4dpl
CldnK:Gal4;Uas:GFP
% of lesion site covered
ns
*
*
***
*
ns
13
13
10
7
D
Unlesioned
Xla.Tubb:DsREDfli1:GFP
fli1:GFP
% of lesion site covered
**
*
*
ns
ns
ns
10
9
4
3

Fig. 1: Presence of fibroblast-like cells, but not myelinated cells or endothelial cells correlates with axonal regeneration. **A:** The thickness of the axonal bridge observed in *XIa.tubb*:DsRed transgenic animals increases after injury, starting at 1 dpl and plateauing at 2 dpl (*One-way ANOVA followed by Bonferroni multiple comparisons:* $F_{3, 107} = 17.77$ ***P < 0.0001, ns indicates no significance). **B:** Presence of fibroblast-like cells (*pdfrb*:GFP+) in the lesion site is substantial from 1 dpl, it peaks at 2 dpl, and declines thereafter (*One-way ANOVA followed by Bonferroni multiple comparisons:* $F_{3, 36} = 53.92$, **P<0.01,***P<0.0001, ns indicates no significance). **C:** Myelinating cells (*cldnK*:GFP+) appear in the injury site only at 2 dpl (*One-way ANOVA followed by Bonferroni multiple comparisons:* $F_{3, 39} = 14.52$, *P0.05, ***P<0.0001, ns indicates no significance). **D:** Endothelial cells (*fli1*:GFP+) do not invade the lesion site (*One-way ANOVA followed by Bonferroni multiple comparisons*: $F_{3, 22} = 7.939$, *P0.05, **P<0.01). Identical animals are imaged on consecutive days. Lateral views of the injury site are shown; rostral is left. Scale bar: 25 µm. Error bars indicate SEM. Numbers on figure relate to number of larvae used.

The thickness of the connecting axon bundles positively correlated with the recovery of touch-evoked swimming distance for individual animals at 2 dpl (Fig. 2A-C). This is consistent with previous results showing continuous axon labelling over the lesion site (axon bridging) in 80 % of animals by 2 dpl, which then plateaued. Presence of an axon bridge correlates with functional recovery, as animals without axon bridge showed worse recovery of touch-evoked swimming distance (Wehner et al. 2017) and re-lesioning abolished functional recovery (Ohnmacht et al. 2016). Hence, a percent score of larvae with bridged injury sites is a quick and reliable measure for anatomical repair (Ohnmacht et al. 2016, Wehner et al. 2017).

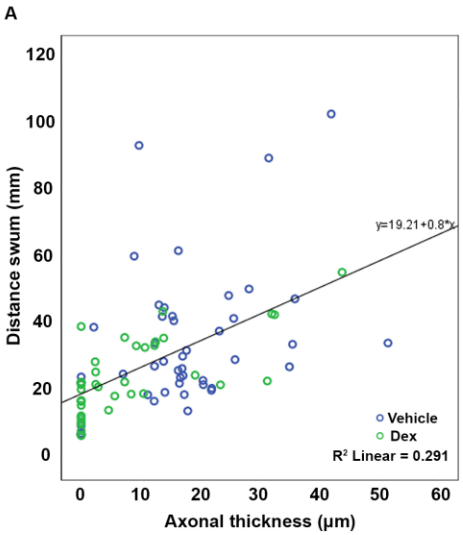

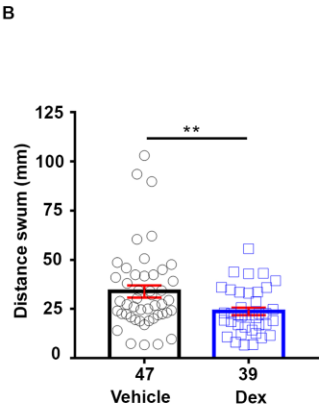

C

Correlations

		Distance swum (mm)	Axonal thickness (µm)	Treatment (Vehicle/Dex)
Distance swum (mm)	Pearson Correlation	1	.540**	-.284**
	Sig. (2-tailed)		.000	.008
	N	86	86	86
Axonal thickness (µm)	Pearson Correlation	.540**	1	-.367**
	Sig. (2-tailed)	.000		.001
	N	86	86	86
Treatment (Vehicle/Dex)	Pearson Correlation	-.284**	-.367**	1
	Sig. (2-tailed)	.008	.001	
	N	86	86	86

**. Correlation is significant at the 0.01 level (2-tailed).

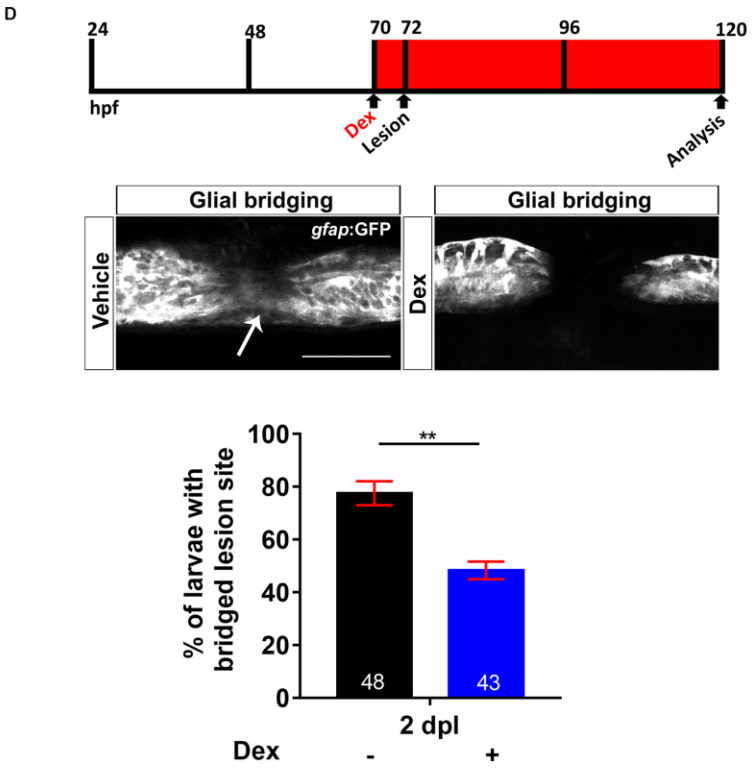

Fig. 2: Dexamethasone treatment impairs axonal and glial crossing of the injury site and recovery of touch-evoked swim distance. A: The thickness of the axonal bridge correlates with the distance swum after injury, following treatment with vehicle or dexamethasone. B: Distance swum is significantly impaired after treatment with dexamethasone (t-test:**P<0.01). C: Correlation table. There is a positive correlation between thickness of the axonal bridge and the distance swum, whereas there is a negative correlation between bridge thickness and dexamethasone treatment and between distance swum and dexamethasone treatment. D: Dexamethasone treatment impairs formation of glial bridges (arrow) over the injury site (Fisher's exact test: **P<0.01). Lateral views of the injury site are shown; rostral is left; Dex = dexamethasone. Scale bar in D: 100 µm. Error bars indicate SEM. Numbers on figure relate to number of larvae used.

After injury, we observed a rapid and massive influx of immune cells, with neutrophils (Mpx^{+}) peaking at 2 hours post-lesion (hpl) and macrophages (*mpeg1*:GFP^{+}; 4C4^{-}) and microglia (*mpeg1*:GFP^{+}; 4C4^{+}) accumulating in the lesion site a few hours later and peaking at 2 dpl (Fig. 3A,).

Myelinating cells (*cldnK*:GFP^{+}) and endothelial cells (*fli1*:GFP^{+}) were not abundant in the lesion site during axonal regrowth (Fig. 1C,D), in contrast to functionally important *pdgfrb:*GFP^{+} fibroblasts[1] that were present in the lesion site at 1 dpl, peaking at 2 dpl (Fig. 1B). This suggests that myelinating cells and endothelial cells are not essential for axon bridging. However, at later time points after injury, axons were clearly associated with processes of myelinating cells (Fig. 1C), which may impact functional repair. In contrast, the spatio- temporal pattern of immune cell invasion of the injury site suggests an early role for the immune system in orchestrating axon growth over the lesion site.

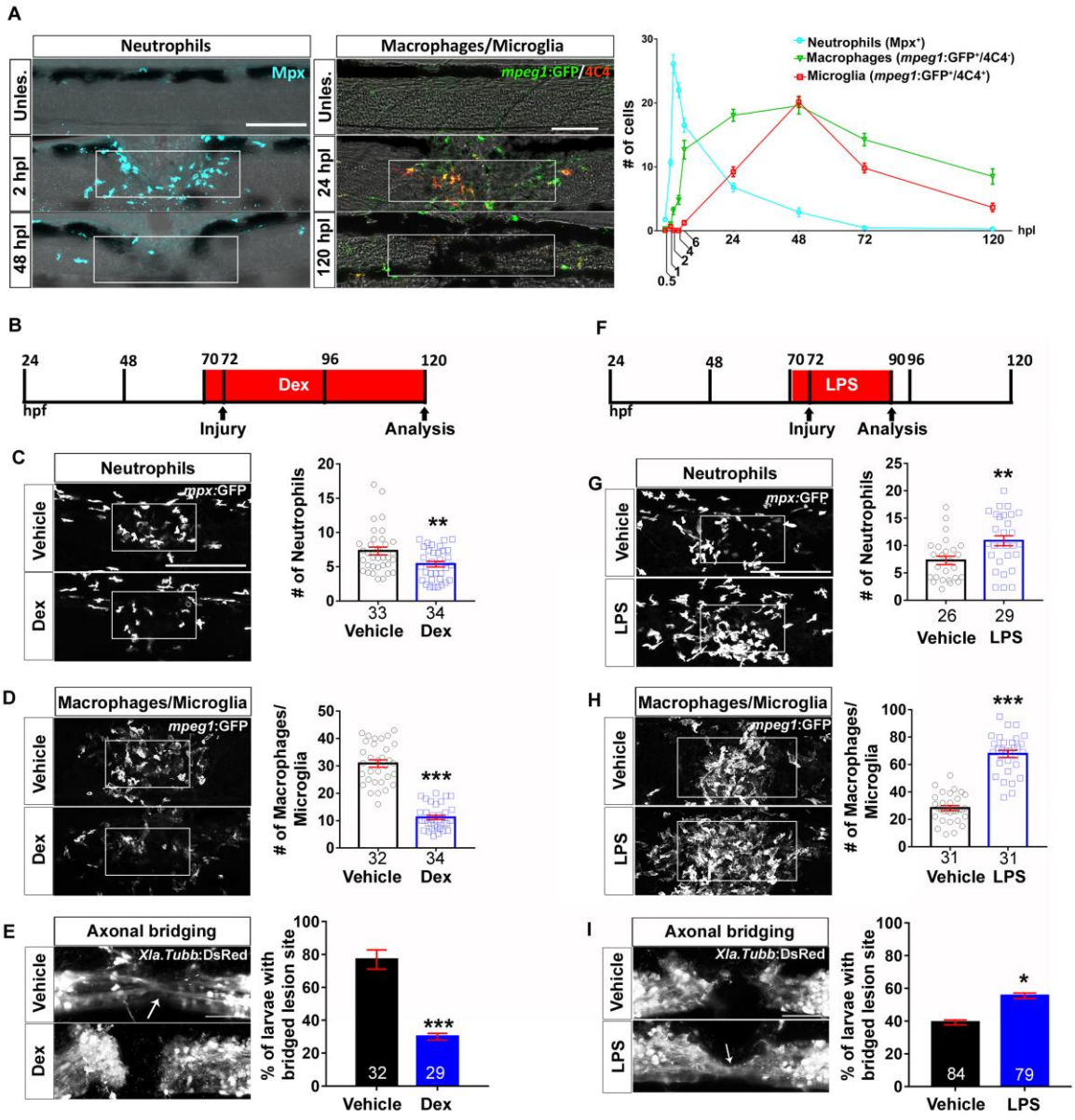

Fig. 3: Spinal injury leads to an inflammatory response that promotes axonal regeneration. A: Neutrophils, macrophages and microglial cells show different dynamics after injury. Neutrophils (Mpx+) accumulate in the injury site very early, peaking at 2 hpl. Macrophages (mpeg1:GFP+/4C4-) and microglial cell (mpeg1:GFP+/4C4+) numbers peak at 48 hpl. Fluorescence images were projected onto transmitted light images. B-E: Incubation with dexamethasone (timeline in B) reduces neutrophil and macrophage numbers (C,D; Mann-Whitney U test: **P<0.01, ***, P<0.001), as well as the proportion of animals with axonal bridging (E; Fisher's exact test: ***P<0.001). F-I: Incubation of animals with LPS during early regeneration (timeline in F) increased numbers of neutrophils and macrophages (G, H; t-test: **P<0.01, ***, P<0.001), as well as the proportion of animals with axonal bridging at

24 hpl (I; Fisher's exact test: *P<0.05). Lateral views of the injury site are shown; rostral is left. Rectangles indicate region of quantification; arrows indicate axonal bridging. Scale bars: 50 µm; Error bars indicate SEM. Numbers on figure relate to number of larvae used.

5.2.2 Immune system activation promotes axonal regeneration

To determine the importance of the immune reaction, we inhibited it using the anti-inflammatory synthetic corticosteroid dexamethasone (Ohnmacht et al. 2016). This reduced the number of microglia, macrophages and neutrophils in the injury site (Fig. 3B-D) and the proportion of larvae exhibiting axon bridging (control: 78 % of examined animals, dexamethasone: 30 %; Fig. 3E).

The average thickness of axon bridges was also reduced by dexamethasone treatment and correlated with impaired recovery of touch- evoked swimming distance (Fig. 2A-C). *gfap*:GFP^{+} astroglia-like processes that cross the injury site slightly later than axons[1] also showed reduced bridging, from 77.6 % of examined animals to 48.3 % (Fig. 2D) under dexamethasone treatment. In addition, depleting the number of immune cells with a well-established morpholino combination against *pu.1* and *gcsfr* (Feng et al. 2012) reduced the proportion of larvae with axonal bridges from 81 % of examined animals to 57 % (Fig. 4A,B).

For a gain-of-function approach, we used incubation with bacterial lipopolysaccharides (LPS) (Novoa et al. 2009). This increased the number of neutrophils and macrophages in the lesion site (Fig. 3F-H). To detect a potential accelerating effect on axonal regrowth, we analysed larvae at 18 hpl, when axonal regeneration was incomplete in untreated animals. This showed an increase in the proportion of larvae with axonal bridges from 41 % of examined animals in wildtype to 60 % in LPS-treated animals (Fig. 3I). Hence, immune system activity is necessary for and promotes axonal regeneration across a spinal lesion site.

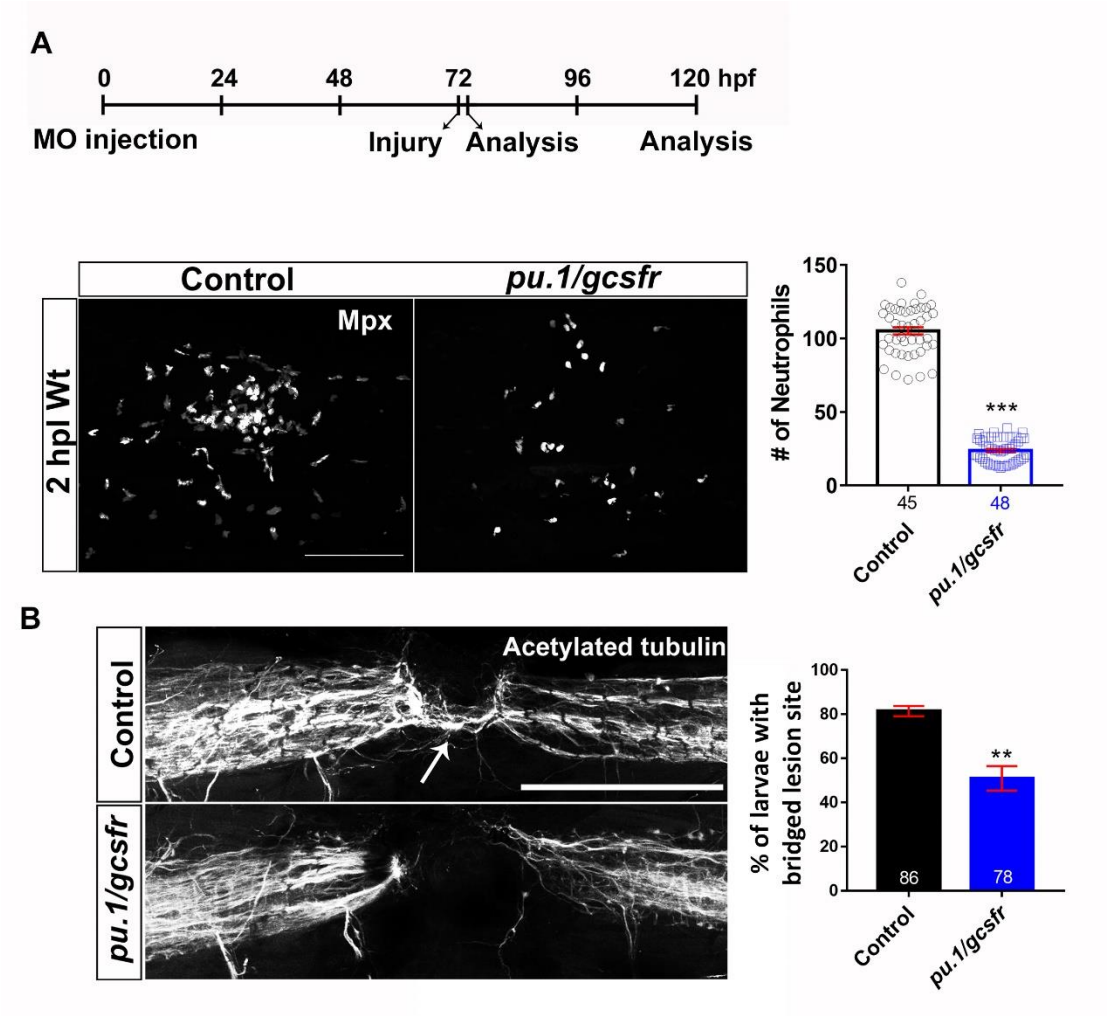

Fig. 4: Inhibiting immune cell development impairs axonal regeneration. A: Neutrophils are strongly reduced in number in pu.1 and gcsfr double morpholino-injected animals (Mann-Whitney test: ***P<0.001). B: Quantification of axonal bridging (arrow; anti-acetylated Tubulin) shows that morpholino injection decreases the proportion of animals with axonal bridges (Fisher's exact test: **P<0.01). Lateral views of the injury site are shown; rostral is left. Scale bar: 100 µm. Error bars indicate SEM. Numbers on figure relate to number of larvae used.

5.2.3 Macrophages determine regenerative success

To analyse the role of different immune cell types in repair, we used mutants. In mutants for the macrophage-lineage determining transcription factor *irf8*, macrophages and microglial cells, but not neutrophils are missing during early

development (Shiau et al. 2015). Homozygous mutants are adult viable and show no overt developmental aberrations, except for an increased number of neutrophils (Shiau et al. 2015).

In situ hybridisation for the macrophage and microglia marker *mpeg1* confirmed expression in the ventral trunk of unlesioned larvae and in a spinal lesion site at 2 dpl in wildtype larvae, but complete absence of signal in unlesioned and lesioned *irf8* larvae (Fig. 5A).

Next, I determined axonal regrowth and recovery of parameters of swimming capacity in *irf8* mutants compared to wildtype animals. Wildtype and mutants showed comparable proportions of animals with axon bridges at 1 dpl (wildtype: 44% of examined animals; *irf8* mutant: 43%). At 2 dpl, however, axonal continuity was observed in 80 % of wildtype animals but only in 41 % of *irf8* mutants (Fig. 5B). At 5 dpl – 2.5 times as long as wildtype animals need for maximal axon bridging – the proportion of mutant larvae with bridged lesion sites was increased compared to 2 dpl (55 % of examined animals vs 41 %), but regenerative success was still strongly reduced compared to wildtype controls (55 % of examined animals vs. 87 %; Fig. 5C).

Analysing touch-evoked swimming, we found that wildtype animals swam comparable distances to unlesioned controls at 2 dpl, as previously described (Wehner et al. 2017). In contrast, recovery of touch-evoked swimming distance in *irf8* larvae plateaued at 2 dpl and did not reach levels of unlesioned animals to at least 5 dpl (Fig. 5C). This indicates that in the absence of macrophages and microglia in *irf8* mutants, initial axonal regeneration is unaffected, but axonal regrowth and functional recovery after spinal cord injury are impaired long-term. To determine the importance of microglia for regeneration, we analysed *csf1ra/b* double-mutants (see Methods) in which the function of colony-stimulating factor 1 receptor (Csf1r) is compromised. Csf1r is selectively needed for microglia differentiation (Oosterhof et al. 2018). After injury in *csf1ra/b* mutants, we observed a strong reduction in the number of microglial cells (to 17 % of wildtype), but an increase in macrophage numbers (by 55 % compared to

wildtype) in the injury site (Fig. 6A,C). Interestingly, neutrophil numbers were also strongly reduced (to 64.1 % of wildtype at 2 hpl and 16 % at 1 dpl) (Fig. 6B), perhaps due to feedback regulation from increased macrophage numbers. Whereas microglia cells were reduced in number in the entire fish, neutrophils were still present in the ventral trunk area. In these mutants, axon bridging was unimpaired (Fig. 6D). Hence, microglia are not necessary for axonal regeneration and reduced numbers of neutrophils do not negatively affect axonal regrowth. Combined with results from the *irf8* mutant, this indicates that recruitment of peripheral macrophages is critical for successful spinal cord regeneration.

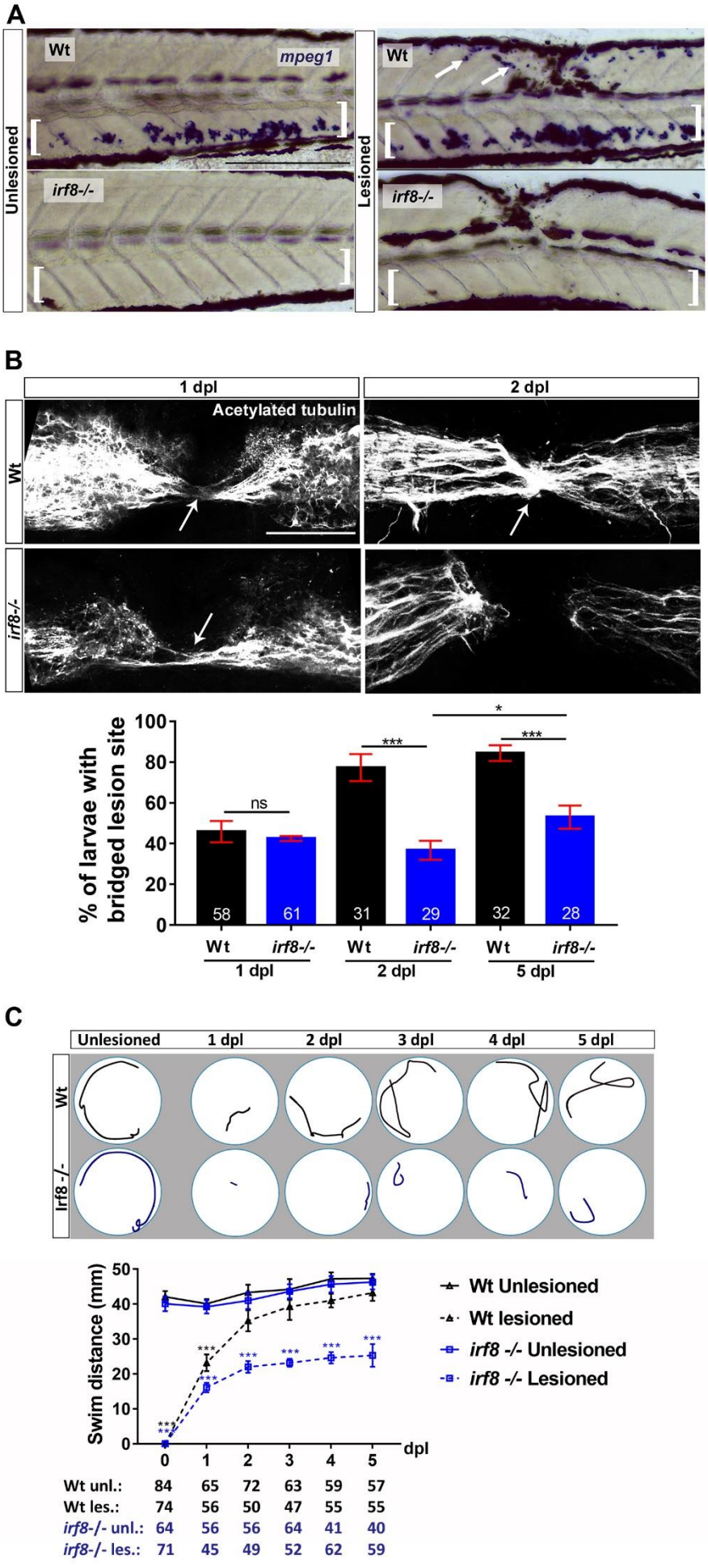
A
Unlesioned
Lesioned
Wt
mpeg1
irf8-/-
Wt
irf8-/-
B
1 dpl
2 dpl
Acetylated tubulin
Wt
irf8-/-
% of larvae with bridged lesion site
100
80
60
40
20
0
ns
***
*
***
58
61
31
29
32
28
Wt
irf8-/-
Wt
irf8-/-
Wt
irf8-/-
1 dpl
2 dpl
5 dpl
C
Unlesioned
1 dpl
2 dpl
3 dpl
4 dpl
5 dpl
Wt
Irf8 -/-
Swim distance (mm)
50
40
30
20
10
0
dpl
0
1
2
3
4
5
Wt Unlesioned
Wt lesioned
irf8 -/- Unlesioned
irf8 -/- Lesioned
Wt unl.: 84 65 72 63 59 57
Wt les.: 74 56 50 47 55 55
irf8-/- unl.: 64 56 56 64 41 40
irf8-/- les.: 71 45 49 52 62 59

Fig. 5: In the *irf8* mutant, axonal regeneration and functional recovery after injury show long-term impairment. A: In situ hybridization for mpeg1 confirms the absence of macrophages and microglial cells before and after injury in the *irf8* mutant compared to controls. Arrows indicate labeling around the injury site and brackets indicate the ventral area of the larvae where the macrophages can be found in the circulation. Note that blackish colour is due to melanocytes. B: Quantification of the proportion of larvae with axonal bridging (anti-acetylated Tubulin) shows that at 1 dpl, axonal bridging is unimpaired in *irf8* mutants, whereas at 2 dpl, *irf8* mutants fail to show full regrowth and even by 5 dpl, the proportion of *irf8* larvae with a bridged lesion site is still lower than in wildtype controls (Fisher's exact test: ***P<0.001, n.s. indicated no significance). C: *Irf8* mutants never fully recover touch-evoked swimming distance in the observation period, whereas wildtype control animals do. Representative swim tracks are displayed. Note that unlesioned *irf8* larvae show swimming distances that are comparable to those in wildtype controls (Two-way ANOVA: $F_{15, 1372} = 11.42$, P<0.001; unles. = unlesioned, les. = lesioned). All lesions are done at 3 dpf. The experiment was performed using 3 different biological replicates and the samples were blinded during the whole experiment. Lateral views of the injury site are shown; rostral is left. Arrows indicate axonal bridging. Scale bars: 200 µm in A and 50 µm in C. Error bars indicate SEM. Numbers on figure relate to number of larvae used.

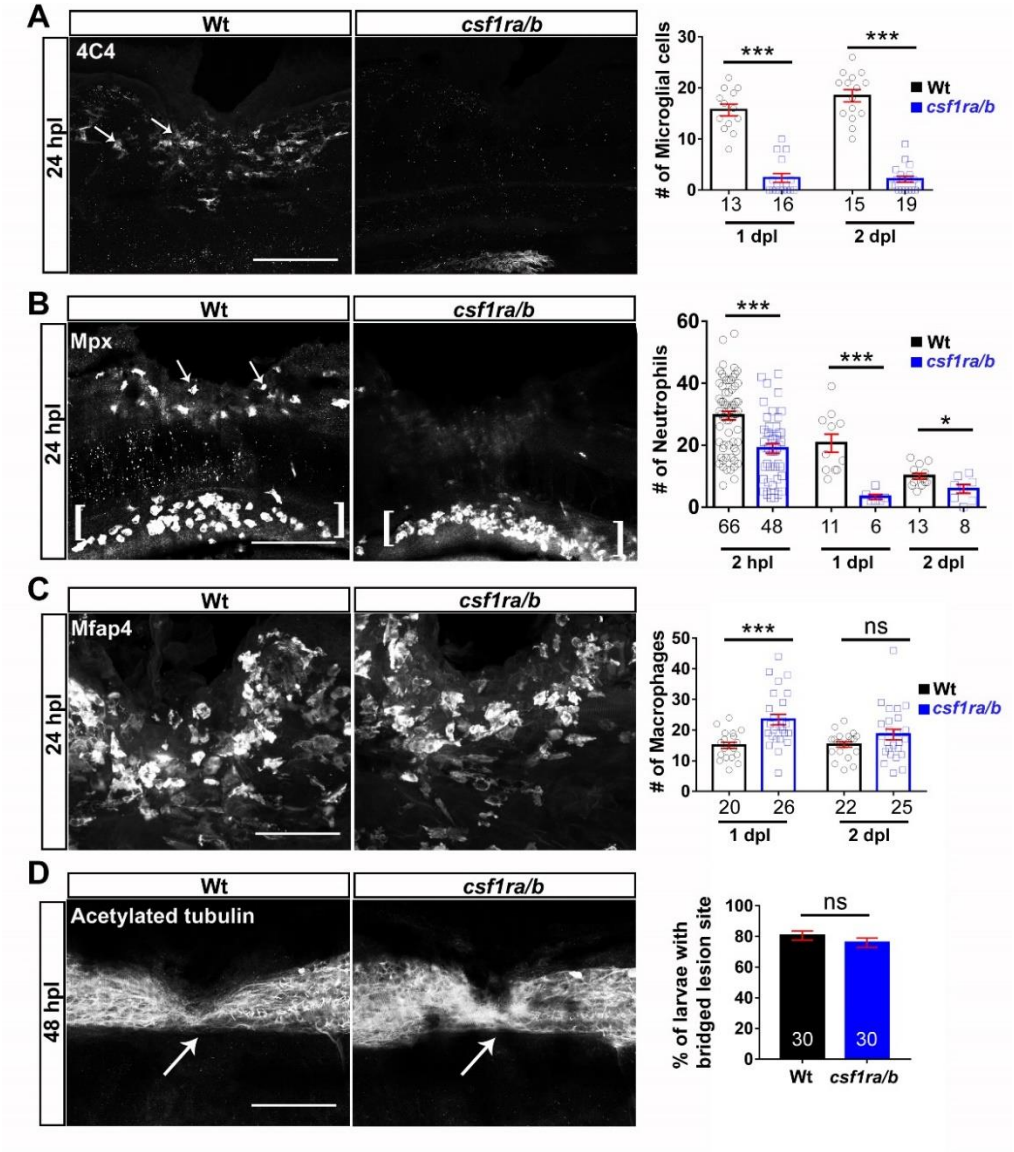

Fig. 6: Absence of microglial cells and reduced neutrophil numbers do not affect axon bridging. A: Numbers of microglial cells (4C4+; arrows) in the injury site of the csfr1a/b mutants are much lower than in wildtype animals (One-way Anova $F_{3, 59} = 87.7$ followed by Bonferroni multiple comparisons: ***P<0.001). B: Fewer neutrophils (Mpx+) are found in the injury site (arrows) of csfr1a/b mutants than in wildtype animals (One-way Anova $F_{5, 146} = 19.91$ followed by Bonferroni multiple comparisons: *P<0.05, ***P<0.001). Note neutrophils ventral to the injury site (brackets). C: The number of macrophages (Mfap4+) is increased in the injury site in the mutants at 1dpl, but not at 2dpl (One-way Anova $F_{3, 89} = 7.224$ followed by Bonferroni multiple comparisons: ***P<0.001, ns indicated no significance). D: Immunostaining against acetylated tubulin shows that axon bridging (arrows) is not affected in the mutants compared to wildtype animals at 2 dpl (Fisher's exact test: ns indicates no significance). Lateral views of the injury site are shown; rostral is left.

Wt = wildtype; Scale bars: 50 µm in A, B, D; 25 µm in B. Error bars indicate SEM. Numbers on figure relate to number of larvae used.

5.2.4 Macrophages are not necessary for Col XII deposition

Next, I asked whether macrophages act via a previously reported regeneration-promoting mechanism, comprising Wnt-dependent deposition of Col XII in the lesion site by *pdgfrb*:GFP^{+} fibroblast-like cells (Wehner et al. 2017). Inhibition of the immune response with dexamethasone did not inhibit appearance of *pdgfrb:*GFP^{+} fibroblast- like cells in the lesion site (Fig. 7A).

By crossing a reporter line for Wnt pathway activity (*6xTCF*:dGFP)[1] into the *irf8* mutant, we found that activation of the pathway was unaltered in the mutant (Fig. 7E). Similarly, expression of *col12a1a* and *col12a1b* mRNA in *irf8* mutants was indistinguishable from that in wildtype animals (Supplementary Fig. 4B). Deposition of Col I protein and mRNA expression of 11 other ECM components were also not altered in the *irf8* mutant at 1 and 2 dpl (Fig. 7B,C). Moreover, immunolabelling against Tp63 showed that by 2 dpl, the injury site in the *irf8* mutants was completely covered by basal keratinocytes, an additional source of Col XII (Wehner et al. 2017), as in wildtype animals (Fig. 7D).

In contrast, a PCR screen of 21 potentially macrophage- derived ECM-modifying matrix metalloproteinases (Newby 2008) (mmps) indicated lower mRNA levels for *mmp11a*, *mmp16a/b*, *mmp24*, and *mmp28* in the injury site of *irf8* mutants compared to wildtype animals (Fig. 8A,B). This suggests a potential for macrophages to alter the lesion site ECM with mmps. Overall, macrophages do not overtly regulate Wnt-signalling, deposition of some crucial ECM components or basal keratinocyte coverage of the injury site during regeneration.

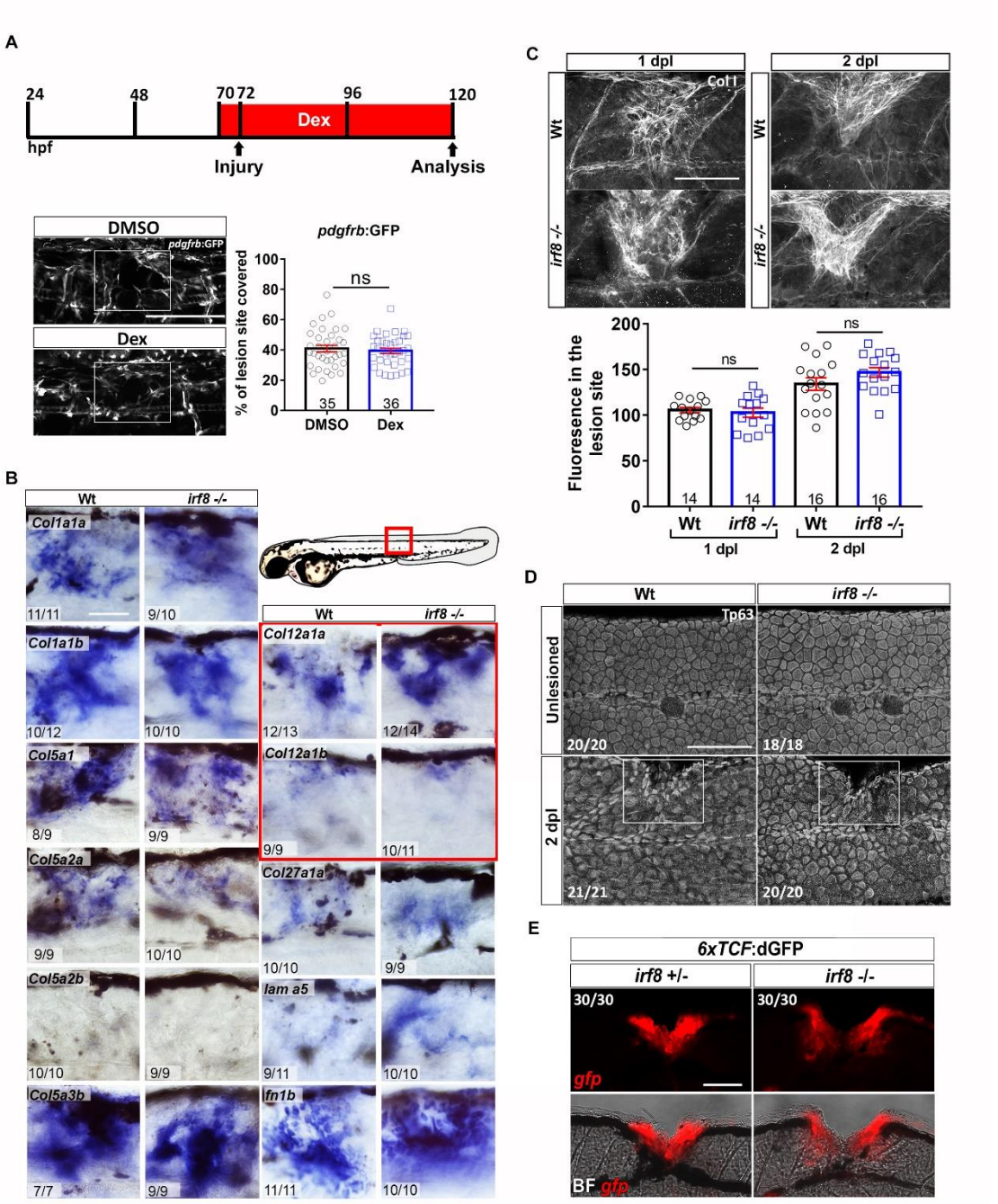

Fig. 7: Wnt-dependent ECM deposition and wound healing are not affected by compromising the immune reaction. A: The density of fibroblast-like cells (pdgfrb:GFP+) in the lesion site is not affected by inhibition of the immune response with dexamethasone (Dex) (t-test, ns = not significant). B: Expression of mRNAs for major ECM components, including col12a1a and col12a1b (red box) is not impaired in the absence of macrophages in *irf8* mutants. C: Immunoreactivity for Collagen I (Col I) is not altered in *irf8* mutants, compared to wildtype controls at 1 dpl and 2 dpl (One-way Anova F (3, 56) = 16.52 followed

by Bonferroni multiple comparisons: ns indicated no significance). D: Basal keratinocytes (anti-Tp63+) cover the injury site (indicated by rectangle) in *irf8* mutants by 2 dpl, similar to wildtype animals. E: Activation of the Wnt pathway is unaltered in *irf8* mutants after injury. The 6xTCF:dGFP reporter line crossed into the *irf8* mutants shows activation of Wnt signalling that is comparable to that in wildtype animals at 2 dpl. Lateral views of the injury site are shown.; rostral is left. Scale bars: 50 μm. Error bars indicate SEM. Numbers on figure relate to number of larvae used.

A

Gene ID	Gene name	Wt	*irf8-/-*
ZDB-GENE-070817-3	*mmp11a-matrix metallopeptidase 11a*	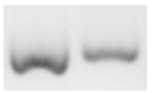	
ZDB-GENE-070820-1	*mmp16a-matrix metallopeptidase 16a*		
ZDB-GENE-061009-22	*mmp16b-matrix metallopeptidase 16b*	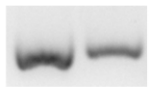	
ZDB-GENE-040724-262	*mmp24-matrix metallopeptidase 24*	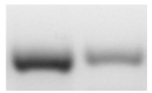	
ZDB-GENE-100226-1	*mmp28-matrix metallopeptidase 28*	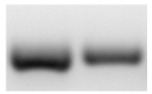	
	β-actin	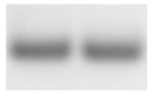	

B

Not regulated

Gene ID	Gene name
ZDB-GENE-030131-9123	*mmp2-matrix metallopeptidase 2*
ZDB-GENE-040426-2132	*mmp9-matrix metallopeptidase 9*
ZDB-GENE-070817-2	*mmp11b-matrix metallopeptidase 11b*
ZDB-GENE-031202-2	*mmp13a-matrix metallopeptidase 13a*
ZDB-GENE-030131-6152	*mmp13b-matrix metallopeptidase 13b*
ZDB-GENE-030901-1	*mmp14a-matrix metallopeptidase 14a*
ZDB-GENE-030901-2	*mmp14b-matrix metallopeptidase 14b*
ZDB-GENE-070817-4	*mmp15a-matrix metallopeptidase 15a*
ZDB-GENE-070817-6	*mmp15b-matrix metallopeptidase 15b*
ZDB-GENE-070820-2	*mmp17a-matrix metallopeptidase 17a*
ZDB-GENE-081107-17	*mmp17b-matrix metallopeptidase 17b*
ZDB-GENE-100308-3	*mmp19-matrix metallopeptidase 19*
ZDB-GENE-100603-2	*mmp20a-matrix metallopeptidase 20a*
ZDB-GENE-100603-3	*mmp20b-matrix metallopeptidase 20b*
ZDB-GENE-050417-448	*mmp23bb-matrix metallopeptidase 23bb*
ZDB-GENE-060421-5765	*mmp30-matrix metallopeptidase 30*

Fig. 8: Some matrix metalloproteases showed reduced expression in *irf8* mutants. A: RT-PCR showed lower expression of 5 mmp genes in the injury site of *irf8* mutants compared to wildtype. B: mmp genes for which no robust change in *irf8* mutants could be detected are listed.

5.2.5 Cellular debris is not a major impediment to regeneration

Macrophages could serve as a substrate for axon growth or promote regeneration by removing debris by phagocytosis - a major function of macrophages in peripheral nerve regeneration in zebrafish (Rosenberg et al. 2012, Villegas et al. 2012). In time-lapse movies of double transgenic animals in which neurons (*Xla.Tubb*:DsRed) and macrophages (*mpeg1*:GFP) were labelled (Fig. 9B) we observed axons crossing the spinal lesion site at the same time macrophages migrated in and out of the injury site.

However, no obvious physical interactions between these cell types were observed, making it unlikely that macrophages acted as an axon growth substrate. We frequently observed macrophages ingesting neuronal material and transporting that away from the injury site in time-lapse movies (Fig. 9B).

In agreement with this observation, TUNEL labelling indicated strongly increased levels of dead or dying cells in the late (48 hpl), but not the early (24 hpl) phase of axonal regeneration in the injury site of *irf8* mutants (Fig. 9A). To determine the impact of debris on regeneration, we prevented cell death and consequently debris accumulation in *irf8* larvae using the pan-caspase inhibitor QVD (Keoni and Brown 2015), that is functional in zebrafish (Ogryzko et al. 2014).

This treatment led to lower debris levels that were comparable to those seen in wildtype larvae at 2 dpl (Fig. 9C) but failed to increase regenerative success in *irf8* mutants (control, 38 % of examined larvae with axon bridges; QVD, 40 %. Thickness of axon bridge: control 19.03 µm +/- 2.14 µm; QVD: 18.32 µm +/- 2.53 µm; t-test: $P > 0.05$. Supplementary Fig. 6E). Conversely, inhibiting debris phagocytosis with the pharmacological inhibitor O- phospho-L-serine (L-SOP) (Witting et al. 2000) in wildtype animals increased levels of debris in the injury site, but did not impair axonal bridging (Fig. 10A-C).

This suggests no obvious connection between debris levels and/or phagocytosis and regenerative success.

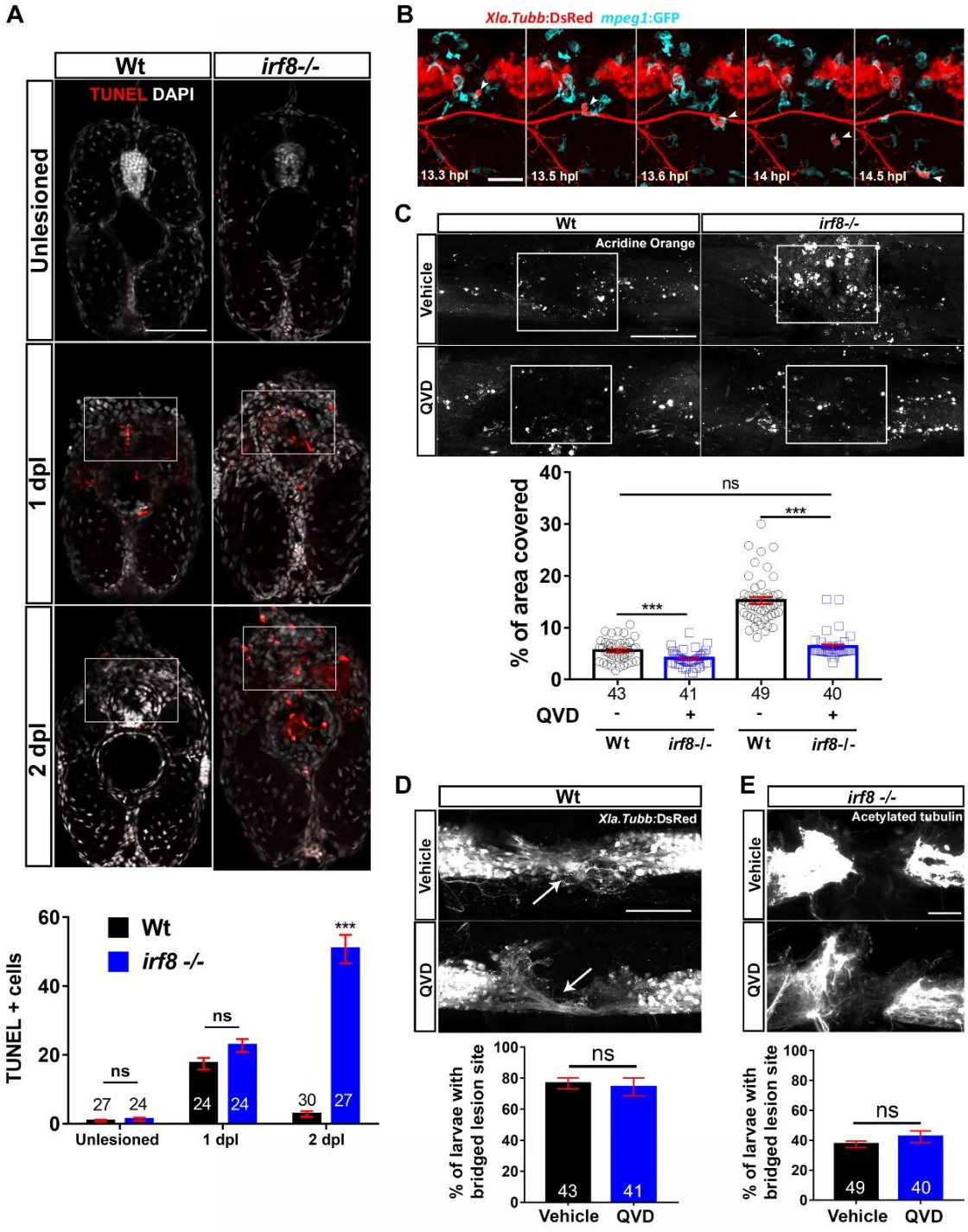

Fig. 9: Debris removal by macrophages is not a major factor for axonal regeneration. A: TUNEL labelling on cross sections of larvae (dorsal is up) shows an increased number of TUNEL+ cells in the injury site (indicated by rectangle) of the *irf8* mutant fish at 2

dpl, but not at 1 dpl (Two-way Anova $_{F\ 3,\ 121}$ = 112.5 followed by Bonferroni multiple comparisons: ***P<0.001, ns = not significant). B: Time-lapse video-microscopy shows that macrophages (cyan, mpeg1:EGFP) are in the injury site and remove neuronal debris (XIa.tubb:DsRed). Arrowheads point out a macrophage with phagocytosed neuronal material. C: Acridine orange labelling at 2 dpl indicates increased levels of debris in the *irf8* mutant, which is reduced to wildtype levels with the pan-caspase inhibitor QVD (Kruskal-Wallis with Dunn's multiple comparisons post-test: *** P<0.001, ns indicates no significance). D,E: Inhibition of cell death with QVD does not alter regenerative success in wildtype animals (D) or *irf8* mutants (E) at 2 dpl (Fisher's exact test: ns indicates no significance). Rectangles indicate regions of quantification and arrows indicate axonal bridges. Lateral views of the injury site are shown (except A); rostral is left. Scale bars: 25µm A, 100 µm B, C, D, E, 50 µm. Error bars indicate SEM. Numbers on figure relate to number of larvae used.

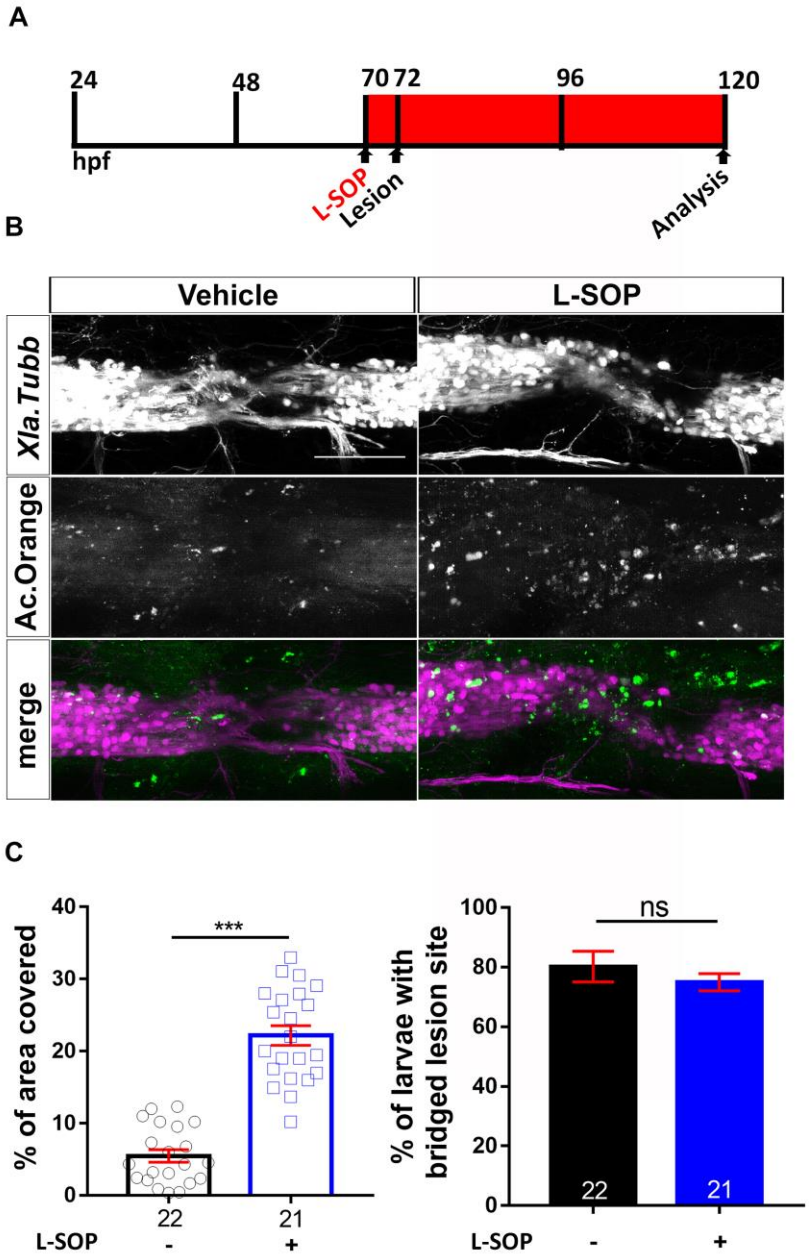

Fig. 10: Treatment with the phagocytosis inhibitor O-Phospho-L-serine (L-SOP) does not affect regenerative success. A: The experimental timeline is shown. B: Treatment with L-SOP increases the amount of debris, detected with acridine orange (t-test: ***P<0.001), but has no effect on axon bridging (XIa.tubb:DsRed; Fisher's exact test: ns indicates no significance) at 2 dpl. Lateral views of the injury site are shown; rostral is left. Scale bar: 100 µm. Error bars indicate SEM. Numbers on figure relate to number of larvae used.

5.2.6 Pro-and anti-inflammatory phases are altered in irf8 mutants

To determine a possible role of cytokines in the regenerative failure of *irf8* mutants, we analysed relative levels of pro-and anti-inflammatory cytokines in the lesion site during regeneration in wildtype animals and *irf8* mutants by qRT-PCR. In wildtype animals, expression levels of pro-inflammatory cytokines *Il-1β* and *TNF-α* were high during initial regeneration (> 25-fold for *Il-1β*; >12-fold for *TNF-α* for approximately to 12 hpl) and reduced again during late regeneration (12- 48 hpl), although still elevated compared to unlesioned controls (Fig. 11A,B). Anti-inflammatory cytokines, such as *tgf-β1a* and *tgf-β3* were expressed at low levels during initial regeneration, and upregulated during late regeneration (approximately 3-fold for *tgf-β1a* and 2-fold for *tgf-β3*), indicating a bi-phasic immune response within the 48-hour time frame of analysis (Fig. 11C,D).

In *irf8* mutants, levels of pro-inflammatory cytokines remained high during the late phase of regeneration (Fig. 11A,B) and anti-inflammatory cytokines were not upregulated (Fig. 11C,D), resulting in a sustained pro-inflammatory environment in *irf8* mutants.

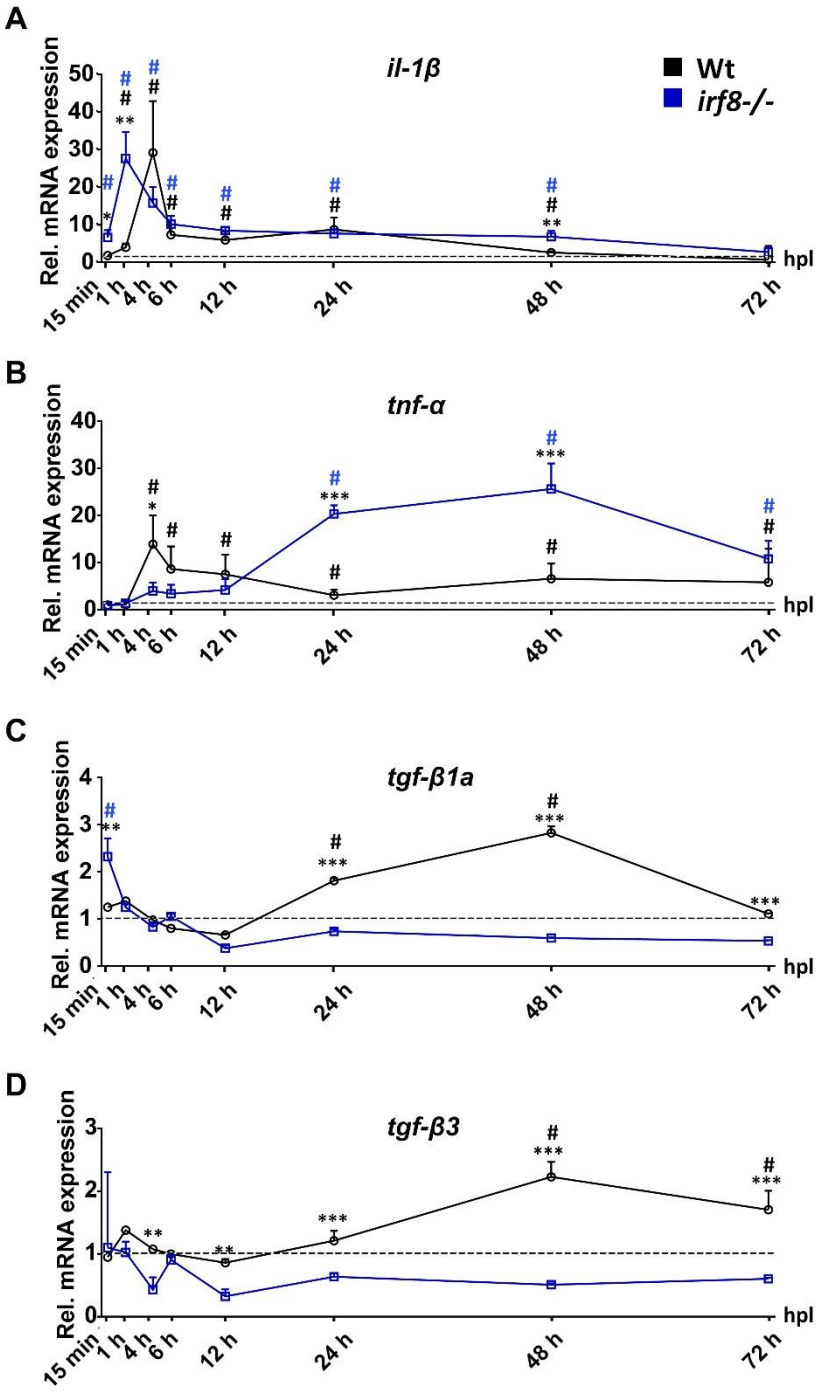

Fig. 11: Inflammation is bi-phasic and dysregulated in *irf8* mutants. A,B: Absence of macrophages in the *irf8* mutant fish leads to increased Il-1β and TNF-α mRNA levels during the late stage of inflammation (>12hpl). An early peak in TNF-α expression is missing in *irf8* mutants. C,D: Expression of anti- inflammatory cytokines, tgf-β1a and tgf-β3, which peak during late regenerative phases in wildtype animals, is strongly reduced in *irf8* mutants (t-

tests: *P<0.05, **P<0.01, ***P<0.001; wt = wildtype animals). # indicates statistical significance when compared to unlesioned animals. Error bars indicate SEM.

The lack of anti-inflammatory cytokines correlated with the lack of macrophages and microglia in *irf8* mutants. We performed qRT-PCR in fluorescence activated flow sorted *mpeg1*:GFP cells in wildtype animals to determine whether macrophages and microglial cells expressed *tgf-β1a and tgf-β3. mpeg1*:GFP+ cells, but also *mpeg1*:GFP negative cells expressed these cytokines (Fig. 12A). In situ hybridisation showed wide-spread labelling with some more strongly labelled cells around the injury site in wildtype, but not *irf8* mutants (Fig. 12B). This is consistent with expression of *tgf-β1a* and *tgf-β3* in microglia/macrophages and other cell types (Finnson et al. 2013). Hence, the immune response is bi-phasic with an initial pro-inflammatory phase, followed by an anti-inflammatory phase in wildtype animals. In the absence of macrophages in *irf8* mutants, animals fail to switch to an anti-inflammatory state.

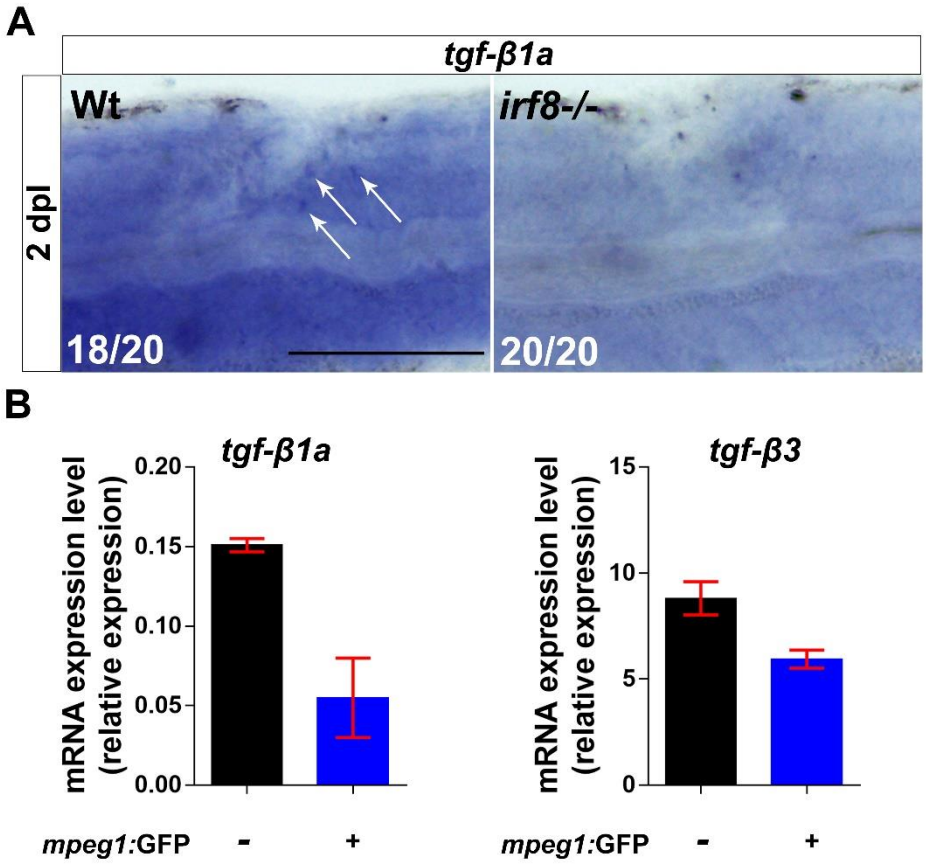

Fig. 12: Tgf-β is expressed by macrophages and other cell types. A: In situ hybridization for tgf-β1a shows widespread expression in the lesioned trunk of wildtype and *irf8* mutant larvae at 2 dpl. Arrows show possible macrophages around the injury site of wildtype larvae that are not present around the injury site of *irf8* mutant larvae. B: Quantitative RT-PCR using the GFP+ and the GFP- cell populations of the injury site tissue of lesioned mpeg1:GFP larvae shows expression of tgf-β1a and tgf-β3 in purified macrophages (GFP+) and other cell types (GFP-). Lateral views of the injury site are shown; rostral is left. Scale bar: 200 µm. Error bars indicate SEM. Numbers on figure relate to number of larvae used.

5.2.7 TNF-α promotes axonal regeneration

To determine whether increased levels of pro-inflammatory cytokines contributed to impaired axon growth in *irf8* mutants, we first inhibited TNF-α signaling. The animals were originally treated with pomalidomide, a selective pharmacological inhibitor of TNF-α release (Muller et al. 1999). The animals were pre-treated with the inhibitor, injured and then transferred back to the inhibitor until the analysis. Previous work in the lab has shown that pre-treatment is more efficient than treatment after injury. The working concentration that was used (170 µM) was selected based on the work from (Mahony et al. 2013) which showed that this concentration has anti-inflammatory effects in zebrafish, it's able to reduce the levels of TNF-α protein and is not teratogenic for zebrafish larvae. The treatment had no effect on axonal regrowth in *irf8* mutants. In contrast, in wildtype animals Pomalidomide strongly inhibited axon bridging at 1 dpl (control: 62 % of examined animals showed an axonal bridge; Pomalidomide: 36 %) and 2 dpl (control: 75 % of examined animals; Pomalidomide: 45 %) (Fig. 13A). To confirm pharmacological results, we targeted *TNF-α* by using CRISPR manipulation with a gene–specific guideRNA (gRNA). Injection of the gRNA into the zygote efficiently mutated the gene as shown by restriction fragment length polymorphism (RFLP) analysis (Fig. 13B) and produced function-disrupting insertion- deletion mutations in a highly conserved domain (Savan et al. 2005) (Table 1). Western blots of 4-day old larvae and immunohistochemistry in the injury site showed robustly reduced TNF-α protein levels (Fig. 14A,B).

Axon bridging was inhibited in wildtype animals by *TNF-α* gRNA injection in a way that was comparable to drug treatment (1 dpl: control: 51 % of examined animals showed bridging; gRNA: 27 %; 2 dpl: control: 88 % of examined animals showed bridging; gRNA: 40 %). At 5 dpl, axon bridging was still strongly impaired (control: 84.1 % of examined animals showed bridging; gRNA: 38.3 %; Fig. 13C), indicating long-term impairment of regeneration. Hence, *TNF-α* dysregulation is not a major

cause of regenerative failure in *irf8* mutants, but *TNF-α* is necessary for axonal regeneration in wildtype animals.

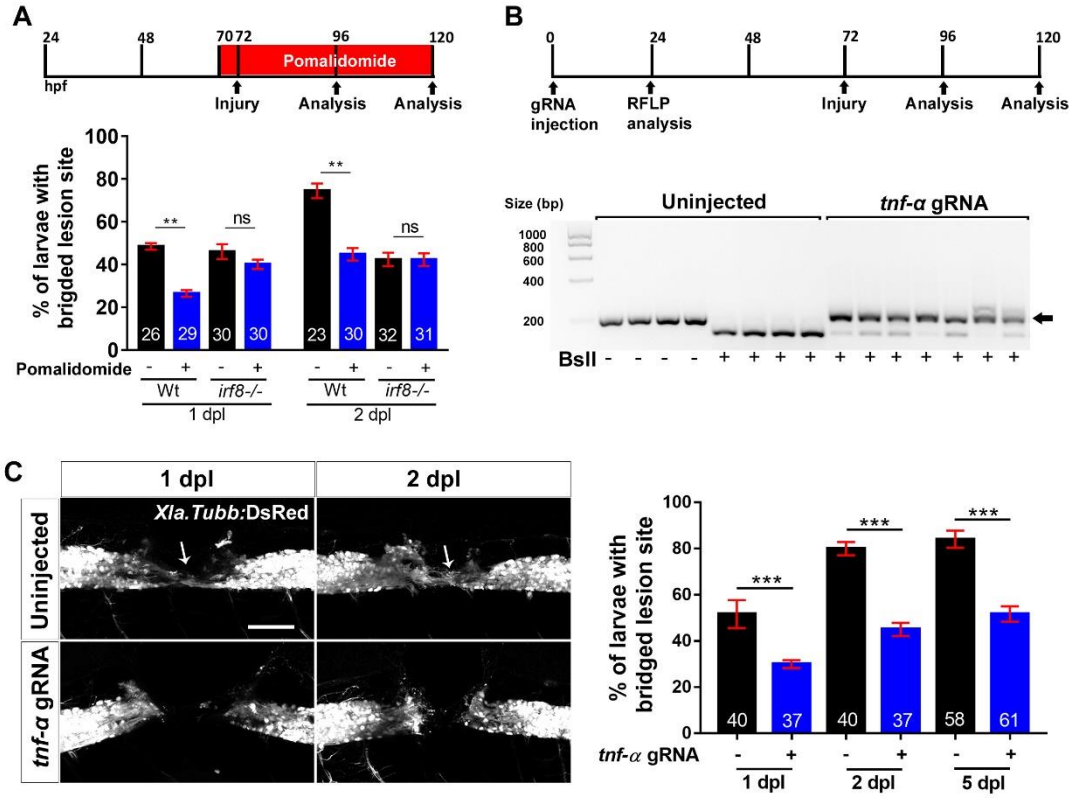

Fig. 13: TNF-α is essential for axonal regeneration. A: TNF-α inhibition by Pomalidomide reduces the proportion of wildtype animals with axon bridging at 1 and 2 dpl. No effect is observed in *irf8* mutants (Two-way ANOVA followed by Bonferroni post-test: $F_{3, 16} = 12.16$, **P<0.01, n.s indicates no significance). B: CRISPR/Cas9-mediated disruption of TNF-α is effective as shown by RFLP analysis. This reveals efficient somatic mutation in the gRNA target site, indicated by resistance to restriction endonuclease digestion (arrow). C: Axonal bridging (arrow; Xla.Tubb:DsRed+) is strongly impaired after disruption of the TNF-α gene. (Fisher's exact test: **P<0.01) and the impairment persists at 5 dpl. Lateral views of the injury site are shown; rostral is left. Scale bar: 50 µm. Error bars indicate SEM. Numbers on figure relate to number of larvae used.

To determine which cells expressed *TNF-α* in wildtype animals, we used immunohistochemistry for L-Plastin, labelling all immune cells, in *TNF-α:*GFP

transgenic fish (Fig. 14D). Nearly all *TNF-α:*GFP^{+} cells co-labelled with L-Plastin (96 %) at 12 hpl. Thus, expression of *TNF-α* occurred mainly in immune cells (Fig. 14A). Double-labelling *TNF-α:*GFP reporter fish with neutrophil (Mpx), microglia (4C4) and macrophage (Mfap4) markers at 24 hpl, when axons were actively growing, indicated that >95 % of *TNF-α:*GFP^{+} cells in the injury were peripheral macrophages. However other cell types, such as neurons (Kisiswa et al. 2013), may also express *TNF-α.* More than 72 % of macrophages were *TNF- α:*GFP^{+}, whereas for microglia (< 6.5 %) and neutrophils (< 0.7 %) the proportion was much smaller. Over time, the proportion of *TNF-α:*GFP^{+} macrophages was reduced (from 72.5 % at 1dpl to 59 % at 2 dpl) (Fig. 6B). Our observations suggest that macrophages promote regeneration by expressing *TNF-α*. To elucidate effects of *TNF-α* inhibition, we determined numbers of neutrophils and macrophages/microglia at 24 and 48 hpl in *TNF-α* gRNA injected animals. This showed no changes in macrophages, but a 49.7 % increase in the number of neutrophils at 1 dpl (Fig. 14C). qRT-PCR indicated that *Il-1β* mRNA levels were increased by 108 %, whereas *TNF-α, tgf-β1a* and *tgf-β3* mRNA levels remained unchanged at 2 dpl (Fig. 14D). This suggests a moderate enhancement of the pro- inflammatory response when TNF-α is inhibited.

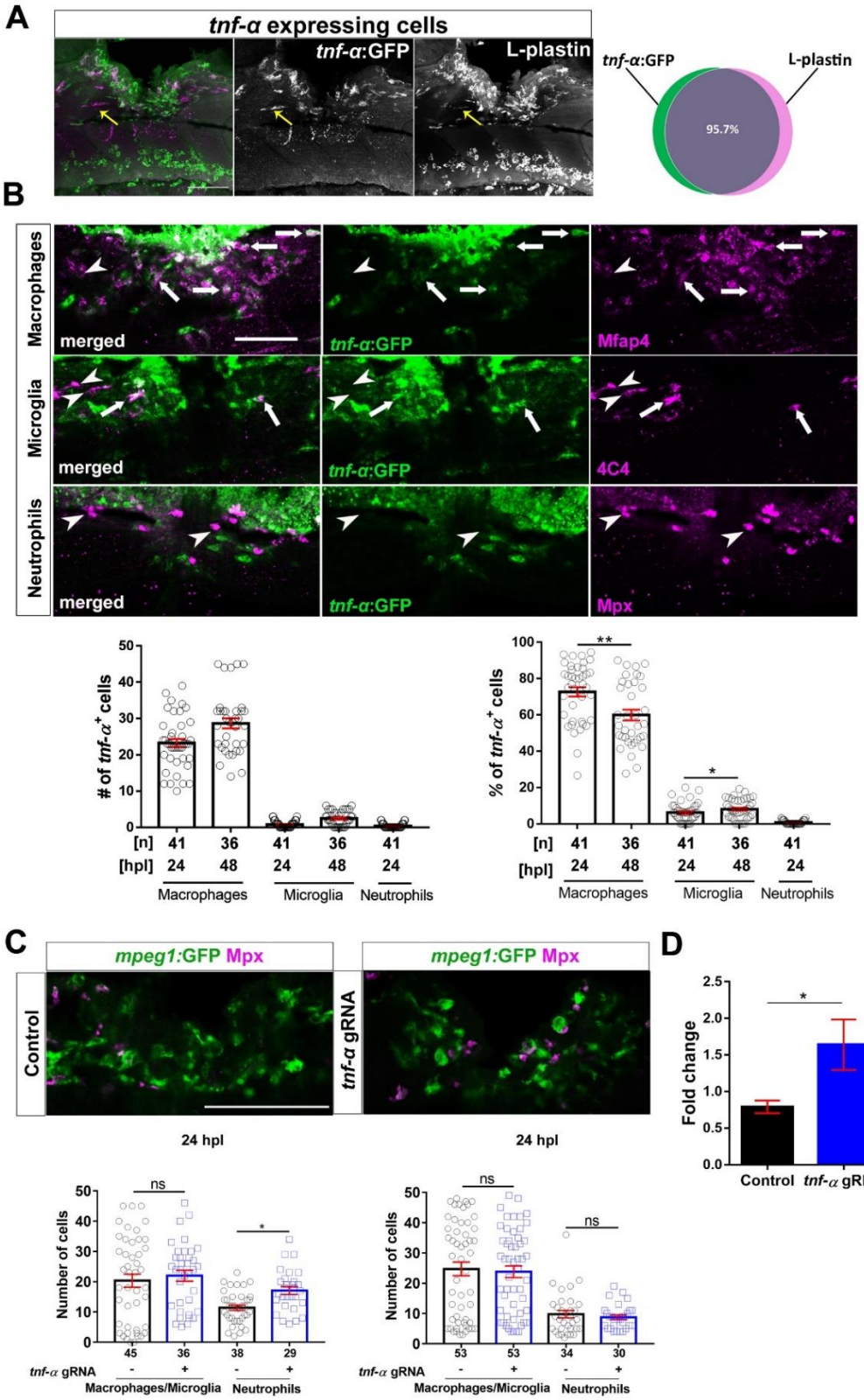
A
tnf-α expressing cells
tnf-α:GFP
L-plastin
tnf-α:GFP
L-plastin
95.7%
B
Macrophages
Microglia
Neutrophils
merged
tnf-α:GFP
Mfap4
4C4
Mpx
# of tnf-α+ cells
% of tnf-α+ cells
[n] 41 36 41 36 41
[hpl] 24 48 24 48 24
Macrophages
Microglia
Neutrophils
C
mpeg1:GFP Mpx
Control
tnf-α gRNA
24 hpl
Number of cells
ns
*
45 36 38 29
tnf-α gRNA - + - +
Macrophages/Microglia
Neutrophils
53 53 34 30
D
Fold change
Control
tnf-α gRNA

Fig. 14: TNF-α is mostly expressed by macrophages in the lesion site of wildtype animals. A: Top row: TNF-α:GFP labelling occurs almost exclusively in L-plastin+ immune cells (L-plastin in green; TNF-α:GFP in magenta; yellow arrow indicates a rare TNF- α:GFP+ microglial cell; 12 hpl) B: In the injury site, the number and proportion of macrophages (Mfap4+) that are TNF-α:GFP+ are much higher than numbers and proportions of microglia (4C4+) and neutrophils (Mpx+), indicating that the main source of TNF-α is the macrophages. Arrows indicate double-labelled cells and arrowheads indicate immune cells that are TNF-α:GFP-. Single optical sections are shown; the proportion of macrophages that are TNF-α:GFP+ decreases over time, whereas the proportion of TNF-α:GFP+ microglial cells slightly increases (One-way ANOVA followed by Bonferroni post-test: F 4, 195 = 376.3, **P<0.01, *P<0.05). C: Quantification of the immune cells after TNF-α gRNA injection shows that TNF-α disruption leads to increased numbers of neutrophils (Mpx+) at 1 dpl but not at 2 dpl, whereas the numbers of macrophages/microglia (mpeg1:GFP+) remains unchanged (Kruskal-Wallis test followed by Dunn's multiple comparisons: *P<0.05, ns indicates no significance). D: qRT-PCR indicates that TNFTNF-α disruption leads to increased levels of Il-1β mRNA at 2 dpl (t- tests: *P<0.05). Lateral views of the injury site are shown; rostral is left. Scale bars: 50 μm. Error bars indicate SEM. Numbers on figure relate to number of larvae used.

Table **1.** List of mutations after CRISPR/Cas9 editing of *TNF-α*.

5.2.8 Il-1β inhibits regeneration in irf8 mutants

To test whether sustained high levels of Il-1β were responsible for regenerative failure in *irf8* mutants, we interfered with *Il-1β* function in three different ways. Firstly, we inhibited caspase-1, which is necessary for activation of Il-1β, using the pharmacological inhibitor YVAD that is functional in zebrafish (Vojtech et al. 2012) (Fig.15A-E). Secondly, we disrupted *Il-1β* RNA splicing with an established morpholino (Supplementary Fig. 10A-D) (Nguyen-Chi et al. 2014). Finally, we targeted *Il-1β* in a CRISPR approach (Fig. 16E- H).

To determine whether interfering with Il-1β function mitigated inflammation in *irf8* mutants, we quantified immune cells, expression of *Il-1β*, *TNF-α* and dead cells. Indeed, after YVAD treatment we observed a reduction of neutrophil peak numbers (by 38 % at 2 hpl; Fig. 15B), as well as strongly reduced levels of *Il-1β* and *TNF-α* mRNA expression (at 2 dpl; Fig. 15A) in *irf8* mutants. Moreover, the number of TUNEL^{+} cells was reduced at 2 dpl in the *irf8* mutant, but not to wildtype levels (Fig. 15C). In lesioned wildtype animals, YVAD reduced peak numbers of neutrophils (by 40 % at 2 hpl) and macrophages (by 28 % at 48 hpl), but no influence on low numbers of TUNEL^{+} cells at 2 dpl was observed. Hence, interfering with Il-1β function reduces inflammation in *irf8* mutants and wildtype animals. Axon bridging in wildtype animals was not affected by YVAD treatment at 2 dpl (control: 79 % of examined animals showed bridging; YVAD: 78 %) (Fig. 15D), indicating that high levels of Il-1β were not necessary for axonal regeneration. In contrast, in YVAD-treated *irf8* mutants, we observed a remarkable rescue of axon bridging at 2 dpl (control: 38 % of examined animals showed bridging; YVAD: 69 %) (Fig. 15D).

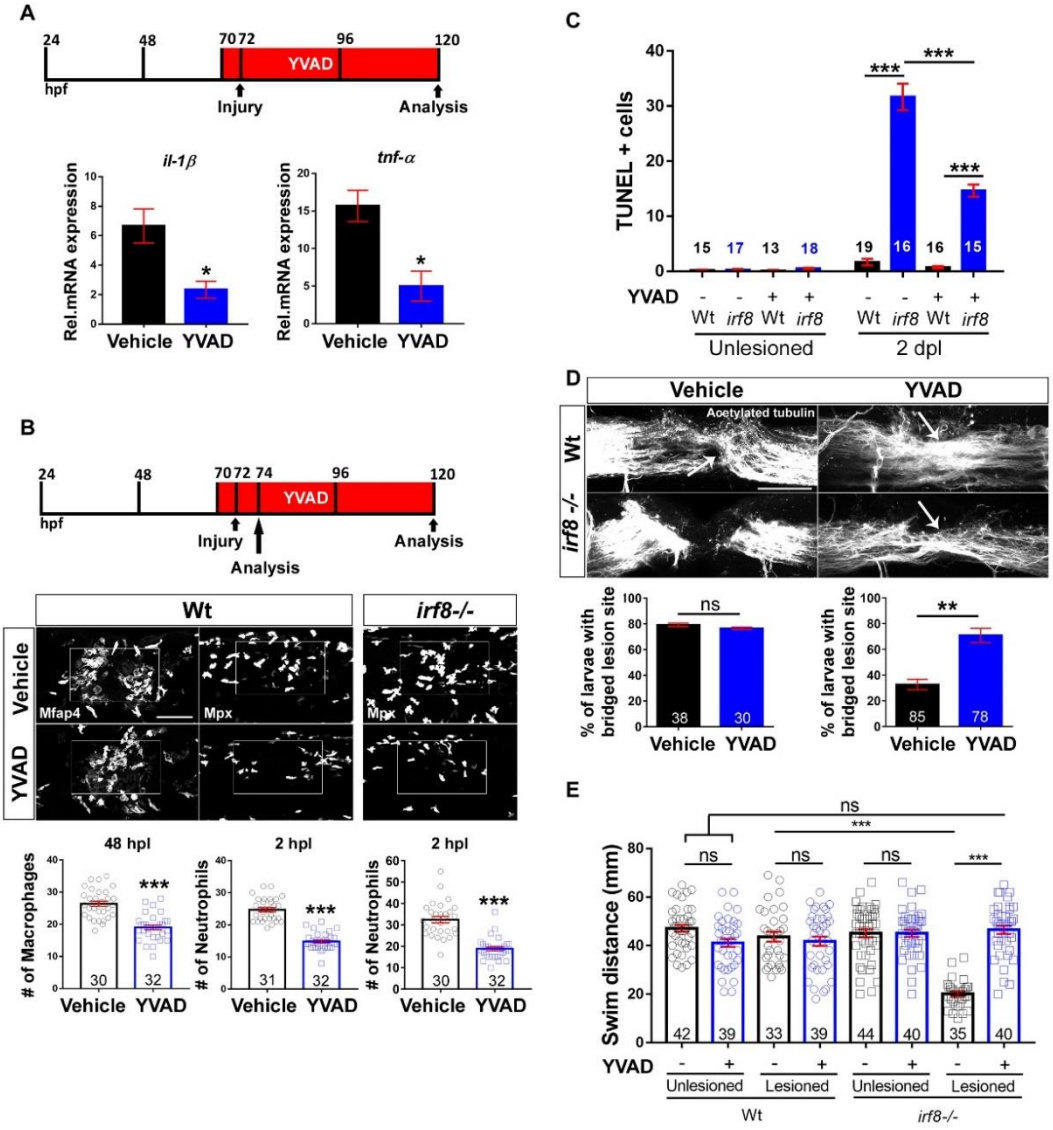

Fig. 15: Inhibition of Il-1β function rescues axonal regeneration in *irf8* mutants. Lateral views of the injury site are shown; rostral is left. A: YVAD reduces expression levels of Il-1β and TNF-α in *irf8* mutants (two-sample t-test: *P<0.05) at 2 dpl. B: YVAD impairs migration of peripheral macrophages (Mfap4+) and neutrophils (Mpx+) in wildtype animals and *irf8* mutants (only neutrophils quantified, due to absence of macrophages) (t-tests: ***P<0.001). C: YVAD moderately reduces the number of TUNEL+ cells in the *irf8* mutants at 2 dpl. (Two-Way ANOVA followed by Bonferroni multiple comparisons: $F_{3, 121} = 112.5$, ***P<0.001). D: YVAD does not influence axonal regeneration in wildtype animals but rescues axonal bridging (arrows) in *irf8* mutants (Fisher's exact test: **P<0.01, ns indicates no significance) at 2 dpl. E: Impaired touch-evoked swimming distance in *irf8* mutants is rescued by YVAD treatment, to levels that are no longer different from lesioned and unlesioned wildtype animals at 2 dpl. YVAD has no influence on swimming distance in

lesioned or unlesioned wildtype animals (Two-way ANOVA followed by Bonferroni multiple comparisons: F 1, 309 = 35.229, ***P<0.0001, ns indicates no significance). Rectangle in B denotes quantification area. Scale bar: 50 µm for B, D. Error bars indicate SEM. Numbers on figure relate to number of larvae used.

Injecting a well-established (Nguyen-Chi et al. 2014) morpholino targeting *Il-1β* into *irf8* mutants at the one-cell-stage inhibited *Il-1β* splicing (Fig. 16A,D). Morpholino-injected animals showed a rescue of axon bridging at 2 dpl (control: 40 % of examined animals showed bridging; YVAD: 60 %) (Fig. 16B,C). Finally, injecting a gRNA targeting *Il-1β* at the one-cell stage led to somatic mutation in the target site of *Il-1β*, indicated by RFLP analysis (Fig. 16E,H). This strongly rescued axonal bridging in lesioned *irf8* mutants (control: 40 % of examined animals showed bridging; acute *Il-1β* gRNA: 70 %) (Fig. 16F,G). Hence, three independent manipulations show that excessive *Il-1β* levels in *irf8* mutants are a key reason for impaired axonal regeneration.

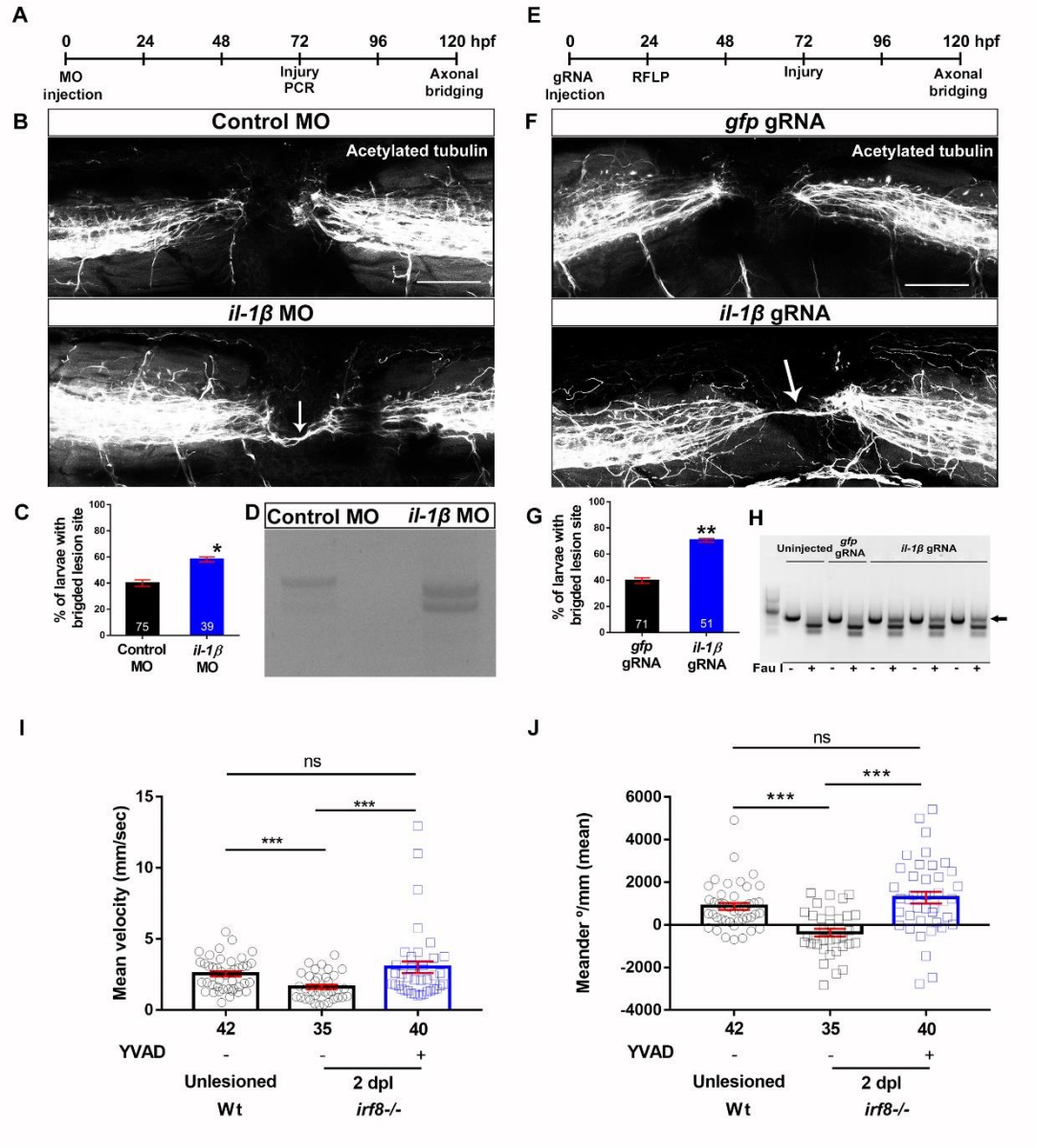

Fig. 16: Inhibition of *Il-1β* expression or disruption of the gene rescue axon bridging and parameters of touch-evoked swimming in *irf8* mutants. A: The timeline for the morpholino manipulations is given. B-D: Morpholino gene knockdown of Il-1β by injecting into the zygote shows characteristic mis-splicing of *Il-1β* mRNA, compared to wildtype animals (D) and partially rescues the bridging phenotype of the *irf8* mutant fish (B,C; Fisher's exact test: *P<0.05). D: Morpholino gene knockdown of Il-1β shows characteristic mis-splicing *of Il-1β* mRNA, compared to wildtype animals. E: The timeline for gRNA manipulation is given. F-G: CRISPR/Cas9-mediated disruption of Il-1β by injecting specific gRNA into the zygote leads to somatic mutations, as shown by RFLP analysis (arrow in H) and rescues the bridging phenotype in *irf8* mutants (F,G; Fisher's exact test: **P<0.01). I,J: YVAD incubation rescues speed (mean velocity) and path shape (meander) that the *irf8* larvae achieve after

injury (Kruskal-Wallis with Dunn's multiple comparisons post-test: *** P<0.001, ** P<0.01, ns indicates no significance). Lateral views of the injury site are shown; rostral is left. Scale bars: 50 µm. Error bars represent SEM. Numbers on figure relate to number of larvae used.

5.2.9 Reduction of Il-1β levels rescues swimming in irf8 mutants.

To determine whether Il-1β inhibition also rescued recovery of swimming function in *irf8* mutants, we analysed touch-evoked swimming distances. YVAD had no effect in unlesioned mutant or wildtype animals and did not affect recovery in lesioned wildtype animals (Fig. 15E). In contrast, YVAD-treatment rescued the touch-evoked swimming distance in *irf8* mutants to levels that were indistinguishable from wildtype lesioned or unlesioned animals (Fig. 15E). Mean velocity and path shape (meandering) were also rescued (Fig. 16I,J). These observations indicate that inhibition of Il-1β alone restores most axonal regeneration and recovery of touch- evoked swimming parameters in the absence of macrophages.

5.2.10 Neutrophils are a major source of Il-1β.

To understand *Il-1β* regulation, we determined the source of Il-1β in wildtype and *irf8* mutants. Using Il-1β immunohistochemistry and a transgenic reporter line (*il- 1β*:GFP), we found expression in microglia, macrophages, neutrophils and basal keratinocytes in the injury site (Figs 17C,D; 18A). Neuronal labelling (HuC/D^{+}) did not overlap with *Il-1β*:GFP labeling (Fig. 18B). While numbers of *Il-1β*:GFP^{+} immune cells did not change significantly between 1 and 2 dpl, the percentage of macrophages (from 50.6 % to 34.3 %) and neutrophils that were labelled for the *Il-1β*:GFP transgene were reduced (from 53.3% to 23.7%), likely reflecting resolution of inflammation (Fig. 18A).

In *irf8* mutants, detection of *Il-1β* mRNA by qRT-PCR and in situ hybridisation

confirmed increased levels at 2 dpl, but not 1 dpl (Fig. 17A,B), despite lack of *Il-1β* expressing microglia and macrophages. Instead, we observed increased numbers of Il-1β^{+} neutrophils (by 97 %) and basal keratinocytes (by 58 %) compared to wildtype animals at 1 dpl (Fig. 17C,D). Importantly, the proportion of neutrophils that were Il-1β^{+} was also increased from 33.6 % in wildtype animals to 49 % in the *irf8* mutant at 1 dpl. This demonstrates that neutrophils are more likely to express *Il-1β* in the absence of macrophages.

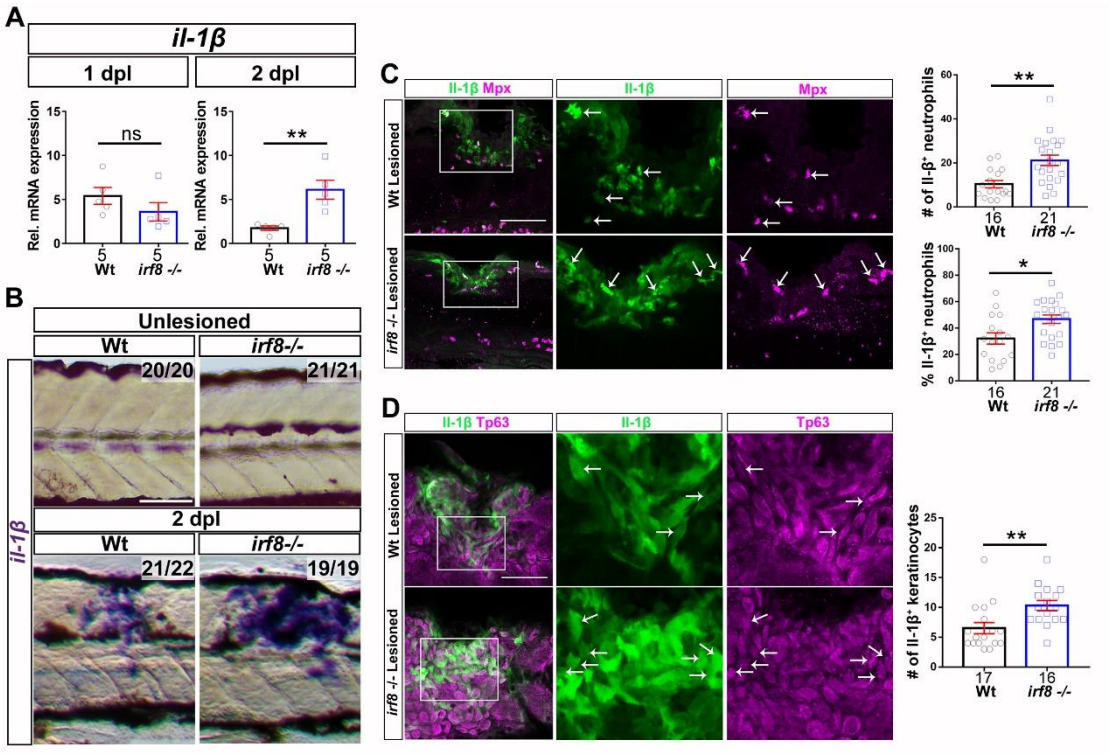

Fig. 17: Levels of Il-1β expression are increased in the injury site of *irf8* mutants. A: At 1 dpl, expression levels of Il-1β are comparable between *irf8* mutants and wildtype (Wt) animals but are higher in the mutant at 2 dpl in qRT-PCR (t-test: **P<0.01, ns indicates no significance). B: In situ hybridization confirms increased expression of Il-1β mRNA at 2 dpl. C: In the injury site, the number and proportion of neutrophils (Mpx+) that are Il-1β immuno-positive (arrows) are increased in *irf8* mutants at 1 dpl compared to wildtype animals. D: The number of basal keratinocytes (Tp63+) that are Il-1β immuno-positive is increased in *irf8* mutants. Single optical sections are shown; boxed areas are shown in higher magnifications (t-test: *P<0.05, **P<0.01). Lateral views of the injury site are shown; rostral is left. Scale

bars: 100 µm in B,C,D and 50 µm for higher magnification areas. Error bars indicate SEM. Numbers on figure relate to number of larvae used.

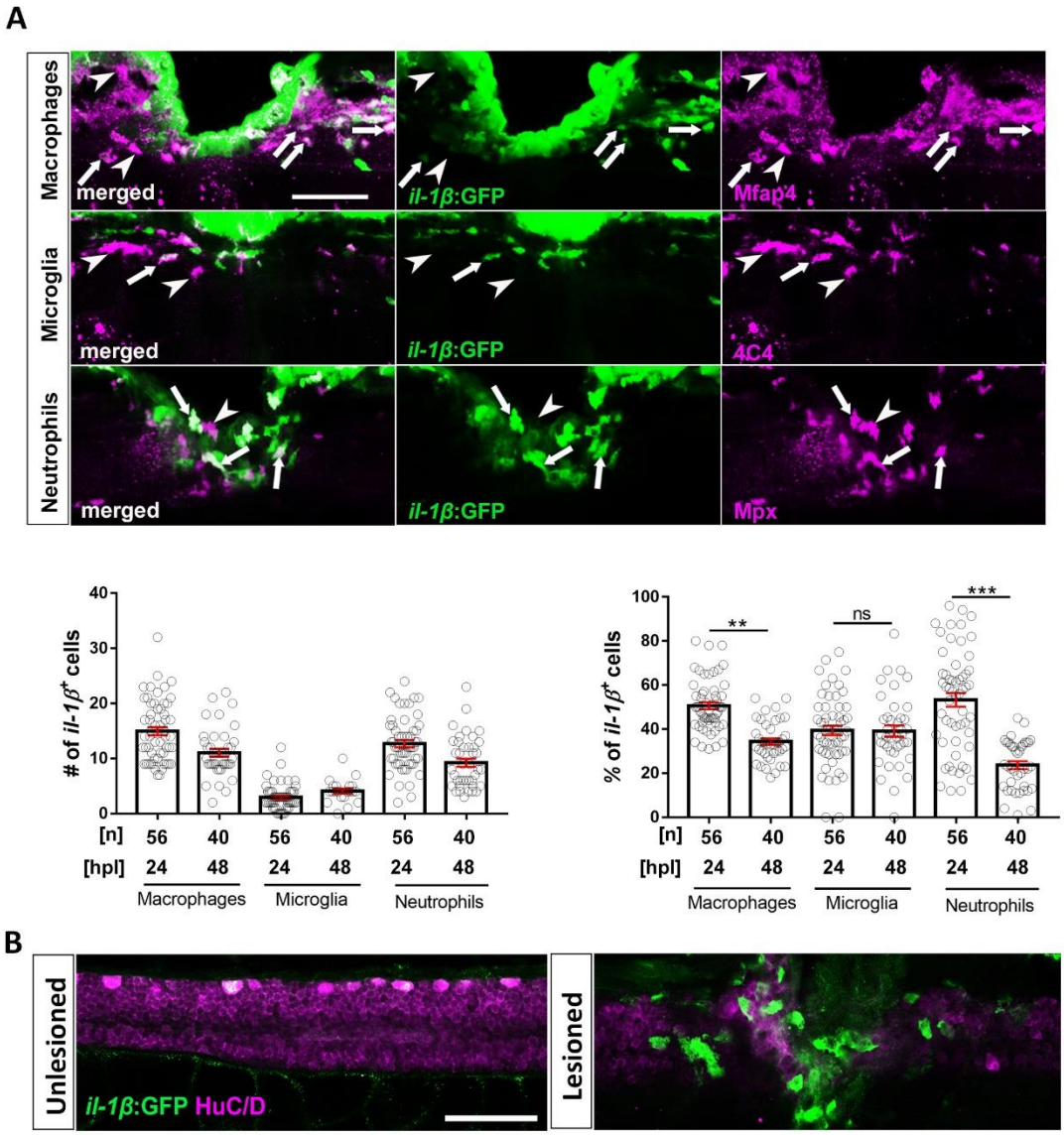

Fig. 18: Il-1β is expressed in immune cells, but not neurons in wildtype animals. A: In the Il-1β reporter line, Il-1β:GFP+ cells are co- labelled (arrows) with the macrophage marker Mfap4, microglial marker 4C4 and the neutrophil marker Mpx. Arrowheads indicate immune cells that are negative for Il-1β:GFP. The proportion of macrophages (Mfap4+) and neutrophils (Mpx+) that are Il-1β:GFP+ changes over time, whereas the proportion of microglial cells that are Il-1β:GFP+ remains the same (One-way ANOVA followed by Bonferroni post-test: $F_{5, 282} = 22.55$, ***P<0.001, **P<0.01, ns = no significance). B: Il-1β:GFP+ cells were rarely co-labelled with the neuronal marker HuC/D at 1 dpl. Lateral views of the

injury site are shown; rostral is left. Single optical sections are shown. Scale bars: 50 µm. Error bars represent SEM. Numbers on figure relate to number of larvae used.

5.2.11 Neutrophils inhibit regeneration in irf8 mutants.

Increased numbers of Il-1β^{+} neutrophils in *irf8* mutants could, at least in part, be due to higher overall numbers of neutrophils in the injury site. We found a peak of neutrophil numbers in the lesion site of *irf8* mutants at 2 hpl, as in wildtype animals (Fig. 19A). However, the number of neutrophils was 27 % higher than in wildtype, potentially due to the higher abundance of this cell type in the *irf8* mutant (Shiau et al. 2015). While neutrophil numbers declined over time in wildtype and *irf8* mutants, they did so more slowly in *irf8* mutants. At 24 hpl, twice, and at 48 hpl, three times the number of neutrophils as in wildtype animals remained in the mutant. Hence, macrophages control number of and cytokine expression by neutrophils (Tauzin et al. 2014), leading to prolonged presence of Il-1β^{+} neutrophils in the injury site of *irf8* mutants.

To determine the relative importance of the neutrophils for regenerative failure in *irf8* mutants, we reduced their numbers using *pu.1*/*gcsfr* morpholino treatment. This strongly reduced numbers of neutrophils by 84.6 % in the injury site at 2 hpl, when the neutrophil reaction peaked in untreated *irf8* mutants (Fig. 19B). *pu.1*/*gcsfr* morpholino treatment also reduced *Il-1β* mRNA levels by 54 % and *TNF-α* mRNA levels by 70 % at 2 dpl (Fig. 19C).

Remarkably, axon bridging (control: 43 % of examined animals showed bridging; *pu.1*/*gcsfr* morpholino: 60 %; Fig. 19D) and recovery of touch-evoked swimming distance were partially rescued in these neutrophil-depleted mutants at 2 dpl (Fig. 19E). This shows that in the absence of macrophages, the prolonged presence of Il-1β^{+} neutrophils is detrimental to regeneration.

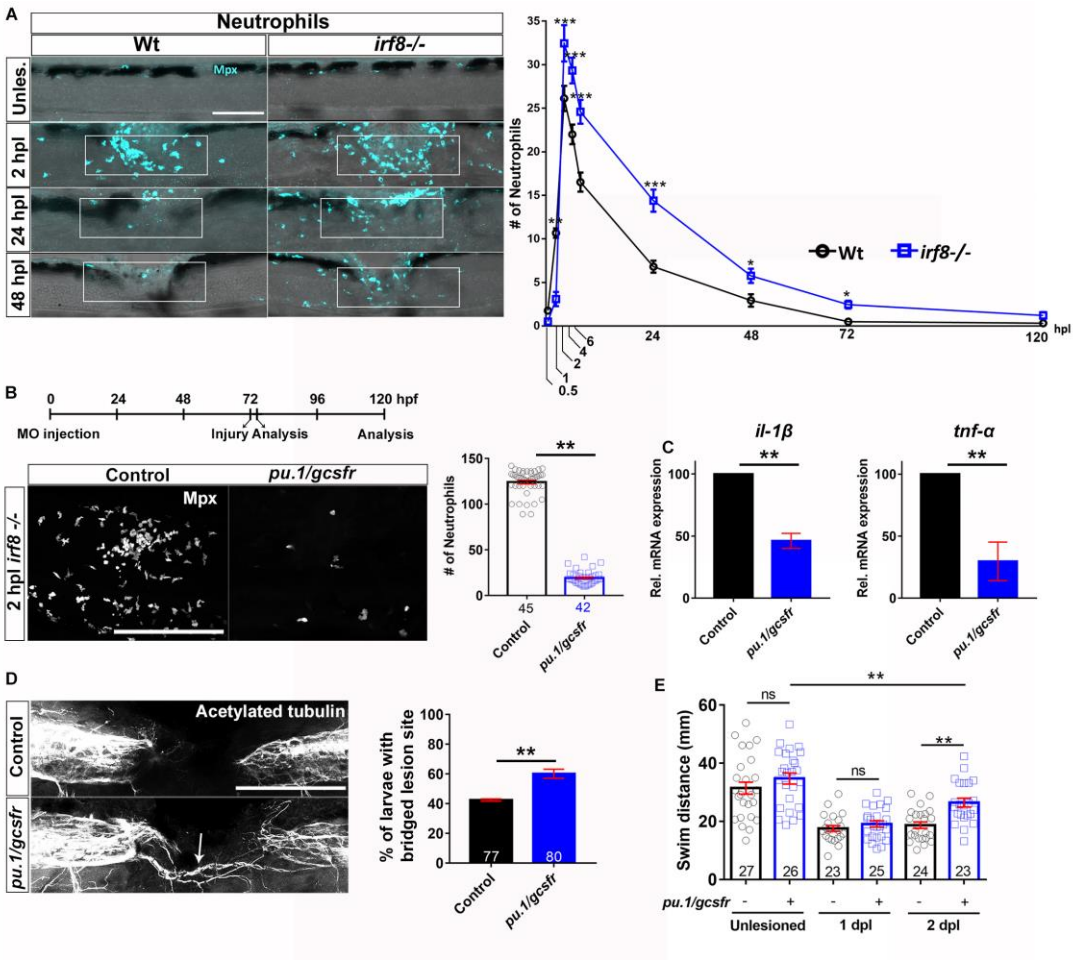

Fig.19: Preventing neutrophil formation partially rescues functional spinal cord regeneration in the *irf8* mutant. A: In *irf8* mutants, higher peak numbers of neutrophils (Mpx+) at 2 hpl and slower clearance over the course of regeneration are observed (Two-Way ANOVA followed by Bonferroni multiple comparisons: $F_{8, 427} = 13.19$ *P<0.05, **P<0.01, ***P<0.001). Note that wildtype data are the same as shown in Fig. 1A, as counts in *irf8* mutants and wildtype animals were done in the same experiments. B: Combination treatment with pu.1 and gcsfr morpholinos efficiently prevents neutrophil accumulation in the lesion site (Mann-Whitney U-test: ***P<0.001). C: In pu.1/gcsfr morpholino injected *irf8* mutant fish, levels of *Il-1β* and *TNF-α* mRNA expression are reduced at 2 dpl, as shown by qRT-PCR (t-test: ***P<0.001). D,E: In pu.1/gcsfr morpholino injected *irf8* mutant fish, axonal bridging (arrows, D; Fisher's exact test: **P<0.01) and behavioural recovery (E; One-Way ANOVA followed by Bonferroni multiple comparisons: $F_{5, 142} = 23.21$, **P<0.01, ns indicates no significance) are partially rescued. Lateral views of the injury site are shown; rostral is left.

Scale bars: 100 µm. Error bars indicate SEM. Numbers on figure relate to number of larvae used.

5.2.12 Il-1β promotes axonal regeneration during the early regeneration.

To determine whether roles of Il-1β and general inflammation differed for different phases of the inflammation, we separately analysed early (0-1 dpl; Fig. 20A) and late (1-2 dpl; Fig. 20B) regeneration by drug incubation. During the early phase, YVAD treatment led to a weak inhibition of axonal regeneration in both wildtype (control: 58 % of examined animals showed bridging; YVAD: 41 %) and *irf8* mutants (control: 41 % of examined animals showed bridging; YVAD: 36 %).

Similarly, dexamethasone treatment inhibited axonal regeneration in both wildtype (control: 57.5 % of examined animals showed bridging; dexamethasone: 36.6 %) and *irf8* (control: 44.6 % of examined animals showed bridging; dexamethasone: 34 %). Interestingly, while LPS promoted regeneration in the early phase in wildtype animals (control: 53.2 % of examined animals showed bridging; LPS: 68.7 %), it was detrimental in *irf8* mutants (control: 39 % of examined animals showed bridging; LPS: 25.5 %), perhaps because baseline inflammation was already high in the mutant. During late regeneration, only dexamethasone had an inhibitory effect in wildtype animals (from 82.1 % of examined animals that showed bridging to 64.4 %). YVAD had no effect in wildtype animals during late regeneration, when *Il-1β* was already down-regulated (control: 81 % crossing; YVAD: 78 % crossing), but a strong rescue effect of YVAD was observed in the *irf8* mutant (control: 37 % of examined animals showed bridging; YVAD: 68 %). This rescue effect was comparable to that observed when Il-1β was suppressed for the entire 48 hours (cf. Fig. 15D). LPS had no effect in wildtype or mutants during late regeneration. Hence, early inflammation and *Il-1β* upregulation promote regeneration, but *Il-1β* must be down-regulated at later phases of axonal regeneration.

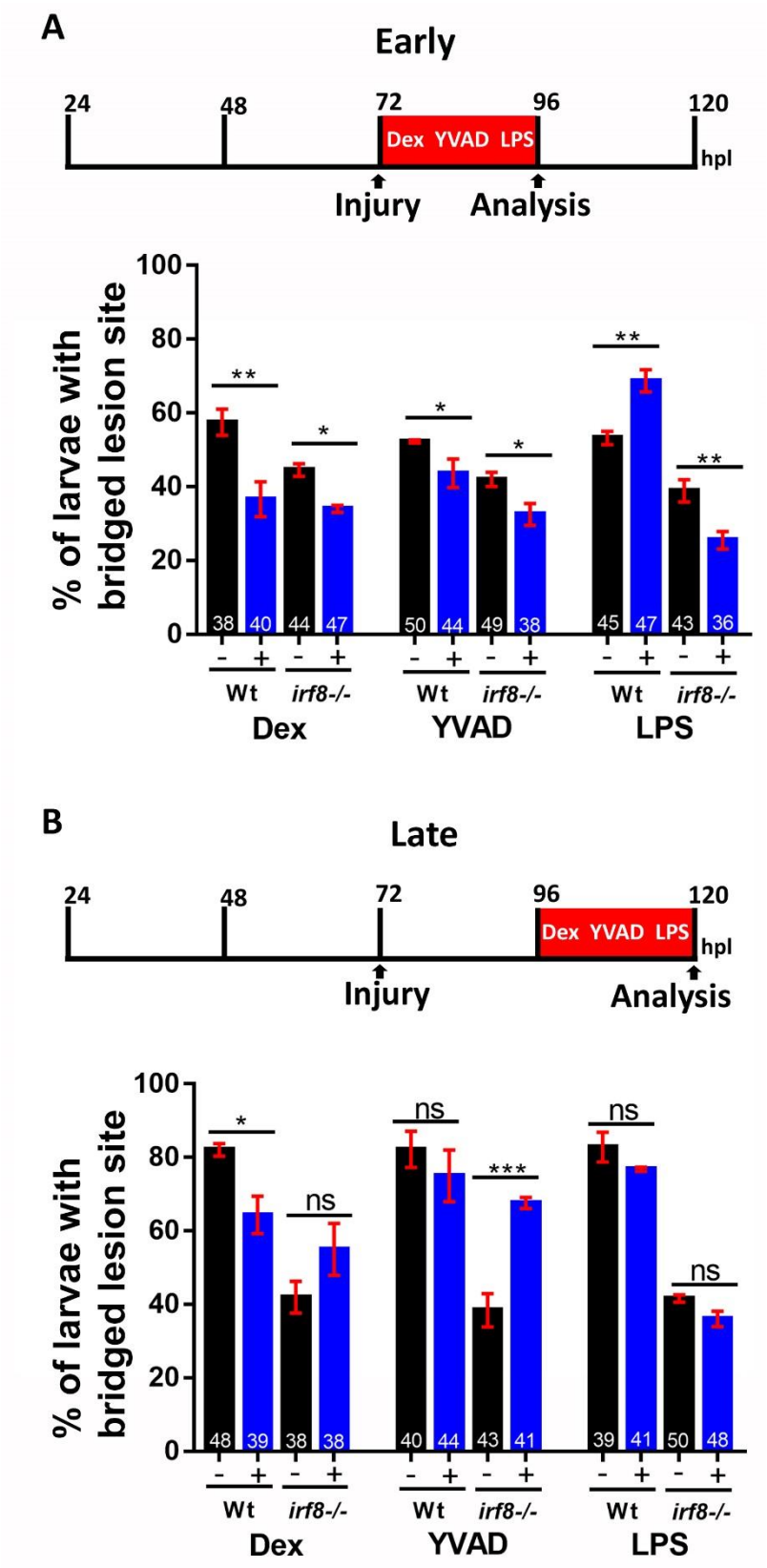

Fig. 20: Temporally restricted manipulations of the immune response reveal time-dependent effects on axon bridging. A: During early regeneration, dexamethasone and YVAD

treatments impair regeneration in both wildtype animals and *irf8* mutants. Stimulation of the immune response with LPS promotes regeneration in wildtype animals but inhibits it in *irf8* mutants (Two-way ANOVA followed by Bonferroni multiple comparisons: $F_{5, 12} = 25.32$. *P<0.05, **P<0.01). B: Manipulations during late regeneration show persistent negative effects of dexamethasone in wildtype animals and a strong rescuing effect of YVAD in *irf8* mutants (Two-way ANOVA followed by Bonferroni multiple comparisons: $F_{5, 12} = 16.05$. *P<0.05, ***P<0.001, ns = no significance; Dex = dexamethasone). Error bars represent SEM. Numbers on figure relate to number of larvae used.

5.3 DISCUSSION

In this chapter I identified a biphasic role of the innate immune response during axonal regeneration in zebrafish larvae. Initiation of the inflammatory response is beneficial for regeneration and the presence of Il-1β promotes axon bridging, whereas later, *Il-1β* expression is regulated by peripheral macrophages (Fig.22). Pharmacological and genetic Inhibition of Il-1β largely was able to improve axonal regeneration in macrophage-deficient larvae, highlighting the essential role of Il-1β as a central regulator for axonal re-growth.

On the other hand, TNF-α derived from the macrophages, although being a pro-inflammatory cytokine like Il-1β, has a pro-regenerative role, by reducing neutrophil number and *Il-1β* expression. These observations indicate that the inflammatory response is highly dynamic, and its tight regulation is essential for successful axonal regeneration (Fig. 22).

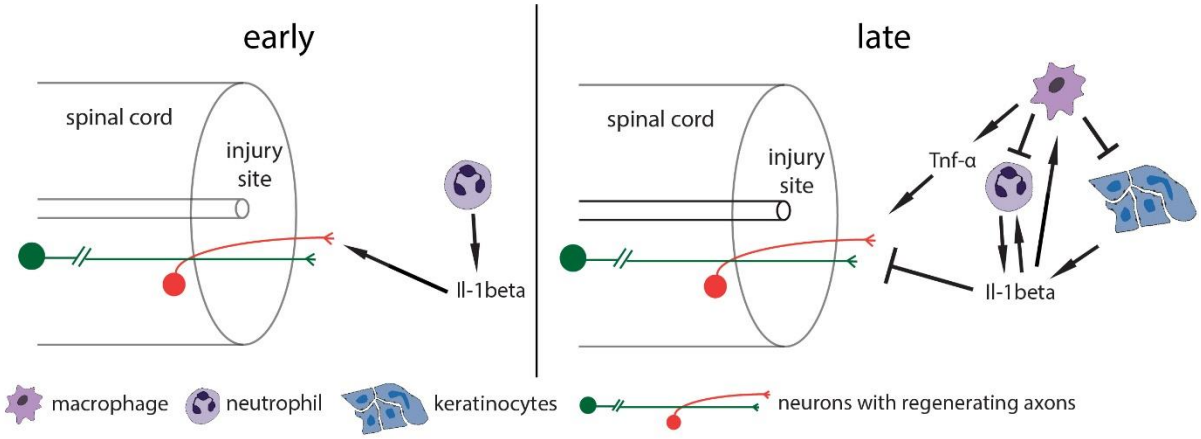

Fig. 21: Working model of the influence of the innate immune system on axonal regrowth. During the early stage, within hours of inflammation, spinal cord injury triggers neutrophil invasion of the injury site and initiation of the inflammatory response, including Il-1β production. This initially promotes regeneration but is later strongly inhibitory. At later stages, Il-1β positively regulates presence of neutrophil and macrophages in a feedback mechanism. Macrophages invade the lesion site and down-regulate levels of Il-

1β in neutrophils and basal keratinocytes, while promoting regeneration by releasing TNF-α. This leads to successful axonal regeneration and recovery of parameters of touch-evoked swimming.

5.3.1 The role of Il-1β

After injury the reaction of the immune system changes rapidly over time. Very soon after injury, neutrophils are the first cells that accumulate to the injury site and the levels of pro-inflammatory *Il-1β* and *TNF-α* increase in the injury site. This is essential for axonal growth initially, indicated by the increased axonal bridging after LPS stimulation during the early stages of inflammation and by the decreased bridging after Il-1β inhibition during the same time point. In agreement to this, other studies have shown that Il-1β can promote neurite growth (Temporin et al. 2008, Boato et al. 2013).

The next crucial event that occurs after injury is the migration of macrophages to the lesion site, where by producing anti-inflammatory cytokines like tgf-β resolve the inflammation and promote tissue regeneration during the late stages of inflammation. This doesn't occur to the macrophage-less *irf8* mutants where the absence of macrophages together with increased levels of Il-1β and decreased levels of anti-inflammatory cytokines inhibit regeneration.

Furthermore, *irf8* mutants are characterized by increased numbers of neutrophils, levels of *Il-1β* and *TNF-α* expression, as well as cell death in the lesion environment. Inhibition of Il-1β led to significant decrease of the numbers of neutrophils accumulating to the injury site, decreased the levels of pro-inflammatory cytokines and decreased also the cell death levels. Indicating that increased levels of Il-1β may condition the lesion environment to be hostile for axonal regeneration. Additionally, some matrix metalloproteinases showed decreased expression in the *irf8* mutant suggesting that the lesion site ECM may be altered. However, the expression of several ECM components, including functionally important Col XII (Wehner et al. 2017), was not altered in the *irf8* mutant. Similar to these observations, (Boato et al. 2013) showed that

Il-1β deficient mice exhibit slightly increased axonal regrowth after SCI.

5.3.2 The role of TNF-α

Inhibition of TNF-α showed a pro-regenerative role of this pro-inflammatory cytokine during axonal regeneration. Axonal regeneration is promoted by TNF-α. Even though both *Il-1β* and *TNF-α* were upregulated in the *irf8* mutant, only reducing Il-1β levels was able to rescue the mutant. This is similar to what has previously been shown by the work of (Turrin and Rivest 2006) which showed that the two-proinflammatory cytokines exhibit different roles. Another key difference in their cellular source in the injury site. Whereas Il-1β is expressed by a substantial proportion of neutrophils, microglia and macrophages, TNF-α is mainly expressed by macrophages. In mammals, *TNF-α* is produced by both microglia and macrophages (Kroner et al. 2014). TNF-α may exert its pro-regenerative role partially by controlling neutrophil numbers and Il-1β levels. Both of these parameters are increased when TNF-α is inhibited. The anti-inflammatory role of TNF-α has been described in the context of auto-immunity (Liu et al. 1998), but whether this interaction between TNF-α and Il-1β is direct or indirect, is still unclear. During fin regeneration, TNF-α has an important promoting function for blastema formation (Nguyen-Chi et al. 2017) suggesting that TNF-α may be involved in tissue remodeling in the lesion site after spinal injury, which then creates an axon growth-promoting environment. However, the role of TNF-α during axonal regeneration in mammals is not clear. There are some studies indicating the promoting properties of TNF-α during axonal growth (Schwartz et al. 1991, Saleh et al. 2011), whereas others show inhibition of axon growth (Kato et al. 2010). However, TNF-α deficient mice had no reported effect after spinal cord injury (Farooque et al. 2001).

5.3.3 The role of macrophages

Preventing neutrophil formation in *irf8* mutants, led to partial rescue of axon regrowth and swimming function. This could be explained by the absence of the early pro-regenerative role of the inflammation after injury. In mammals, it has been reported that neutrophils cause secondary cell death (Saiwai et al. 2010, Kubota et al. 2012) whereas neutrophil depletion leads to favorable injury outcomes (Taoka et al. 1997), similar to my data. Macrophages control inflammatory response, as their absence in *irf8* mutants leads to abnormally high expression levels of pro-inflammatory cytokines *Il-1β* and *TNF-α* and increased numbers of neutrophils, similarly to observations during fin regeneration (Hasegawa et al. 2017). Moreover, higher proportion of neutrophils were Il-1β^{+} in *irf8* mutants, indicates that macrophages prevent neutrophils from obtaining a more pro- inflammatory phenotype.

Using FACS and ISH I show that macrophages/microglia, together with other tissues, express *tgf-β1a* and *tgf-β3* and could thus be partially responsible for reducing pro-inflammatory phenotypes in wildtype animals.

Macrophages do not promote regeneration primarily by preventing cell death or removing debris. Debris levels were clearly increased in the absence of macrophages in *irf8* mutants. However, during Il-1β inhibition and rescue of decreased axonal bridging, debris levels were still higher than in controls. Furthermore, prevention of cell death did not rescue axon growth and inhibition of phagocytosis in wildtype animals did not impair regeneration. Hence, debris abundance is not a major determinant for regenerative success. Interestingly, in fin regeneration paradigm, lack of macrophages leads to death of tissue progenitor cells, and subsequently, fin regeneration is impaired (Hasegawa et al. 2017). On the other hand, studies in mammalian models have shown that debris and especially myelin debris have an inhibitory role during regeneration (Church et al. 2017). Microglial cells may not be essential for axonal re-growth as the unimpaired axonal bridging was observed in the *csfr1a/b* mutant. However, the increase in peripheral macrophages in this

mutant within the lesion site could have compensated for a possible regeneration-promoting role of microglia.

5.3.4 What about the other cell types present in the injury site?

The use of different reporter lines to visualize the neuronal elements of the spinal cord alongside with other cell populations that respond to the injury site showed that the endothelial cells from the injured blood vessels were slow to reform blood vessels. In contrast, in mammals, endothelial cells accumulate in the injury site, where they may have anti-inflammatory functions (Kadl and Leitinger 2005, Al-Soudi et al. 2017, Cohen et al. 2017).

The use of cldnK reporter line showed that after injury there is myelinating cells bridged the lesion site, when axons had already crossed the lesion site, which may contribute to recovery of swimming behavior after injury. In mammals SCI models, transplanted myelinating cells, have been shown to improve recovery after spinal injury (Bunge 2016, Nakhjavan-Shahraki et al. 2018).

In order to assess how glial processes, respond after injury I treated zebrafish larvae with dexamethasone. I found that glial processes cross the injury site, and this depends on the immune response similarly to the axons. Although these processes cross the injury site independently of axons and axons still cross when these cells are ablated (Wehner et al. 2017), astroglia-like processes have been shown to support axonal growth by producing growth factors like Fgf and ctgfa (Goldshmit et al. 2012, Mokalled et al. 2016).

In summary I've shown that tight control of the inflammatory response after SCI is crucial for regenerative success in zebrafish larvae. Inflammation is rapidly down-regulated in zebrafish concurrent with the upregulation of anti-inflammatory cytokines, which does not readily occur in mammals (Kigerl et al. 2009).

Furthermore, the use of the zebrafish larval model provides an in vivo system to study the complexity of the inflammatory response alone or with combination of the regenerative events that occur after SCI and allow zebrafish to regain their

swimming capacity. In addition to this, the larval model can be used an easily accessible high-throughput model which can give insights to help understand mammalian SCI and test specific molecules leading eventually to the development of efficient therapeutic strategies against SCI.

Chapter 6: General Discussion

6.1 Zebrafish larva as a model to study regeneration

Unlike mammals, adult zebrafish are able to regenerate their CNS and spinal cord after injury. Several studies have elegantly demonstrated that adult zebrafish can replace a plethora of lost neurons by regenerating new neurons such as motor neurons (Reimer et al. 2008), interneurons (Kuscha et al. 2012, Barreiro-Iglesias et al. 2015) and radial glia progenitor cells (Briona and Dorsky 2014, Ghosh and Hui 2016). The adult zebrafish is a very well-established model to study regenerative neurogenesis (Reimer et al. 2009, Kuscha et al. 2012, Reimer et al. 2013, Barreiro-Iglesias et al. 2015, Becker and Becker 2015). However, it takes up to 3-4 months for them to reach adulthood and the study of regenerative events includes further tissue handling in order for the CNS to be accessible, such as surgery, perfusion, dissection and section for antibody staining. Furthermore, another limiting factor is the number of animals that can be processed in each round of experiments and the time that the regeneration is complete, as it takes up to 6 weeks for an adult zebrafish to functionally repair its spinal cord (Becker et al. 2004).

In contrast to the adult animals, zebrafish larvae are transparent and small in size. Spinal cord injury can be easily performed with an injection needle and we can easily proceed with further analysis. We have established larval zebrafish as a model for lesion induced motor neurogenesis (Ohnmacht et al. 2016) and have shown that zebrafish larvae have the ability to reclose the wound, regenerate motor neurons and restore swimming ability within 2 days postinjury (dpi), with a survival rate of 85%-90% after a lesion (Ohnmacht et al. 2016). Other studies from our group (Becker et al. 1997, Becker and Becker 2001, Schweitzer et al. 2005) have shown that adult fish are able to repair severed axons and regain swimming behaviour and this is also observed in the larval injury model (Wehner et al. 2017). Zebrafish larvae exhibit functional regeneration within 48 hours post injury, much quicker than the 4-6 weeks in adults. Furthermore, they are very easy to handle, and a high number of animals can be handled during each experiment, such that high statistical power is easier to achieve than in adults. It is also very important to mention that zebrafish larvae up to

5 days post fertilization are not protected under the A(SP)A 1986 which regulates the use of animals in research. This allowed us to replace the adult zebrafish with larval zebrafish and therefore to reduce at the same time the number of adult experiments, in agreement with the 3R guidelines that regulate the use of animals in research.

One of the key features of the larval model is the transparency of the larvae which makes them ideal for live imaging. This feature combined with the high number of reporter lines allows the live observation of the cell types of interest. These offer a lot of possibilities. Live imaging combined with different manipulations allows us to perform regenerative or drug screening using a vertebrate in vivo model which is highly plastic. For these reasons I used the larval injury model for my experiments in this thesis.

6.2 Zebrafish larva as a model to study inflammation after injury in the CNS

The immune response is one of the key events that occur after an infection or an injury. There are many different injury models that show the orchestrated events that occur during the different stages of inflammation after injury. The presence of immune cells in the CNS was considered to be detrimental and was characterized as a hallmark for pathology. However, over the last few years several groups were able to go into more detail regarding the interaction between CNS and immunity. Several studies challenged the dogma that immune system can have a negative effect on neurons by providing data that show that multiple signals and reactions from the immune response can have neuroprotective effects on the injured CNS (Baumert 1995, Kyritsis et al. 2012, Ohnmacht et al. 2016).

Injury to the CNS leads to an inflammatory cascade that begins with cell death and continues through complex cellular and molecular interactions. Briefly, after injury DAMPS and ATP are released by the injured cells. This activates the inflammasome which produces mature cytokines like Il-1β which is the principal cytokine that responds immediately after injury. Studies have shown that Il-1β can be produced

directly and very rapidly by cells within the injured CNS, like neurons (Watt and Hobbs 2000), microglia (Giulian et al. 1986) and oligodendrocytes (Blasi et al. 1999). Subsequently neutrophils arrive to the injury site and amplify the immune response by producing cytokines, ROS and proteases while during the first day monocytes start to accumulate in the lesion environment and remain there until the resolution of inflammation (Gadani et al. 2015). These cells produce specific molecules during the different stages of inflammation. However, the consequences of the immune response for the CNS remain controversial. Some groups report aspects of it that can be beneficial like oncomodulin that is produced by the neutrophils and has been shown to promote optic nerve regeneration (Kurimoto et al. 2013) and il4 that activates CD4+ T cells which have a neuroprotective role after injury (Walsh et al. 2015) whereas other studies suggest that immunity can be destructive for the CNS. Work from Kroner et al., show that TNF signalling can alter macrophage polarization towards the so-called M1 phenotype leading to extensive tissue damage after SCI (Kroner et al. 2014). Similarly, Yawata et al., showed that macrophages can exhibit a neurotoxic role through glutamate which can be attenuated by glutaminase inhibition (Yawata et al. 2008). These studies and others elegantly highlight the complexity of the events that occur in the CNS after injury. Another aspect that adds extra difficulty is in all vertebrate injury models there is an interaction between innate and adaptive immunity. As a result, we cannot assess accurately the role of each of the cellular and molecular players during inflammation.

In order to tackle this caveat, I used the larval zebrafish injury model for the purposes of this thesis to study the role of the innate immune response during the regeneration of the spinal cord after transection. While the adult zebrafish model exhibits regeneration of the spinal cord and can be considered closer to mammalian models since it's a fully developed system, the larval model was used due to certain advantages. After complete transection we can study how axons grow and establish new functional axonal connections that allow zebrafish to swim again within 48 hours (larval model) (Wehner et al. 2017) instead of 6 weeks (adult model) (Becker et al. 2004).

Furthermore, one advantage over the other models and also the adult zebrafish model is the lag between the development of the innate and adaptive immune system (Meijer and Spaink 2011). This is very important because it allows the study of the contribution of the innate immune response to the regeneration of the spinal cord after injury without having to considering the influence of the adaptive immunity. This way the exact role of the macrophages, neutrophils or microglial cells, can be assessed without implications derived from the interaction between innate and adaptive immunity as occur in mammalian injury models or in the adult zebrafish injury model.

After SCI in zebrafish larvae the innate immune response is initiated within minutes. The injury site is characterized by an influx of immune cells. Live imaging using reporter lines showed that the cellular response is similar to the mammalian in terms of timing, with the neutrophils being the first cell population that responds. After the initial response of the neutrophils the inflammatory response continues with the recruitment of the macrophages from the periphery that migrate into the injury site and phagocytose debris and release cytokines. Il-1β and TNF-α are the key cytokines that can be found in the lesion environment which, as in mammals, regulate the inflammatory response and the regenerative events. However, the whole process, from the initiation to the resolution of inflammation, occurs much faster compared to mammals, where the immune response after injury is prolonged. Zebrafish larvae are able to resolve the inflammation and regenerate their injured spinal cord in 48 hours which makes them ideal model for studying the inflammatory response after injury.

6.3 The role of the innate immune response to the axonal regeneration

Using the larval zebrafish model, I was able to characterize how axons are re-growing and establishing new functional connections after injury. Time lapse imaging and immunohistochemical observations showed that axons are starting to grow within 15

hours after injury. During this time window, only axons were found to cross the injury site. The majority of the fascicles that were observed consisted only of axonal processes whereas only 20% of the fascicles quantified were positive for glial markers indicating that axons can grow independently of the glial scaffold which is in contrast with previous studies where the importance of the glial bridge for axonal regeneration was mentioned (Goldshmit et al. 2012, Mokalled et al. 2016). By 48 hours post injury the glial fascicles have been caught up with the axons and the majority of the fascicles contain axonal and glial processes (Fig. 4.1.C). In order to give a more definitive answer, to the question regarding the glial contribution I selectively ablated the glial population, performed spinal cord injuries and assess the axonal regrowth after ablation. Interestingly what I found was that the axons were able to navigate through the lesion site even after the glial ablation. This showed that indeed the axons do not necessarily need the glial population to re-grow and establish functional connections with the distal stump. In agreement with this observation a study from Dervan and Roberts showed that adult eel exhibits axonal regeneration after spinal cord injury without glial support as GFAP+ processes were found in the injury site 16 days after lesion (Dervan and Roberts 2003). Similar results were obtained after optic nerve (Nona 2005) and spinal cord transection in goldfish (Nona and Stafford 1995). Optic nerve axons are able to regenerate after transection without glial bridges.

Regeneration of axons after injury is something that many groups have worked on and continue working. Several studies in zebrafish and other injury models have mentioned the role of inflammation during this regenerative process (Becker and Becker 2001, Gadani et al. 2015, Ohtake et al. 2015, Jin and Yamashita 2016, D'Rozario et al. 2017, Hill 2017, Filous and Schwab 2018). However, it is very difficult to exactly determine the actual contribution of the immune response during axonal regeneration.

In order to address this question I used the larval zebrafish model which allowed me to focus my analysis only on the innate immune system due to the fact that the

adaptive immune system needs a few weeks to be functionally developed and mature (Meijer and Spaink 2011) (Fig.6.3.1).

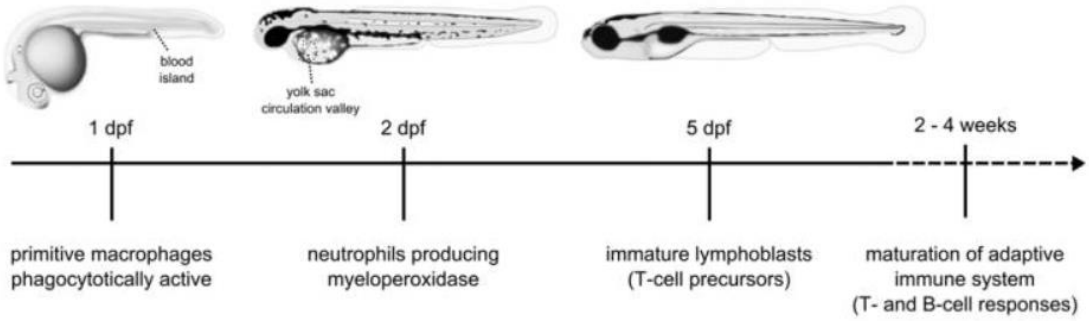

Fig. 6.3.1. Schematic overview of the development of the zebrafish immune system (adapted from (Meijer and Spaink 2011))

Firstly, I manipulated the immune system using pharmacology to see how the system will respond. After inhibition using dexamethasone the bridging score was decreased compared to the control group. On the other hand, stimulation with LPS led to increased inflammatory response which subsequently resulted in increased axonal regeneration (Fig. 3). Taken together, these data indicate that inflammatory response is essential for axonal growth after injury, similar to what has been found in adult zebrafish for which acute inflammation is beneficial for neuronal and axonal regeneration (Becker and Becker 2001, Kyritsis et al. 2012).

In order to go one step further I used genetic tools to manipulate the immune response because the use of drugs very often has adverse effects. Using the csf1ra/b double knock-out line I assessed the role of the microglia during regeneration of the injured axons. These animals retain their neutrophils and macrophages, but do not have microglia. After injury the bridging score was similar between wt and csf1ra/b mutants indicating that the microglia cells are not the major cell type necessary for axonal regeneration (Fig. 6).

Next, I used the macrophage-less *irf8* mutant line and I found that after injury there is increased number of neutrophils in the injury site (Fig. 17), the levels of the pro-inflammatory cytokines Il-1β and TNF-α were increased compared to the wt control group where they were initially increased and then by 2 days post injury returned to

basal levels (Fig. 11), indicating prolong inflammation which resulted in decreased bridging score in the mutant fish.

Cytokine mediated inflammation plays an important role after CNS injury. Il-1β and TNF-α have been shown to induce neurotoxicity through glutamate release (Ye et al. 2013). In order to assess the role of these cytokines during my injury paradigm I manipulated them separately using pharmacology and CRISPR/Cas mediated genome editing. Pharmacological inhibition of Il-1β rescued the decreased bridging phenotype in the *irf8* mutants (Fig. 15). Furthermore, it rescued the swimming behaviour, indicating that axonal re-growth leads to functional connections and that increased levels of Il-1β can be detrimental for regeneration. This is similar to what was found by Hasegawa et al.,2017 who showed that after ablation of macrophages using *irf8* morpholino the levels of Il-1β were increased and this led to impaired regeneration of the zebrafish fin fold (Hasegawa et al. 2017). Also modulation of the immune system and more specifically pro-inflammatory modulators promotes successful tissue regeneration (Julier et al. 2017).

In contrast to what I found after inhibition of Il-1β, manipulation of TNF-α either by blocking its release using pharmacology or by CRISPR had a negative effect on regeneration (Fig. 13). The bridging score was significantly decreased and this impairment persisted even up to 5 days post injury, indicating a pro-regenerative role of TNF-α similar to what was found in the past during fin (Nguyen-Chi et al. 2017) and vascular (Bowers et al. 2018) regeneration respectively.

Interestingly, manipulation of TNF-α led to a phenotype similar to what has been observed in the *irf8* mutants. The number of neutrophils was increased after injury and also the expression of Il-1β was doubled two days post-injury, coinciding with the decreased bridging (Fig. 14). This indicated a paradoxical anti-inflammatory role of TNF-α that was not expected. However, there are studies in the past that mention that treatment of neutrophils with TNF-α in vitro decreases their chemotactic ability (Vollmer et al. 1992). Furthermore, Il-1β can be indirectly controlled by TNF-α as it has been shown that TNF-α regulates the transcription of NLRP3 inflammasome

components (McGeough et al. 2017). Il-1β production occurs via NLRP3 inflammasome. TNF-α knockout mice show decreased mRNA expression of Nlrp3, Pycard and pro-Casp-1 and subsequently decreased pro-Il-1β and pro-il-18 (McGeough et al. 2017).

In summary, I propose that inflammation has a very dynamic role during axonal regeneration which is finely tuned by the macrophages. More specifically, after injury there are two phases of the inflammatory response. During the early phase, within hours of inflammation, spinal cord injury triggers neutrophil invasion of the injury site and initiation of the inflammatory response, including Il-1β production which amplifies the immune response and through specific signals they attract macrophages to the injury site. This initially promotes regeneration, but if it persists becomes inhibitory. During the late phase, Il-1β positively regulates the presence of neutrophil and macrophages in a feedback mechanism. Macrophages invade the lesion site and down-regulate levels of Il-1β in other cells like neutrophils and basal keratinocytes, while promoting regeneration by releasing TNF-α. This leads to successful axonal regeneration and recovery of parameters of touch-evoked swimming.

Concluding remarks and future directions

In this thesis I presented how axons are able to regenerate after mechanical injury of the spinal cord and found that axons are able to navigate through the non-neural lesion site without the glial support and manage to establish functional axonal connections. However, one cannot exclude that we may have missed some glial processes that have already bridged the lesion site and acted as a substrate for the axons.

Further experiments need to be carried out in order to identify what is the substrate for the axons to grow if not the glial processes. As mentioned in Chapter 4, mRNA sequencing of the injury site will provide useful information regarding the molecular

components of the lesion site that are essential for axonal re-growth during different time points post injury. Furthermore, the lesion site after the spinal cord injury is characterized by a complex composition consisted of many different cell types and molecules that condition the environment. Several cell types have been previously identified in the spinal cord lesion site, like endothelial cells that regulate myeloid cell activity (Cohen et al. 2017), immune cells (Kasinathan et al. 2015), oligodendrocytes (Almad et al. 2011), matrix metalloproteinases (Zhang et al. 2011), fibroblasts (Wehner et al. 2017) and ECM molecules like chondroitin sulphate proteoglycans (Iaci et al. 2007). These can all be possible substrates for the axons that cross the injury site after injury. Their role during axonal regeneration can be easily assessed because there are zebrafish reporter lines available so their response and interaction with axons can be observed in vivo performing high-resolution time-lapse imaging on the larvae. Furthermore, ablation studies targeting these cells and molecules can be performed quote easily on zebrafish due to the easiness in manipulating their genome using the CRISPR/Cas system or other genetic tools.

In addition to this, another experiment that can be done is an expression profile of mammalian embryonic and adult tissue that show robust and limited regenerative potential respectively. These data will be compared with data from embryonic and larval zebrafish in order to identify differential regulated genes like Epac that it has been shown to regulate the c-AMP dependent guidance in rats and shows differential expression during (Murray and Shewan 2008, Murray et al. 2009).Furthermore, there are genes like Nogo that in mammals has been shown to negatively regulate neuronal plasticity (Vanek et al. 1998) whereas in zebrafish the Nogo-A homologue Rtn4b has been discovered in differentiating CNS regions and downregulation caused severed effects in retinal axonal projections (Welte et al. 2015). The RNA-seq data possibly will show other differentially expressed genes between mammals and zebrafish. Their role could be further assessed in vivo using the CRISPR/Cas system or pharmacological approaches combined with the zebrafish larval injury model.

I found that the inflammatory response is important for axonal and neuronal regeneration in the zebrafish larval model which recapitulates the findings in adult

zebrafish, indicating that adult zebrafish can be replaced to some extend with zebrafish larvae which allows more rapid conduction of experiments.

I also found that peripheral macrophages appear to be the most important innate immune cell type during spinal cord regeneration. However, one cannot exclude that in terms of neuronal regeneration this may be different. (Kyritsis et al. 2012) have shown that activation of microglia is important for neuronal proliferation after injury in the adult zebrafish CNS. In the csf1ra/b double KO microglia did not appear to be necessary for axonal regeneration, possibly because of the infiltration of peripheral macrophages, but it would be interesting to assess the neuronal regeneration in a system that lacks microglial cells both during the larval and the adult stages.

The findings derived from the CRISPR manipulations indicate the different roles of two mainly proinflammatory cytokines. In order to go one step further these findings can be verified using stable mutant lines instead of just using acutely gRNA injected embryos. However, there is still the risk of genetic compensation which is the ability that the cells have to fix mutations that have been introduced to the genome and affect their functionality and survival. The loss of one gene may be compensated by another that exhibits similar functions and expression pattern. This is something that has been reported in different models (El-Brolosy and Stainier 2017).

During this thesis the role of anti-inflammatory cytokines like tgf-β was not assessed. Anti-inflammaotry cytokines have been found to be beneficial for axonal regeneration (Vidal et al. 2013). It would be useful for better understanding of the system to assess the role of anti-inflammatory molecules during axonal and neuronal regeneration of the spinal cord. One example can be the overexpression of the tgf-β1a and tgf-β3 in the *irf8* embryos which exhibited decreased expression of these two anti-inflammatory cytokines after injury.

It is very important to see how the neurons respond to the different manipulations of the innate immune response. What are the cues that are detected by the progenitors and can lead to proliferation or differentiation after injury ? Neurons and axons may exhibit differential requirements regarding the immune response.

Possibly during neuronal regeneration microglial cells may be the most important cell type. In order to address this, expression profiling experiments of the injury site of zebrafish larvae after different manipulations or from different mutant lines will provide a better insight of the lesion environment and help to identify possible targets that are key mediators of neuronal and axonal regeneration.

Current interventions for the treatment of the spinal cord injury are focusing on protecting the surviving cells from secondary damage, replacing injured or dead cells, and promoting axon regeneration from the glial scar formed by reactive astrocytes that plays a crucial part in the regeneration failure in mammals. To achieve these goals requires to develop economical and powerful model organisms that could be used for real-time imaging of pathogenesis and to provide gene or drug target information. Similar to the adult zebrafish, neuronal replacement, axonal outgrowth and functional recovery also occurred in larval zebrafish. However, the axonal repair is quicker as it happened within 48 hours as opposed to 6 weeks in adults. In this regard, larval zebrafish are amenable to study the intrinsic and extrinsic signals that control regeneration in vivo and to identify how the regenerated axons integrate into the CNS circuit to restore neural function.

In this context the findings of this thesis can be validated in adult zebrafish and then in mammals. There are mutant lines in house available for Il-1β and TNF-α and tools that can be used and assess the effect on axonal and neuronal regeneration.

The temporal separation that zebrafish larvae exhibit during the development and the maturation of their innate and adpative immune system although is very useful, because it allows the separate study of the contribution of the innate immune response during regeneration, can potentially be also a caveat of the model. One main reason is that previous studies have shown that adaptive immunity plays significant roles in shaping post-traumatic inflammation and downstream cascades of neurodegeneration and repair (Ankeny and Popovich 2009, Gadani et al. 2015). Furthermore, important factors and interactions that are more typical in injury models may be overlooked. In order to assess the role of the adaptive immune

response experiments in adult zebrafish should be carried out. However, the larval model is still powerful because the innate inflammatory response occurs very early after injury and is essential in order to condition the lesion environment in such a way so that the tissue can start to regenerate whereas the adaptive response occurs much later (days or weeks post injury) (Gadani et al. 2015).Another aspect that should be taken into account is the type of injury. For the purpose of this thesis I performed a complete transection of the spinal cord and assessed the regenerative events that occur. However, around 70% of the spinal cord injuries are incomplete which partially impedes the spinal cord and can be caused by a spinal cord contusion (bruising), a partial severance of the spinal cord, stretching, having something pressing against the spinal cord, or even having bone fragments or foreign bodies embedded or otherwise affecting it. Although complete transections are clinically rare, they provide specificity and allow us to assess the regenerative potential that mammals and other animal models exhibit. On the other hand, it would be useful if more clinically relevant injury models were used. However, the problem with this would be the reproducibility because it can be more variable in terms of tissue and axonal sparing compared to the complete transection. Previous studies have shown that crush injury can be performed in zebrafish optic nerve in a reproducible way (Liu and Londraville 2003, Diekmann et al. 2015). Based on this, contusion injuries on the zebrafish spinal cord should be feasible in order to establish a model which could exhibit more clinical relevance.

Taken together the data presented in this thesis could ultimately help to consolidate our understanding on how axons regenerate and manage to establish new functional connections after injury and what is the role of the immune response. The clinical relevance of the larval regeneration model is that it can be used for screening drugs in living animals and genetic manipulations that are not feasible in models such as mouse. Early drug screens for clinical use involves the identification of a protein or pathways that may result in a therapeutic effect, validation of the discovered development candidate in experimental models, and the screening of compounds that are likely to have activity at the target protein. The transparency of zebrafish

larvae enables small molecule screens that assay compound libraries against disease targets to identify drug-like compounds in vivo. The VAST (Vertebrate Automated Screening Technology) Biolmager system, which is designed for high-resolution imaging of 2-7 dpf zebrafish larvae automatically, can be used for chemical or genetic screening in a more efficient manner to identify “hit” molecules and genes that are immune related and may have an effect on successful motor neuron and axonal regeneration. These hits can be further validated in adult zebrafish and then in mammalian models leading eventually to the development of efficient therapeutic strategies of SCI.

Furthermore, following up on this, future studies on zebrafish could try to investigate if the new-born neurons are able to extend new processes across the injury site and reinnervate their original or new targets or if the axons that regenerate are derived from neurons that were spared during injury and its’ downstream events. This could be relatively easily answered using the zebrafish larval model and more specifically the Zebrabow reporter line which allows multispectral cell labelling that can be used for cell tracing and lineage analysis (Pan et al. 2013). This will provide very useful information because it could possibly show which is more important; axonal regeneration or neurogenesis. There is evidence that axons in the mammalian CNS have an intrinsic regenerative potential, whereas the evidence that new neurons can be born are very limited, so the knowledge obtained from this experiment could change completely the focus of research and the development of therapeutic strategies.

Appendix

Materials

Chemicals and reagents

Name	Cat. No.	Source
Agarose	BPE1356	Sigma-Aldrich
Aminobenzoic acid ethylmethylester (MS222)	A5040	Sigma-Aldrich
Ampicillin	A9518	Sigma-Aldrich
BCIP/NBT tablet	B5655	Sigma-Aldrich
β-Mercaptoethanol	M6250	Sigma-Aldrich
Bovine serum albumin (BSA)	A3912	Sigma-Aldrich
Calcium Chloride, $CaCl_2$	C/1500/53	Fisher Scientific
α-Digoxygenin-AP conjugate	11093274910	Roche
Digoxygenin-11-UTP	3359247910	Roche
Dimethyl sulfoxide (DMSO)	D2650	Sigma-Aldrich
Ethanol	E7023	Sigma-Aldrich
Ethylenediaminetetraacetic acid (EDTA)	E6635	Sigma-Aldrich
Formamide	47670	Sigma-Aldrich
Glycerol	G5516	Sigma-Aldrich
Glycine	50046	Fisher Scientific
Heparin sodium salt	H3393	Sigma-Aldrich
Hydrochloric acid, HCl	320331	Sigma-Aldrich
Magnesium Chloride, $MgCl_2$	31413	Sigma-Aldrich
Methanol	M/4000/17	Fisher

Normal donkey serum	S30	Millipore
Normal goat serum	ab7481	Abcam
Normal sheep serum	SMI-6050C	Covance
Paraformaldehyde (PFA)	P6148	Sigma-Aldrich
2-Propanol; Isopropanol	I9516	Sigma-Aldrich
Potassium chloride, KCl	P4504	Sigma-Aldrich
Potassium dihydrogen orthophosphate, KH2PO4	60218	Sigma-Aldrich
RNaseZAP	R2020	Sigma-Aldrich
Sodium acetate, CH3COONa	241245	Sigma-Aldrich
Sodium chloride, NaCl	S7653	Sigma-Aldrich
Sodium citrate	S1804	Sigma-Aldrich
Sodium hydroxide	30620	Sigma-Aldrich
Sodium phosphate dibasic	S0876	Sigma-Aldrich
Sodium dihydrogen phosphate,	S5011	Sigma-Aldrich
Superfrost coated glass slides	48311-703	VWR International
Torula yeast tRNA	10109517001	Roche
Triton X-100	93426	Sigma-Aldrich
Trizma Base	93362	Sigma-Aldrich
Tween 20	P1379	Sigma-Aldrich
X-Gal	B8503	Sigma-Aldrich
EdU Click-iT	C10340	Invitrogen
MAXIScript® Kit	AM1322	Ambion
Qiaprep Spin Miniprep kit	27106	Qiagen
pGEM-T Easy Vector kit	A1360	Promega

MinElute Gel Extraction kit	28604	Qiagen
iScript cDNA synthesis kit	170-8891	Bio-rad
Rneasy Mini kit	74104	Qiagen
SsoAdvancedTM Universal SBR Green Supermix	172-5271	Bio-rad
Collagenase	C9891	Sigma-Aldrich
Proteinase K	03115887001	Roche
Trypsin-EDTA	25200-056	Gibco
Dexamethasone	D1756	Sigma
LPS	L2880	Sigma
Ac-YVAD-cmk	SML0429	Sigma
Q-VD-OPh	SML0063	Sigma
IWR-1	I0161	Sigma
O-Phospho-L-serine	P0878	Sigma
TAG DNA polymerase	M023X	NEB
In Situ Cell Death Detection Kit TMR red	2156792910	Roche
Acridine orange	A9231	Sigma

Antibodies

Name	**Host**	**Source**	**Cat.no**	**Dilution**
Anti-GFP (Wehner et al. 2018)	chicken	Abcam	AB13970	1:300

Anti-HB9 arreiro-Iglesias et 2015)	mouse	DSHB	81.5c10	1:500
Anti-4c4 (Ohnmacht et al. 2016)	mouse	European Collection of Authenticated Cell Cultures (ECACC)	7.4.C4 (ECACC 92092321)	1:50
Monoclonal Anti-Tubulin, Acetylated (Wehner et al. 2018)	mouse	Sigma	T6793	1:300
Anti-tp63 (Wehner et al. 2018)	rabbit	Sigma	SAB2701838	1:300
Anti-collagen I (Wehner et al. 2018)	rabbit	Abcam	ab23730	1:300
Anti-GFAP (Wehner et al. 2018)	rabbit	Dako	Z0334	1:300
Anti-HuC/HuD (Ulrich et al. 2016)	mouse	Invitrogen	A-21271	1:100
Anti-mpx (Kenyon et al. 2018)	rabbit	GeneTex	GTX128379	1:300
Anti-mfap4	rabbit	GeneTex	GTX132692	1:300

Anti-Il-1β (Zheng et al. 2015)	rabbit	Proteintech	16806-1-AP	1:200
Anti-TNF-α (Nelson et al. 2013)	rabbit	AnaSpec	AS-55383	1-2000 1-500
Anti l-plastin(Ohnmacht et al. 2016)	rabbit	Yi Feng	-	1:500
AffiniPure Fab Fragment Donkey Anti-Rabbit IgG (H^+L) (Laresgoiti et al. 2016, Prost et al. 2016)	donkey	Jackson ImmunoResearch	711-007-003	40 µg/ml
Cy5 Anti-rabbit	donkey	Jackson ImmunoResearch	711-175-152	1:300
Cy™3 Anti-Rabbit IgG (H^+L)	donkey	Jackson ImmunoResearch	711-165-152	1:300
Cy™3 Aff Anti-Mouse IgG (H^+L)	donkey	Jackson ImmunoResearch	715-165-150	1:300
Alexa Fluor® 488 Anti-Mouse IgG(H^+L)	donkey	Jackson ImmunoResearch	715-545-150	1:300
Cy™5- Anti-Mouse IgG (H^+L)	donkey	Jackson ImmunoResearch	715-175-150	1:300

Solutions

Alkaline Tris buffer

100 mM Tris HCl (1 M stock, pH 9.5)

50 mM $MgCl_2$

100 mM NaCl

0.1% Tween® 20

EDTA – Trypsin

0.25% trypsin

1mM EDTA

PBS

Hybridisation Mix

50% Formamide

5 x SSC

0.1% Tween® 20

50 µg / ml heparin

5 mg / ml tRNA from Torula yeast

complete with RNase free H_2O, adjust

pH to 6.0

Hybridisation mix for washes (HMW)

50% Formamide5 x SSC

complete with RNase free water

ISH blocking buffer

1x PBS

0.1% Tween® 20

5% normal sheep serum

10mg / ml Bovine Serum Albumin (BSA)

IHC blocking buffer

1x PBS

1% DMSO

1% BSA

1% normal donkey

serum 0.7% TritonX 100

Paraformaldehyde 4%

16g paraformaldehyde

40 ml 10 x PBS

complete with d H_2O up to 400 ml

10 x Phosphate buffered saline (PBS), pH 7.5

80 g NaCl

14.16 g Na_2HPO_4

2.4 g KH_2PO_4

2 g KCl

adjust pH to 7.5

complete with d H_2O up to 1L

1 x Phosphate buffered saline (PBS), pH 7.5

100 ml of 10x Phosphate buffered saline (PB)

complete with d H_2O up to 1L

0.2% Phosphate buffered saline (PBS), TritonX-100

100 ml of 10x Phosphate buffered saline (PBS)

2ml TritonX-100

complete with d H_2O up to 1L

0.5% Phosphate buffered saline (PBS), TritonX-100

100 ml of 10x Phosphate buffered saline (PBS)

5ml TritonX-100

complete with d H_2O up to 1L

1% Phosphate buffered saline (PBS), TritonX-100

25 ml of 10x Phosphate buffered saline (PBS)

2,5ml TritonX-100

complete with d H_2O up to 250mL

0,1% Phosphate buffered saline (PBS), Tween-20

100 ml of 10x Phosphate buffered saline (PBS)

1 ml Tween-20

complete with d H_2O up to 1L

Sodium citrate (10 mM)

2.94 g sodium citrate

complete with d H_2O up to 1L

adjust pH to 6.5

20 x SSC stock solution, pH 7

175.3 g NaCl

88.2 g Citric acid trisodium salt

complete with RNase free H_2O up

to 1L

Staining Buffer

100 mM Tris-HCL pH 9,5

50mM $MgCl_2$

100mM NaCl

0.1% Tween 20

Staining Solution

1 tablet NBT/BCIP

10ml Staining Buffer

Stop solution

1 x PBS, pH 5.5

1 mM EDTA

0.1% Tween® 20

50 x TAE buffer

484 g Tris Base

114.2 ml Acetic Acid

1000 ml 0.1 EDTA, pH 8

adjust pH to 6.5 with HCl

complete with dd H_2O up to 2L

Tris HCl (1 M), pH 9.5

121.1 g Trizma base dissolved in 900 ml RNase free H_2O

adjust pH to 9.5 with HCl

complete with RNase free H_2O up to 1L

References

Abe, N., S. H. Borson, M. J. Gambello, F. Wang and V. Cavalli (2010). "Mammalian target of rapamycin (mTOR) activation increases axonal growth capacity of injured peripheral nerves." J Biol Chem **285**(36): 28034-28043.

Acuner Ozbabacan, S. E., A. Gursoy, R. Nussinov and O. Keskin (2014). "The structural pathway of interleukin 1 (IL-1) initiated signaling reveals mechanisms of oncogenic mutations and SNPs in inflammation and cancer." PLoS computational biology **10**(2): e1003470-e1003470.

Aghaallaei, N., B. Bajoghli, H. Schwarz, M. Schorpp and T. Boehm (2010). "Characterization of mononuclear phagocytic cells in medaka fish transgenic for a cxcr3a:gfp reporter." Proc Natl Acad Sci U S A **107**(42): 18079-18084.

Ahuja, C. S., J. R. Wilson, S. Nori, M. R. N. Kotter, C. Druschel, A. Curt and M. G. Fehlings (2017). "Traumatic spinal cord injury." Nat Rev Dis Primers **3**: 17018.

Akira, S. and H. Hemmi (2003). "Recognition of pathogen-associated molecular patterns by TLR family." Immunol Lett **85**(2): 85-95.

Al-Soudi, A., M. H. Kaaij and S. W. Tas (2017). "Endothelial cells: From innocent bystanders to active participants in immune responses." Autoimmunity Reviews **16**(9): 951-962.

Allan, S. M. and N. J. Rothwell (2003). "Inflammation in central nervous system injury." Philosophical Transactions of the Royal Society B: Biological Sciences **358**(1438): 1669-1677.

Almad, A., F. R. Sahinkaya and D. M. McTigue (2011). "Oligodendrocyte fate after spinal cord injury." Neurotherapeutics **8**(2): 262-273.

Alunni, A. and L. Bally-Cuif (2016). "A comparative view of regenerative neurogenesis in vertebrates." Development **143**(5): 741-753.

Alvarez-Buylla, A. and J. M. García-Verdugo (2002). "Neurogenesis in Adult Subventricular Zone." The Journal of Neuroscience **22**(3): 629.

Ambriz-Peña, X., E. A. García-Zepeda, I. Meza and G. Soldevila (2014). "Jak3 Enables Chemokine-Dependent Actin Cytoskeleton Reorganization by Regulating Cofilin and Rac/Rhoa GTPases Activation." PLOS ONE **9**(2): e88014.

Anand, S. K. and A. C. Mondal (2018). "TrkB receptor antagonism inhibits stab injury induced proliferative response in adult zebrafish (Danio rerio) brain." Neurosci Lett **672**: 28-33.

Ando, K., S. Fukuhara, N. Izumi, H. Nakajima, H. Fukui, R. N. Kelsh and N. Mochizuki (2016). "Clarification of mural cell coverage of vascular endothelial cells by live imaging of zebrafish." Development **143**(8): 1328-1339.

Ankeny, D. P. and P. G. Popovich (2009). "Mechanisms and implications of adaptive immune responses after traumatic spinal cord injury." Neuroscience **158**(3): 1112-1121.

Bao, F., Y. Chen, G. A. Dekaban and L. C. Weaver (2004). "Early anti-inflammatory treatment reduces lipid peroxidation and protein nitration after spinal cord injury in rats." Journal of Neurochemistry **88**(6): 1335-1344.

Bao, F., Y. Chen, K. A. Schneider and L. C. Weaver (2008). "An integrin inhibiting molecule decreases oxidative damage and improves neurological function after spinal cord injury." Experimental Neurology **214**(2): 160-167.

Barreiro-Iglesias, A., K. S. Mysiak, A. L. Scott, M. M. Reimer, Y. Yang, C. G. Becker and T. Becker (2015). "Serotonin Promotes Development and Regeneration of Spinal Motor Neurons in Zebrafish." Cell Rep **13**(5): 924-932.

Bartholdi, D. and M. E. Schwab (1997). "Expression of pro-inflammatory cytokine and chemokine mRNA upon experimental spinal cord injury in mouse: An in situ hybridization study." European Journal of Neuroscience **9**(7): 1422-1438.

Bassity, E. and T. G. Clark (2012). "Functional identification of dendritic cells in the teleost model, rainbow trout (Oncorhynchus mykiss)." PLoS One **7**(3): e33196.

Baumert, P. W., Jr. (1995). "Acute inflammation after injury. Quick control speeds rehabilitation." Postgrad Med **97**(2): 35-36, 39, 42 passim.

Baumgart, E. V., J. S. Barbosa, L. Bally-Cuif, M. Gotz and J. Ninkovic (2012). "Stab wound injury of the zebrafish telencephalon: A model for comparative analysis of reactive gliosis." Glia **60**(3): 343-357.

Beattie, M. S., J. C. Bresnahan and G. Lopate (1990). "Metamorphosis alters the response to spinal

cord transection in Xenopus laevis frogs." J Neurobiol **21**(7): 1108-1122.
Becker, C. G. and T. Becker (2002). "Repellent guidance of regenerating optic axons by chondroitin sulfate glycosaminoglycans in zebrafish." J Neurosci **22**(3): 842-853.
Becker, C. G. and T. Becker (2007). "Growth and pathfinding of regenerating axons in the optic projection of adult fish." J Neurosci Res **85**(12): 2793-2799.
Becker, C. G. and T. Becker (2008). "Adult zebrafish as a model for successful central nervous system regeneration." Restor Neurol Neurosci **26**(2-3): 71-80.
Becker, C. G. and T. Becker (2015). "Neuronal Regeneration from Ependymo-Radial Glial Cells: Cook, Little Pot, Cook!" Developmental Cell **32**(4): 516-527.
Becker, C. G., B. C. Lieberoth, F. Morellini, J. Feldner, T. Becker and M. Schachner (2004). "L1.1 is involved in spinal cord regeneration in adult zebrafish." Journal of Neuroscience **24**(36): 7837-7842.
Becker, C. G., B. C. Lieberoth, F. Morellini, J. Feldner, T. Becker and M. Schachner (2004). "L1.1 is involved in spinal cord regeneration in adult zebrafish." J Neurosci **24**(36): 7837-7842.
Becker, T. and C. G. Becker (2001). "Regenerating descending axons preferentially reroute to the gray matter in the presence of a general macrophage/microglial reaction caudal to a spinal transection in adult zebrafish." J Comp Neurol **433**(1): 131-147.
Becker, T. and C. G. Becker (2014). "Axonal regeneration in zebrafish." Curr Opin Neurobiol **27**: 186-191.
Becker, T., R. R. Bernhardt, E. Reinhard, M. F. Wullimann, E. Tongiorgi and M. Schachner (1998). "Readiness of zebrafish brain neurons to regenerate a spinal axon correlates with differential expression of specific cell recognition molecules." Journal of Neuroscience **18**(15): 5789-5803.
Becker, T., M. F. Wullimann, C. G. Becker, R. R. Bernhardt and M. Schachner (1997). "Axonal regrowth after spinal cord transection in adult zebrafish." J Comp Neurol **377**(4): 577-595.
Becker, T., M. F. Wullimann, C. G. Becker, R. R. Bernhardt and M. Schachner (1997). "Axonal regrowth after spinal cord transection in adult zebrafish." Journal of Comparative Neurology **377**(4): 577-595.
Bernardos, R. L. and P. A. Raymond (2006). "GFAP transgenic zebrafish." Gene Expression Patterns **6**(8): 1007-1013.
Bernardos, R. L. and P. A. Raymond (2006). "GFAP transgenic zebrafish." Gene Expr Patterns **6**(8): 1007-1013.
Bernhardt, R. R. (1999). "Cellular and molecular bases of axonal regeneration in the fish central nervous system." Exp Neurol **157**(2): 223-240.
Blackmore, M. G., Z. M. Wang, J. K. Lerch, D. Motti, Y. P. Zhang, C. B. Shields, J. K. Lee, J. L. Goldberg, V. P. Lemmon and J. L. Bixby (2012). "Kruppel-like Factor 7 engineered for transcriptional activation promotes axon regeneration in the adult corticospinal tract." Proceedings of the National Academy of Sciences of the United States of America **109**(19): 7517-7522.
Blasi, F., M. Riccio, A. Brogi, M. Strazza, M. L. Taddei, S. Romagnoli, A. Luddi, R. D'Angelo, S. Santi, E. Costantino-Ceccarini and M. Melli (1999). "Constitutive expression of interleukin-1beta (IL-1beta) in rat oligodendrocytes." Biol Chem **380**(2): 259-264.
Boato, F., K. Rosenberger, S. Nelissen, L. Geboes, E. M. Peters, R. Nitsch and S. Hendrix (2013). "Absence of IL-1beta positively affects neurological outcome, lesion development and axonal plasticity after spinal cord injury." J Neuroinflammation **10**: 6.
Bollaerts, I., J. Van Houcke, L. Andries, L. De Groef and L. Moons (2017). "Neuroinflammation as Fuel for Axonal Regeneration in the Injured Vertebrate Central Nervous System." Mediators Inflamm **2017**: 9478542.
Bollaerts, I., J. Van houcke, L. Andries, L. De Groef and L. Moons (2017). "Neuroinflammation as Fuel for Axonal Regeneration in the Injured Vertebrate Central Nervous System." Mediators of Inflammation **2017**: 14.
Bonilla, F. A. and H. C. Oettgen (2010). "Adaptive immunity." J Allergy Clin Immunol **125**(2 Suppl 2): S33-40.
Bosch, X. and M. Ramos-Casals (2014). Chapter 14 - Granulocytes: Neutrophils, Basophils, Eosinophils. The Autoimmune Diseases (Fifth Edition). N. R. Rose and I. R. Mackay. Boston, Academic Press**:** 201-215.
Bowers, E., A. Slaughter, P. S. Frenette, R. Kuick, O. M. Pello and D. Lucas (2018). "Granulocyte-derived TNFα promotes vascular and hematopoietic regeneration in the bone marrow." Nature medicine **24**(1): 95-102.
Bradbury, E. J., L. D. Moon, R. J. Popat, V. R. King, G. S. Bennett, P. N. Patel, J. W. Fawcett and S. B. McMahon (2002). "Chondroitinase ABC promotes functional recovery after spinal cord injury."

Nature **416**(6881): 636-640.
Briona, L. K. and R. I. Dorsky (2014). "Radial glial progenitors repair the zebrafish spinal cord following transection." Experimental neurology **256**: 81-92.
Bunge, M. B. (2016). "Efficacy of Schwann cell transplantation for spinal cord repair is improved with combinatorial strategies." J Physiol **594**(13): 3533-3538.
Canty, A. J., L. Huang, J. S. Jackson, G. E. Little, G. Knott, B. Maco and V. De Paola (2013). "In-vivo single neuron axotomy triggers axon regeneration to restore synaptic density in specific cortical circuits." Nature Communications **4**: 2038.
Cardozo, M. J., K. S. Mysiak, T. Becker and C. G. Becker (2017). "Reduce, reuse, recycle - Developmental signals in spinal cord regeneration." Dev Biol **432**(1): 53-62.
Carrillo, S. A., C. Anguita-Salinas, O. A. Pena, R. A. Morales, S. Munoz-Sanchez, C. Munoz-Montecinos, S. Paredes-Zuniga, K. Tapia and M. L. Allende (2016). "Macrophage Recruitment Contributes to Regeneration of Mechanosensory Hair Cells in the Zebrafish Lateral Line." J Cell Biochem **117**(8): 1880-1889.
Chaplin, D. D. (2010). "Overview of the Immune Response." The Journal of allergy and clinical immunology **125**(2 Suppl 2): S3-23.
Chassot, B., D. Pury and A. Jazwinska (2016). "Zebrafish fin regeneration after cryoinjury-induced tissue damage." Biol Open **5**(6): 819-828.
Chen, L., H. Deng, H. Cui, J. Fang, Z. Zuo, J. Deng, Y. Li, X. Wang and L. Zhao (2018). "Inflammatory responses and inflammation-associated diseases in organs." Oncotarget **9**(6): 7204-7218.
Chen, Z. L., W. M. Yu and S. Strickland (2007). "Peripheral regeneration." Annual Review of Neuroscience **30**: 209-233.
Cheng, X., H. Wang, X. Zhang, S. Zhao, Z. Zhou, X. Mu, C. Zhao and W. Teng (2017). "The Role of SDF-1/CXCR4/CXCR7 in Neuronal Regeneration after Cerebral Ischemia." Front Neurosci **11**: 590.
Chung, K. F. (2009). Chapter 27 - Cytokines. Asthma and COPD (Second Edition). P. J. Barnes et al. Oxford, Academic Press**:** 327-341.
Church, J. S., L. M. Milich, J. K. Lerch, P. G. Popovich and D. M. McTigue (2017). "E6020, a synthetic TLR4 agonist, accelerates myelin debris clearance, Schwann cell infiltration, and remyelination in the rat spinal cord." Glia **65**(6): 883-899.
Clark, R. and T. Kupper (2005). "Old Meets New: The Interaction Between Innate and Adaptive Immunity." Journal of Investigative Dermatology **125**(4): 629-637.
Cohen, M., H. Ben-Yehuda, Z. Porat, C. Raposo, S. Gordon and M. Schwartz (2017). "Newly Formed Endothelial Cells Regulate Myeloid Cell Activity Following Spinal Cord Injury via Expression of CD200 Ligand." J Neurosci **37**(4): 972-985.
Colaco, H. G. and L. F. Moita (2016). "Initiation of innate immune responses by surveillance of homeostasis perturbations." Febs j **283**(13): 2448-2457.
Côté, M.-P., A. A. Amin, V. J. Tom and J. D. Houle (2011). "Peripheral Nerve Grafts Support Regeneration after Spinal Cord Injury." Neurotherapeutics **8**(2): 294-303.
Coupe, P., M. Munz, J. V. Manjon, E. S. Ruthazer and D. L. Collins (2012). "A CANDLE for a deeper in vivo insight." Med Image Anal **16**(4): 849-864.
Cregg, J. M., M. A. DePaul, A. R. Filous, B. T. Lang, A. Tran and J. Silver (2014). "Functional regeneration beyond the glial scar." Experimental Neurology **253**: 197-207.
Curado, S., D. Y. Stainier and R. M. Anderson (2008). "Nitroreductase-mediated cell/tissue ablation in zebrafish: a spatially and temporally controlled ablation method with applications in developmental and regeneration studies." Nat Protoc **3**(6): 948-954.
D'Rozario, M., K. R. Monk and S. C. Petersen (2017). Analysis of myelinated axon formation in zebrafish. Zebrafish: Disease Models and Chemical Screens. H. W. Detrich et al. San Diego, Elsevier Academic Press Inc. **138:** 383-414.
Danilova, N. and L. A. Steiner (2002). "B cells develop in the zebrafish pancreas." Proceedings of the National Academy of Sciences of the United States of America **99**(21): 13711-13716.
Davalos, D., J. Grutzendler, G. Yang, J. V. Kim, Y. Zuo, S. Jung, D. R. Littman, M. L. Dustin and W. B. Gan (2005). "ATP mediates rapid microglial response to local brain injury in vivo." Nat Neurosci **8**(6): 752-758.
David, S. and A. J. Aguayo (1981). "Axonal elongation into peripheral nervous system "bridges" after central nervous system injury in adult rats." Science **214**(4523): 931.
David, S., C. Bouchard, O. Tsatas and N. Giftochristos (1990). "Macrophages can modify the nonpermissive nature of the adult mammalian central nervous system." Neuron **5**(4): 463-469.

David, S. and S. Lacroix (2003). "Molecular approaches to spinal cord repair." Annual Review of Neuroscience **26**: 411-440.
Davis, O., R. Merrison-Hort, S. R. Soffe and R. Borisyuk (2017). "Studying the role of axon fasciculation during development in a computational model of the Xenopus tadpole spinal cord." Scientific Reports **7**(1): 13551.
den Haan, J. M., R. Arens and M. C. van Zelm (2014). "The activation of the adaptive immune system: cross-talk between antigen-presenting cells, T cells and B cells." Immunol Lett **162**(2 Pt B): 103-112.
Dervan, A. G. and B. L. Roberts (2003). "Reaction of spinal cord central canal cells to cord transection and their contribution to cord regeneration." J Comp Neurol **458**(3): 293-306.
Dervan, A. G. and B. L. Roberts (2003). "Reaction of spinal cord central canal cells to cord transection and their contribution to cord regeneration." Journal of Comparative Neurology **458**(3): 293-306.
Dias, T. B., Y. J. Yang, K. Ogai, T. Becker and C. G. Becker (2012). "Notch signaling controls generation of motor neurons in the lesioned spinal cord of adult zebrafish." J Neurosci **32**(9): 3245-3252.
Diekmann, H., P. Kalbhen and D. Fischer (2015). "Active mechanistic target of rapamycin plays an ancillary rather than essential role in zebrafish CNS axon regeneration." Front Cell Neurosci **9**: 251.
Diekmann, H., P. Kalbhen and D. Fischer (2015). "Active mechanistic target of rapamycin plays an ancillary rather than essential role in zebrafish CNS axon regeneration." Frontiers in Cellular Neuroscience **9**: 11.
Diekmann, H., P. Kalbhen and D. Fischer (2015). "Characterization of optic nerve regeneration using transgenic zebrafish." Frontiers in Cellular Neuroscience **9**(118).
Diekmann, H., P. Kalbhen and D. Fischer (2015). "Characterization of optic nerve regeneration using transgenic zebrafish." Frontiers in Cellular Neuroscience **9**: 118.
Dinarello, C. A. (1996). "Biologic basis for interleukin-1 in disease." Blood **87**(6): 2095-2147.
Dinarello, C. A. (2005). "The many worlds of reducing interleukin-1." Arthritis Rheum **52**(7): 1960-1967.
Donat, C. K., G. Scott, S. M. Gentleman and M. Sastre (2017). "Microglial Activation in Traumatic Brain Injury." Frontiers in Aging Neuroscience **9**: 208.
Donnelly, D. J. and P. G. Popovich (2008). "Inflammation and its role in neuroprotection, axonal regeneration and functional recovery after spinal cord injury." Exp Neurol **209**(2): 378-388.
Donnelly, D. J. and P. G. Popovich (2008). "Inflammation and its role in neuroprotection, axonal regeneration and functional recovery after spinal cord injury." Experimental Neurology **209**(2): 378-388.
Eda, S., M. Yamanaka and M. Beppu (2004). "Carbohydrate-mediated phagocytic recognition of early apoptotic cells undergoing transient capping of CD43 glycoprotein." J Biol Chem **279**(7): 5967-5974.
Edelson, B. T., W. Kc, R. Juang, M. Kohyama, L. A. Benoit, P. A. Klekotka, C. Moon, J. C. Albring, W. Ise, D. G. Michael, D. Bhattacharya, T. S. Stappenbeck, M. J. Holtzman, S. S. Sung, T. L. Murphy, K. Hildner and K. M. Murphy (2010). "Peripheral CD103+ dendritic cells form a unified subset developmentally related to CD8alpha+ conventional dendritic cells." J Exp Med **207**(4): 823-836.
El-Brolosy, M. A. and D. Y. R. Stainier (2017). "Genetic compensation: A phenomenon in search of mechanisms." PLOS Genetics **13**(7): e1006780.
Elkabes, S., E. M. DiCicco-Bloom and I. B. Black (1996). "Brain microglia/macrophages express neurotrophins that selectively regulate microglial proliferation and function." J Neurosci **16**(8): 2508-2521.
Ellett, F., L. Pase, J. W. Hayman, A. Andrianopoulos and G. J. Lieschke (2011). "mpeg1 promoter transgenes direct macrophage-lineage expression in zebrafish." Blood **117**(4): e49.
Ellett, F., L. Pase, J. W. Hayman, A. Andrianopoulos and G. J. Lieschke (2011). "mpeg1 promoter transgenes direct macrophage-lineage expression in zebrafish." Blood **117**(4): e49-56.
Elsaeidi, F., M. A. Bemben, X.-F. Zhao and D. Goldman (2014). "Jak/Stat Signaling Stimulates Zebrafish Optic Nerve Regeneration and Overcomes the Inhibitory Actions of Socs3 and Sfpq." The Journal of Neuroscience **34**(7): 2632-2644.
Elsaeidi, F., M. A. Bemben, X. F. Zhao and D. Goldman (2014). "Jak/Stat Signaling Stimulates Zebrafish Optic Nerve Regeneration and Overcomes the Inhibitory Actions of Socs3 and Sfpq." Journal of Neuroscience **34**(7): 2632-2644.

Emlet, D. R., H. Gomez and J. A. Kellum (2019). Chapter 21 - Pathogen-Associated Molecular Patterns, Damage-Associated Molecular Patterns, and Their Receptors in Acute Kidney Injury. Critical Care Nephrology (Third Edition). C. Ronco et al. Philadelphia, Content Repository Only!**:** 121-127.e123.
Esche, C., C. Stellato and L. A. Beck (2005). "Chemokines: Key Players in Innate and Adaptive Immunity." Journal of Investigative Dermatology **125**(4): 615-628.
Farasat, S., I. Aksentijevich and J. R. Toro (2008). "Autoinflammatory diseases: clinical and genetic advances." Arch Dermatol **144**(3): 392-402.
Farooque, M., J. Isaksson and Y. Olsson (2001). "Improved recovery after spinal cord injury in neuronal nitric oxide synthase-deficient mice but not in TNF-alpha-deficient mice." J Neurotrauma **18**(1): 105-114.
Faul, F., E. Erdfelder, A. Buchner and A. G. Lang (2009). "Statistical power analyses using G*Power 3.1: tests for correlation and regression analyses." Behav Res Methods **41**(4): 1149-1160.
Feng, Y., S. Renshaw and P. Martin (2012). "Live imaging of tumor initiation in zebrafish larvae reveals a trophic role for leukocyte-derived PGE(2)." Curr Biol **22**(13): 1253-1259.
Feng, Y., S. Renshaw and P. Martin (2012). "Live Imaging of Tumor Initiation in Zebrafish Larvae Reveals a Trophic Role for Leukocyte-Derived PGE(2)." Current Biology **22**(13): 1253-1259.
Feng, Y., C. Santoriello, M. Mione, A. Hurlstone and P. Martin (2010). "Live imaging of innate immune cell sensing of transformed cells in zebrafish larvae: Parallels between tumor initiation and wound inflammation." PLoS Biology **8**(12).
Ferguson, A. R., R. N. Christensen, J. C. Gensel, B. A. Miller, F. Sun, E. C. Beattie, J. C. Bresnahan and M. S. Beattie (2008). "Cell death after spinal cord injury is exacerbated by rapid TNFα-induced trafficking of GluR2-lacking AMPARs to the plasma membrane." Journal of Neuroscience **28**(44): 11391-11400.
Fernandez-Klett, F. and J. Priller (2014). "The fibrotic scar in neurological disorders." Brain Pathol **24**(4): 404-413.
Fetcho, J. (2003). "Zebrafish: A Practical Approach. The Practical Approach Series, Volume 261. Edited by Christiane Nüsslein-Volhard and Ralf Dahm." The Quarterly Review of Biology **78**(4): 477-478.
Fialkow, L., Y. Wang and G. P. Downey (2007). "Reactive oxygen and nitrogen species as signaling molecules regulating neutrophil function." Free Radic Biol Med **42**(2): 153-164.
Filbin, M. T. (2003). "Myelin-associated inhibitors of axonal regeneration in the adult mammalian CNS." Nature Reviews Neuroscience **4**: 703.
Filous, A. R. and J. M. Schwab (2018). "Determinants of Axon Growth, Plasticity, and Regeneration in the Context of Spinal Cord Injury." American Journal of Pathology **188**(1): 53-62.
Finnson, K. W., S. McLean, G. M. Di Guglielmo and A. Philip (2013). "Dynamics of Transforming Growth Factor Beta Signaling in Wound Healing and Scarring." Adv Wound Care (New Rochelle) **2**(5): 195-214.
Flaherty, D. K. (2012). Chapter 5 - Antigen-Presenting Cells. Immunology for Pharmacy. D. K. Flaherty. Saint Louis, Mosby**:** 37-44.
Franze, K., P. A. Janmey and J. Guck (2013). "Mechanics in Neuronal Development and Repair." Annual Review of Biomedical Engineering **15**(1): 227-251.
Gadani, Sachin P., James T. Walsh, John R. Lukens and J. Kipnis (2015). "Dealing with Danger in the CNS: The Response of the Immune System to Injury." Neuron **87**(1): 47-62.
Gage, F. H. and S. Temple (2013). "Neural stem cells: generating and regenerating the brain." Neuron **80**(3): 588-601.
Gallo, R. L. and V. Nizet (2008). "Innate barriers against infection and associated disorders." Drug discovery today. Disease mechanisms **5**(2): 145-152.
Ganger, M. T., G. D. Dietz and S. J. Ewing (2017). "A common base method for analysis of qPCR data and the application of simple blocking in qPCR experiments." BMC Bioinformatics **18**(1): 534.
Gao, Y., K. W. Deng, J. W. Hou, J. B. Bryson, A. Barco, E. Nikulina, T. Spencer, W. Mellado, E. R. Kandel and M. T. Filbin (2004). "Activated CREB is sufficient to overcome inhibitors in myelin and promote spinal axon regeneration in vivo." Neuron **44**(4): 609-621.
Genovese, T., E. Mazzon, C. Crisafulli, R. Di Paola, C. Muià, P. Bramanti and S. Cuzzocrea (2006). "Immunomodulatory effects of etanercept in an experimental model of spinal cord injury." Journal of Pharmacology and Experimental Therapeutics **316**(3): 1006-1016.
Genovese, T., E. Mazzon, C. Crisafulli, R. Di Paola, C. Muià, E. Esposito, P. Bramanti and S. Cuzzocrea (2008). "TNF-α blockage in a mouse model of SCI: Evidence for improved outcome."

Shock **29**(1): 32-41.
Gensel, J. C., S. Nakamura, Z. Guan, N. van Rooijen, D. P. Ankeny and P. G. Popovich (2009). "Macrophages Promote Axon Regeneration with Concurrent Neurotoxicity." The Journal of neuroscience : the official journal of the Society for Neuroscience **29**(12): 3956-3968.
Geoffroy, C. G. and B. Zheng (2014). "Myelin-Associated Inhibitors in Axonal Growth After CNS Injury." Current opinion in neurobiology **0**: 31-38.
Geremia, N. M., F. Bao, T. E. Rosenzweig, T. Hryciw, L. Weaver, G. A. Dekaban and A. Brown (2012). "CD11d antibody treatment improves recovery in spinal cord-injured mice." Journal of Neurotrauma **29**(3): 539-550.
Gesuete, R., M. P. Stenzel-Poore and S. G. Kohama (2014). "Toll-Like Receptors and Ischemic Brain Injury." Journal of Neuropathology & Experimental Neurology **73**(5): 378-386.
Geurtzen, K., F. Knopf, D. Wehner, L. F. Huitema, S. Schulte-Merker and G. Weidinger (2014). "Mature osteoblasts dedifferentiate in response to traumatic bone injury in the zebrafish fin and skull." Development **141**(11): 2225-2234.
Ghosh, S. and S. P. Hui (2016). "Regeneration of Zebrafish CNS: Adult Neurogenesis." Neural Plast **2016**: 5815439.
Ghosh, S. and S. P. Hui (2016). "Regeneration of Zebrafish CNS: Adult Neurogenesis." Neural Plasticity **2016**: 5815439.
Ghosh, S. and S. P. Hui (2018). "Axonal regeneration in zebrafish spinal cord." Regeneration (Oxford, England) **5**(1): 43-60.
Ghosh, S. and S. P. Hui (2018). "Axonal regeneration in zebrafish spinal cord." Regeneration (Oxf) **5**(1): 43-60.
Giulian, D., T. J. Baker, L. C. Shih and L. B. Lachman (1986). "Interleukin 1 of the central nervous system is produced by ameboid microglia." J Exp Med **164**(2): 594-604.
Goldshmit, Y., F. Frisca, A. R. Pinto, A. Pébay, J.-K. K. Y. Tang, A. L. Siegel, J. Kaslin and P. D. Currie (2014). "Fgf2 improves functional recovery—decreasing gliosis and increasing radial glia and neural progenitor cells after spinal cord injury." Brain and Behavior **4**(2): 187-200.
Goldshmit, Y., T. E. Sztal, P. R. Jusuf, T. E. Hall, M. Nguyen-Chi and P. D. Currie (2012). "Fgf-Dependent Glial Cell Bridges Facilitate Spinal Cord Regeneration in Zebrafish." Journal of Neuroscience **32**(22): 7477-7492.
Goldshmit, Y., T. E. Sztal, P. R. Jusuf, T. E. Hall, M. Nguyen-Chi and P. D. Currie (2012). "Fgf-dependent glial cell bridges facilitate spinal cord regeneration in zebrafish." J Neurosci **32**(22): 7477-7492.
Goldshmit, Y., T. E. Sztal, P. R. Jusuf, T. E. Hall, M. Nguyen-Chi and P. D. Currie (2012). "Fgf-Dependent Glial Cell Bridges Facilitate Spinal Cord Regeneration in Zebrafish." The Journal of Neuroscience **32**(22): 7477.
Gong, Y. F., L. X. Xiang and J. Z. Shao (2009). "CD154-CD40 interactions are essential for thymus-dependent antibody production in zebrafish: insights into the origin of costimulatory pathway in helper T cell-regulated adaptive immunity in early vertebrates." J Immunol **182**(12): 7749-7762.
Graciarena, M., C. Dambly-Chaudiere and A. Ghysen (2014). "Dynamics of axonal regeneration in adult and aging zebrafish reveal the promoting effect of a first lesion." Proceedings of the National Academy of Sciences of the United States of America **111**(4): 1610-1615.
Grandel, H., J. Kaslin, J. Ganz, I. Wenzel and M. Brand (2006). "Neural stem cells and neurogenesis in the adult zebrafish brain: Origin, proliferation dynamics, migration and cell fate." Developmental Biology **295**(1): 263-277.
Grandel, H., J. Kaslin, J. Ganz, I. Wenzel and M. Brand (2006). "Neural stem cells and neurogenesis in the adult zebrafish brain: origin, proliferation dynamics, migration and cell fate." Dev Biol **295**(1): 263-277.
Grandpre, T. and S. M. Strittmatter (2001). "Nogo: a molecular determinant of axonal growth and regeneration." Neuroscientist **7**(5): 377-386.
Gris, D., D. R. Marsh, M. A. Oatway, Y. Chen, E. F. Hamilton, G. A. Dekaban and L. C. Weaver (2004). "Transient Blockade of the CD11d/CD18 Integrin Reduces Secondary Damage after Spinal Cord Injury, Improving Sensory, Autonomic, and Motor Function." Journal of Neuroscience **24**(16): 4043-4051.
Gross, C. G. (2000). "Neurogenesis in the adult brain: death of a dogma." Nat Rev Neurosci **1**(1): 67-73.
Guth, L., C. R. Brewer, W. F. Collins, Jr., M. E. Goldberger and E. R. Perl (1980). "Criteria for evaluating spinal cord regeneration experiments." Exp Neurol **69**(1): 1-3.

Halloum, I., S. Carrère-Kremer, M. Blaise, A. Viljoen, A. Bernut, V. Le Moigne, C. Vilchèze, Y. Guérardel, G. Lutfalla, J.-L. Herrmann, W. R. Jacobs and L. Kremer (2016). "Deletion of a dehydratase important for intracellular growth and cording renders rough Mycobacterium abscessus avirulent." Proceedings of the National Academy of Sciences **113**(29): E4228.
Hamilton, F. (1822). An account of the fishes found in the river Ganges and its branches. Edinburgh :, Printed for A. Constable and company; [etc., etc.].
Hanke, M. L. and T. Kielian (2011). "Toll-like receptors in health and disease in the brain: mechanisms and therapeutic potential." Clinical science (London, England : 1979) **121**(9): 367-387.
Hasegawa, T., C. J. Hall, P. S. Crosier, G. Abe, K. Kawakami, A. Kudo and A. Kawakami (2017). "Transient inflammatory response mediated by interleukin-1beta is required for proper regeneration in zebrafish fin fold." Elife **6**.
Hasegawa, T., C. J. Hall, P. S. Crosier, G. Abe, K. Kawakami, A. Kudo and A. Kawakami (2017). "Transient inflammatory response mediated by interleukin-1β is required for proper regeneration in zebrafish fin fold." eLife **6**: e22716.
Hashimoto, M., A. Nitta, H. Fukumitsu, H. Nomoto, L. Shen and S. Furukawa (2005). "Involvement of glial cell line-derived neurotrophic factor in activation processes of rodent macrophages." J Neurosci Res **79**(4): 476-487.
Haugland, G. T., A. E. Jordal and H. I. Wergeland (2012). "Characterization of small, mononuclear blood cells from salmon having high phagocytic capacity and ability to differentiate into dendritic like cells." PLoS One **7**(11): e49260.
He, Z. and Y. Jin (2016). "Intrinsic Control of Axon Regeneration." Neuron **90**(3): 437-451.
Hill, C. E. (2017). "A view from the ending: Axonal dieback and regeneration following SCI." Neuroscience Letters **652**: 11-24.
Hilton, B. J. and F. Bradke (2017). "Can injured adult CNS axons regenerate by recapitulating development?" Development **144**(19): 3417-3429.
Hoffman, W., F. G. Lakkis and G. Chalasani (2016). "B Cells, Antibodies, and More." Clinical Journal of the American Society of Nephrology : CJASN **11**(1): 137-154.
Howe, K., M. D. Clark, C. F. Torroja, J. Torrance, C. Berthelot, M. Muffato, J. E. Collins, S. Humphray, K. McLaren, L. Matthews, S. McLaren, I. Sealy, M. Caccamo, C. Churcher, C. Scott, J. C. Barrett, R. Koch, G.-J. Rauch, S. White, W. Chow, B. Kilian, L. T. Quintais, J. A. Guerra-Assunção, Y. Zhou, Y. Gu, J. Yen, J.-H. Vogel, T. Eyre, S. Redmond, R. Banerjee, J. Chi, B. Fu, E. Langley, S. F. Maguire, G. K. Laird, D. Lloyd, E. Kenyon, S. Donaldson, H. Sehra, J. Almeida-King, J. Loveland, S. Trevanion, M. Jones, M. Quail, D. Willey, A. Hunt, J. Burton, S. Sims, K. McLay, B. Plumb, J. Davis, C. Clee, K. Oliver, R. Clark, C. Riddle, D. Elliott, G. Threadgold, G. Harden, D. Ware, S. Begum, B. Mortimore, G. Kerry, P. Heath, B. Phillimore, A. Tracey, N. Corby, M. Dunn, C. Johnson, J. Wood, S. Clark, S. Pelan, G. Griffiths, M. Smith, R. Glithero, P. Howden, N. Barker, C. Lloyd, C. Stevens, J. Harley, K. Holt, G. Panagiotidis, J. Lovell, H. Beasley, C. Henderson, D. Gordon, K. Auger, D. Wright, J. Collins, C. Raisen, L. Dyer, K. Leung, L. Robertson, K. Ambridge, D. Leongamornlert, S. McGuire, R. Gilderthorp, C. Griffiths, D. Manthravadi, S. Nichol, G. Barker, S. Whitehead, M. Kay, J. Brown, C. Murnane, E. Gray, M. Humphries, N. Sycamore, D. Barker, D. Saunders, J. Wallis, A. Babbage, S. Hammond, M. Mashreghi-Mohammadi, L. Barr, S. Martin, P. Wray, A. Ellington, N. Matthews, M. Ellwood, R. Woodmansey, G. Clark, J. D. Cooper, A. Tromans, D. Grafham, C. Skuce, R. Pandian, R. Andrews, E. Harrison, A. Kimberley, J. Garnett, N. Fosker, R. Hall, P. Garner, D. Kelly, C. Bird, S. Palmer, I. Gehring, A. Berger, C. M. Dooley, Z. Ersan-Ürün, C. Eser, H. Geiger, M. Geisler, L. Karotki, A. Kirn, J. Konantz, M. Konantz, M. Oberländer, S. Rudolph-Geiger, M. Teucke, C. Lanz, G. Raddatz, K. Osoegawa, B. Zhu, A. Rapp, S. Widaa, C. Langford, F. Yang, S. C. Schuster, N. P. Carter, J. Harrow, Z. Ning, J. Herrero, S. M. J. Searle, A. Enright, R. Geisler, R. H. A. Plasterk, C. Lee, M. Westerfield, P. J. de Jong, L. I. Zon, J. H. Postlethwait, C. Nüsslein-Volhard, T. J. P. Hubbard, H. R. Crollius, J. Rogers and D. L. Stemple (2013). "The zebrafish reference genome sequence and its relationship to the human genome." Nature **496**: 498.
Hu, X., J. Cai, J. Yang and G. M. Smith (2010). "Sensory axon targeting is increased by NGF gene therapy within the lesioned adult femoral nerve." Experimental Neurology **223**(1): 153-165.
Huang, Z., W. Wang, J. Ma, B. Li, J. Chen, H. Yang and Saijilafu (2017). "mTOR signaling pathway differently regulates central and peripheral axon regeneration." Acta Biochimica et Biophysica Sinica **49**(8): 689-695.
Hui, S. P., A. Dutta and S. Ghosh (2010). "Cellular Response After Crush Injury in Adult Zebrafish Spinal Cord." Developmental Dynamics **239**(11): 2962-2979.
Hui, S. P., A. Dutta and S. Ghosh (2010). "Cellular response after crush injury in adult zebrafish

spinal cord." Dev Dyn **239**(11): 2962-2979.
Hui, S. P., D. Z. Sheng, K. Sugimoto, A. Gonzalez-Rajal, S. Nakagawa, D. Hesselson and K. Kikuchi (2017). "Zebrafish Regulatory T Cells Mediate Organ-Specific Regenerative Programs." Dev Cell **43**(6): 659-672.e655.
Iaci, J. F., A. M. Vecchione, M. P. Zimber and A. O. Caggiano (2007). "Chondroitin sulfate proteoglycans in spinal cord contusion injury and the effects of chondroitinase treatment." J Neurotrauma **24**(11): 1743-1759.
Ito, T., J. M. Connett, S. L. Kunkel and A. Matsukawa (2013). "The linkage of innate and adaptive immune response during granulomatous development." Frontiers in Immunology **4**: 10.
Iversen, M. B., L. S. Reinert, M. K. Thomsen, I. Bagdonaite, R. Nandakumar, N. Cheshenko, T. Prabakaran, S. Y. Vakhrushev, M. Krzyzowska, S. K. Kratholm, F. Ruiz-Perez, S. V. Petersen, S. Goriely, B. M. Bibby, K. Eriksson, J. Ruland, A. R. Thomsen, B. C. Herold, H. H. Wandall, S. Frische, C. K. Holm and S. R. Paludan (2015). "An innate antiviral pathway acting before interferons at epithelial surfaces." Nature Immunology **17**: 150.
Iwasaki, A. and R. Medzhitov (2010). "Regulation of adaptive immunity by the innate immune system." Science (New York, N.Y.) **327**(5963): 291-295.
James, N. D., J. Shea, E. M. Muir, J. Verhaagen, B. L. Schneider and E. J. Bradbury (2015). "Chondroitinase gene therapy improves upper limb function following cervical contusion injury." Exp Neurol **271**: 131-135.
Jault, C., L. Pichon and J. Chluba (2004). Toll-like receptor gene family and TIR-domain adapters in Danio rerio.
Jeschke, A. and A. Haas (2016). "Deciphering the roles of phosphoinositide lipids in phagolysosome biogenesis." Communicative & Integrative Biology **9**(3): e1174798.
Jin, X. M. and T. Yamashita (2016). "Microglia in central nervous system repair after injury." Journal of Biochemistry **159**(5): 491-496.
Julier, Z., A. J. Park, P. S. Briquez and M. M. Martino (2017). "Promoting tissue regeneration by modulating the immune system." Acta Biomaterialia **53**: 13-28.
Kadl, A. and N. Leitinger (2005). "The role of endothelial cells in the resolution of acute inflammation." Antioxid Redox Signal **7**(11-12): 1744-1754.
Kasinathan, N., M. B. Vanathi, V. M. Subrahmanyam and J. V. Rao (2015). "A review on response of immune system in spinal cord injury and therapeutic agents useful in treatment." Curr Pharm Biotechnol **16**(1): 26-34.
Kato, K., H. Liu, S. Kikuchi, R. R. Myers and V. I. Shubayev (2010). "Immediate anti-tumor necrosis factor-alpha (etanercept) therapy enhances axonal regeneration after sciatic nerve crush." J Neurosci Res **88**(2): 360-368.
Kawano, H., J. Kimura-Kuroda, Y. Komuta, N. Yoshioka, H. P. Li, K. Kawamura, Y. Li and G. Raisman (2012). "Role of the lesion scar in the response to damage and repair of the central nervous system." Cell and Tissue Research **349**(1): 169-180.
Kenyon, A., D. Gavriouchkina, J. Zorman, V. Chong-Morrison, G. Napolitani, V. Cerundolo and T. Sauka-Spengler (2018). "Generation of a double binary transgenic zebrafish model to study myeloid gene regulation in response to oncogene activation in melanocytes." Disease Models & Mechanisms.
Keoni, C. L. and T. L. Brown (2015). "Inhibition of Apoptosis and Efficacy of Pan Caspase Inhibitor, Q-VD-OPh, in Models of Human Disease." J Cell Death **8**: 1-7.
Kerschensteiner, M., E. Gallmeier, L. Behrens, V. V. Leal, T. Misgeld, W. E. Klinkert, R. Kolbeck, E. Hoppe, R. L. Oropeza-Wekerle, I. Bartke, C. Stadelmann, H. Lassmann, H. Wekerle and R. Hohlfeld (1999). "Activated human T cells, B cells, and monocytes produce brain-derived neurotrophic factor in vitro and in inflammatory brain lesions: a neuroprotective role of inflammation?" J Exp Med **189**(5): 865-870.
Kiefer, R., D. Lindholm and G. W. Kreutzberg (1993). "Interleukin-6 and transforming growth factor-beta 1 mRNAs are induced in rat facial nucleus following motoneuron axotomy." Eur J Neurosci **5**(7): 775-781.
Kigerl, K. A., J. C. Gensel, D. P. Ankeny, J. K. Alexander, D. J. Donnelly and P. G. Popovich (2009). "Identification of two distinct macrophage subsets with divergent effects causing either neurotoxicity or regeneration in the injured mouse spinal cord." J Neurosci **29**(43): 13435-13444.
Kigerl, K. A., V. M. McGaughy and P. G. Popovich (2006). "Comparative analysis of lesion development and intraspinal inflammation in four strains of mice following spinal contusion injury." Journal of Comparative Neurology **494**(4): 578-594.

Kigerl, K. A., V. M. McGaughy and P. G. Popovich (2006). "Comparative analysis of lesion development and intraspinal inflammation in four strains of mice following spinal contusion injury." J Comp Neurol **494**(4): 578-594.
Kim, G. M., J. Xu, J. Xu, S. K. Song, P. Yan, G. Ku, X. M. Xu and C. Y. Hsu (2001). "Tumor necrosis factor receptor deletion reduces nuclear factor-κB activation, cellular inhibitor of apoptosis protein 2 expression, and functional recovery after traumatic spinal cord injury." Journal of Neuroscience **21**(17): 6617-6625.
Kim, S. U. and J. de Vellis (2005). "Microglia in health and disease." J Neurosci Res **81**(3): 302-313.
Kipnis, J. (2016). "Multifaceted interactions between adaptive immunity and the central nervous system." Science **353**(6301): 766.
Kisiswa, L., C. Osório, C. Erice, T. Vizard, S. Wyatt and A. M. Davies (2013). "TNFα reverse signaling promotes sympathetic axon growth and target innervation." Nature neuroscience **16**(7): 865-873.
Kizil, C., J. Kaslin, V. Kroehne and M. Brand (2011). "Adult neurogenesis and brain regeneration in zebrafish." Developmental Neurobiology **72**(3): 429-461.
Kizil, C., N. Kyritsis, S. Dudczig, V. Kroehne, D. Freudenreich, J. Kaslin and M. Brand (2012). "Regenerative Neurogenesis from Neural Progenitor Cells Requires Injury-Induced Expression of Gata3." Developmental Cell **23**(6): 1230-1237.
Knopf, F., K. Schnabel, C. Haase, K. Pfeifer, K. Anastassiadis and G. Weidinger (2010). "Dually inducible TetON systems for tissue-specific conditional gene expression in zebrafish." Proceedings of the National Academy of Sciences of the United States of America **107**(46): 19933-19938.
Kobayashi, T., P. T. Walsh, M. C. Walsh, K. M. Speirs, E. Chiffoleau, C. G. King, W. W. Hancock, J. H. Caamano, C. A. Hunter, P. Scott, L. A. Turka and Y. Choi (2003). "TRAF6 is a critical factor for dendritic cell maturation and development." Immunity **19**(3): 353-363.
Kolaczkowska, E. and P. Kubes (2013). "Neutrophil recruitment and function in health and inflammation." Nature Reviews Immunology **13**: 159.
Kroehne, V., D. Freudenreich, S. Hans, J. Kaslin and M. Brand (2011). "Regeneration of the adult zebrafish brain from neurogenic radial glia-type progenitors." Development **138**(22): 4831-4841.
Kroner, A., A. D. Greenhalgh, J. G. Zarruk, R. Passos Dos Santos, M. Gaestel and S. David (2014). "TNF and increased intracellular iron alter macrophage polarization to a detrimental M1 phenotype in the injured spinal cord." Neuron **83**(5): 1098-1116.
Kroner, A., A. D. Greenhalgh, J. G. Zarruk, R. PassosdosSantos, M. Gaestel and S. David (2014). "TNF and Increased Intracellular Iron Alter Macrophage Polarization to a Detrimental M1 Phenotype in the Injured Spinal Cord." Neuron **83**(5): 1098-1116.
Kubota, K., H. Saiwai, H. Kumamaru, T. Maeda, Y. Ohkawa, Y. Aratani, T. Nagano, Y. Iwamoto and S. Okada (2012). "Myeloperoxidase exacerbates secondary injury by generating highly reactive oxygen species and mediating neutrophil recruitment in experimental spinal cord injury." Spine (Phila Pa 1976) **37**(16): 1363-1369.
Kumamaru, H., P. Lu, E. S. Rosenzweig and M. H. Tuszynski (2018). "Activation of Intrinsic Growth State Enhances Host Axonal Regeneration into Neural Progenitor Cell Grafts." Stem Cell Reports **11**(4): 861-868.
Kumar, H., H. Choi, M.-J. Jo, H. P. Joshi, M. Muttigi, D. Bonanomi, S. B. Kim, E. Ban, A. Kim, S.-H. Lee, K.-T. Kim, S. Sohn, X. Zeng and I. Han (2018). "Neutrophil elastase inhibition effectively rescued angiopoietin-1 decrease and inhibits glial scar after spinal cord injury." Acta Neuropathologica Communications **6**(1): 73.
Kuno, K. and K. Matsushima (1994). "The IL-1 receptor signaling pathway." Journal of Leukocyte Biology **56**(5): 542-547.
Kurimoto, T., Y. Yin, G. Habboub, H. Y. Gilbert, Y. Li, S. Nakao, A. Hafezi-Moghadam and L. I. Benowitz (2013). "Neutrophils express oncomodulin and promote optic nerve regeneration." Journal of Neuroscience **33**(37): 14816-14824.
Kuscha, V., A. Barreiro-Iglesias, C. G. Becker and T. Becker (2012). "Plasticity of tyrosine hydroxylase and serotonergic systems in the regenerating spinal cord of adult zebrafish." J Comp Neurol **520**(5): 933-951.
Kuscha, V., S. L. Frazer, T. B. Dias, M. Hibi, T. Becker and C. G. Becker (2012). "Lesion-induced generation of interneuron cell types in specific dorsoventral domains in the spinal cord of adult zebrafish." J Comp Neurol **520**(16): 3604-3616.
Kyritsis, N., C. Kizil, S. Zocher, V. Kroehne, J. Kaslin, D. Freudenreich, A. Iltzsche and M. Brand (2012). "Acute inflammation initiates the regenerative response in the adult zebrafish brain." Science

338(6112): 1353-1356.
Labonte, A. C., S. S. J. Sung, L. T. Jennelle, A. P. Dandekar and Y. S. Hahn (2017). "Expression of scavenger receptor-AI promotes alternative activation of murine macrophages to limit hepatic inflammation and fibrosis." Hepatology (Baltimore, Md.) **65**(1): 32-43.
Lam, S. H., H. L. Chua, Z. Gong, T. J. Lam and Y. M. Sin (2004). "Development and maturation of the immune system in zebrafish, Danio rerio: A gene expression profiling, in situ hybridization and immunological study." Developmental and Comparative Immunology **28**(1): 9-28.
Lam, S. H., H. L. Chua, Z. Gong, Z. Wen, T. J. Lam and Y. M. Sin (2002). "Morphologic transformation of the thymus in developing zebrafish." Developmental Dynamics **225**(1): 87-94.
Laresgoiti, U., M. Z. Nikolic, C. Rao, J. L. Brady, R. V. Richardson, E. J. Batchen, K. E. Chapman and E. L. Rawlins (2016). "Lung epithelial tip progenitors integrate glucocorticoid- and STAT3-mediated signals to control progeny fate." Development **143**(20): 3686-3699.
Lawrence, C. B., S. M. Allan and N. J. Rothwell (1998). "Interleukin-1β and the interleukin-1 receptor antagonist act in the striatum to modify excitotoxic brain damage in the rat." European Journal of Neuroscience **10**(3): 1188-1195.
Lawson, N. D. and B. M. Weinstein (2002). "In vivo imaging of embryonic vascular development using transgenic zebrafish." Dev Biol **248**(2): 307-318.
Lee, S. M., S. Rosen, P. Weinstein, N. Van Rooijen and L. J. Noble-Haeusslein (2011). "Prevention of both neutrophil and monocyte recruitment promotes recovery after spinal cord injury." Journal of Neurotrauma **28**(9): 1893-1907.
Lee, W. L., R. E. Harrison and S. Grinstein (2003). "Phagocytosis by neutrophils." Microbes Infect **5**(14): 1299-1306.
Lerch, J. K., Y. R. Martinez-Ondaro, J. L. Bixby and V. P. Lemmon (2014). "cJun promotes CNS axon growth." Molecular and Cellular Neuroscience **59**: 97-105.
Lewko, W. M. and R. K. Oldham (2009). Cytokines. Principles of Cancer Biotherapy. R. K. Oldham and R. O. Dillman. Dordrecht, Springer Netherlands**:** 155-276.
Li, J. Y., K. Gao, T. Shao, D. D. Fan, C. B. Hu, C. C. Sun, W. R. Dong, A. F. Lin, L. X. Xiang and J. Z. Shao (2018). "Characterization of an NLRP1 Inflammasome from Zebrafish Reveals a Unique Sequential Activation Mechanism Underlying Inflammatory Caspases in Ancient Vertebrates." J Immunol **201**(7): 1946-1966.
Li, L., B. Yan, Y. Q. Shi, W. Q. Zhang and Z. L. Wen (2012). "Live imaging reveals differing roles of macrophages and neutrophils during zebrafish tail fin regeneration." J Biol Chem **287**(30): 25353-25360.
Li, Y., Y. Li, X. Cao, X. Jin and T. Jin (2017). "Pattern recognition receptors in zebrafish provide functional and evolutionary insight into innate immune signaling pathways." Cellular and Molecular Immunology **14**(1): 80-89.
Libardo, M. D. J., C. de la Fuente-Nuñez, K. Anand, G. Krishnamoorthy, P. Kaiser, S. C. Pringle, C. Dietz, S. Pierce, M. B. Smith, A. Barczak, S. H. E. Kaufmann, A. Singh and A. M. Angeles-Boza (2018). "Phagosomal Copper-Promoted Oxidative Attack on Intracellular Mycobacterium tuberculosis." ACS Infectious Diseases.
Liddelow, S. A. and B. A. Barres (2016). "Not everything is scary about a glial scar." Nature **532**: 182.
Liston, A. and S. L. Masters (2017). "Homeostasis-altering molecular processes as mechanisms of inflammasome activation." Nature Reviews Immunology **17**: 208.
Liu, J., M. W. Marino, G. Wong, D. Grail, A. Dunn, J. Bettadapura, A. J. Slavin, L. Old and C. C. Bernard (1998). "TNF is a potent anti-inflammatory cytokine in autoimmune-mediated demyelination." Nat Med **4**(1): 78-83.
Liu, K., A. Tedeschi, K. K. Park and Z. G. He (2011). Neuronal Intrinsic Mechanisms of Axon Regeneration. Annual Review of Neuroscience, Vol 34. S. E. Hyman et al. Palo Alto, Annual Reviews. **34:** 131-152.
Liu, Q. and R. L. Londraville (2003). "Using the adult zebrafish visual system to study cadherin-2 expression during central nervous system regeneration." Methods Cell Sci **25**(1-2): 71-78.
Liu, S., G. Y. Xu, K. M. Johnson, C. Echetebu, Z. S. Ye, C. E. Hulsebosch and D. J. McAdoo (2008). "Regulation of interleukin-1beta by the interleukin-1 receptor antagonist in the glutamate-injured spinal cord: endogenous neuroprotection." Brain Res **1231**: 63-74.
Liu, X., Y.-S. Li, S. A. Shinton, J. Rhodes, L. Tang, H. Feng, C. A. Jette, A. T. Look, K. Hayakawa and R. R. Hardy (2017). "Zebrafish B Cell Development without a Pre-B Cell Stage, Revealed by CD79 Fluorescence Reporter Transgenes." Journal of immunology (Baltimore, Md. : 1950) **199**(5):

1706-1715.
Livak, K. J. and T. D. Schmittgen (2001). "Analysis of relative gene expression data using real-time quantitative PCR and the 2(-Delta Delta C(T)) Method." Methods **25**(4): 402-408.
Loddick, S. A. and N. J. Rothwell (1996). "Neuroprotective effects of human recombinant interleukin-1 receptor antagonist in focal cerebral ischaemia in the rat." Journal of Cerebral Blood Flow and Metabolism **16**(5): 932-940.
Lois, C. and A. Alvarez-Buylla (1994). "Long-distance neuronal migration in the adult mammalian brain." Science **264**(5162): 1145-1148.
Long, H., W. Liao, L. Wang and Q. Lu (2016). "A Player and Coordinator: The Versatile Roles of Eosinophils in the Immune System." Transfusion Medicine and Hemotherapy **43**(2): 96-108.
Love, S. (2006). "Demyelinating diseases." Journal of Clinical Pathology **59**(11): 1151-1159.
Lugo-Villarino, G., K. M. Balla, D. L. Stachura, K. Banuelos, M. B. Werneck and D. Traver (2010). "Identification of dendritic antigen-presenting cells in the zebrafish." Proc Natl Acad Sci U S A **107**(36): 15850-15855.
MacLeod, A. S. and J. N. Mansbridge (2016). "The Innate Immune System in Acute and Chronic Wounds." Advances in Wound Care **5**(2): 65-78.
Maggio, D. M., K. Chatzipanteli, N. Masters, S. P. Patel, W. D. Dietrich and D. D. Pearse (2012). "Acute molecular perturbation of inducible nitric oxide synthase with an antisense approach enhances neuronal preservation and functional recovery after contusive spinal cord injury." Journal of Neurotrauma **29**(12): 2244-2249.
Mahar, M. and V. Cavalli (2018). "Intrinsic mechanisms of neuronal axon regeneration." Nature reviews. Neuroscience **19**(6): 323-337.
Mahony, C., L. Erskine, J. Niven, N. H. Greig, W. D. Figg and N. Vargesson (2013). "Pomalidomide is nonteratogenic in chicken and zebrafish embryos and nonneurotoxic in vitro." Proc Natl Acad Sci U S A **110**(31): 12703-12708.
Makuloluwa, K. K., A. Midgley and M. Beresford (2014). "Neutrophil extracellular trap-mediated activation of endosomal toll-like receptors induce immune activation in juvenile-onset systemic lupus erythematosus." Pediatric Rheumatology Online Journal **12**(Suppl 1): P110-P110.
Martinon, F., A. Mayor and J. Tschopp (2009). "The inflammasomes: guardians of the body." Annu Rev Immunol **27**: 229-265.
Matsuoka, R. L., M. Marass, A. Avdesh, C. S. Helker, H. M. Maischein, A. S. Grosse, H. Kaur, N. D. Lawson, W. Herzog and D. Y. Stainier (2016). "Radial glia regulate vascular patterning around the developing spinal cord." Elife **5**.
Matsuoka, R. L., M. Marass, A. Avdesh, C. S. M. Helker, H. M. Maischein, A. S. Grosse, H. Kaur, N. D. Lawson, W. Herzog and D. Y. R. Stainier (2016). "Radial glia regulate vascular patterning around the developing spinal cord." eLife **5**(NOVEMBER2016).
McGeough, M. D., A. Wree, M. E. Inzaugarat, A. Haimovich, C. D. Johnson, C. A. Peña, R. Goldbach-Mansky, L. Broderick, A. E. Feldstein and H. M. Hoffman (2017). "TNF regulates transcription of NLRP3 inflammasome components and inflammatory molecules in cryopyrinopathies." The Journal of Clinical Investigation **127**(12): 4488-4497.
McHedlishvili, L., V. Mazurov and E. M. Tanaka (2012). "Reconstitution of the central nervous system during salamander tail regeneration from the implanted neurospheres." Methods Mol Biol **916**: 197-202.
McKerracher, L. and K. M. Rosen (2015). "MAG, myelin and overcoming growth inhibition in the CNS." Frontiers in Molecular Neuroscience **8**: 51.
McMurran, C. E., C. A. Jones, D. C. Fitzgerald and R. J. M. Franklin (2016). "CNS Remyelination and the Innate Immune System." Frontiers in Cell and Developmental Biology **4**: 38.
Meijer, A. H., A. Chatzopoulou, H. P. Spaink, M. J. M. Schaaf, U. Roy and A. Alia (2015). "Transcriptional and Metabolic Effects of Glucocorticoid Receptor α and β Signaling in Zebrafish." Endocrinology **156**(5): 1757-1769.
Meijer, A. H. and H. P. Spaink (2011). "Host-pathogen interactions made transparent with the zebrafish model." Curr Drug Targets **12**(7): 1000-1017.
Merino, J. J. and M. J. Oset-Gasque (2013). "The CXCR7 activation by SDF1 induces Neural progenitor migration (NPC): a dual effect on CXCR4/CXCR7 axis within the vascular niche of ischemic rats." Int J Stroke **8**(8): E56.
Métayer, L. E., A. Vilalta, G. A. A. Burke and G. C. Brown (2017). "Anti-CD47 antibodies induce phagocytosis of live, malignant B cells by macrophages via the Fc domain, resulting in cell death by phagoptosis." Oncotarget **8**(37): 60892-60903.

Metchnikoff, É. (1892). Leçons sur la pathologie comparée de l'inflammation: faites à l'Institut Pasteur in 1891. Paris: Masson.
Ming, G.-l. and H. Song (2005). Adult neurogenesis in the mammalian central nervous system.
Moens, C. B. and V. E. Prince (2002). "Constructing the hindbrain: Insights from the zebrafish." Developmental Dynamics **224**(1): 1-17.
Mogensen, T. H. (2009). "Pathogen Recognition and Inflammatory Signaling in Innate Immune Defenses." Clinical Microbiology Reviews **22**(2): 240-273.
Mokalled, M. H., C. Patra, A. L. Dickson, T. Endo, D. Y. Stainier and K. D. Poss (2016). "Injury-induced ctgfa directs glial bridging and spinal cord regeneration in zebrafish." Science **354**(6312): 630-634.
Mokalled, M. H., C. Patra, A. L. Dickson, T. Endo, D. Y. R. Stainier and K. D. Poss (2016). "Injury-induced ctgfa directs glial bridging and spinal cord regeneration in zebrafish." Science **354**(6312): 630.
Moore, M. A. S. (2014). Chapter 47 - Hematopoietic Stem Cells. Principles of Tissue Engineering (Fourth Edition). R. Lanza et al. Boston, Academic Press**:** 989-1040.
Moore, W. (2011). "The Edwin Smith papyrus." BMJ **342**.
Moreno, R. L., M. Josey and A. B. Ribera (2017). "Zebrafish In Situ Spinal Cord Preparation for Electrophysiological Recordings from Spinal Sensory and Motor Neurons." J Vis Exp(122).
Mothe, A. J. and C. H. Tator (2013). "Review of transplantation of neural stem/progenitor cells for spinal cord injury." International Journal of Developmental Neuroscience **31**(7): 701-713.
Muller, G. W., R. Chen, S. Y. Huang, L. G. Corral, L. M. Wong, R. T. Patterson, Y. Chen, G. Kaplan and D. I. Stirling (1999). "Amino-substituted thalidomide analogs: potent inhibitors of TNF-alpha production." Bioorg Med Chem Lett **9**(11): 1625-1630.
Munzel, E. J., K. Schaefer, B. Obirei, E. Kremmer, E. A. Burton, V. Kuscha, C. G. Becker, C. Brosamle, A. Williams and T. Becker (2012). "Claudin k is specifically expressed in cells that form myelin during development of the nervous system and regeneration of the optic nerve in adult zebrafish." Glia **60**(2): 253-270.
Murray, A. J. and D. A. Shewan (2008). "Epac mediates cyclic AMP-dependent axon growth, guidance and regeneration." Mol Cell Neurosci **38**(4): 578-588.
Murray, A. J., S. J. Tucker and D. A. Shewan (2009). "cAMP-Dependent Axon Guidance Is Distinctly Regulated by Epac and Protein Kinase A." The Journal of Neuroscience **29**(49): 15434.
Nakajima, K., S. Honda, Y. Tohyama, Y. Imai, S. Kohsaka and T. Kurihara (2001). "Neurotrophin secretion from cultured microglia." J Neurosci Res **65**(4): 322-331.
Nakajima, K. and S. Kohsaka (2004). "Microglia: neuroprotective and neurotrophic cells in the central nervous system." Curr Drug Targets Cardiovasc Haematol Disord **4**(1): 65-84.
Nakhjavan-Shahraki, B., M. Yousefifard, V. Rahimi-Movaghar, M. Baikpour, F. Nasirinezhad, S. Safari, M. Yaseri, A. Moghadas Jafari, P. Ghelichkhani, A. Tafakhori and M. Hosseini (2018). "Transplantation of olfactory ensheathing cells on functional recovery and neuropathic pain after spinal cord injury; systematic review and meta-analysis." Scientific Reports **8**(1): 325.
Naoi, M. and W. Maruyama (1999). "Cell death of dopamine neurons in aging and Parkinson's disease." Mech Ageing Dev **111**(2-3): 175-188.
Naruo, S., K. Okajima, Y. Taoka, M. Uchiba, T. Nakamura, H. Okabe and K. Takagi (2003). "Prostaglandin E<inf>1</inf>reduces compression trauma-induced spinal cord injury in rats mainly by inhibiting neutrophil activation." Journal of Neurotrauma **20**(2): 221-228.
Neirinckx, V., C. Coste, R. Franzen, A. Gothot, B. Rogister and S. Wislet (2014). "Neutrophil contribution to spinal cord injury and repair." Journal of neuroinflammation **11**: 150-150.
Nelson, C. M., K. M. Ackerman, P. O'Hayer, T. J. Bailey, R. A. Gorsuch and D. R. Hyde (2013). "Tumor necrosis factor-alpha is produced by dying retinal neurons and is required for Muller glia proliferation during zebrafish retinal regeneration." J Neurosci **33**(15): 6524-6539.
Neumann, H., M. R. Kotter and R. J. M. Franklin (2009). "Debris clearance by microglia: an essential link between degeneration and regeneration." Brain **132**: 288-295.
Newby, A. C. (2008). "Metalloproteinase expression in monocytes and macrophages and its relationship to atherosclerotic plaque instability." Arterioscler Thromb Vasc Biol **28**(12): 2108-2114.
Nguyen-Chi, M., B. Laplace-Builhe, J. Travnickova, P. Luz-Crawford, G. Tejedor, G. Lutfalla, K. Kissa, C. Jorgensen and F. Djouad (2017). "TNF signaling and macrophages govern fin regeneration in zebrafish larvae." Cell Death Dis **8**(8): e2979.
Nguyen-Chi, M., B. Laplace-Builhé, J. Travnickova, P. Luz-Crawford, G. Tejedor, G. Lutfalla, K. Kissa, C. Jorgensen and F. Djouad (2017). "TNF signaling and macrophages govern fin regeneration

in zebrafish larvae." Cell Death & Disease **8**(8): e2979.
Nguyen-Chi, M., B. Laplace-Builhe, J. Travnickova, P. Luz-Crawford, G. Tejedor, Q. T. Phan, I. Duroux-Richard, J. P. Levraud, K. Kissa, G. Lutfalla, C. Jorgensen and F. Djouad (2015). "Identification of polarized macrophage subsets in zebrafish." Elife **4**: e07288.
Nguyen-Chi, M., Q. T. Phan, C. Gonzalez, J. F. Dubremetz, J. P. Levraud and G. Lutfalla (2014). "Transient infection of the zebrafish notochord with E. coli induces chronic inflammation." Dis Model Mech **7**(7): 871-882.
Nona, S. N. and C. A. Stafford (1995). "Glial repair at the lesion site in regenerating goldfish spinal cord: an immunohistochemical study using species-specific antibodies." J Neurosci Res **42**(3): 350-356.
Norden, D. M., M. M. Muccigrosso and J. P. Godbout (2015). "Microglial priming and enhanced reactivity to secondary insult in aging, and traumatic CNS injury, and neurodegenerative disease." Neuropharmacology **96**(Pt A): 29-41.
Novoa, B., T. V. Bowman, L. Zon and A. Figueras (2009). "LPS response and tolerance in the zebrafish (Danio rerio)." Fish Shellfish Immunol **26**(2): 326-331.
Nussenzweig, M. C. and R. M. Steinman (1980). "Contribution of dendritic cells to stimulation of the murine syngeneic mixed leukocyte reaction." J Exp Med **151**(5): 1196-1212.
O'Connell, E. M. and T. B. Nutman (2015). "Eosinophilia in Infectious Diseases." Immunology and allergy clinics of North America **35**(3): 493-522.
Odeberg, H. and I. Olsson (1976). "Microbicidal mechanisms of human granulocytes: synergistic effects of granulocyte elastase and myeloperoxidase or chymotrypsin-like cationic protein." Infect Immun **14**(6): 1276-1283.
Ogai, K., A. Kuwana, S. Hisano, M. Nagashima, Y. Koriyama, K. Sugitani, K. Mawatari, H. Nakashima and S. Kato (2014). "Upregulation of Leukemia Inhibitory Factor (LIF) during the Early Stage of Optic Nerve Regeneration in Zebrafish." PLOS ONE **9**(8): e106010.
Ogryzko, N. V., E. E. Hoggett, S. Solaymani-Kohal, S. Tazzyman, T. J. Chico, S. A. Renshaw and H. L. Wilson (2014). "Zebrafish tissue injury causes upregulation of interleukin-1 and caspase-dependent amplification of the inflammatory response." Dis Model Mech **7**(2): 259-264.
Ogryzko, N. V., A. Lewis, H. L. Wilson, A. H. Meijer, S. A. Renshaw and P. M. Elks (2018). "Macrophage Il-1beta protects against mycobacterial infection downstream of Hif-1alpha in zebrafish." bioRxiv.
Ohnmacht, J., Y. Yang, G. W. Maurer, A. Barreiro-Iglesias, T. M. Tsarouchas, D. Wehner, D. Sieger, C. G. Becker and T. Becker (2016). "Spinal motor neurons are regenerated after mechanical lesion and genetic ablation in larval zebrafish." Development **143**(9): 1464-1474.
Ohtake, Y., U. Hayat and S. X. Li (2015). "PTEN inhibition and axon regeneration and neural repair." Neural Regeneration Research **10**(9): 1363-1368.
Oosterhof, N., L. E. Kuil, H. C. van der Linde, S. M. Burm, W. Berdowski, W. F. J. van Ijcken, J. C. van Swieten, E. M. Hol, M. H. G. Verheijen and T. J. van Ham (2018). "Colony-Stimulating Factor 1 Receptor (CSF1R) Regulates Microglia Density and Distribution, but Not Microglia Differentiation In Vivo." Cell Rep **24**(5): 1203-1217 e1206.
Oshiumi, H., M. Matsumoto, K. Funami, T. Akazawa and T. Seya (2003). "TICAM-1, an adaptor molecule that participates in Toll-like receptor 3-mediated interferon-beta induction." Nat Immunol **4**(2): 161-167.
Oshiumi, H., M. Sasai, K. Shida, T. Fujita, M. Matsumoto and T. Seya (2003). "TIR-containing adapter molecule (TICAM)-2, a bridging adapter recruiting to toll-like receptor 4 TICAM-1 that induces interferon-beta." J Biol Chem **278**(50): 49751-49762.
Otero-Ortega, L., M. C. Gómez-de Frutos, F. Laso-García, A. Sánchez-Gonzalo, A. Martínez-Arroyo, E. Díez-Tejedor and M. Gutiérrez-Fernández (2017). "NogoA Neutralization Promotes Axonal Restoration After White Matter Injury In Subcortical Stroke." Scientific Reports **7**(1): 9431.
Oudkhir, M., I. Martelly, B. Boilly and M. Castagna (1992). "Increased protein kinase C activity in the central nervous system of the newt during limb regeneration." Biochem Biophys Res Commun **184**(1): 433-440.
Pan, Y. A., T. Freundlich, T. A. Weissman, D. Schoppik, X. C. Wang, S. Zimmerman, B. Ciruna, J. R. Sanes, J. W. Lichtman and A. F. Schier (2013). "Zebrabow: multispectral cell labeling for cell tracing and lineage analysis in zebrafish." Development **140**(13): 2835-2846.
Panayiotou, E. and S. Malas (2013). "Adult spinal cord ependymal layer: a promising pool of quiescent stem cells to treat spinal cord injury." Front Physiol **4**: 340.
Pasare, C. and R. Medzhitov (2003). "Toll pathway-dependent blockade of CD4+CD25+ T cell-

mediated suppression by dendritic cells." Science **299**(5609): 1033-1036.
Pasare, C. and R. Medzhitov (2004). "Toll-dependent control mechanisms of CD4 T cell activation." Immunity **21**(5): 733-741.
Pauwels, A.-M., M. Trost, R. Beyaert and E. Hoffmann (2017). "Patterns, Receptors, and Signals: Regulation of Phagosome Maturation." Trends in Immunology **38**(6): 407-422.
Pearse, D. D., K. Chatzipanteli, A. E. Marcillo, M. B. Bunge and W. D. Dietrich (2003). "Comparison of iNOS Inhibition by Antisense and Pharmacological Inhibitors after Spinal Cord Injury." Journal of Neuropathology and Experimental Neurology **62**(11): 1096-1107.
Pennock, N. D., J. T. White, E. W. Cross, E. E. Cheney, B. A. Tamburini and R. M. Kedl (2013). "T cell responses: naïve to memory and everything in between." Advances in Physiology Education **37**(4): 273-283.
Peri, F. and C. Nusslein-Volhard (2008). "Live imaging of neuronal degradation by microglia reveals a role for v0-ATPase a1 in phagosomal fusion in vivo." Cell **133**(5): 916-927.
Perrin, F. E., S. Lacroix, M. Avilés-Trieueros and S. David (2005). "Involvement of monocyte chemoattractant protein-1, macrophage inflammatory protein-1α and interleukin-1β Wallerian degeneration." Brain **128**(4): 854-866.
Piccinini, A. M. and K. S. Midwood (2010). "DAMPening Inflammation by Modulating TLR Signalling." Mediators of Inflammation **2010**: 21.
Pineau, I. and S. Lacroix (2007). "Proinflammatory cytokine synthesis in the injured mouse spinal cord: Multiphasic expression pattern and identification of the cell types involved." Journal of Comparative Neurology **500**(2): 267-285.
Pineau, I. and S. Lacroix (2007). "Proinflammatory cytokine synthesis in the injured mouse spinal cord: multiphasic expression pattern and identification of the cell types involved." J Comp Neurol **500**(2): 267-285.
Pineau, I., L. Sun, D. Bastien and S. Lacroix (2010). "Astrocytes initiate inflammation in the injured mouse spinal cord by promoting the entry of neutrophils and inflammatory monocytes in an IL-1 receptor/MyD88-dependent fashion." Brain, Behavior, and Immunity **24**(4): 540-553.
Porcelli, S. A. (2017). Chapter 17 - Innate Immunity. Kelley and Firestein's Textbook of Rheumatology (Tenth Edition). G. S. Firestein et al., Elsevier**:** 274-287.
Prost, S., R. E. Kishen, D. C. Kluth and C. O. Bellamy (2016). "Working with Commercially Available Quantum Dots for Immunofluorescence on Tissue Sections." PLoS One **11**(9): e0163856.
Pruss, H., M. A. Kopp, B. Brommer, N. Gatzemeier, I. Laginha, U. Dirnagl and J. M. Schwab (2011). "Non-resolving aspects of acute inflammation after spinal cord injury (SCI): indices and resolution plateau." Brain Pathol **21**(6): 652-660.
Rao, M. B., D. Didiano and J. G. Patton (2017). "Neurotransmitter-Regulated Regeneration in the Zebrafish Retina." Stem Cell Reports **8**(4): 831-842.
Reimer, M. M., V. Kuscha, C. Wyatt, I. Sorensen, R. E. Frank, M. Knuwer, T. Becker and C. G. Becker (2009). "Sonic hedgehog is a polarized signal for motor neuron regeneration in adult zebrafish." J Neurosci **29**(48): 15073-15082.
Reimer, M. M., V. Kuscha, C. Wyatt, I. Sörensen, R. E. Frank, M. Knüwer, T. Becker and C. G. Becker (2009). "Sonic hedgehog is a polarized signal for motor neuron regeneration in adult zebrafish." Journal of Neuroscience **29**(48): 15073-15082.
Reimer, M. M., A. Norris, J. Ohnmacht, R. Patani, Z. Zhong, T. B. Dias, V. Kuscha, A. L. Scott, Y. C. Chen, S. Rozov, S. L. Frazer, C. Wyatt, S. Higashijima, E. E. Patton, P. Panula, S. Chandran, T. Becker and C. G. Becker (2013). "Dopamine from the brain promotes spinal motor neuron generation during development and adult regeneration." Dev Cell **25**(5): 478-491.
Reimer, M. M., I. Sorensen, V. Kuscha, R. E. Frank, C. Liu, C. G. Becker and T. Becker (2008). "Motor neuron regeneration in adult zebrafish." J Neurosci **28**(34): 8510-8516.
Relton, J. K., D. Martin, R. C. Thompson and D. A. Russell (1996). "Peripheral administration of interleukin-1 receptor antagonist inhibits brain damage after focal cerebral ischemia in the rat." Experimental Neurology **138**(2): 206-213.
Renshaw, S. A., C. A. Loynes, D. M. Trushell, S. Elworthy, P. W. Ingham and M. K. Whyte (2006). "A transgenic zebrafish model of neutrophilic inflammation." Blood **108**(13): 3976-3978.
Renshaw, S. A. and N. S. Trede (2012). "A model 450 million years in the making: zebrafish and vertebrate immunity." Dis Model Mech **5**(1): 38-47.
Renshaw, S. A. and N. S. Trede (2012). "A model 450 million years in the making: zebrafish and vertebrate immunity." Disease models & mechanisms **5**(1): 38-47.
Reynolds, B. A. and S. Weiss (1992). "Generation of neurons and astrocytes from isolated cells of the

adult mammalian central nervous system." Science **255**(5052): 1707-1710.
Rhodes, J., A. Hagen, K. Hsu, M. Deng, T. X. Liu, A. T. Look and J. P. Kanki (2005). "Interplay of pu.1 and gata1 determines myelo-erythroid progenitor cell fate in zebrafish." Dev Cell **8**(1): 97-108.
Richardson, P. M., U. M. McGuinness and A. J. Aguayo (1980). "Axons from CNS neurones regenerate into PNS grafts." Nature **284**(5753): 264-265.
Riera Romo, M., D. Pérez-Martínez and C. Castillo Ferrer (2016). "Innate immunity in vertebrates: an overview." Immunology **148**(2): 125-139.
Ritter, M. A. (1978). "Embryonic mouse thymus development: stem cell entry and differentiation." Immunology **34**(1): 69-75.
Rock, K. L. and H. Kono (2008). "The inflammatory response to cell death." Annu Rev Pathol **3**: 99-126.
Rolls, A., R. Shechter and M. Schwartz (2009). "The bright side of the glial scar in CNS repair." Nat Rev Neurosci **10**(3): 235-241.
Rosales, C., C. A. Lowell, M. Schnoor and E. Uribe-Querol (2017). "Neutrophils: Their Role in Innate and Adaptive Immunity 2017." Journal of Immunology Research **2017**: 9748345.
Rosenberg, A. F., M. A. Wolman, C. Franzini-Armstrong and M. Granato (2012). "In vivo nerve-macrophage interactions following peripheral nerve injury." J Neurosci **32**(11): 3898-3909.
Rosenberg, A. F., M. A. Wolman, C. Franzini-Armstrong and M. Granato (2012). "In Vivo Nerve–Macrophage Interactions Following Peripheral Nerve Injury." The Journal of Neuroscience **32**(11): 3898.
Ross, K. F. and M. C. Herzberg (2016). "Autonomous immunity in mucosal epithelial cells: fortifying the barrier against infection." Microbes and Infection **18**(6): 387-398.
Rossi, F., A. Jankovski and C. Sotelo (1995). "Differential regenerative response of purkinje cell and inferior olivary axons confronted with embryonic grafts: Environmental cues versus intrinsic neuronal determinants." Journal of Comparative Neurology **359**(4): 663-677.
Saiwai, H., Y. Ohkawa, H. Yamada, H. Kumamaru, A. Harada, H. Okano, T. Yokomizo, Y. Iwamoto and S. Okada (2010). "The LTB4-BLT1 axis mediates neutrophil infiltration and secondary injury in experimental spinal cord injury." Am J Pathol **176**(5): 2352-2366.
Saleem, S. and R. R. Kannan (2018). "Zebrafish: an emerging real-time model system to study Alzheimer's disease and neurospecific drug discovery." Cell Death Discovery **4**(1): 45.
Saleh, A., D. R. Smith, S. Balakrishnan, L. Dunn, C. Martens, C. W. Tweed and P. Fernyhough (2011). "Tumor necrosis factor-alpha elevates neurite outgrowth through an NF-kappaB-dependent pathway in cultured adult sensory neurons: Diminished expression in diabetes may contribute to sensory neuropathy." Brain Res **1423**: 87-95.
Savan, R., T. Kono, D. Igawa and M. Sakai (2005). "A novel tumor necrosis factor (TNF) gene present in tandem with theTNF-alpha gene on the same chromosome in teleosts." Immunogenetics **57**(1-2): 140-150.
Schindelin, J., I. Arganda-Carreras, E. Frise, V. Kaynig, M. Longair, T. Pietzsch, S. Preibisch, C. Rueden, S. Saalfeld, B. Schmid, J. Y. Tinevez, D. J. White, V. Hartenstein, K. Eliceiri, P. Tomancak and A. Cardona (2012). "Fiji: an open-source platform for biological-image analysis." Nat Methods **9**(7): 676-682.
Schneider, W. M., M. D. Chevillotte and C. M. Rice (2014). "Interferon-Stimulated Genes: A Complex Web of Host Defenses." Annual Review of Immunology **32**(1): 513-545.
Schnyder, J. and M. Baggiolini (1978). "Role of phagocytosis in the activation of macrophages." The Journal of Experimental Medicine **148**(6): 1449-1457.
Schürch, C. M., S. Forster, F. Brühl, S. H. Yang, E. Felley-Bosco and E. Hewer (2018). "The "don't eat me" signal CD47 is a novel diagnostic biomarker and potential therapeutic target for diffuse malignant mesothelioma." Oncoimmunology **7**(1): e1373235.
Schwartz, M., A. Solomon, V. Lavie, S. Ben-Bassat, M. Belkin and A. Cohen (1991). "Tumor necrosis factor facilitates regeneration of injured central nervous system axons." Brain Res **545**(1-2): 334-338.
Schweitzer, J., T. Becker, J. Lefebvre, M. Granato, M. Schachner and C. G. Becker (2005). "Tenascin-C is involved in motor axon outgrowth in the trunk of developing zebrafish." Dev Dyn **234**(3): 550-566.
Segawa, K. and S. Nagata (2015). "An Apoptotic ‘Eat Me’ Signal: Phosphatidylserine Exposure." Trends in Cell Biology **25**(11): 639-650.
Selles-Navarro, I., B. Ellezam, R. Fajardo, M. Latour and L. McKerracher (2001). "Retinal ganglion cell and nonneuronal cell responses to a microcrush lesion of adult rat optic nerve." Exp Neurol

167(2): 282-289.
Shah, B., N. Burg and M. H. Pillinger (2017). Chapter 11 - Neutrophils. Kelley and Firestein's Textbook of Rheumatology (Tenth Edition). G. S. Firestein et al., Elsevier**:** 169-188.e163.
Shiau, C. E., Z. Kaufman, A. M. Meireles and W. S. Talbot (2015). "Differential requirement for irf8 in formation of embryonic and adult macrophages in zebrafish." PLoS One **10**(1): e0117513.
Shimizu, I., R. W. Oppenheim, M. O'Brien and A. Shneiderman (1990). "Anatomical and functional recovery following spinal cord transection in the chick embryo." J Neurobiol **21**(6): 918-937.
Sieger, D., C. Moritz, T. Ziegenhals, S. Prykhozhij and F. Peri (2012). "Long-range Ca2+ waves transmit brain-damage signals to microglia." Dev Cell **22**(6): 1138-1148.
Silva, M. T. and M. Correia-Neves (2012). "Neutrophils and Macrophages: the Main Partners of Phagocyte Cell Systems." Frontiers in Immunology **3**: 174.
Simon, S. I. and M.-H. Kim (2010). "A day (or 5) in a neutrophil's life." Blood **116**(4): 511.
Smith, P. D., F. Sun, K. K. Park, B. Cai, C. Wang, K. Kuwako, I. Martinez-Carrasco, L. Connolly and Z. G. He (2009). "SOCS3 Deletion Promotes Optic Nerve Regeneration In Vivo." Neuron **64**(5): 617-623.
Smith, R. P., J. K. Lerch-Haner, J. R. Pardinas, W. J. Buchser, J. L. Bixby and V. P. Lemmon (2011). "Transcriptional profiling of intrinsic PNS factors in the postnatal mouse." Molecular and Cellular Neuroscience **46**(1): 32-44.
Soderblom, C., X. Luo, E. Blumenthal, E. Bray, K. Lyapichev, J. Ramos, V. Krishnan, C. Lai-Hsu, K. K. Park, P. Tsoulfas and J. K. Lee (2013). "Perivascular Fibroblasts Form the Fibrotic Scar after Contusive Spinal Cord Injury." The Journal of Neuroscience **33**(34): 13882-13887.
Sofroniew, M. V. (2009). "Molecular dissection of reactive astrogliosis and glial scar formation." Trends in neurosciences **32**(12): 638-647.
Sorrells, S. F., M. F. Paredes, A. Cebrian-Silla, K. Sandoval, D. Qi, K. W. Kelley, D. James, S. Mayer, J. Chang, K. I. Auguste, E. F. Chang, A. J. Gutierrez, A. R. Kriegstein, G. W. Mathern, M. C. Oldham, E. J. Huang, J. M. Garcia-Verdugo, Z. Yang and A. Alvarez-Buylla (2018). "Human hippocampal neurogenesis drops sharply in children to undetectable levels in adults." Nature **555**: 377.
Spangler, J. B., I. Moraga, J. L. Mendoza and K. C. Garcia (2015). "Insights into Cytokine–Receptor Interactions from Cytokine Engineering." Annual review of immunology **33**: 139-167.
St John, A. L. and S. N. Abraham (2013). "Innate Immunity and its Regulation by Mast Cells." Journal of immunology (Baltimore, Md. : 1950) **190**(9): 4458-4463.
Stirling, D. P., S. Liu, P. Kubes and V. W. Yong (2009). "Depletion of Ly6G/Gr-1 leukocytes after spinal cord injury in mice alters wound healing and worsens neurological outcome." Journal of Neuroscience **29**(3): 753-764.
Streisinger, G., C. Walker, N. Dower, D. Knauber and F. Singer (1981). "Production of clones of homozygous diploid zebra fish (Brachydanio rerio)." Nature **291**(5813): 293-296.
Sultani, M., A. Stringer, J. Bowen and R. Gibson (2012). Anti-Inflammatory Cytokines: Important Immunoregulatory Factors Contributing to Chemotherapy-Induced Gastrointestinal Mucositis.
Sun, F. and Z. G. He (2010). "Neuronal intrinsic barriers for axon regeneration in the adult CNS." Current Opinion in Neurobiology **20**(4): 510-518.
Tanaka, E. M. and P. Ferretti (2009). "Considering the evolution of regeneration in the central nervous system." Nat Rev Neurosci **10**(10): 713-723.
Tanaka, Y., H. Kojima, H. Miyazaki, T. Koga and H. Moriyama (2009). "Roles of Cytokines and Cell Cycle Regulating Substances in Proliferation of Cholesteatoma Epithelium." The Laryngoscope **109**(7): 1102-1107.
Taoka, Y., K. Okajima, M. Uchiba, K. Murakami, S. Kushimoto, M. Johno, M. Naruo, H. Okabe and K. Takatsuki (1997). "Role of neutrophils in spinal cord injury in the rat." Neuroscience **79**(4): 1177-1182.
Tauzin, S., T. W. Starnes, F. B. Becker, P.-y. Lam and A. Huttenlocher (2014). "Redox and Src family kinase signaling control leukocyte wound attraction and neutrophil reverse migration." The Journal of Cell Biology **207**(5): 589.
Tazaki, A., E. M. Tanaka and J. F. Fei (2017). "Salamander spinal cord regeneration: The ultimate positive control in vertebrate spinal cord regeneration." Dev Biol **432**(1): 63-71.
Temporin, K., H. Tanaka, Y. Kuroda, K. Okada, K. Yachi, H. Moritomo, T. Murase and H. Yoshikawa (2008). "IL-1beta promotes neurite outgrowth by deactivating RhoA via p38 MAPK pathway." Biochem Biophys Res Commun **365**(2): 375-380.
Terman, J. R., X. M. Wang and G. F. Martin (2000). "Repair of the transected spinal cord at different stages of development in the North American opossum, Didelphis virginiana." Brain Res Bull **53**(6):

845-855.
Thompson, M. R., J. J. Kaminski, E. A. Kurt-Jones and K. A. Fitzgerald (2011). "Pattern Recognition Receptors and the Innate Immune Response to Viral Infection." Viruses **3**(6): 920-940.
Tran, A. P., P. M. Warren and J. Silver (2018). "The Biology of Regeneration Failure and Success After Spinal Cord Injury." Physiol Rev **98**(2): 881-917.
Traver, D., P. Herbomel, E. E. Patton, R. D. Murphey, J. A. Yoder, G. W. Litman, A. Catic, C. T. Amemiya, L. I. Zon and N. S. Trede (2003). "The zebrafish as a model organism to study development of the immune system." Adv Immunol **81**: 253-330.
Tsarouchas, T. M., D. Wehner, L. Cavone, T. Munir, M. Keatinge, M. Lambertus, A. Underhill, T. Barrett, E. Kassapis, N. Ogryzko, Y. Feng, T. J. van Ham, T. Becker and C. G. Becker (2018). "Dynamic control of proinflammatory cytokines Il-1β and Tnf-α by macrophages is necessary for functional spinal cord regeneration in zebrafish." bioRxiv.
Tseng, W.-Y., Y.-S. Huang, H.-H. Lin, S.-F. Luo, F. McCann, K. McNamee, F. Clanchy and R. Williams (2018). "TNFR signalling and its clinical implications." Cytokine **101**: 19-25.
Tu, W. Y., J. E. Simpson, J. R. Highley and P. R. Heath (2017). "Spinal muscular atrophy: Factors that modulate motor neurone vulnerability." Neurobiol Dis **102**: 11-20.
Turrin, N. P. and S. Rivest (2006). "Tumor necrosis factor alpha but not interleukin 1 beta mediates neuroprotection in response to acute nitric oxide excitotoxicity." J Neurosci **26**(1): 143-151.
Tuttolomondo, A., R. Pecoraro and A. Pinto (2014). "Studies of selective TNF inhibitors in the treatment of brain injury from stroke and trauma: a review of the evidence to date." Drug Design, Development and Therapy **8**: 2221-2239.
Ulrich, F., J. Carretero-Ortega, J. Menéndez, C. Narvaez, B. Sun, E. Lancaster, V. Pershad, S. Trzaska, E. Véliz, M. Kamei, A. Prendergast, K. R. Kidd, K. M. Shaw, D. A. Castranova, V. N. Pham, B. D. Lo, B. L. Martin, D. W. Raible, B. M. Weinstein and J. Torres-Vázquez (2016). "Reck enables cerebrovascular development by promoting canonical Wnt signaling." Development (Cambridge, England) **143**(1): 147-159.
Valitutti, S., D. Coombs and L. Dupre (2010). "The space and time frames of T cell activation at the immunological synapse." FEBS Lett **584**(24): 4851-4857.
Van houcke, J., I. Bollaerts, E. Geeraerts, B. Davis, A. Beckers, I. Van Hove, K. Lemmens, L. De Groef and L. Moons (2017). "Successful optic nerve regeneration in the senescent zebrafish despite age-related decline of cell intrinsic and extrinsic response processes." Neurobiology of Aging **60**: 1-10.
Vanek, P., M. Thallmair, M. E. Schwab and J. P. Kapfhammer (1998). "Increased lesion-induced sprouting of corticospinal fibres in the myelin-free rat spinal cord." European Journal of Neuroscience **10**(1): 45-56.
Vargas, M. E. and B. A. Barres (2007). "Why is Wallerian degeneration in the CNS so slow?" Annual Review of Neuroscience **30**: 153-179.
Vidal, P. M., E. Lemmens, D. Dooley and S. Hendrix (2013). "The role of "anti-inflammatory" cytokines in axon regeneration." Cytokine Growth Factor Rev **24**(1): 1-12.
Villegas, R., S. M. Martin, K. C. O'Donnell, S. A. Carrillo, A. Sagasti and M. L. Allende (2012). "Dynamics of degeneration and regeneration in developing zebrafish peripheral axons reveals a requirement for extrinsic cell types." Neural Dev **7**: 19.
Vitetta, E. S., M. T. Berton, C. Burger, M. Kepron, W. T. Lee and X. M. Yin (1991). "Memory B and T cells." Annu Rev Immunol **9**: 193-217.
Vojtech, L. N., N. Scharping, J. C. Woodson and J. D. Hansen (2012). "Roles of inflammatory caspases during processing of zebrafish interleukin-1beta in Francisella noatunensis infection." Infect Immun **80**(8): 2878-2885.
Vollmer, K. L., J. S. Alberts, H. T. Carper and G. L. Mandell (1992). "Tumor necrosis factor-alpha decreases neutrophil chemotaxis to N-formyl-1-methionyl-1-leucyl-1-phenylalanine: analysis of single cell movement." J Leukoc Biol **52**(6): 630-636.
Walsh, J. T., S. Hendrix, F. Boato, I. Smirnov, J. Zheng, J. R. Lukens, S. Gadani, D. Hechler, G. Gölz, K. Rosenberger, T. Kammertöns, J. Vogt, C. Vogelaar, V. Siffrin, A. Radjavi, A. Fernandez-Castaneda, A. Gaultier, R. Gold, T. D. Kanneganti, R. Nitsch, F. Zipp and J. Kipnis (2015). "MHCII-independent CD4+ T cells protect injured CNS neurons via IL-4." Journal of Clinical Investigation **125**(2): 699-714.
Wang, L. F., S. B. Huang, H. D. Zhao, C. J. Liu, L. Yao and Y. Q. Shen (2017). "Activating transcription factor 3 promotes spinal cord regeneration of adult zebrafish." Biochem Biophys Res Commun **488**(3): 522-527.

Wang, X., K. Cao, X. Sun, Y. Chen, Z. Duan, L. Sun, L. Guo, P. Bai, D. Sun, J. Fan, X. He, W. Young and Y. Ren (2015). "Macrophages in spinal cord injury: phenotypic and functional change from exposure to myelin debris." Glia **63**(4): 635-651.
Wang, X. J., K. M. Kong, W. L. Qi, W. L. Ye and P. S. Song (2005). "Interleukin-1 beta induction of neuron apoptosis depends on p38 mitogen-activated protein kinase activity after spinal cord injury." Acta Pharmacologica Sinica **26**(8): 934-942.
Watt, J. A. and N. K. Hobbs (2000). "Interleukin-1beta immunoreactivity in identified neurons of the rat magnocellular neurosecretory system: evidence for activity-dependent release." J Neurosci Res **60**(4): 478-489.
Weber, A., P. Wasiliew and M. Kracht (2010). "Interleukin-1 (IL-1) pathway." Sci Signal **3**(105): cm1.
Wehner, D., T. Becker and C. G. Becker (2018). "Restoration of anatomical continuity after spinal cord transection depends on Wnt/beta-catenin signaling in larval zebrafish." Data Brief **16**: 65-70.
Wehner, D., T. M. Tsarouchas, A. Michael, C. Haase, G. Weidinger, M. M. Reimer, T. Becker and C. G. Becker (2017). "Wnt signaling controls pro-regenerative Collagen XII in functional spinal cord regeneration in zebrafish." Nat Commun **8**(1): 126.
Welte, C., S. Engel and C. A. Stuermer (2015). "Upregulation of the zebrafish Nogo-A homologue, Rtn4b, in retinal ganglion cells is functionally involved in axon regeneration." Neural Dev **10**: 6.
Welte, C., S. Engel and C. A. O. Stuermer (2015). "Upregulation of the zebrafish Nogo-A homologue, Rtn4b, in retinal ganglion cells is functionally involved in axon regeneration." Neural Development **10**(1): 6.
Westerfield, M. (2000). The Zebrafish Book. A Guide for the Laboratory Use of Zebrafish (Danio Rerio).
Weyd, H., L. Abeler-Dörner, B. Linke, A. Mahr, V. Jahndel, S. Pfrang, M. Schnölzer, C. S. Falk and P. H. Krammer (2013). "Annexin A1 on the Surface of Early Apoptotic Cells Suppresses CD8(+) T Cell Immunity." PLoS ONE **8**(4): e62449.
White, D. T., S. Sengupta, M. T. Saxena, Q. Xu, J. Hanes, D. Ding, H. Ji and J. S. Mumm (2017). "Immunomodulation-accelerated neuronal regeneration following selective rod photoreceptor cell ablation in the zebrafish retina." Proc Natl Acad Sci U S A **114**(18): E3719-e3728.
Wilgus, T. A., S. Roy and J. C. McDaniel (2013). "Neutrophils and Wound Repair: Positive Actions and Negative Reactions." Adv Wound Care (New Rochelle) **2**(7): 379-388.
Wilson, K. S., C. S. Tucker, E. A. Al-Dujaili, M. C. Holmes, P. W. Hadoke, C. J. Kenyon and M. A. Denvir (2016). "Early-life glucocorticoids programme behaviour and metabolism in adulthood in zebrafish." J Endocrinol **230**(1): 125-142.
Winterbourn, C. C., A. J. Kettle and M. B. Hampton (2016). "Reactive Oxygen Species and Neutrophil Function." Annu Rev Biochem **85**: 765-792.
Witting, A., P. Muller, A. Herrmann, H. Kettenmann and C. Nolte (2000). "Phagocytic clearance of apoptotic neurons by Microglia/Brain macrophages in vitro: involvement of lectin-, integrin-, and phosphatidylserine-mediated recognition." J Neurochem **75**(3): 1060-1070.
Wojdasiewicz, P., Ł. A. Poniatowski and D. Szukiewicz (2014). "The Role of Inflammatory and Anti-Inflammatory Cytokines in the Pathogenesis of Osteoarthritis." Mediators of Inflammation **2014**: 561459.
Wolman, M. A., A. M. Regnery, T. Becker, C. G. Becker and M. C. Halloran (2007). "Semaphorin3D regulates axon axon interactions by modulating levels of L1 cell adhesion molecule." J Neurosci **27**(36): 9653-9663.
Xiao, T. S. (2017). "Innate immunity and inflammation." Cellular and Molecular Immunology **14**(1): 1-3.
Yang, L., P. C. Blumbergs, N. R. Jones, J. Manavis, G. T. Sarvestani and M. N. Ghabriel (2004). "Early Expression and Cellular Localization of Proinflammatory Cytokines Interleukin-1β, Interleukin-6, and Tumor Necrosis Factor-α in Human Traumatic Spinal Cord Injury." Spine **29**(9): 966-971.
Yang, L., N. R. Jones, P. C. Blumbergs, C. Van Den Heuvel, E. J. Moore, J. Manavis, G. T. Sarvestani and M. N. Ghabriel (2005). "Severity-dependent expression of pro-inflammatory cytokines in traumatic spinal cord injury in the rat." Journal of Clinical Neuroscience **12**(3): 276-284.
Yang, W. and P. Hu (2018). "Skeletal muscle regeneration is modulated by inflammation." Journal of Orthopaedic Translation **13**: 25-32.
Yawata, I., H. Takeuchi, Y. Doi, J. Liang, T. Mizuno and A. Suzumura (2008). "Macrophage-induced neurotoxicity is mediated by glutamate and attenuated by glutaminase inhibitors and gap junction

inhibitors." Life Sciences **82**(21-22): 1111-1116.
Ye, L., Y. Huang, L. Zhao, Y. Li, L. Sun, Y. Zhou, G. Qian and J. C. Zheng (2013). "IL-1β and TNF-α induce neurotoxicity through glutamate production: a potential role for neuronal glutaminase." Journal of neurochemistry **125**(6): 897-908.
Yeo, S. Y., M. Kim, H. S. Kim, T. L. Huh and A. B. Chitnis (2007). "Fluorescent protein expression driven by her4 regulatory elements reveals the spatiotemporal pattern of Notch signaling in the nervous system of zebrafish embryos." Dev Biol **301**(2): 555-567.
Yeo, S. Y., M. Kim, H. S. Kim, T. L. Huh and A. B. Chitnis (2007). "Fluorescent protein expression driven by her4 regulatory elements reveals the spatiotemporal pattern of Notch signaling in the nervous system of zebrafish embryos." Developmental Biology **301**(2): 555-567.
Yin, Y., M. T. Henzl, B. Lorber, T. Nakazawa, T. T. Thomas, F. Jiang, R. Langer and L. I. Benowitz (2006). "Oncomodulin is a macrophage-derived signal for axon regeneration in retinal ganglion cells." Nat Neurosci **9**(6): 843-852.
Yuan, Y. and C. He (2013). The glial scar in spinal cord injury and repair.
Yuan, Y. M. and C. He (2013). "The glial scar in spinal cord injury and repair." Neurosci Bull **29**(4): 421-435.
Zhang, H., M. Chang, C. N. Hansen, D. M. Basso and L. J. Noble-Haeusslein (2011). "Role of matrix metalloproteinases and therapeutic benefits of their inhibition in spinal cord injury." Neurotherapeutics **8**(2): 206-220.
Zhang, J.-M. and J. An (2007). "Cytokines, Inflammation and Pain." International anesthesiology clinics **45**(2): 27-37.
Zhang, Y. and D. L. Wiest (2016). "Using the Zebrafish Model to Study T Cell Development." Methods Mol Biol **1323**: 273-292.
Zhang, Z., F. Li and T. Sun (2012). "Does repair of spinal cord injury follow the evolutionary theory?" Neural Regeneration Research **7**(11): 849-852.
Zheng, X., W. Dai, X. Chen, K. Wang, W. Zhang, L. Liu and J. Hou (2015). "Caffeine reduces hepatic lipid accumulation through regulation of lipogenesis and ER stress in zebrafish larvae." J Biomed Sci **22**: 105.
Zhou, X., X. He and Y. Ren (2014). "Function of microglia and macrophages in secondary damage after spinal cord injury." Neural Regeneration Research **9**(20): 1787-1795.
Ziv, Y. and M. Schwartz (2008). "Orchestrating brain-cell renewal: the role of immune cells in adult neurogenesis in health and disease." Trends Mol Med **14**(11): 471-478.
Zong, S., G. Zeng, B. Wei, C. Xiong and Y. Zhao (2012). "Beneficial effect of interleukin-1 receptor antagonist protein on spinal cord injury recovery in the rat." Inflammation **35**(2): 520-526.

Publications

© 2016. Published by The Company of Biologists Ltd | Development (2016) 143, 1464-1474 doi:10.1242/dev.129155

STEM CELLS AND REGENERATION

RESEARCH ARTICLE

Spinal motor neurons are regenerated after mechanical lesion and genetic ablation in larval zebrafish

Jochen Ohnmacht*,‡, Yujie Yang (杨宇婕)‡, Gianna W. Maurer, Antón Barreiro-Iglesias, Themistoklis M. Tsarouchas, Daniel Wehner, Dirk Sieger, Catherina G. Becker§ and Thomas Becker§

ABSTRACT

In adult zebrafish, relatively quiescent progenitor cells show lesion-induced generation of motor neurons. Developmental motor neuron generation from the spinal motor neuron progenitor domain (pMN) sharply declines at 48 hours post-fertilisation (hpf). After that, mostly oligodendrocytes are generated from the same domain. We demonstrate here that within 48 h of a spinal lesion or specific genetic ablation of motor neurons at 72 hpf, the pMN domain reverts to motor neuron generation at the expense of oligodendrogenesis. By contrast, generation of dorsal Pax2-positive interneurons was not altered. Larval motor neuron regeneration can be boosted by dopaminergic drugs, similar to adult regeneration. We use larval lesions to show that pharmacological suppression of the cellular response of the innate immune system inhibits motor neuron regeneration. Hence, we have established a rapid larval regeneration paradigm. Either mechanical lesions or motor neuron ablation is sufficient to reveal a high degree of developmental flexibility of pMN progenitor cells. In addition, we show an important influence of the immune system on motor neuron regeneration from these progenitor cells.

KEY WORDS: Dopamine, Macrophage, Microglia, Nitroreductase, Hb9, Olig2, Sox10

INTRODUCTION

In contrast to mammals, adult zebrafish are capable of regenerating neurons in the central nervous system (CNS), including the spinal cord (Grandel and Brand, 2013; Goldman, 2014; Becker and Becker, 2015; Than-Trong and Bally-Cuif, 2015). To understand these differences, it is important to elucidate the signals and mechanisms leading to successful CNS regeneration in fish. In adult zebrafish, a lesion to the spinal cord induces ependymo-radial glial cells (ERGs) to proliferate and, subsequently, distinct ERG domains give rise to different types of neurons (Reimer et al., 2008; Goldshmit et al., 2012; Kuscha et al., 2012a,b). For example, *olig2*-expressing ERGs in the ventromedial aspect of the spinal cord generate new motor neurons after a lesion (Reimer et al., 2008).

Motor neuron-generating adult ERGs are likely to be derived from embryonic motor neuron progenitor (pMN) cells. The spinal pMN domain thus transitions from a motor neuron generating program during early development [up to 48 hours post-fertilisation (hpf)] (Reimer et al., 2013) to generation of oligodendrocytes (Kirby et al., 2006; Kim et al., 2008; Czopka et al., 2013) and eventually, to relative quiescence at the adult stage (Reimer et al., 2008).

A mechanical lesion in adults reinitiates the program for motor neuron generation (Reimer et al., 2008). This is positively regulated by Hedgehog (Reimer et al., 2009), dopamine signalling acting on the Hedgehog pathway (Reimer et al., 2013) and serotonin (Barreiro-Iglesias et al., 2015). To explore the plasticity of spinal progenitors, we asked whether motor neuron regeneration can be triggered when their developmental generation has been completed but cells in the pMN domain are still proliferating and generate oligodendrocytes, and if so, whether progenitors react to signals similar to those during adult regeneration.

The immune system probably plays an important role in regeneration. For example, there is a strong microglia/macrophage reaction to a spinal lesion (Becker and Becker, 2001) and activation of microglia/macrophages alone is sufficient to trigger neuronal regeneration in the adult zebrafish telencephalon (Kyritsis et al., 2012). This suggests that signalling of microglia/macrophages to progenitor cells occurs.

However, with mechanical lesions, it is difficult to dissociate the effects of extrinsic signals from those of injuring the intricate radial processes of the progenitors themselves. For example, it has been shown that the stem cell potential of astrocytes in mammals differs following mechanical lesion versus cell ablation or a chronic disease state (Sirko et al., 2013). Therefore, we use a genetic strategy (Curado et al., 2008) to selectively ablate motor neurons in order to determine whether this loss is sufficient to trigger motor neuron regeneration in the larval spinal cord.

We find that a mechanical lesion of the larval spinal cord leads to regeneration of motor neurons close to the spinal lesion site and that this can be enhanced with a dopamine agonist, similar to adult regeneration. A macrophage/microglial reaction promotes motor neuron regeneration. Cell type-specific ablation is sufficient to induce motor neuron regeneration. Hence, motor neuron regeneration can be studied in larvae, as it replicates some features of adult regeneration. Motor neuron regeneration can be dissociated from mechanical lesion of progenitors and is promoted by the innate immune system.

RESULTS

Larval lesion induces local regeneration of motor neurons

Embryonic motor neuron generation from the pMN domain largely ceases by 48-51 hpf (Reimer et al., 2013), whereas oligodendrogenesis from these progenitors continues for weeks (Park et al., 2007). To determine whether pMN progenitors can switch to generating motor neurons during oligodendrogenesis, we inflicted a mechanical lesion to the spinal cord at 3 days post-fertilisation (dpf), leaving the notochord and major blood vessels

Centre for Neuroregeneration, The University of Edinburgh, 49 Little France Crescent, Edinburgh EH16 4SB, UK.
*Present address: Institute of Experimental and Clinical Pharmacology and Toxicology, University of Lübeck, 23562 Lübeck, Germany.
‡These authors contributed equally to this work

§Authors for correspondence (catherina.becker@ed.ac.uk; thomas.becker@ed.ac.uk)

Received 28 July 2015; Accepted 25 February 2016

Development (2016) 143, 1464-1474 doi:10.1242/dev.129155

intact (Fig. 1A-C). Such a wound closes quickly (within 48 h; Fig. 1D) and larvae recover swimming capability within 2 days post-lesion, as measured by distance moved after tail touch (Fig. S1). This indicates that functional regeneration is extremely quick at the larval stage.

To label newly generated motor neurons, we applied the DNA base analogue and proliferation marker EdU to *Hb9:*GFP (also known as *mnx1:*GFP) transgenic animals directly after the lesion at 3 dpf and counted double labelled neurons at 4, 5 and 6 dpf. No increase in the number of *Hb9:*GFP$^+$ neurons that incorporated EdU, which would have been newly generated after the lesion, was observed at 4 dpf. However, at both 5 and 6 dpf, the number of *Hb9:*GFP$^+$/EdU$^+$ cells was strongly increased by up to 400% close to (within 50 µm), but not far from (within 50-100 µm) the lesion site, compared with unlesioned controls (Fig. 1E-H). To test whether regenerative neurogenesis would also occur at later stages, we shifted the injury paradigm to 5 dpf, when larvae had become fully behaving predators (Semmelhack et al., 2014; Bianco and Engert, 2015). Analysis of *Hb9:*GFP$^+$/EdU$^+$ neurons at 7 dpf indicated a 257% increase in the number of new motor neurons, comparable to the 3 to 5 dpf standard protocol (Fig. S2). This supports the presence of local lesion-induced signals that lead to motor neuron regeneration within 48 h of the lesion.

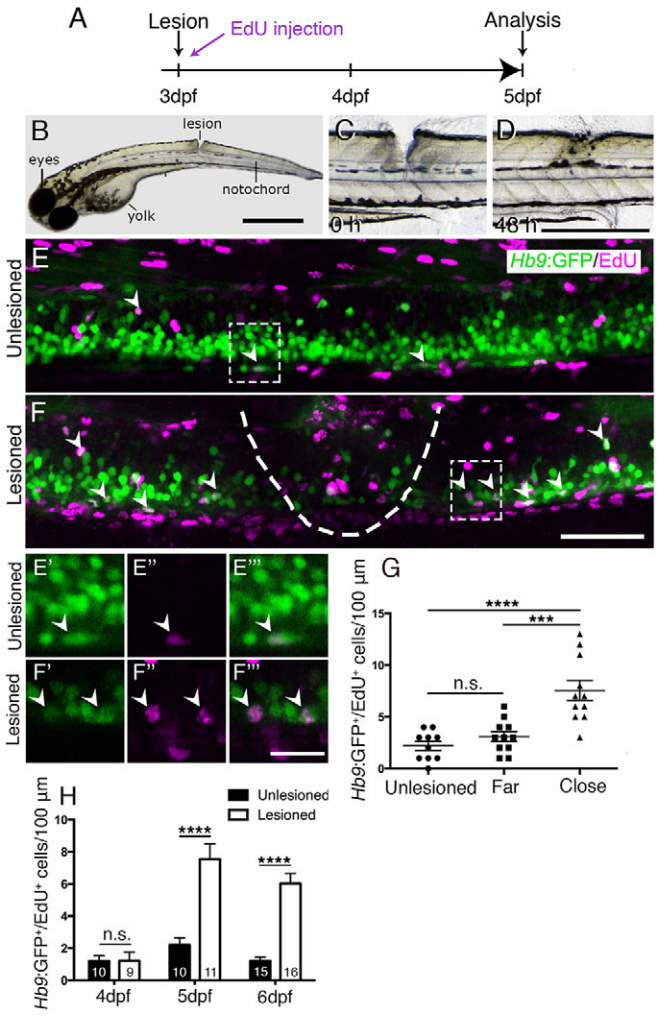

Fig. 1. A mechanical lesion to the spinal cord heals within 48 h and leads to motor neuron regeneration close to the lesion site. (A) Time line for experiments. (B) A zebrafish larva with a lesion in the dorsal trunk area, leaving the notochord intact at 3 dpf. (C,D) The same larva imaged at 0 and 48 h post lesion shows closure of the wound. (E,F) The lesion area is outlined with double-labelled *Hb9:*GFP$^+$/EdU$^+$ neurons indicated by arrowheads. A lesion leads to increased numbers of *Hb9:*GFP$^+$/EdU$^+$ double-labelled motor neurons (compare E and F). E′ to F‴ show higher magnifications of areas boxed in E and F, respectively, in single optical sections indicating double labelling. (G) Motor neurons are regenerated close to (<50 µm rostral and caudal), but not far from (100 µm>×>50 µm rostral and caudal) the lesion site (one-way ANOVA with Bonferroni's multiple comparisons test, ***P<0.001, ****P<0.0001; unlesioned, n=10; far, n=11; close, n=11). (H) Time line of the increase in the number of EdU-labelled motor neurons (t-test, ****P<0.0001). Values are means±s.e.m. Lateral views of larvae are shown (rostral is left; dorsal is up). Scale bars: 100 µm in B; 500 µm in D for C,D; 50 µm in F for E,F; 15 µm in F‴ for E′-F‴.

To determine whether larval pMN progenitor cells react to a lesion with increased proliferation, we injected EdU into *olig2*:DsRed transgenic larvae, in which pMN progenitors and motor neurons contain DsRed protein. To label acutely proliferating cells in the pMN domain, we chose a paradigm in which larvae were lesioned at 3 dpf and EdU was injected at 4 dpf with a subsequent survival time of 4 h. This indicated a 165% increase in the number of *olig2*:DsRed$^+$/EdU$^+$ cells (Fig. 2A-D). Hence, proliferation in the pMN domain was increased after a lesion.

To assess whether newly generated motor neurons in larvae were derived from the *olig2*-expressing cells, we used EdU labelling in *Hb9*:GFP; *olig2*:DsRed double transgenic larvae. If newly generated motor neurons are derived from these progenitors, they retain the DsRed protein, which is expressed in progenitors under the regulatory sequences for *olig2*. Thus DsRed protein acts as short-term lineage tracer. Indeed, all newly generated motor neurons (*Hb9*:GFP$^+$/EdU$^+$; 23 neurons in 4 animals) were also positive for DsRed (Fig. 2E). This suggests that after a lesion, newly generated motor neurons originate from *olig2*-expressing pMN progenitor cells.

To determine whether generation of oligodendrocytes, which are derived from the same progenitor domain (Kucenas et al., 2008; Czopka et al., 2013), was altered by the lesion, we assessed numbers of *olig2*:GFP/*sox10*:mRFP/EdU triple-labelled cells, representing newly generated oligodendrocytes and their precursors (Kirby et al., 2006), at 5 dpf, after a lesion at 3 dpf. These cells were present in unlesioned larvae, confirming previous evidence for continuous generation of oligodendrocytes in unlesioned larvae (Kucenas et al., 2008; Czopka et al., 2013), and reduced in number by 88% after a lesion (Fig. 3A-D). We assessed the number of newly generated differentiated oligodendrocytes in the *mbp*:GFP (Almeida et al., 2011) transgenic line, in which oligodendrocytes are labelled under the regulatory sequences of the *myelin basic protein a* (*mbpa*) gene. The number of EdU double-labelled *mbp*:GFP$^+$ cells was also strongly reduced by 94% (Fig. 3E-G).

Importantly, we did not observe any *olig2*:GFP/*sox10*:mRFP double-labelled cells that were labelled by the TUNEL reaction, indicating that lower numbers of oligodendrocyte-lineage cells were not due to increased cell death (Fig. S3). To determine whether a sub-class of pMN progenitors show selective cell death, we also assessed the number of *olig2*:GFP/TUNEL double-labelled cells within the pMN domain, but did not detect increased cell death after a lesion. Occasionally, we observed double-labelled cells in the pMN domain outside the area of interest in both conditions, demonstrating that we were able to detect such cells (not shown). Taken together, these observations suggest that after a lesion, progenitor cells in the pMN domain switch from oligodendrocyte generation to motor neuron generation.

To elucidate whether other progenitor cells are induced to generate new neurons after a lesion, we analysed the number of

Development (2016) 143, 1464-1474 doi:10.1242/dev.129155

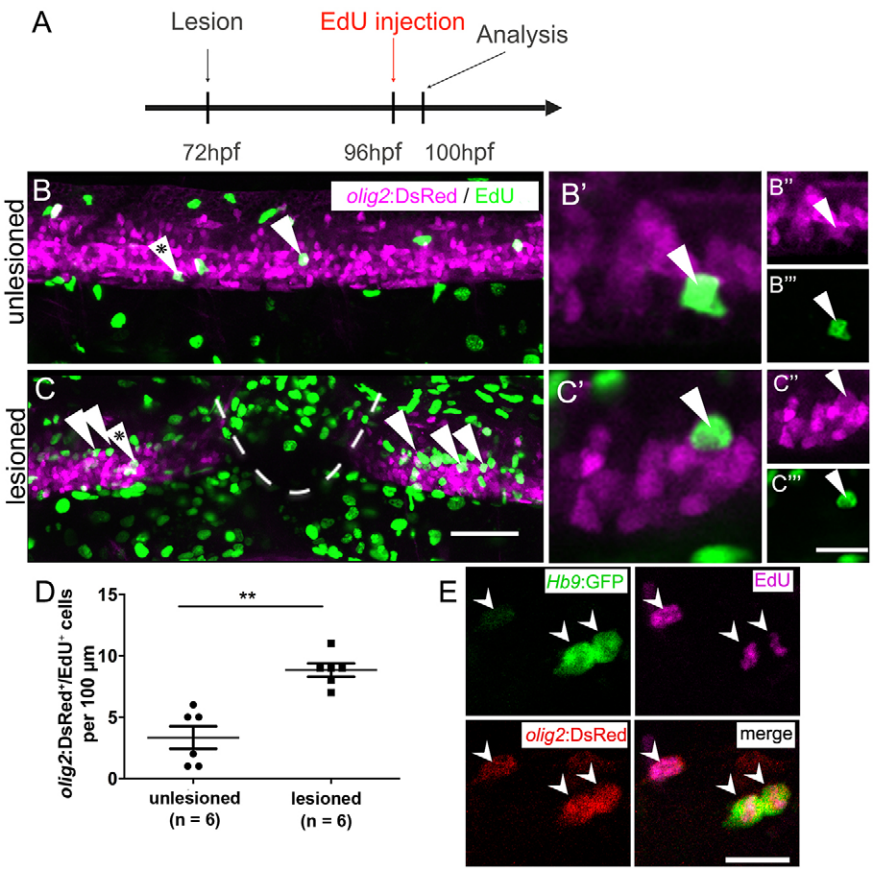

Fig. 2. After a lesion, the pMN domain shows increased proliferation and gives rise to motor neurons. (A) Time line of the experiment. (B,C) *olig2*:DsRed^{+} cells (arrowheads) in the pMN domain that incorporated EdU within the last 4 h. (B′-C‴) Higher magnifications of single optical sections of the cells indicated by asterisks in B and C, respectively, showing double labelling. (D) The number of proliferating cells in the pMN domain is significantly increased in the vicinity of the lesion site (Mann–Whitney test; ***P*=0.0049). (E) In *Hb9*:GFP and *olig2*:DsRed double-transgenic larvae (lesion: 3 dpf; analysis: 5 dpf), newly generated motor neurons (*Hb9*:GFP^{+}/EdU^{+}) that retain DsRed protein are indicated by arrowheads. Lateral views are shown; rostral is left, dorsal is up. Values are means±s.e.m. Scale bars: 50 µm in C for B,C; 20 µm in C‴ for B″-C‴ and 10 µm for B′,C′; 15 µm in E.

newly generated dorsal *pax2a*:GFP^{+} interneurons, which are regenerated after an adult spinal cord lesion (Kuscha et al., 2012b). *pax2a*:GFP^{+} post-mitotic neurons have been suggested to be derived from more dorsal progenitor domains and not the pMN domain (England et al., 2011). The analysis in larvae showed equally low numbers of *pax2a*:GFP/EdU double-labelled cells in unlesioned controls and lesioned larvae (Fig. S4). This suggests that for some dorsal progenitor domains, a lesion might not be sufficient to trigger increased generation of neurons.

To determine whether larval regeneration shares mechanisms with adult regeneration, we decided to analyse dopamine signalling, which is shown to promote spinal motor neuron regeneration in adults (Reimer et al., 2013). To detect an endogenous source for dopamine, we labelled descending, mostly dopaminergic axons, by immunohistochemistry for tyrosine hydroxylase 1 (TH1; the rate-limiting enzyme in dopamine synthesis). Thus, we could detect descending TH1^{+} axons in the spinal cord of unlesioned larval zebrafish at 78 hpf (Fig. S5). In lesioned larvae, TH1^{+} axons were not detected caudal to the lesion site, 6 h after the lesion. These distal axon segments had most likely degenerated. Incubation in the dopamine agonist pergolide after a lesion (3-5 dpf), increased the number of newly generated *Hb9*:GFP^{+} motor neurons by 63% (Fig. 4), with no difference between the rostral and caudal spinal cord. These data suggest that larval pMN progenitors react to similar signals as adult pMN-like progenitors after a lesion.

The immune response is important for motor neuron regeneration

Reactive immune cells promote neuronal regeneration (Kyritsis et al., 2012) and the larval spinal cord offers the opportunity to study the innate immune system in isolation from the adaptive immune response, which develops only later (Danilova and Steiner, 2002; Lam et al., 2004). To determine whether the innate immune system promoted motor neuron generation after a larval lesion, we labelled microglial cells with a 4C4 antibody (Becker and Becker, 2001), and all macrophages and neutrophils with an L-plastin (Lcp1) antibody (Feng et al., 2010). Labelling with the 4C4 antibody was significantly increased in the lesion site by 369% (data not shown). At 48 h after the lesion, labelling of both 4C4 and L-plastin was concentrated at the lesion site (Fig. 5A,B,D). Suppressing this response by incubation of larvae in the immunosuppressant dexamethasone (Kyritsis et al., 2012), strongly dampened the microglia/macrophage response (Fig. 5C,E,F). This treatment also led to a reduction in the number of newly generated *Hb9*:GFP^{+}/EdU^{+} motor neurons by 60% within 48 h of the lesion (3-5 dpf; Fig. 5G-I), suggesting that macrophages/microglial cells exert a positive influence on motor neuron regeneration.

Genetic ablation of motor neurons triggers specific motor neuron apoptosis and macrophage/microglial activation

To determine whether a mechanical lesion is necessary to trigger motor neuron regeneration or whether loss of motor neurons alone is sufficient to trigger a regenerative response, we expressed a nitroreductase transgene in motor neurons for selective ablation in *Tg(mnx1:Gal4, UAS:nfsB-mCherry)* double-transgenic fish. Lateral views of larvae showed obvious labelling in motor neurons in the ventral half of the spinal cord with axons growing into the muscle periphery, as well as in the heart and pancreas at 3 dpf (Fig. 6A). Expression levels varied, but could be substantially increased through selective breeding. There was a

Development (2016) 143, 1464-1474 doi:10.1242/dev.129155

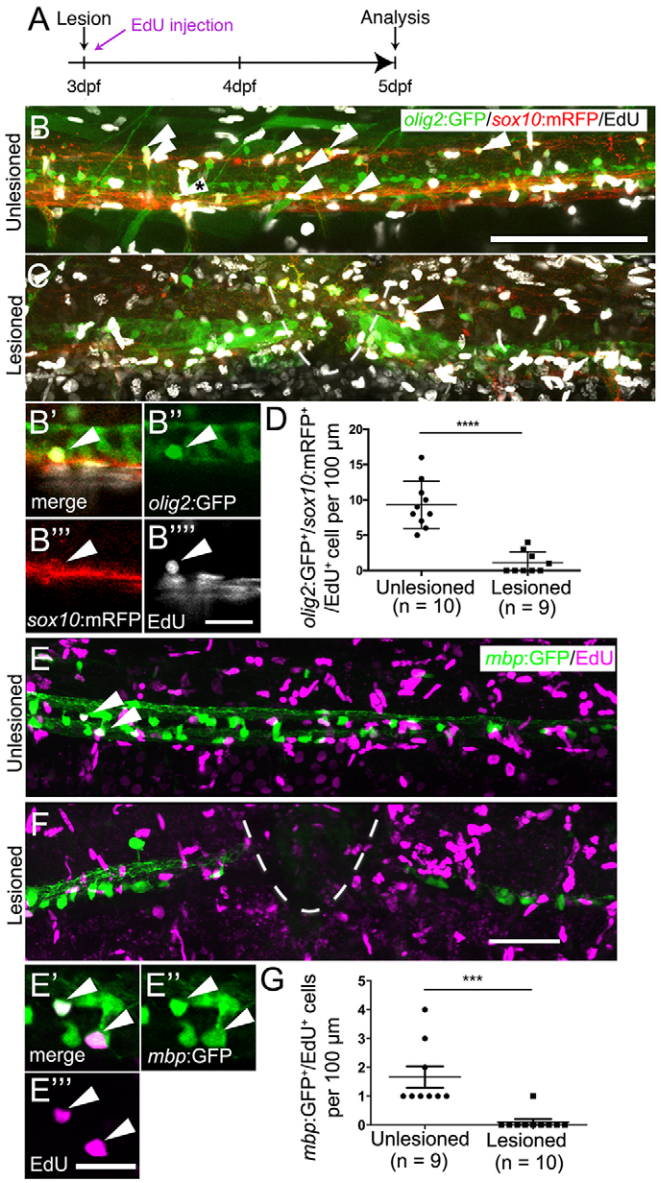

Fig. 3. Oligodendrocyte generation is reduced after a spinal lesion. (A) Time line of the experiment. (B,C) Newly generated oligodendrocytes and their precursors, triple labelled by *olig2*:GFP, *sox10*:mRFP and EdU (arrowheads), are reduced in number after lesion. (B′-B‴′) A triple-labelled cell (indicated with asterisk in B) in a single optical section at higher magnification. (D) The number of triple-labelled cells is reduced (Student's *t*-test, ****P<0.0001). (E) *mbp*:GFP$^+$ oligodendrocytes incorporate EdU (indicated by arrowheads) in unlesioned larvae. (E′-E‴) Two double-labelled neurons indicated in E at higher magnification in a single optical section. (F) Fewer double-labelled cells are observed after a lesion. (G) The number of new oligodendrocytes is significantly reduced after a lesion (Mann–Whitney *U*-test; ***P=0.0005). Lateral views are shown; rostral is left, dorsal is up. The lesion site is indicated by a dashed line. Values are means±s.e.m. Scale bars: 100 µm in B for B,C; 20 µm in B‴′ for B′-B‴′; 50 µm in F for E,F; 20 µm in E‴.

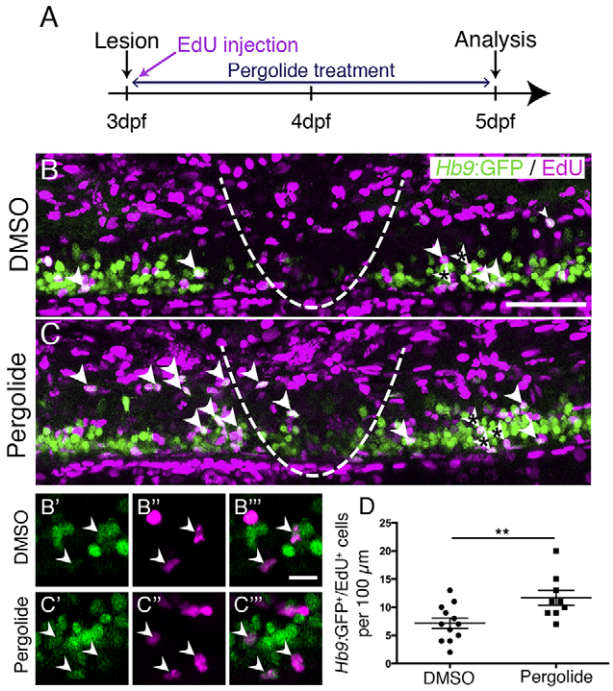

Fig. 4. Motor neuron regeneration is enhanced by application of a dopamine agonist. (A) Experimental time line. (B,C) Double-labelled *Hb9:*GFP$^+$/EdU$^+$ neurons are indicated by arrowheads. (B′-C‴′) Double-labelled cells from B,C (asterisks) are indicated by arrowheads in single optical sections at higher magnification. (D) Pergolide treatment during the regeneration phase significantly increases the number of *Hb9:*GFP$^+$/EdU$^+$ double-labelled motor neurons (*t*-test, **P=0.0092; DMSO, n=12; Pergolide, n=9). Lateral views are shown; rostral is left, dorsal is up. The lesion site is indicated by a dashed line. Values are means±s.e.m. Scale bars: 50 µm in B for B,C; 10 µm in B‴′ for B′-C‴′.

general decline in the number of labelled cells with progressing development. mCherry$^+$ cells were still detectable at 10 dpf, but had completely disappeared in adults (data not shown).

At 3 dpf, triple labelling of Hb9, ChAT and mCherry revealed that 86% of the mCherry-labelled spinal cells were also positive for Hb9, ChAT or both, indicating that the vast majority of mCherry$^+$ cells were indeed motor neurons (Fig. 6B,C). Conversely, 42% of Hb9$^+$ and 54% of ChAT$^+$ motor neurons expressed the *nfsB-mCherry* transgene at 3 dpf (Table S1). At 5 dpf, the proportion of Hb9$^+$ motor neurons that were also labelled by mCherry was reduced to 25% (data not shown), in line with the developmental reduction in transgene and endogenous *hb9* expression.

Incubation with metronidazole (MTZ) led to a visible loss of mCherry signal starting 4-5 h into the treatment and by 24 h, almost no intact cell bodies were observable in the spinal cord of whole-mounted larvae or sections (Fig. 7A-D; Fig. S6). TUNEL and FLICA labelling of motor neurons confirmed loss of these cells (Fig. S7). In *Tg(mnx1:Gal4, UAS:nfsB-mCherry); slc6a5*:GFP triple-transgenic fish, in which glycinergic neurons in the ventral spinal cord are additionally labelled for GFP (McLean et al., 2007), mCherry$^+$ motor neurons, but not *slc6a5*:GFP$^+$ interneurons were ablated, indicating specificity of ablation (Fig. S8). Counts of Hb9 and ChAT immunoreactive neurons showed a reduction by 12% and 17%, respectively (Fig. 8I). Treatment of *Hb9:*GFP larvae with 5 and 10 mM MTZ did not result in any cell loss, indicating that MTZ alone was not toxic to motor neurons (data not shown).

mCherry fluorescence was also reduced in the heart (Fig. S6), suggesting ablation of heart tissue and blood flow in ventral and intersegmental vessels had stopped in at 24 h into the treatment (n=5), but not in MTZ-treated control animals (n=5). These larvae still survived the treatment for several days. This is probably because small zebrafish larvae do not depend on circulation for oxygen diffusion until about 14 dpf (Jacob et al., 2002). For example, mutants without a heartbeat show no obvious aberrations in the first week of development (Rottbauer et al., 2001). The latest time point we analysed was at 9 dpf.

Development (2016) 143, 1464-1474 doi:10.1242/dev.129155

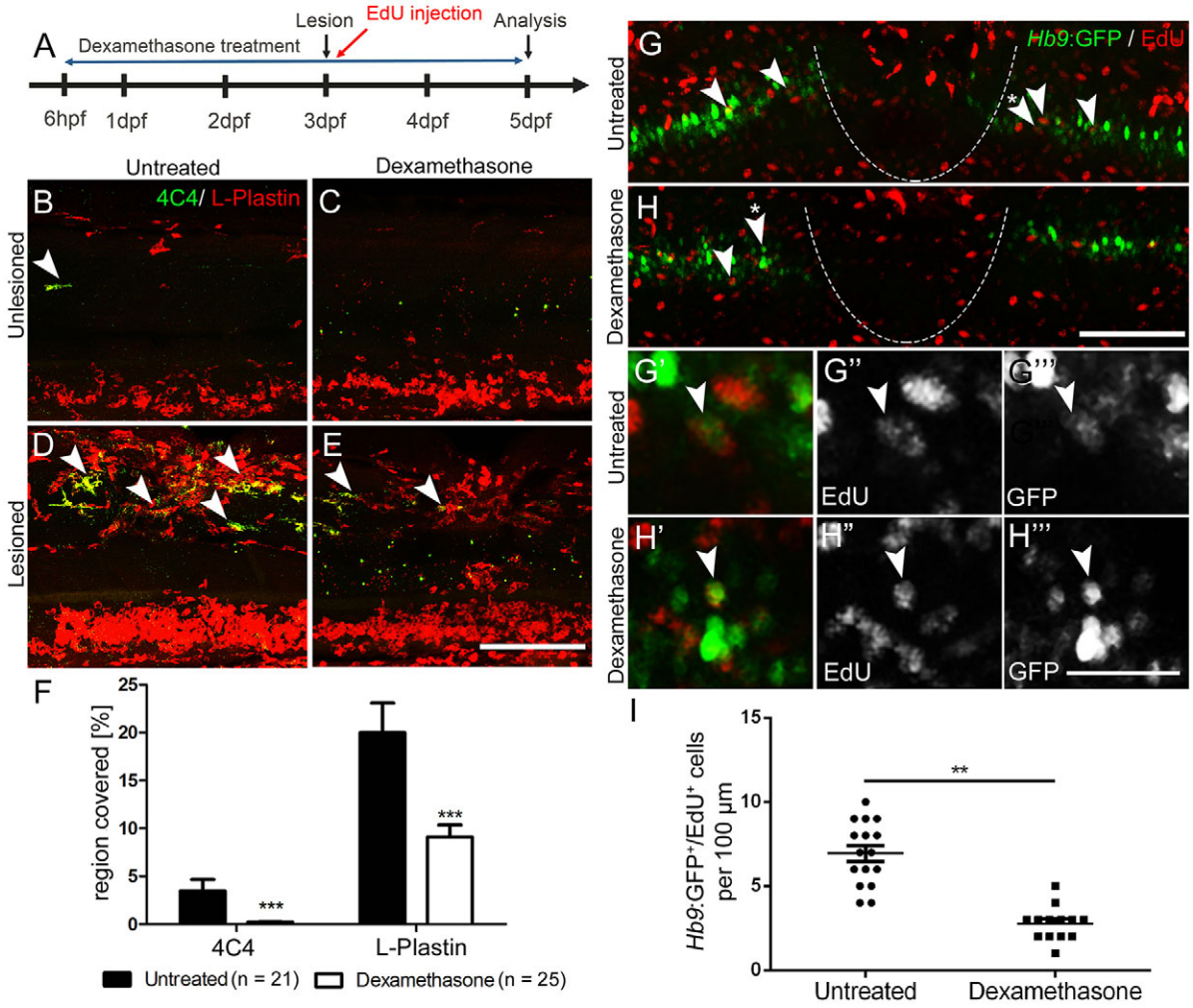

Fig. 5. Suppression of the immune response inhibits motor neuron regeneration. (A) Time line for the experiments. (B-F) Incubation with dexamethasone does not lead to visible changes in unlesioned larvae (B,C), but strongly reduces the immune reaction at the lesion site (D,E) as indicated by reduced 4C4 (arrowheads indicate 4C4$^+$ cells) and L-plastin immunoreactivity. Quantification of immunoreactivity is shown in F (Student's *t*-test, ***P<0.001). (G-I) Dexamethasone treatment reduces the number EdU-labelled *Hb9:*GFP$^+$ motor neurons (arrowheads). Higher magnifications of double-labelled neurons indicated by asterisks in G,H are shown in single optical sections in G′-H‴. (I) Quantification of the reduction in newly generated motor neurons (*t*-test; **P=0.0085; unlesioned, n=16; dexamethasone, n=13). Lateral views are shown; rostral is left, dorsal is up. The lesion site is indicated by a dashed line. Values are means±s.e.m. Scale bars: 100 µm in E for B-E; 100 µm in H for G,H; 50 µm in H‴ for G′-H‴.

Using the 4C4 antibody, we detected that MTZ treatment resulted in an increased number of 4C4$^+$ cell profiles in the spinal cord, which were often found to contain red fluorescing debris from mCherry$^+$ cells after 24 h of MTZ incubation (Fig. 7E-G). The increase in numbers of macrophages/microglial cells was specific to the spinal cord, because we did not observe an increase in cell numbers in the eyes or brain (Fig. S9). Moreover, in wild-type larvae, no increase in macrophage/microglial cell counts was observed after MTZ treatment (data not shown). Hence, ablation of motor neurons leads to a specific reaction of macrophages/microglial cells in the spinal cord.

Motor neurons regenerate after targeted ablation

As ablation of mCherry$^+$ cells in *Tg(mnx1:Gal4, UAS:nfsB-mCherry)* double transgenic fish was almost complete, reappearance of these cells would indicate regeneration of motor neurons. However, we did not observe any new mCherry$^+$ cells for at least 7 days post-ablation (n=7). To test whether this was due to a lack of regeneration or an inability to re-express the transgene, we treated larvae with MTZ from 3 to 4 dpf and additionally inflicted a mechanical lesion at 4 dpf, because mechanical lesions trigger motor neuron regeneration (see above). However, no mCherry$^+$ cells were observed for up to 8 dpf (n=7, data not shown). In addition, at 2 weeks after a spinal lesion in adult *Tg(mnx1:Gal4, UAS:nfsB-mCherry)* fish (n=3), we observed small strongly Hb9 immunoreactive cells, previously shown to be lesion-induced newly generated motor neurons (Reimer et al., 2008), but none of these were mCherry$^+$ (data not shown). This indicates that the transgene is not expressed by newly generated motor neurons at later stages of development or in adult fish.

To determine whether motor neuron regeneration took place after ablation of motor neurons, we used Hb9 immunohistochemistry after EdU injections at different injection and detection time points. After two injections of EdU at 16 and 22 h into the MTZ treatment, we observed a significant increase in the number of Hb9$^+$/EdU$^+$ motor neurons at 9 dpf (Fig. 8A-C,F,G) but not at 5 dpf (48 h after treatment onset; n=4, data not shown). By contrast, the number of Pax2 immunoreactive interneurons that were double labelled with

Development (2016) 143, 1464-1474 doi:10.1242/dev.129155

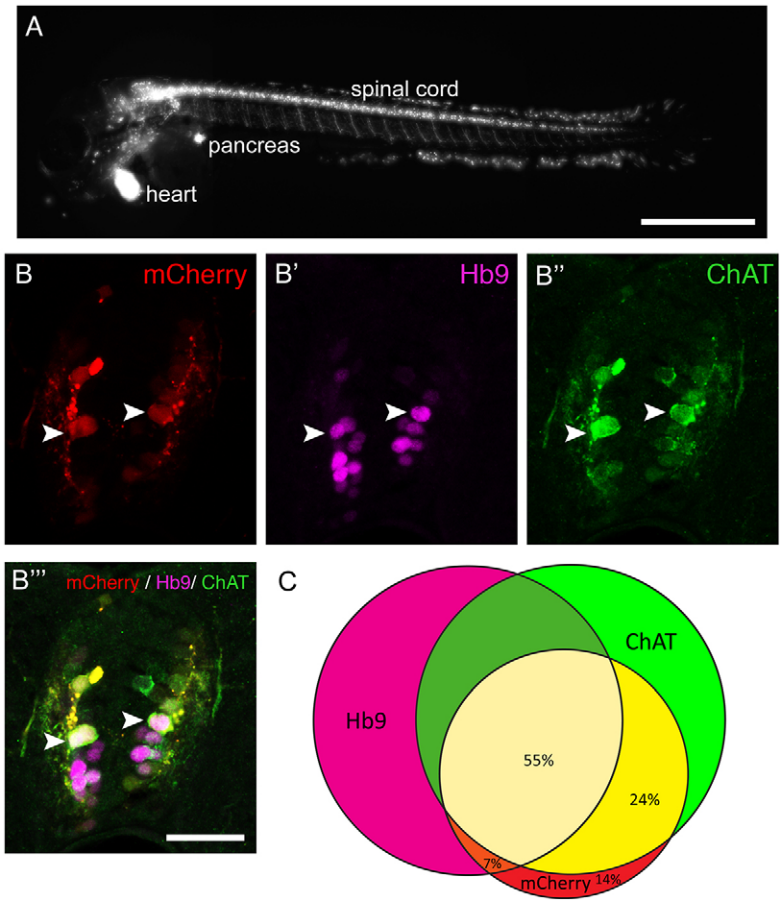

Fig. 6. The *Tg(mnx1:Gal4, UAS:nfsB-mCherry)* transgene is expressed in motor neurons. (A) Lateral view of a whole larva (rostral left, dorsal up, 3 dpf) indicates labelling in spinal motor neurons, the pancreas and heart. (B,C) Spinal cross sections (3 dpf) indicate that most mCherry^{+} cells are also Hb9^{+} or ChAT^{+}, or both. Arrowheads indicate triple-labelled cells. (C) Venn diagram showing the overlap of mCherry expression with motor neuron markers. Scale bars: 500 µm in A; 25 µm in B‴ for B-B‴.

EdU was not increased at 9 dpf after motor neuron ablation at 3 dpf (Fig. 8D,E,H). Application of EdU at 48 and 72 h post treatment did not result in Hb9/EdU co-labelled profiles in either controls (n=4) or MTZ-treated larvae (n=4 at 48 h post-treatment; n=4 at 72 h post treatment), indicating that new motor neurons were generated within 48 h of treatment.

The overall number of Hb9^{+} profiles was significantly reduced 24 h after ablation at 3 dpf and was back to control levels at 7 dpf.

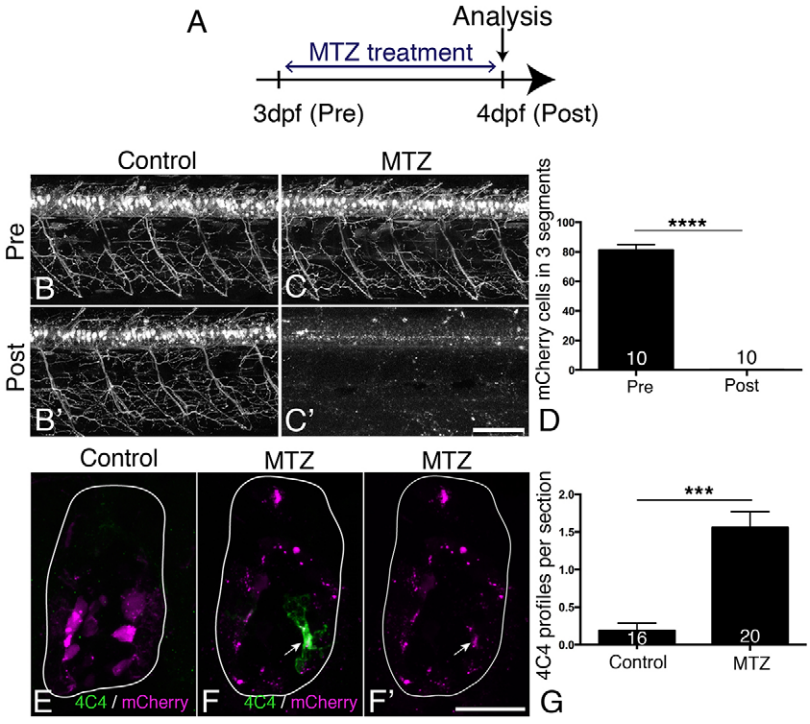

Fig. 7. MTZ treatment leads to ablation of all transgene-expressing cells and to microglia/macrophage activation. (A) Treatment time line. (B-D) mCherry^{+} motor neurons and their axons are visible in untreated control larvae at 3 and 4 dpf (B,B′), but mCherry labelling is completely lost after 24 h treatment with MTZ (C,C′), quantified in D (Mann–Whitney U-test, ****P<0.0001). (E-G) Cross sections show that mCherry-labelled cells fragment during MTZ treatment and that microglia/macrophages appear and phagocytose the cell debris (arrow in F,F′). Microglia/macrophages are quantified in G (Mann–Whitney U-test, ***P<0.0001). Values are means±s.e.m. Scale bars: 100 µm in C′ for B-C′; 25 µm in F′ for E-F′.

Development (2016) 143, 1464-1474 doi:10.1242/dev.129155

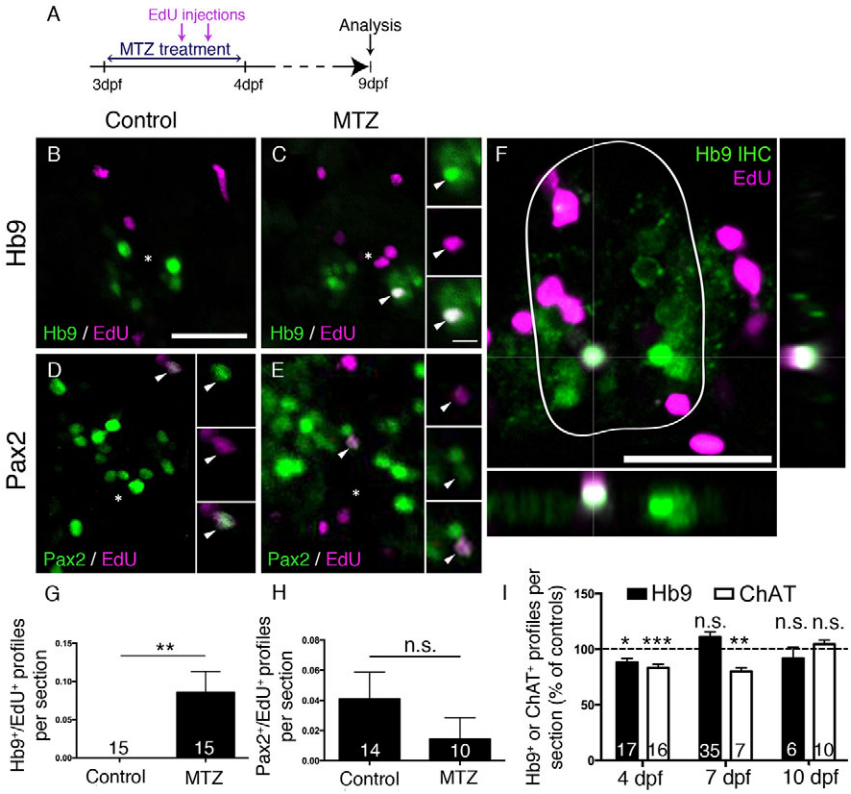

Fig. 8. Motor neuron ablation leads to regeneration of motor neurons. (A) Experimental timeline. (B-H) In spinal cross sections, $Hb9^+/EdU^+$ motor neurons are only observed in MTZ-treated larvae (B,C, shown in a whole cross section of the spinal cord including orthogonal views in F), whereas $Pax2^+$ interneurons are labelled by EdU in untreated and MTZ-treated larvae, quantified in G (Mann–Whitney *U*-test, $^{**}P=0.0063$) and H (Mann–Whitney *U*-test, $P>0.99$), respectively. (I) Overall numbers of $Hb9^+$ and $ChAT^+$ profiles are reduced after a lesion, but return to control values at 7 dpf (Hb9 only) or 10 dpf (ChAT) (*t*-test, $^{*}P=0.0188$; $^{**}P=0.0012$; $^{***}P=0.0004$). Values are means±s.e.m. Scale bars: 25 µm in B for B-E; 5 µm in inset in C for all insets; 25 µm in F.

Similarly, numbers of ChAT profiles were significantly reduced up to 7 dpf and were not significantly different from controls by 10 dpf (Fig. 8I). This suggests that at least some newly generated motor neurons mature into ChAT-positive cells by 10 dpf. Taken together, the data suggest that motor neuron ablation leads to a rapid lesion-induced regeneration of motor neurons, which is completed within 48 h of ablation, followed by slow differentiation of motor neurons, whereas generation of $Pax2^+$ interneurons was unaffected by motor neuron ablation.

DISCUSSION

Here, we demonstrate that spinal progenitors can be induced to regenerate motor neurons in larval zebrafish at the expense of oligodendrocyte generation and identify the immune response as a regeneration-promoting signal. This supports the view that spinal progenitors in zebrafish are highly plastic in terms of the developmental programs they execute. Moreover, we show that genetic ablation of a proportion of motor neurons is sufficient to induce their specific regeneration.

Larval motor neuron regeneration is similar to adult regeneration

Our previous birth dating study of motor neurons indicated that motor neuron generation sharply declines at 48 hpf (Reimer et al., 2013). Our present results confirm that few motor neurons are generated after that time. This allows us to distinguish regenerative from developmental neurogenesis at early larval stages. However, the larval zebrafish spinal cord is still a developing system. This is demonstrated by the observation that $Pax2^+$ interneurons (this report) and other interneurons (Briona and Dorsky, 2014) are still being generated. Nevertheless, some key features of motor neuron regeneration are similar between larval and adult regeneration. For example, the highest numbers of regenerating motor neurons are observed close to the lesion site, motor neurons are derived from *olig2*-expressing progenitors and regeneration is promoted by dopamine (this study and Reimer et al., 2008; Reimer et al., 2013). We show here that motor neuron regeneration and functional recovery in larvae are very rapid, occurring within 48 h, whereas in adults, motor neuron regeneration and recovery of swimming take weeks. However, the possible contribution of regenerated motor neurons to functional recovery still needs to be determined. Our observations show that motor neuron regeneration can be studied in larvae.

Microglia/macrophage signalling might contribute to regeneration

Another aspect that is similar for larval and adult lesions (Becker and Becker, 2001) is activation of the immune system, which might carry pro-regenerative signals. Here, we demonstrate accumulation of immune cells at a spinal lesion site and after motor neuron ablation in larvae and we find that suppression of the immune response using dexamethasone reduces motor neuron regeneration. Manipulation of the adult immune response with dexamethasone in the stab-lesioned telencephalon similarly suppressed neurogenesis from progenitor cells (Kyritsis et al., 2012). Analysis of the immune response at early larval stages has the advantage that the innate immune system can be studied in isolation of the adaptive immune system, because the latter is not functional at early larval stages (Danilova and Steiner, 2002; Lam et al., 2004). Hence, microglia/macrophages are positive regulators of lesion-induced neurogenesis in the lesioned adult and larval CNS.

pMN progenitors are highly plastic

It is likely that regenerated motor neurons are derived from the pMN domain, because they are found close to it in the ventral spinal cord, the pMN domain exhibits increased proliferation after a lesion and

Development (2016) 143, 1464-1474 doi:10.1242/dev.129155

new motor neurons retain DsRed protein expressed from the *olig2* promoter. The pMN progenitor domain generates motor neurons during embryonic development (Shin et al., 2007) and can be reactivated to generate motor neurons from relative quiescence in adults (Reimer et al., 2008). Here, we demonstrate that motor neuron generation can be reactivated by either transection or ablation lesion, even when pMN progenitors are actively generating oligodendrocytes at larval stages (Park et al., 2005; Czopka et al., 2013).

During development, evidence suggests that distinct pMN progenitors generate either motor neurons or oligodendrocytes in a time-dependent fashion (Wu et al., 2006; Ravanelli and Appel, 2015). In the context of larval regeneration, this means that either the oligodendrocyte-restricted progenitors change their developmental program to generate motor neurons, or that new motor neuron progenitors are recruited after lesion/ablation. Our observation that oligodendrogenesis sharply declines during motor neuron regeneration supports a view in which pMN progenitors change fate from oligodendrogenesis to motor neuron generation after a lesion.

Ablated motor neurons are slowly regenerated

Ablation of a specific cell type allows us to ask whether the loss of this cell type is sufficient to elicit its regeneration. We found that after ablation of motor neurons, these are replenished over the course of a few days. Cell numbers for the immature motor neuron marker Hb9 were back to control levels earlier than those for the mature motor neuron marker ChAT. This reflects the differentiation sequence in developing motor neurons and in adult regeneration (Reimer et al., 2008). Interestingly, we observed new motor neurons ($Hb9^+/EdU^+$) by 48 h after the transection lesion, whereas after ablation, these were only observed at later time points. However, new motor neurons could no longer be labelled by EdU application at 48 h or later after the onset of ablation. This suggests rapid generation of new neuroblasts after ablation, followed by a prolonged differentiation phase. Interestingly, in mice, astrocytes in the telencephalon express a neurosphere-forming potential *in vitro* after a mechanical stab injury, but not after cell ablation, indicating that in mammals too, a mechanical lesion might lead to a stronger regenerative response in glial cells (Sirko et al., 2013).

In general, motor neuron regeneration in larvae is substantially quicker than lesion-induced regeneration in adults, in which newly generated, mature $ChAT^+$ motor neurons were observed at 42 days, but not 14 days post injury (Reimer et al., 2008). Rapid motor neuron regeneration is an advantage of larval regeneration studies.

Progenitor domains differ in their regenerative potential

Generation of *pax2a*:GFP^+ or $Pax2^+$ neurons was not enhanced in either of the experimental paradigms. These cells are most likely derived from a more dorsal progenitor domain than the pMN domain (England et al., 2011), indicating that progenitors for dorsal $Pax2^+$ cells do not react to either a mechanical spinal lesion or ablation of motor neurons with enhanced generation of $Pax2^+$ neurons. This underscores the highly plastic nature of the pMN progenitor domain.

Technical considerations of genetic motor neuron ablation

The *Tg(mnx1:Gal4, UAS:nfsB-mCherry)* transgene is reliably and specifically expressed in a proportion of motor neurons at 3 dpf. Ablation is complete, with undetectable bystander effects on *slc6a5*:GFP^+ interneurons. This all-or-nothing situation could be harnessed for regeneration screens in the future. However, even though $Hb9^+$ motor neurons regenerate, the transgene, driven by *hb9* regulatory sequences, is not re-expressed. Possible explanations are developmentally reduced expression of the endogenous gene (Reimer et al., 2008) and silencing of the highly repetitive UAS sequences used in the generation of this transgenic model (Akitake et al., 2011).

Motor neuron ablation in this system leads to an impaired swimming behaviour (Reimer et al., 2013). This could become interesting for future studies of behavioural recovery during motor neuron regeneration. Currently, oedema formation due to ablation of heart cells precludes behaviour studies. Finally, we cannot exclude the possibility that the cessation of blood flow affects regeneration dynamics, even though larvae do not depend on oxygen (Jacob et al., 2002) and mutants without circulation develop normally for at least a week (Rottbauer et al., 2001). Next-generation models might employ less-repetitive versions of UAS (Akitake et al., 2011), which could be driven by regulatory sequences of more mature motor neuron markers (e.g. ChAT). Hence, ablation of motor neurons holds promise for future screening and functional studies of regeneration.

Conclusion

Motor neuron progenitor cells can be induced to regenerate motor neurons at larval stages by mechanical lesion or motor neuron ablation and they react to similar signals (e.g. dopamine) as progenitor cells do during adult regeneration. This indicates considerable plasticity of larval progenitor/stem cells. We use this paradigm to demonstrate a pro-regenerative role of the immune system. Of note, some experiments can be performed at very early unprotected larval stages, thus replacing the need for work with older animals in the sense of reduction, refinement and replacement (the 3Rs; Tannenbaum and Bennett, 2015). We expect that the combination of rapid regeneration with the classical advantages of the zebrafish larva, i.e. small size, transparency and genetic accessibility will lead to a wide range of larval regeneration studies.

MATERIALS AND METHODS

Animals

All fish were kept and bred in our laboratory fish facility according to standard methods (Westerfield, 2000) and all experiments were approved by the British Home Office. We used wild-type (*wik*); *Tg(mnx1:GFP^{ml2})*, abbreviated as *Hb9:*GFP (Flanagan-Steet et al., 2005); *Tg(slc6a5:GFP)*, abbreviated as *slc6a5*:GFP (McLean et al., 2007); *Tg(mnx1:Gal4^{s300t})* (Wyart et al., 2009); *Tg(UAS:nfsB-mCherry)* (Davison et al., 2007); *Tg(olig2:EGFP)*, abbreviated as *olig2*:GFP (Shin et al., 2003); *Tg(olig2:DsRed2)*, abbreviated as *olig2*:DsRed (Kucenas et al., 2008); *Tg(pax2a:GFP)*, abbreviated as *pax2a*:GFP (Picker et al., 2002); *Tg(sox10(7.2):mRFP)*, abbreviated as *sox10*:mRFP (Kirby et al., 2006); and *Tg(mbp:EGFP)*, abbreviated as *mbp*:GFP (Almeida et al., 2011). Male and female fish were used for the experiments.

Larval lesion

Larvae were anaesthetized in 0.02% MS222 (Sigma-Aldrich), embedded in 1.5% low melting point agarose and placed in a lateral position on a microscope slide. Lesions were performed using a sharp 30-gauge injection needle, leaving the notochord and major blood vessels intact. After the lesions, larvae were either immediately injected with 5-ethynyl-2′-deoxyuridine (EdU; Sigma-Aldrich) into the yolk (as described below) or immediately released by gently removing the agarose.

Quantification of behavioural recovery

Lesioned and unlesioned control larvae were touched with a glass capillary on the median fin fold caudal to the lesion site. The swim path of their escape response was recorded and analysed using a Noldus behaviour analysis set-up and EthoVision software (v. 7). Data are shown as distance travelled during the first 15 s after touch, averaged from triplicate measures per larva.

Development (2016) 143, 1464-1474 doi:10.1242/dev.129155

Completeness of injury was verified by the absence of an escape response in freshly lesioned larvae. Dependence of recovery on continuity of the spinal cord was tested by re-lesioning at the end of the regeneration period.

Dexamethasone treatment

To suppress the immune system, we used the glucocorticoid receptor agonist dexamethasone (Sigma), which was previously shown to suppress the immune response in adults (Kyritsis et al., 2012) and larvae (Zhang et al., 2008; Hall et al., 2014). Embryos were incubated with 200 µg/ml dexamethasone in fish water containing 1% DMSO (Sigma-Aldrich) from 6 hpf. Embryos were kept in 5 ml Petri dishes in groups of 10 and fish water was changed every day. At 3 dpf, larvae were lesioned as described above and returned into clean Petri dishes with dexamethasone until analysis at day 5.

Genetic ablation

For motor neuron ablation, larvae were treated from 72 hpf onwards for 24 h with 5 mM metronidazole (Sigma-Aldrich) in fish water containing 0.2% DMSO in darkness at 28°C.

TUNEL labelling

Cryosections were dehydrated in methanol for 10 min at −20°C, washed for 10 min in PBS at room temperature. Terminal deoxynucleotidyl transferase dUTP nick end labelling (TUNEL) was performed using the Fluorescein In Situ Cell Death Detection Kit (Roche) according to the manufacturer's protocol. Sections were covered with Parafilm to prevent evaporation and incubated in a humid chamber at 37°C for 1 h. After the labelling procedure, the sections were extensively washed in PBS.

Whole mounted zebrafish larvae at 5 days post lesion were anaesthetized, fixed in 4% paraformaldehyde (PFA)/1% DMSO in PBS at room temperature for 3 h, washed in PBS and PBST (PBS with 0.2% Tween 20). Then larvae were digested with collagenase (Sigma; 0.2 mg/ml in PBST) for 50 min. The TDT reaction cocktail was prepared according to the manufacturer's instructions (Click-iT TUNEL imaging assay; Roche) and larvae were incubated at room temperature overnight. Larvae were washed in PBS and Click-iT reaction cocktail was prepared and larvae were incubated at room temperature in the dark for 3 h. After extensive washing in PBS, larvae were either processed for immunohistochemistry or transferred to 70% glycerol in PBS.

Detection of activated caspases using fluorochrome-labelled inhibitors of caspases

Fluorochrome-labelled inhibitors of caspases (FLICAs) were used for the detection of activated caspases in motor neurons during metronidazole treatment. We adapted this method for *in vivo* zebrafish larvae from that recently reported for the *ex vivo* brain and spinal cord of larval sea lampreys (Barreiro-Iglesias and Shifman, 2012). The Image-iT LIVE Green Poly Caspases Detection Kit (Invitrogen) was used for the detection of activated caspases in motor neurons. This kit contains one vial (component A of the kit) of the lyophilized FLICA reagent (FAM-VAD-FMK). The reagent contains a fluoromethyl ketone (FMK) moiety, associated with a caspase-specific amino acid sequence (VAD). A carboxyfluorescein group (FAM) is attached as a fluorescent reporter. The FLICA reagent interacts with the enzyme active centre of any activated caspase via the recognition sequence, and then attaches covalently through the FMK moiety (Barreiro-Iglesias and Shifman, 2012). The 150× stock FLICA reagent solution was prepared by adding 50 µl of DMSO to the vial.

Six hours after treatment, DMSO control and metronidazole-treated 78 hpf *Tg(mnx1:Gal4, UAS:nfsB-mCherry)* zebrafish were incubated at 28.5°C in 1× FLICA labelling solution (made from 150× FLICA reagent stock diluted in PBS) for 1 h. After incubation, the animals were washed in PBS on a shaker 9×15 min in PBS to remove unbound FLICA (Barreiro-Iglesias and Shifman, 2012). After washes, the animals were anaesthetized and fixed in 4% PFA in PBS for 1 h and then mounted in 70% glycerol in PBS.

Antibodies

We used mouse anti-Hb9 (MNR2, Developmental Studies Hybridoma Bank, 1:400) (Reimer et al., 2013); rabbit anti-Pax2 (PRB-276P, Covance, 1:1000) (Kuscha et al., 2012b), goat anti-choline acetyltransferase (ChAT) (AB144P, Millipore, 1:500) (Reimer et al., 2008), rabbit anti-L-plastin (a gift from Yi Feng, University of Edinburgh; 1:500) recognizing macrophages, microglia and neutrophils (Feng et al., 2010) and the mouse monoclonal antibody 4C4 (hybridoma line 7.4.C4; 92092321, Public Health England; supernatant, 1:50), recognizing microglia/macrophages (Becker and Becker, 2001), as previously described.

Whole-mount immunohistochemistry

Whole larvae were fixed in 4% PFA/1% DMSO in PBS for 2 h. After washing in PBS, larvae were permeabilized in collagenase (2 mg/ml in PBS) for 25 min. After washing with PBStx (0.2% Triton X-100 in PBS) larvae were incubated in 50 mM glycine for 10 min and washed. After blocking in blocking buffer (1% DMSO, 1% goat serum, 1% BSA and 0.7% Triton X-100) for 2 h, larvae were incubated with primary antibodies at 4°C overnight. Secondary antibodies were added after extensive washes at 4°C overnight. After washing, larvae were mounted in 70% glycerol for subsequent imaging.

Section immunohistochemistry

Larvae were fixed in 4% paraformaldehyde for 2 h, cryoprotected in 30% sucrose overnight, flash-frozen and cryosectioned at a thickness of 14 µm. Sections were fixed in ice cold methanol at −20°C for 10 min and then rehydrated in PBS at room temperature for 10 min. After incubation in blocking buffer (2% goat serum in 0.2% Triton X-100 in PBS) at room temperature for 1.5 h they were incubated with primary antibody overnight at 4°C. Sections were washed in PBStx (0.2% Triton X-100 in PBS) before secondary antibody incubation for 1 h at room temperature. After three 5 min washes in PBStx and two 5 min washes in PBS, sections were mounted in Fluoromount (Sigma).

EdU labelling and detection

Zebrafish larvae from 3 days post-lesion onwards were anaesthetized, placed on a silicone elastomere mount (Sylgard 527 A&B; Dow Corning, 1675167) and injected into the yolk with ∼5 nl 5 mM EdU in 0.1 M sterile KCl and 7.5% DMSO. After washing, larvae were allowed to develop under standard conditions. For analysis, larvae were fixed in 4% paraformaldehyde for 2 h, cryoprotected in 30% sucrose overnight, flash-frozen and cryosectioned at 14 µm. Sections were fixed in methanol for 10 min at −20°C and washed for 10 min in PBS at room temperature. The EdU Click-iT reaction solution (Roche) was prepared fresh according to the manufacturer's protocol. Sections on slides were covered with solution and incubated in a humid chamber at room temperature in the dark for 3 h. After three 10 min washes in PBS, sections were used for imaging or subsequent processing for immunohistochemistry.

Whole-mounted larvae were fixed in 4% PFA/1% DMSO in PBS at room temperature for 3 h, washed in PBS, transferred to methanol and incubated at −20°C for at least 2 h. After rehydrating in a dilution row from methanol to PBST (0.2% Tween 20) larvae were washed in PBST and digested with collagenase (Sigma; 0.2 mg/ml in PBST) for 30 min. The EdU Click-iT reaction solution was prepared and larvae were incubated in 2 ml tubes at room temperature in the dark for 3 h. After extensive washing in PBS, larvae were either processed for immunohistochemistry or transferred to 70% glycerol in PBS.

Quantification and statistical analyses

Cell quantifications in whole-mounted larvae were performed manually by analysing all consecutive images in stacks taken with a confocal microscope. Multiply labelled cells were scored when labels occurred on the same optical section (<2 µm). As a standard, counts were performed within the 50 µm rostral and caudal closest to the lesion site and expressed as cells/100 µm, unless stated differently. For quantification in cryosections (14 µm thickness) we counted all cell profiles and expressed this as number of profiles/section. All variability indicated represents s.e.m. All images were captured with a 20× objective on an Zeiss LSM710 confocal microscope. At least two independent experiments were performed per treatment and cell counts were carried out blinded to the treatment. We used *t*-tests (for

Development (2016) 143, 1464-1474 doi:10.1242/dev.129155

normally distributed data) and Mann–Whitney *U*-tests (for non-normal distributions) for comparisons of two conditions. For multiple comparisons, we used one-way analysis of variance followed by Bonferroni's test for comparisons of individual groups (for normally distributed data) or the Kruskal–Wallis test followed by Dunn's test for comparing individual groups (for non-normal distributions), using GraphPad Prism software.

Acknowledgements

We thank Drs Bruce Appel, Herwig Baier, Yi Feng, Joe Fetcho, Shin-ichi Higashijima, Dirk Meyer, Hitoshi Okamoto, Michael Parsons and Bettina Schmid for providing transgenic fish lines and reagents. We are grateful to Maria Rubio and Silvère Santos for expertly running our zebrafish facility.

Competing interests

The authors declare no competing or financial interests.

Author contributions

Conceptualisation: D.S., C.G.B. and T.B. Investigation: J.O., Y.Y., G.W.M., A.B.-I., T.M.T. and D.W. Writing (original draft, review and editing): C.G.B. and T.B. Supervision: D.S.

Funding

This research was supported by the BBSRC [BB/L021498/1 to C.G.B., T.B.], the NC3Rs [grant no. NC/L001063/1 to C.G.B., T.B.], MND Scotland [C.G.B., T.B.], the Robert Packard Center for ALS research at Johns Hopkins [C.G.B., T.B.], the Euan MacDonald Centre for MND Research [C.G.B., T.B.], and postdoctoral fellowships from the Fundación Barrié and Xunta de Galicia [A.B.-I.] and the Deutsche Forschungsgemeinschaft [WE5736/1-1 to D.W.]. Deposited in PMC for immediate release.

Supplementary information

Supplementary information available online at
http://dev.biologists.org/lookup/suppl/doi:10.1242/dev.129155/-/DC1

References

Akitake, C. M., Macurak, M., Halpern, M. E. and Goll, M. G. (2011). Transgenerational analysis of transcriptional silencing in zebrafish. *Dev. Biol.* **352**, 191-201.

Almeida, R. G., Czopka, T., Ffrench-Constant, C. and Lyons, D. A. (2011). Individual axons regulate the myelinating potential of single oligodendrocytes in vivo. *Development* **138**, 4443-4450.

Barreiro-Iglesias, A. and Shifman, M. I. (2012). Use of fluorochrome-labeled inhibitors of caspases to detect neuronal apoptosis in the whole-mounted lamprey brain after spinal cord injury. *Enzyme Res.* **2012**, 835731.

Barreiro-Iglesias, A., Mysiak, K. S., Scott, A. L., Reimer, M. M., Yang, Y., Becker, C. G. and Becker, T. (2015). Serotonin promotes development and regeneration of spinal motor neurons in zebrafish. *Cell Rep.* **13**, 924-932.

Becker, T. and Becker, C. G. (2001). Regenerating descending axons preferentially reroute to the gray matter in the presence of a general macrophage/microglial reaction caudal to a spinal transection in adult zebrafish. *J. Comp. Neurol.* **433**, 131-147.

Becker, C. G. and Becker, T. (2015). Neuronal regeneration from ependymo-radial glial cells - Cook, little pot, cook! *Dev. Cell* **32**, 516-527.

Bianco, I. H. and Engert, F. (2015). Visuomotor transformations underlying hunting behavior in zebrafish. *Curr. Biol.* **25**, 831-846.

Briona, L. K. and Dorsky, R. I. (2014). Radial glial progenitors repair the zebrafish spinal cord following transection. *Exp. Neurol.* **256**, 81-92.

Curado, S., Stainier, D. Y. R. and Anderson, R. M. (2008). Nitroreductase-mediated cell/tissue ablation in zebrafish: a spatially and temporally controlled ablation method with applications in developmental and regeneration studies. *Nat. Protoc.* **3**, 948-954.

Czopka, T., Ffrench-Constant, C. and Lyons, D. A. (2013). Individual oligodendrocytes have only a few hours in which to generate new myelin sheaths in vivo. *Dev. Cell* **25**, 599-609.

Danilova, N. and Steiner, L. A. (2002). B cells develop in the zebrafish pancreas. *Proc. Natl. Acad. Sci. USA* **99**, 13711-13716.

Davison, J. M., Akitake, C. M., Goll, M. G., Rhee, J. M., Gosse, N., Baier, H., Halpern, M. E., Leach, S. D. and Parsons, M. J. (2007). Transactivation from Gal4-VP16 transgenic insertions for tissue-specific cell labeling and ablation in zebrafish. *Dev. Biol.* **304**, 811-824.

England, S., Batista, M. F., Mich, J. K., Chen, J. K. and Lewis, K. E. (2011). Roles of Hedgehog pathway components and retinoic acid signalling in specifying zebrafish ventral spinal cord neurons. *Development* **138**, 5121-5134.

Feng, Y., Santoriello, C., Mione, M., Hurlstone, A. and Martin, P. (2010). Live imaging of innate immune cell sensing of transformed cells in zebrafish larvae: parallels between tumor initiation and wound inflammation. *PLoS Biol.* **8**, e1000562.

Flanagan-Steet, H., Fox, M. A., Meyer, D. and Sanes, J. R. (2005). Neuromuscular synapses can form in vivo by incorporation of initially aneural postsynaptic specializations. *Development* **132**, 4471-4481.

Goldman, D. (2014). Muller glial cell reprogramming and retina regeneration. *Nat. Rev. Neurosci.* **15**, 431-442.

Goldshmit, Y., Sztal, T. E., Jusuf, P. R., Hall, T. E., Nguyen-Chi, M. and Currie, P. D. (2012). Fgf-dependent glial cell bridges facilitate spinal cord regeneration in zebrafish. *J. Neurosci.* **32**, 7477-7492.

Grandel, H. and Brand, M. (2013). Comparative aspects of adult neural stem cell activity in vertebrates. *Dev. Genes Evol.* **223**, 131-147.

Hall, C. J., Boyle, R. H., Sun, X., Wicker, S. M., Misa, J. P., Krissansen, G. W., Print, C. G., Crosier, K. E. and Crosier, P. S. (2014). Epidermal cells help coordinate leukocyte migration during inflammation through fatty acid-fuelled matrix metalloproteinase production. *Nat. Commun.* **5**, 3880.

Jacob, E., Drexel, M., Schwerte, T. and Pelster, B. (2002). Influence of hypoxia and of hypoxemia on the development of cardiac activity in zebrafish larvae. *Am. J. Physiol. Regul. Integr. Comp. Physiol.* **283**, R911-R917.

Kim, H., Shin, J., Kim, S., Poling, J., Park, H.-C. and Appel, B. (2008). Notch-regulated oligodendrocyte specification from radial glia in the spinal cord of zebrafish embryos. *Dev. Dyn.* **237**, 2081-2089.

Kirby, B. B., Takada, N., Latimer, A. J., Shin, J., Carney, T. J., Kelsh, R. N. and Appel, B. (2006). In vivo time-lapse imaging shows dynamic oligodendrocyte progenitor behavior during zebrafish development. *Nat. Neurosci.* **9**, 1506-1511.

Kucenas, S., Takada, N., Park, H.-C., Woodruff, E., Broadie, K. and Appel, B. (2008). CNS-derived glia ensheath peripheral nerves and mediate motor root development. *Nat. Neurosci.* **11**, 143-151.

Kuscha, V., Barreiro-Iglesias, A., Becker, C. G. and Becker, T. (2012a). Plasticity of tyrosine hydroxylase and serotonergic systems in the regenerating spinal cord of adult zebrafish. *J. Comp. Neurol.* **520**, 933-951.

Kuscha, V., Frazer, S. L., Dias, T. B., Hibi, M., Becker, T. and Becker, C. G. (2012b). Lesion-induced generation of interneuron cell types in specific dorsoventral domains in the spinal cord of adult zebrafish. *J. Comp. Neurol.* **520**, 3604-3616.

Kyritsis, N., Kizil, C., Zocher, S., Kroehne, V., Kaslin, J., Freudenreich, D., Iltzsche, A. and Brand, M. (2012). Acute inflammation initiates the regenerative response in the adult zebrafish brain. *Science* **338**, 1353-1356.

Lam, S. H., Chua, H. L., Gong, Z., Lam, T. J. and Sin, Y. M. (2004). Development and maturation of the immune system in zebrafish, *Danio rerio*: a gene expression profiling, in situ hybridization and immunological study. *Dev. Comp. Immunol.* **28**, 9-28.

McLean, D. L., Fan, J., Higashijima, S., Hale, M. E. and Fetcho, J. R. (2007). A topographic map of recruitment in spinal cord. *Nature* **446**, 71-75.

Park, H.-C., Boyce, J., Shin, J. and Appel, B. (2005). Oligodendrocyte specification in zebrafish requires notch-regulated cyclin-dependent kinase inhibitor function. *J. Neurosci.* **25**, 6836-6844.

Park, H.-C., Shin, J., Roberts, R. K. and Appel, B. (2007). An olig2 reporter gene marks oligodendrocyte precursors in the postembryonic spinal cord of zebrafish. *Dev. Dyn.* **236**, 3402-3407.

Picker, A., Scholpp, S., Bohli, H., Takeda, H. and Brand, M. (2002). A novel positive transcriptional feedback loop in midbrain-hindbrain boundary development is revealed through analysis of the zebrafish pax2.1 promoter in transgenic lines. *Development* **129**, 3227-3239.

Ravanelli, A. M. and Appel, B. (2015). Motor neurons and oligodendrocytes arise from distinct cell lineages by progenitor recruitment. *Genes Dev.* **29**, 2504-2515.

Reimer, M. M., Sörensen, I., Kuscha, V., Frank, R. E., Liu, C., Becker, C. G. and Becker, T. (2008). Motor neuron regeneration in adult zebrafish. *J. Neurosci.* **28**, 8510-8516.

Reimer, M. M., Kuscha, V., Wyatt, C., Sörensen, I., Frank, R. E., Knüwer, M., Becker, T. and Becker, C. G. (2009). Sonic hedgehog is a polarized signal for motor neuron regeneration in adult zebrafish. *J. Neurosci.* **29**, 15073-15082.

Reimer, M. M., Norris, A., Ohnmacht, J., Patani, R., Zhong, Z., Dias, T. B., Kuscha, V., Scott, A. L., Chen, Y.-C., Rozov, S. et al. (2013). Dopamine from the brain promotes spinal motor neuron generation during development and adult regeneration. *Dev. Cell* **25**, 478-491.

Rottbauer, W., Baker, K., Wo, Z. G., Mohideen, M.-A. P. K., Cantiello, H. F. and Fishman, M. C. (2001). Growth and function of the embryonic heart depend upon the cardiac-specific L-type calcium channel alpha1 subunit. *Dev. Cell* **1**, 265-275.

Semmelhack, J. L., Donovan, J. C., Thiele, T. R., Kuehn, E., Laurell, E. and Baier, H. (2014). A dedicated visual pathway for prey detection in larval zebrafish. *Elife* **3**, 17968.

Shin, J., Park, H.-C., Topczewska, J. M., Mawdsley, D. J. and Appel, B. (2003). Neural cell fate analysis in zebrafish using olig2 BAC transgenics. *Methods Cell Sci.* **25**, 7-14.

Shin, J., Poling, J., Park, H.-C. and Appel, B. (2007). Notch signaling regulates neural precursor allocation and binary neuronal fate decisions in zebrafish. *Development* **134**, 1911-1920.

Development (2016) 143, 1464-1474 doi:10.1242/dev.129155

Sirko, S., Behrendt, G., Johansson, P. A., Tripathi, P., Costa, M. R., Bek, S., Heinrich, C., Tiedt, S., Colak, D., Dichgans, M. et al. (2013). Reactive glia in the injured brain acquire stem cell properties in response to sonic hedgehog. [corrected]. *Cell Stem Cell* **12**, 426-439.

Tannenbaum, J. and Bennett, B. T. (2015). Russell and Burch's 3Rs then and now: the need for clarity in definition and purpose. *J. Am. Assoc. Lab. Anim. Sci.* **54**, 120-132.

Than-Trong, E. and Bally-Cuif, L. (2015). Radial glia and neural progenitors in the adult zebrafish central nervous system. *Glia* **63**, 1406-1428.

Westerfield, M. (2000). *The Zebrafish Book: A Guide for The Laboratory Use of Zebrafish (Danio rerio)*, 4th edn. Eugene: University of Oregon Press.

Wu, S., Wu, Y. and Capecchi, M. R. (2006). Motoneurons and oligodendrocytes are sequentially generated from neural stem cells but do not appear to share common lineage-restricted progenitors in vivo. *Development* **133**, 581-590.

Wyart, C., Del Bene, F., Warp, E., Scott, E. K., Trauner, D., Baier, H. and Isacoff, E. Y. (2009). Optogenetic dissection of a behavioural module in the vertebrate spinal cord. *Nature* **461**, 407-410.

Zhang, Y., Bai, X.-T., Zhu, K.-Y., Jin, Y., Deng, M., Le, H.-Y., Fu, Y.-F., Chen, Y., Zhu, J., Look, A. T. et al. (2008). In vivo interstitial migration of primitive macrophages mediated by JNK-matrix metalloproteinase 13 signaling in response to acute injury. *J. Immunol.* **181**, 2155-2164.

nature COMMUNICATIONS

ARTICLE

DOI: 10.1038/s41467-017-00143-0 OPEN

Wnt signaling controls pro-regenerative Collagen XII in functional spinal cord regeneration in zebrafish

Daniel Wehner[1], Themistoklis M. Tsarouchas[1], Andria Michael[1], Christa Haase[2], Gilbert Weidinger[3], Michell M. Reimer[4], Thomas Becker[1] & Catherina G. Becker[1]

The inhibitory extracellular matrix in a spinal lesion site is a major impediment to axonal regeneration in mammals. In contrast, the extracellular matrix in zebrafish allows substantial axon re-growth, leading to recovery of movement. However, little is known about regulation and composition of the growth-promoting extracellular matrix. Here we demonstrate that activity of the Wnt/β-catenin pathway in fibroblast-like cells in the lesion site is pivotal for axon re-growth and functional recovery. Wnt/β-catenin signaling induces expression of *col12a1a/b* and deposition of Collagen XII, which is necessary for axons to actively navigate the non-neural lesion site environment. Overexpression of *col12a1a* rescues the effects of Wnt/β-catenin pathway inhibition and is sufficient to accelerate regeneration. We demonstrate that in a vertebrate of high regenerative capacity, Wnt/β-catenin signaling controls the composition of the lesion site extracellular matrix and we identify Collagen XII as a promoter of axonal regeneration. These findings imply that the Wnt/β-catenin pathway and Collagen XII may be targets for extracellular matrix manipulations in non-regenerating species.

[1] Centre for Neuroregeneration, University of Edinburgh, The Chancellor's Building, 49 Little France Crescent, Edinburgh EH16 4SB, UK. [2] Institute for Immunology, TechnischeUniversität Dresden, Fetscherstraße 74, Dresden 01307, Germany. [3] Institute of Biochemistry and Molecular Biology, Ulm University, Albert-Einstein-Allee 11, Ulm 89081, Germany. [4] Technische Universität Dresden, DFG-Center of Regenerative Therapies Dresden, Cluster of Excellence at the TU Dresden, Fetscherstraße 105, Dresden 01307, Germany. Thomas Becker and Catherina G. Becker contributed equally to this work. Correspondence and requests for materials should be addressed to T.B. (email: Thomas.Becker@ed.ac.uk) or to C.G.B. (email: Catherina.Becker@ed.ac.uk)

After a spinal injury, non-neural cells invade the lesion site and set up a complex extracellular matrix (ECM)[1, 2]. The lesion site ECM consists of a plethora of molecules that may be inhibitory, permissive, or promoting for axon re-growth. In mammals, the balance of ECM molecules is shifted towards an inhibitory matrix that does not allow axons to cross the lesion site, in turn preventing recovery of function[1, 2]. In vertebrates capable of functional spinal cord regeneration, such as fishes and salamanders, the lesion site ECM naturally allows crossing of regenerating axons, offering potential insight into how this ECM is controlled and which ECM molecules may promote regeneration[3–6].

A candidate to control the composition of the lesion site ECM in zebrafish is the Wnt/β-catenin pathway, because Wnt/β-catenin signaling has been shown to control fibroblast biology and ECM deposition[7–10]. Moreover, axonal reconnection, which is necessary for functional recovery in adult[11] and larval zebrafish[12, 13], also depends on Wnt/β-catenin pathway activity in both systems[14, 15]. Wnt/β-catenin signaling involves extracellular Wnt ligand-induced stabilization and translocation of β-catenin into the nucleus where it modifies target gene transcription together with Tcf/Lef family proteins[16]. To understand how Wnt/β-catenin signaling promotes spinal cord regeneration, cell types of action and downstream mechanisms of pathway activation, such as deposition of ECM factors, need to be identified.

Different ECM molecules have specific functions for axon growth and regeneration. For example, among the collagens, *col19a1, col18a1*, and *col15a1b* promote growth of developing motor axons, whereas only *col4a5* is necessary for the correct growth of regenerating motor axons in zebrafish[17–20]. Hence, it is important to identify specific axon re-growth-promoting ECM components in the lesion site.

Adult and larval zebrafish show robust axonal and functional regeneration after complete spinal cord transection[11–13, 21]. Importantly, axon regeneration in larvae is rapid and can be observed in real-time. Lesion-induced paralysis at 3 days-post fertilization (dpf) is followed by recovery of touch-evoked swimming within 2 days post-lesion (dpl)[13]. Swimming capacity is lost upon re-transection[15, 16]. This makes zebrafish larvae a powerful tool to identify mechanisms responsible for establishing a lesion environment that is conducive to axon growth. Moreover, sensitive reporter lines and inducible cell-type specific pathway inhibition using the TetON system can be used to interrogate the Wnt/β-catenin signaling pathway in zebrafish[22–25].

Here, we find that Wnt/β-catenin signaling in fibroblast-like cells accumulating in the lesion site is pivotal for axon re-growth and functional regeneration. A gene expression screen identifies *col12a1a/b* expression and deposition of Collagen XII downstream of Wnt/β-catenin signaling to be required for regeneration. Hence, Wnt/β-catenin signaling in non-neural cells controls the composition of an axon-growth promoting ECM environment in the spinal lesion site in zebrafish.

Results

Axonal bridging correlates with functional recovery. To identify molecular mechanisms regulating the spinal lesion ECM, we first analysed dynamics of axon regeneration in zebrafish larvae. Using anti-acetylated Tubulin immunohistochemistry we observed little to no axonal re-growth within the first 12 h after a spinal lesion. At 12 h post-lesion (hpl) mainly axonal debris, indicated by fragmented anti-acetylated Tubulin immunoreactivity, and only very few and thin re-growing axon fascicles were found in the lesion site (5/20 animals; Supplementary Fig. 1a). We found no animals with a completely bridged lesion site (0/20 animals). Analysis of stills from time-lapse video microscopy imaging at this time point confirmed little axonal re-growth (2/9 animals with axons in the lesion site, 0/9 animals with axonal bridge; Supplementary Movies 1 and 2). After this initial lag phase axons rapidly re-grew (Supplementary Fig. 1a). At 1 dpl, 57% of all larvae showed axonal bridging of the lesion site, as indicated by continuous axonal labelling between rostral and caudal spinal cord ($n = 112$). Bridging further increased to >80% of the animals at 2 dpl ($n = 111$; Fig. 1c). Remarkably, we found that in the 18% of lesioned larvae in which no axonal bridge was established by 2 dpl, functional recovery, as measured by touch-evoked swim distance, was also impaired (analysed in *Xla.Tubb*:DsRED[26] transgenic fish; Supplementary Fig. 1b,c). This underscores the importance of axonal re-growth for functional recovery in larvae.

Axons navigate a non-neural lesion site that is rich in ECM. To determine how axons cross the lesion site, we analysed their relationship with astroglia-like processes, as these have been shown to be supportive for axon regeneration in zebrafish[27, 28]. We imaged axonal and glial processes in time-lapse video microscopy using double transgenic fish for *Xla.Tubb*:DsRED, to visualize neuronal processes, and either *gfap*:GFP[29] ($n = 6$ fish, 33 fasicles) or *her4.3*:EGFP[30] ($n = 3$ fish, 30 fasicles) to label astroglia-like processes. This revealed that the majority of fascicles that entered the lesion site were composed of axons without detectable glial processes (49–53%). Some fascicles contained both glial and axonal processes (20–21%) and some pure glial fascicles were observed (27–30%; Fig. 1a and Supplementary Movies 1 and 2; see Methods section for scoring criteria). To confirm these findings we used a range of combinations of immunohistochemical and transgenic markers for neuronal and glial processes in static images of live animals and histological preparations at 1 dpl. This showed that 63–77% of axon-containing fascicles (≙46–62% of all fascicles analysed) were devoid of detectable glial processes (Fig. 1b). Nineteen to 26% contained both axonal and glial processes and 19–28% of all analysed fascicles were only composed of glial processes. Moreover, double-immunohistochemistry for anti-acetylated Tubulin and anti-GFAP showed that at 1 dpl, only 36% of animals had glial processes bridging the lesion site, in contrast to 57% of the fish with an axonal bridge. At 2 dpl, glial processes had caught up (Fig. 1c). This suggests that axons cross the lesion site more rapidly than glial processes. In summary, these observations support that many axons rapidly extend into the lesion site and cross it independently of detectable glial processes.

To experimentally test a role of astroglia-like processes in supporting axonal regeneration, we ablated the majority of glial cells using *gfap*:Gal4ff;*UAS*:NTR-mCherry transgenic fish that express the enzyme nitroreductase under regulatory sequences of the *gfap* gene[31]. Adding the prodrug Metronidazole (MTZ) at 1 dpf, which is converted by nitroreductase into a cytotoxic compound, almost completely eliminated transgene-expressing glial cells by 3 dpf (Fig. 1d)[31]. A dramatic depletion of astroglia-like processes in the lesion site was confirmed by anti-GFAP immunohistochemistry (Fig. 1e). Remarkably, this treatment did not reduce the proportion of animals with axonal bridge (anti-acetylated Tubulin$^+$; Fig. 1e). This further supports that glial processes do not have a major role in facilitating axonal re-growth across a spinal lesion site. However, we cannot rule out that glial processes that were not detected with our markers and were spared by the ablation still supported axonal regeneration.

To explore possible substrates for the highly dynamic growth cones other than glia, we determined regulation and protein deposition for two major ECM components, *collagen1a2* (*col1a2*) and *fibronectin1a* (*fn1a*). Both genes showed robust upregulation

of expression in the lesion site (Fig. 1f). Using specific antibodies we indeed observed an accumulation of Collagen I (Col I) and Fibronectin proteins in the lesion matrix (Fig. 1g). The Col I and Fibronectin immunoreactivity appeared diffuse, but also formed fibrous structures, often with a longitudinal orientation. Double immunohistochemistry at 1 dpl revealed close apposition of regenerating axonal fascicles (anti-acetylated Tubulin^{+}) with anti-Col I (11 of 13 fascicles associated with Col I immunoreactivity; $n = 7$ fish) or anti-Fibronectin (15 of 22 fascicles associated with Fibronectin immunoreactivity; $n = 6$

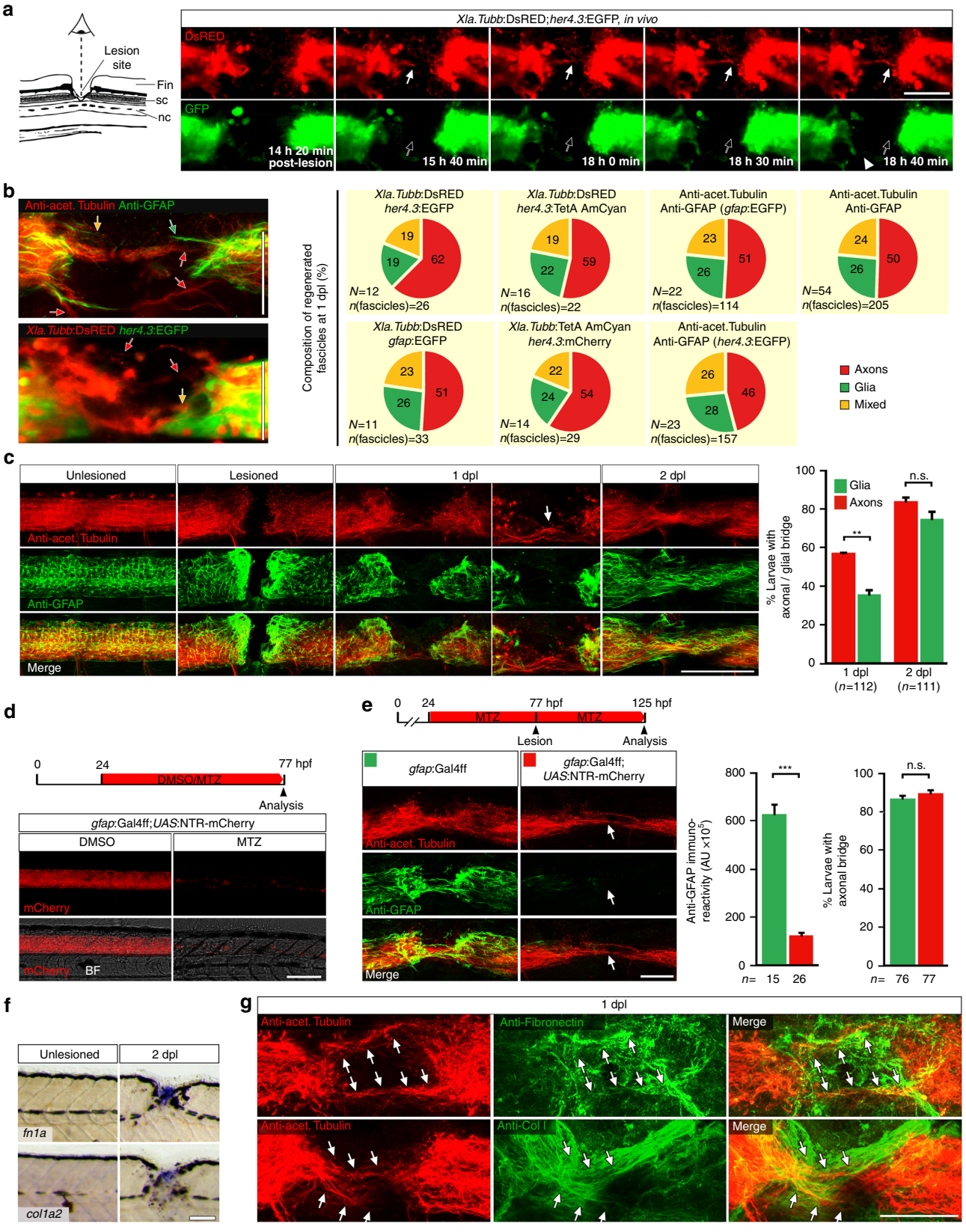

fish) immunoreactive fibres in the lesion site (arrows in Fig. 1g, Supplementary Movies 3 and 4). Hence, regenerating axons navigate the non-neural lesion environment in close association with ECM, suggesting that axon-ECM interactions might be important for axonal re-growth.

Wnt signaling is activated after spinal cord lesion. To determine a potential role of the Wnt/β-catenin pathway in controlling the composition of the spinal lesion ECM, we first characterized the cells in which the pathway was active after lesion. We used in situ hybridisation to detect transcripts of three different transgenic reporter lines of Wnt/β-catenin-dependent transcription, *6xTCF*:dGFP, *Top*:dGFP, *7xTCF*:mCherry[22–24]. We also determined expression levels of direct Wnt/β-catenin target genes *axin2* and *lef1*[32, 33], which are commonly used as read-outs of pathway activation and act as feedback inhibitor (*axin2*) and transcriptional activator (*lef1*) in the pathway, respectively (see Fig. 2a). All probes showed increased labelling in the lesion site at 2 dpl (Fig. 2b; Supplementary Fig. 2a,b). Time course analysis in the highly sensitive *6xTCF*:dGFP Wnt reporter line indicated incipient pathway activity in the lesion site at 0.5 dpl (12 hpl; arrows in Supplementary Fig. 2c), increased activity at 1 dpl, maximal activation at 2 dpl and return to undetectable control levels by 5 dpl after dorsal incision lesion or lateral stab lesion (Fig. 2b, Supplementary Fig. 2d,e). This correlates well with the time course of axonal regeneration. The 6*xTCF*:dGFP reporter also labelled a few additional cells within the spinal cord at 1 and 2 dpl (empty arrows in Fig. 2c). These cells have previously been described as glial cells[14].

6xTCF:dGFP reporter labelling was specific for Wnt/β-catenin pathway activity in our experimental paradigm, as pharmacological inhibition (IWR-1) or heat shock-induced ubiquitous overexpression of the negative regulator *axin1* in *hs*:Axin1[34] transgenic larvae strongly reduced the signal in the lesion site (Supplementary Fig. 2f,g). Importantly, using anti-GFP immunohistochemistry on whole mounts and sections confirmed the strong signal in the lesion site and only sparse labelling in the adjacent spinal cord in *6xTCF*:dGFP transgenic animals (Supplementary Fig. 2h,i). Moreover, our in situ hybridization protocol allowed us to detect *gfp*-expressing glial cells throughout the spinal cord in whole mount preparations of 5 dpf *her4.3*:EGFP transgenic fish (Supplementary Fig. 2j). This shows that lack of labelling in neural tissue was not due to potential probe penetration issues in whole mount preparations. Hence, after spinal cord lesion, Wnt/β-catenin signaling is mainly increased in the non-neural lesion site, which is a major, previously undescribed, domain of Wnt/β-catenin pathway activity.

Wnt signaling is active mainly in fibroblast-like cells. To characterize the Wnt-responding cell types in the non-neural lesion site environment, we utilized *6xTCF*:dGFP transgenic fish. GFP protein and mRNA was mainly detectable at the lesion edge at 1 and 2 dpl (Fig. 2c; Supplementary Fig. 2h). Wnt-responding cells did not co-label with markers of muscle fibres (MyHC/F59[35], $n > 10$; Supplementary Fig. 3a,b) or immune cells (L-Plastin[36], $n > 10$; Supplementary Fig. 3c). In contrast, 31% of GFP-labeled cells (cell counts in immunolabeled sections of individual animals, $n = 10$) were co-labeled with the basal keratinocyte marker p63[37] (arrowheads in Fig. 2d; Supplementary Fig. 3d). The remaining two thirds of the Wnt-responsive cells (*6xTCF*:dGFP$^+$/p63$^-$) were located subepidermally in the lesion site and could thus be fibroblasts. There is no definitive fibroblast marker. However, fibroblasts are known to express the ECM core components *col1a2* and *fn1a* during dermal stroma formation in developing zebrafish[38, 39]. Indeed we found that at 1 dpl and 2 dpl, Wnt-responding subepidermal cells were positive for *col1a2* and *fn1a* transcripts (arrows in Fig. 2e; Supplementary Fig. 3e–g), which were both upregulated in the lesion site (Fig. 1f). Interestingly, in the peripheral lesion area, where the myotome was still intact, a population of *6xTCF*:dGFP$^+$/p63$^-$ cells, continuous with the subepidermal cells in the lesion site, were found sandwiched between basal keratinocytes (p63$^+$) and slow twitch muscle fibres (MyHC/F59$^+$) (insets in Supplementary Fig. 3a,b). Additional *6xTCF*:dGFP$^+$/p63$^-$ cells were found covering the spinal cord (arrows in Supplementary Fig. 3h). These positions correspond to previously described dermal and meningeal fibroblast locations in the developing zebrafish and adult eel[39, 40]. Based on these observations, we tentatively identify the vast majority of Wnt-responding cells as fibroblast-like. Importantly, we found fibroblast-like Wnt-responding cells (*6xTCF*:dGFP$^+$/p63$^-$) in close proximity to regenerating axons (anti-acetylated Tubulin$^+$) in the spinal lesion site at 1 dpl (arrows in Fig. 2f). Hence, the majority of Wnt-responding cells after a lesion are non-neural fibroblast-like cells that are part of the lesion environment through which axons navigate.

Regeneration requires Wnt signaling in non-neural cells. To functionally inhibit Wnt/β-catenin pathway activity selectively in lesion site cells, we took advantage of the TetON system that allows for Doxycycline (DOX)-inducible (Supplementary Fig. 4a), cell type-specific pathway manipulation[41]. To interfere with Wnt/β-catenin signaling, we used *TetRE*:Axin1-YFP transgenic fish, a TetResponder line that has been shown to efficiently inhibit the pathway when activated during zebrafish development or adult tail fin regeneration[25, 41]. To specifically target cells that activate

Fig. 1 Regenerating axons navigate a non-neural lesion environment that is rich in ECM independently of astroglia-like processes. **a** Time-lapse video-microscopy reveals that axonal growth cones (arrow, *Xla.Tubb*:DsRED) extend into the lesion site independently of astroglia-like processes (*her4.3*:EGFP, *empty arrow* points out lack of glial labelling). *Arrowhead* indicates glial process extending into the lesion site. Single frames are shown. Abbreviations: fin, dorsal fin fold; sc, spinal cord; nc, notochord. **b** Quantification of fascicle composition at 1 dpl using different combinations of immunohistochemical and transgenic markers for astroglia-like processes and axons indicates that the majority of fascicles are neuronal with no detectable glial component (46–62% of all fascicles analyzed). In the example scans on the left, *yellow arrows* indicate mixed fascicles, containing neurites and glial processes; *green arrows* indicate pure glial fascicles and *red arrows* indicate pure axonal fascicles. **c** Time course of re-growth of axons (anti-acetylated Tubulin$^+$) and astroglia-like processes (anti-GFAP$^+$) after spinal cord transection. Quantification of labelling continuity between rostral and caudal spinal cord stumps at 1 dpl and 2 dpl suggests faster bridging of the lesion site by neuronal rather than glial processes. *Arrow points* to axonal bridge with very few glial processes in the lesion site at 1 dpl at higher magnification (Fischer's exact test: $^{**}P < 0.01$; n.s. indicates not significant). **d** Treatment of *gfap*:Gal4ff;*UAS*:NTR-mCherry transgenic fish with the pro-drug Metronidozole (MTZ) almost completely ablates transgene-expressing glial cells by 3 dpf. **e** Treatment of *gfap*:Gal4ff;*UAS*:NTR-mCherry transgenic fish with MTZ dramatically reduces anti-GFAP$^+$astroglia-like processes (*t*-test: $^{***}P < 0.001$) but does not reduce the proportion of larvae with axonal bridges at 2 dpl (Fischer's exact test: n.s indicates not significant). **f** *fn1a* and *col1a2* expression is upregulated after lesion, shown by in situ hybridization. **g** Regenerating axons (anti-acetylated Tubulin$^+$; *arrows*) are closely associated with Collagen I and Fibronectin immunoreactivity in a lesion site (confocal depth was limited to spinal cord). Also see Supplementary Movies 3 and 4. **a**–**g** Views are dorsal (**a**; rostral is *left*) or lateral (b-g; dorsal is *up*, rostral is *left*). BF: brightfield. *Scale bars*: 100 μm **a**,**c**–**f** and 50 μm **b**,**g**. *Error bars* indicate s.e.m

the Wnt/β-catenin pathway in the lesion site, we generated a TetActivator line using regulatory elements of the direct Wnt/β-catenin target *lef1* (*lef1*:TetA AmCyan; Supplementary Fig. 4b). Indeed, this strategy showed injury-induced TetActivator expression (*amcyan* mRNA) in Wnt-responding cells in the lesion site in *lef1*:TetA AmCyan;*6xTCF*:dGFP double-transgenic fish (Supplementary Fig. 4c). YFP fluorescence was likewise concentrated in the lesion site in *lef1*:TetA AmCyan;*TetRE*:Axin1-YFP double-transgenic fish after DOX treatment (Fig. 3a,b). This indicates successful selective targeting of Wnt-responding cells in the lesion site. The inhibition was effective, as lesion site expression of *axin2*, an established read-out for Wnt/β-catenin pathway activity[33] (Fig. 2a), was strongly reduced (Supplementary Fig. 4d).

To determine whether functional spinal cord regeneration was impaired in *lef1*:TetA AmCyan; *TetRE*:Axin1-YFP

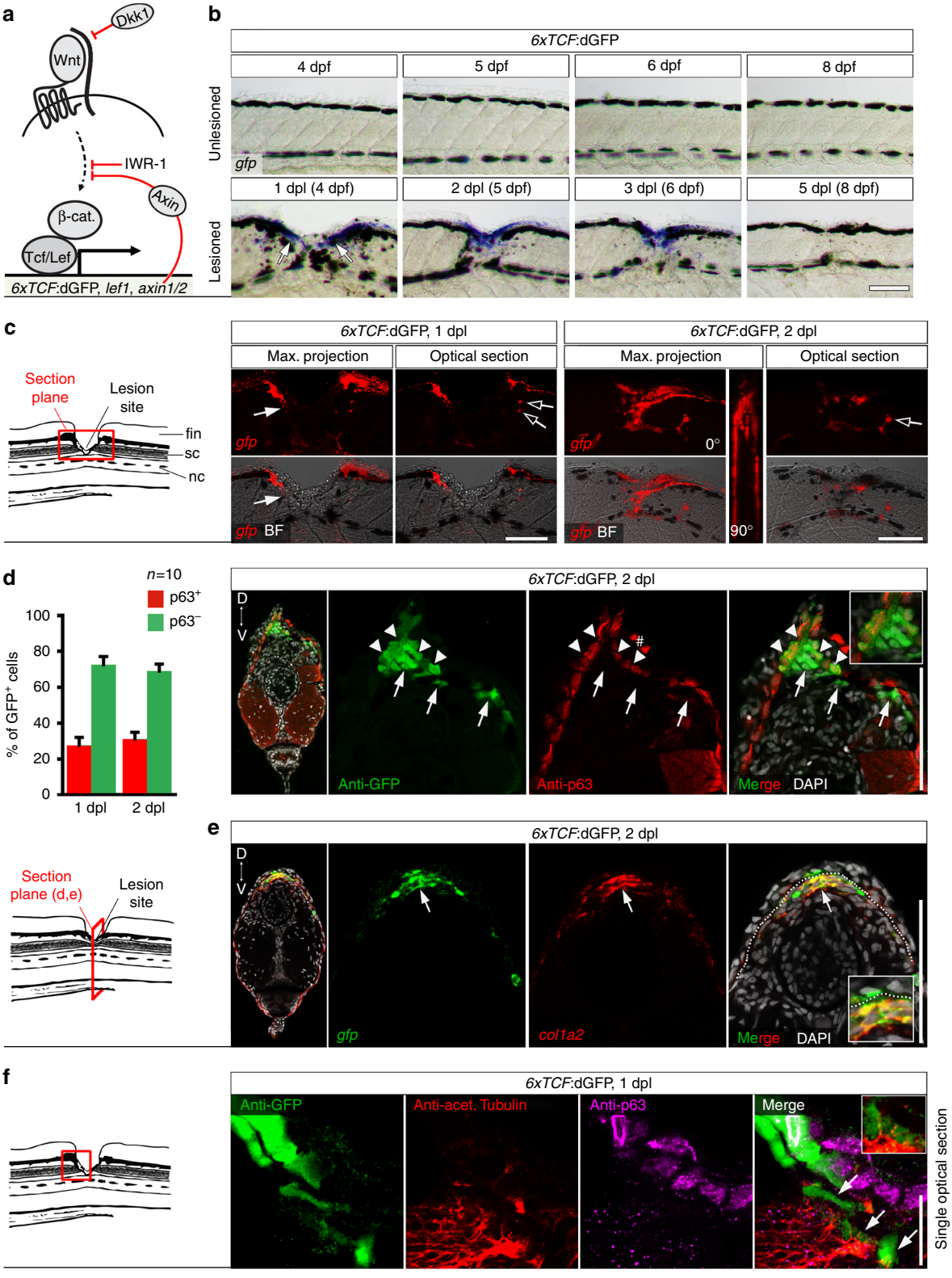

double-transgenic fish after DOX treatment, we scored fish showing continuity of axonal labeling over the lesion site (anti-acetylated Tubulin$^+$) and quantified swim distance after touch at 2 dpl. The proportion of larvae with bridged lesion sites was reduced by 48% (Fig. 3c). Moreover, larvae recovered to swim only less than half the distance (42%) of unlesioned Wnt-inhibited animals, whereas lesioned control larvae recovered to swim the same distance as their unlesioned age-matched controls (Fig. 3d).

Importantly, neuronal (*Xla.Tubb*:TetA AmCyan) and glial (*her4.3*:TetA AmCyan[25])-specific Axin1 induction did not induce a phenotype, whereas ubiquitous expression (*ubi*:TetA AmCyan[25]) recapitulated the axonal and behaviour phenotypes of lesion site-specific manipulations (Fig. 3e–m; Supplementary Fig. 4e). Of note, Axin1 was correctly targeted in all of these lines, as indicated by YFP fluorescence of the Axin1-YFP fusion protein in neurons (*Xla.Tubb*:TetA AmCyan), glia (*her4.3*:TetA AmCyan) or throughout the larvae (*ubi*:TetA AmCyan). Moreover, *axin1* induction in neural cells reached functional levels. This is indicated in the neuronal-driven TetActivator line (*Xla.Tubb*:TetA AmCyan), in which *axin2* expression in the lesion site remained unaffected but was strongly reduced in a constitutively Wnt-responsive domain in the brain (Supplementary Fig. 4f,g). Hence, Wnt/β-catenin pathway activity in neurons or glia is not detectably involved in axonal regeneration. To exclude non-specific effects of the TetON system or Axin1-YFP induction, we also interfered systemically with Wnt/β-catenin signaling using a pharmacological approach (IWR-1) or via heat shock-induced ubiquitous overexpression of the pathway antagonists *axin1* or *dkk1* in *hs*:Axin1 or *hs*:dkk1[42] transgenic fish, respectively. Using *dkk1* overexpression as an additional control was important, as it specifically antagonizes the pathway at the receptor level, whereas *axin1* overexpression and IWR-1 promote degradation of the transcriptional co-activator β-catenin (Fig. 2a; Supplementary Note 1). All of these manipulations robustly reduced the proportion of larvae with an axonal bridge (reduction by 51–72%) and functional recovery ($\leq$ 48% of the swim distance covered by unlesioned Wnt-inhibited animals; Supplementary Fig. 5a–c). Inhibition of Wnt/β-catenin signaling (IWR-1 treatment) starting at different time points post-lesion showed that axon re-growth was still maximally inhibited when the treatment was started at 0.5 dpl (12 hpl), but the effect of IWR-1 was greatly diminished when the treatment was started at 1 dpl and had no effect when it was started at 1.5 dpl (Supplementary Fig. 5d). Hence, Wnt/β-catenin pathway activity is required mainly between 0.5 dpl and 1 dpl for axon regeneration, when axons actively grow across the lesion site.

Two lines of evidence support that effects of Wnt/β-catenin pathway inhibition on axon regeneration were not merely a secondary consequence of potential defects in wound healing. Firstly, a lateral stab lesion, which generates minimal tissue disruption (Supplementary Fig. 2e), showed a similar reduction in axonal regeneration and functional recovery after pharmacological Wnt/β-catenin pathway inhibition, as was observed after dorsal incision lesion (Supplementary Fig. 5e). Second, wound re-epithelialization by basal keratinocytes, providing a protective layer over the lesion site[43], robustly occurred in controls (30/30) and in larvae in which Wnt/β-catenin signaling had been systemically inhibited using IWR-1 (30/30) (visualized in *krtt1c19e*:EGFP transgenic fish[44]; arrow in Supplementary Fig. 6; also see Fig. 4h). We conclude that Wnt/β-catenin signaling in fibroblast-like cells in the lesion site, but not in neural cells, is necessary for functional axon regeneration.

Interestingly, systemic but not glial cell-specific Wnt-inhibition also reduced the number of animals with glial bridges. This suggests that glial crossing of the lesion site also depends on Wnt/β-catenin signaling in a non-cell autonomous way (Supplementary Fig. 7a,b).

Wnt signaling promotes Col XII deposition. We hypothesized that Wnt/β-catenin signaling in lesion site fibroblast-like cells controls ECM deposition, as fibroblasts are a major source of ECM under physiological and pathological conditions. To identify relevant Wnt/β-catenin-controlled ECM components, we compared labelling intensities between control and IWR-1-treated stab-lesioned larvae in an in situ hybridisation screen for two fibronectins and 44 collagen chain-encoding genes at 1 dpl (Fig. 4a; Supplementary Fig. 8a). These genes were chosen, because of roles of these ECM protein classes in axon growth and regeneration[17–20, 45]. In DMSO-treated controls we found expression of both fibronectins and 10 collagens to be locally upregulated in the lesion site compared to adjacent unlesioned trunk tissue. Of these upregulated genes, only expression of *col6a2* and of the paralogs *col12a1a* and *col12a1b* were noticeably reduced when Wnt/β-catenin signaling was inhibited (IWR-1 treatment). We did not find any increased expression of ECM molecules after IWR-1 treatment. We focused our further analysis on *col12a1a* and *col12a1b*, because both paralogs code for the essential α-chain of Collagen XII (Col XII) and are regulated by Wnt/β-catenin signaling. Since functional Col XII molecules assemble as α-chain trimers, Col XII protein expression likely also depends on Wnt/β-catenin signaling, as no other paralogs were found in the genome that could substitute for *col12a1a* and *col12a1b*[46].

First we determined the time course of *col12a1a/b* expression after a lesion. Parallel to the time course of Wnt/β-catenin pathway activation, *col12a1a/b* transcripts were detectable in the lesion site at 0.5 dpl (12 hpl). Further increased expression was detected at 1 dpl, when axons started to regenerate. Expression peaked at 2 dpl and had returned to baseline levels by 5 dpl (Fig. 4b; Supplementary Fig. 8b).

To verify control of *col12a1a/b* expression by Wnt/β-catenin signaling, we quantified fluorescence in situ hybridisation signals for *col12a1a/b* transcripts at 1 dpl after 24 h of IWR-1 treatment. This confirmed transcriptional downregulation of *col12a1a* and

Fig. 2 Wnt/β-catenin signaling is mainly active in fibroblast-like cells after spinal cord lesion. **a** Cartoon showing relevant transcriptional read-outs of Wnt/β-catenin pathway activity, feedback regulatory mechanisms and strategies to interfere with signaling at different levels of the pathway. Abbreviation: β-cat., β-catenin. **b** Detection of *gfp* mRNA in the *6xTCF*:dGFP transgenic reporter line shows transient activity of the Wnt/β-catenin pathway in the lesion site during regeneration. **c** *gfp* expression is largely confined to the lesion edge in *6xTCF*:dGFP transgenic larvae (arrow). A few additional cells are labelled within the presumptive spinal cord region (*empty arrows*). Abbreviations: nc, notochord; sc, spinal cord; fin, dorsal fin fold. **d** The *6xTCF*:dGFP Wnt reporter is mostly active in subepidermal p63$^-$ cells (*arrows*; $\geq$ 69% of all *6xTCF*:dGFP$^+$ cells at 1 dpl and 2 dpl), but also in p63$^+$ basal keratinocytes (*arrowheads*) in the lesion site. # indicates non-specific signal. **e** Consistent with a fibroblast identity, subepidermal cells (below *dashed line*) co-express *col1a2* (*red*) and *gfp* mRNA (*green*) in a lesioned *6xTCF*:dGFP transgenic animal (*arrow*). *Dashed line* indicates junction between basal epithelium and adjacent connective tissue. **f** Fibroblast-like (*6xTCF*:dGFP$^+$/p63$^-$) cells are found in close proximity to regenerating axons (anti-acetylated Tubulin$^+$) in the spinal lesion site at 1 dpl (*arrows*). A single optical section is shown. **a**–**f** Views are lateral (**b**,**c**,**f**; dorsal is *up*, rostral is *left*) or transversal (**d**,**e**; dorsal is *up*) as indicated. BF: brightfield. *Scale bars*: whole mounts, 100 µm **b**,**c** and 25 µm **f**; sections: 100 µm. *Error bars* indicate s.e.m

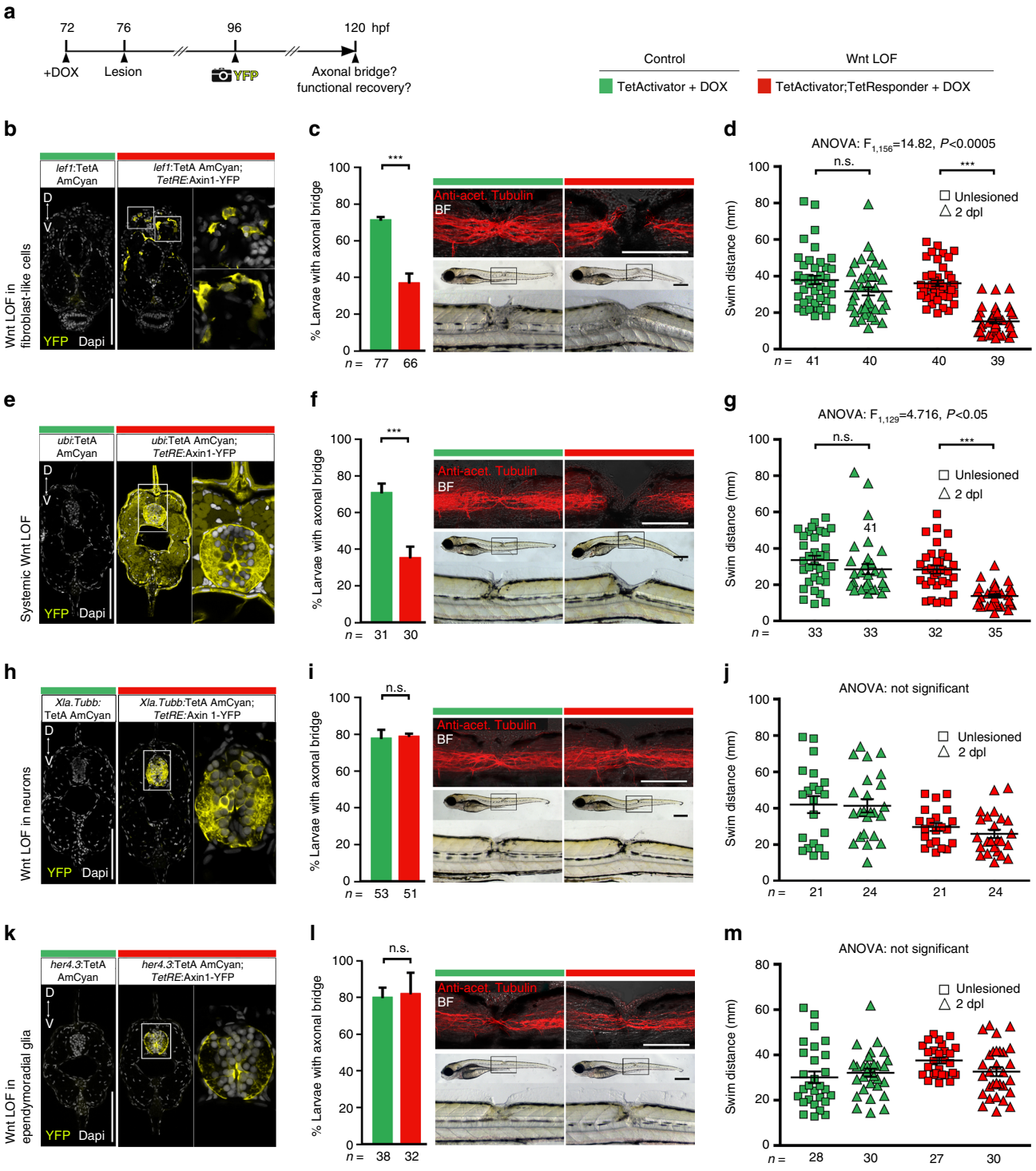

Fig. 3 Wnt/β-catenin signaling in non-neural cells is required for axon regeneration and functional recovery. **a** Schematic timeline of the experimental design using the TetON system. **b**–**d** *axin1* overexpression selectively in cells in the lesion site (**b**; *lef1*$^{+}$) is sufficient to interfere with axon regeneration (**c**; Fischer's exact test: $^{***}P < 0.001$) and functional recovery (**d**; two-way ANOVA: $F_{1,156} = 14.82$, $P < 0.0005$; *t*-test: $^{***}P < 0.001$). **e**–**g** *axin1* overexpression throughout the fish **e** interferes with axon regeneration (**f**; Fischer's exact test: $^{*}P < 0.05$) and functional recovery (**g**; two-way ANOVA: $F_{1,129} = 4.716$, $P < 0.05$; *t*-test: $^{***}P < 0.001$). **h**–**j** Neuronal *axin1* overexpression, indicated by YFP labelling of parenchymal cell bodies and neuropil in the spinal cord **h**, does not interfere with axon regeneration **i** or functional recovery (**j**; two-way ANOVA shows no interaction between lesion and treatment). **k**–**m** *axin1* overexpression in ependymoradial glial cells, indicated by YFP labeling in cell bodies lining the central canal, their radial processes and pial end feet **k** does not interfere with axon regeneration **l** or functional recovery (**m**; two-way ANOVA shows no interaction between lesion and treatment). **b**–**e** Views are transversal (**b**,**e**,**h**,**k**; dorsal is *up*) or lateral (**c**,**f**,**i**,**l**; dorsal is *up*, rostral is *left*). BF: brightfield. n.s.: not significant. *Scale bars*: whole mounts, 200 and 100 µm; sections: 100 µm. *Error bars* indicate s.e.m

col12a1b by 88% and 98% respectively (Fig. 4c). RT-PCR of lesion site-enriched trunk tissue confirmed that IWR-1 treatment interfered with lesion-induced *col12a1a* and *col12a1b* upregulation at 1 dpl, while *col1a1a* expression levels remained unaffected by Wnt/β-catenin pathway inhibition (Supplementary Fig. 8c). Consistent with our finding that Wnt/β-catenin pathway activity is mainly required within the first 24 h after a lesion for axonal re-growth (Supplementary Fig. 5d), IWR-1 treatment for 24 h between 1 dpl and 2 dpl had no effect on *col12a1a/b* expression. (Supplementary Fig. 8d). This indicates that sustained Wnt/β-catenin pathway activity was not needed for *col12a1a/b* transcription.

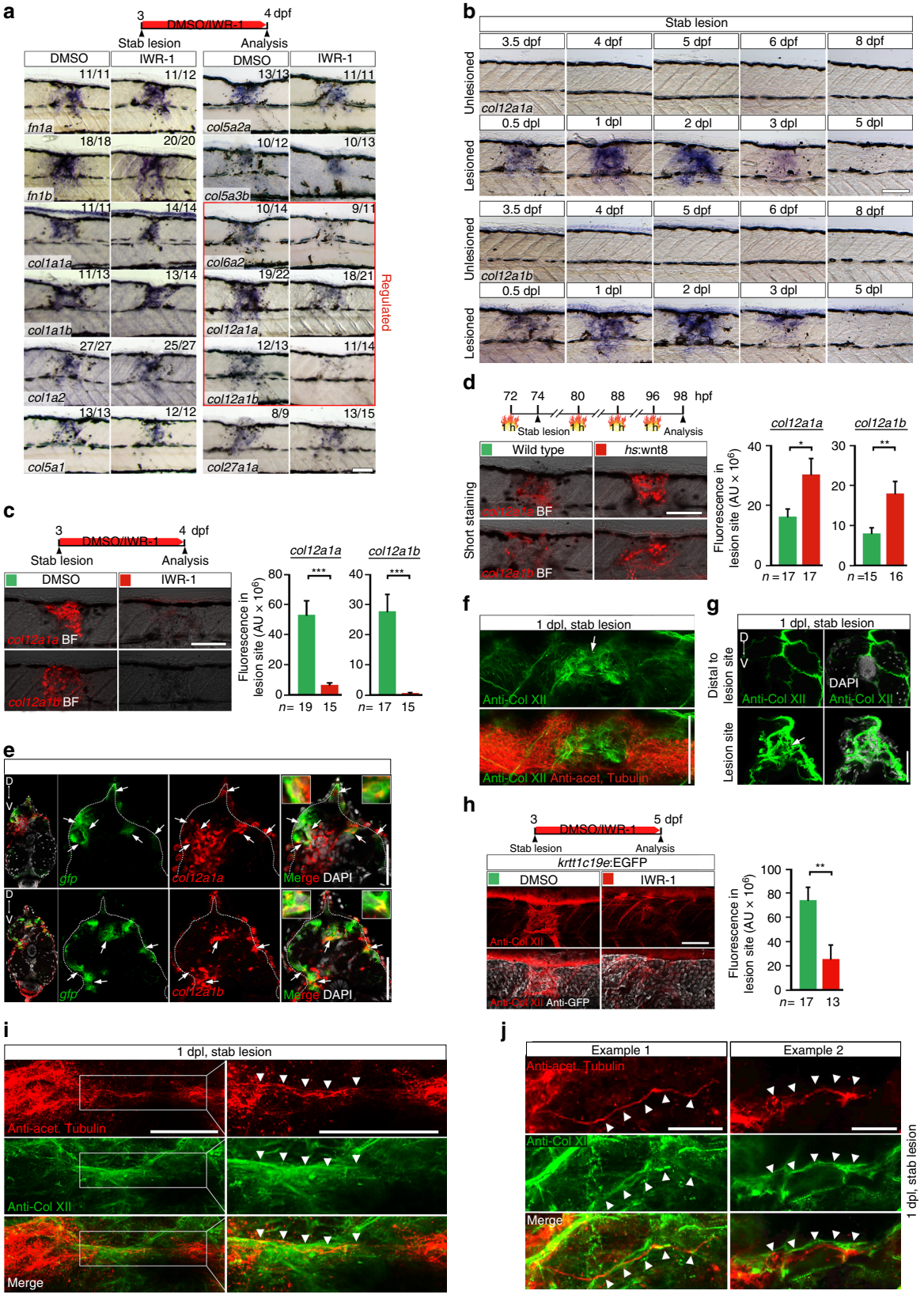

Activation of Wnt/β-catenin signaling through overexpression of *wnt8* for 24 h in *hs*:wnt8 transgenic fish[47] enhanced expression of both *col12a1* genes at 1 dpl specifically in the lesion site (Fig. 4d). Thus, gain- and loss-of-function experiments for Wnt/β-catenin pathway activity support that zebrafish orthologs of the *col12a1* gene are transcriptionally controlled by Wnt/β-catenin signaling in a spinal lesion site in zebrafish larvae during the initial phase of axon regeneration.

To determine whether Wnt/β-catenin signaling regulates *col12a1a/b* transcription in the lesion site likely directly or indirectly, we compared the kinetics of down-regulation of *col12a1a/b* expression after pathway inhibition with that of the direct transcriptional target gene *axin2* at 1 dpl. Short-term inhibition of Wnt/β-catenin pathway activity through *axin1* overexpression in *hs*:Axin1 transgenic fish for 6 h was sufficient to abolish expression of *axin2* while *col12a1a* and *col12a1b* expression was not affected at that early time point (Supplementary Fig. 8e). This indicates delayed and thus indirect control of *col12a1a/b* transcription by Wnt/β-catenin signaling. Taken together, these data support a scenario in which Wnt/β-catenin signaling promotes axonal regeneration by initiating *col12a1a* and *col12a1b* expression after a lesion.

To characterize the *col12a1a* and *col12a1b*-expressing cells in the lesion site, we used multicolour fluorescence in situ hybridization. The majority of *col12a1a* and *col12a1b*-expressing cells co-labeled with *pdgfrb*:GFP[48] reporter transcripts, a marker for pericytes and reactive fibroblasts, at 1 dpl (Supplementary Fig. 8f,g)[49]. Inhibition of Wnt/β-catenin signaling (IWR-1 treatment) did not overtly inhibit appearance of *pdgfrb*:GFP$^+$ cells, indicating that Wnt/β-catenin signaling does not act on potential migration of *col12a1a/b*-expressing cells into the lesion site (Supplementary Fig. 8h). Some of the *col12a1a* and *col12a1b*-expressing cells were also positive for *6xTCF*:dGFP reporter transcripts at 1 dpl (arrows in Fig. 4e). However, a substantial proportion of *col12a1a/b*-expressing cells were not co-labelled with *6xTCF*:dGFP reporter transcripts, indicating that expression of *col12a1a* and *col12a1b* was not exclusive to acutely Wnt-responding cells. Hence, Wnt/β-catenin pathway activity could have already ceased in the majority of *col12a1a* and *col12a1b*-expressing cells at the time point of analysis or Wnt-responding cells could induce additional non-neural cells in the lesion site to express these genes.

We next assessed whether Col XII protein deposition was altered by inhibition of Wnt/β-catenin signaling. We found increased immunoreactivity of Col XII in the lesion site at 1 dpl and 2 dpl in control lesioned larvae compared to adjacent unlesioned trunk tissue or unlesioned control animals (arrows in Figs. 4f,g and Supplementary Fig. 9a). Inhibition of Wnt/β-catenin signaling by IWR-1 treatment or after heat shock-induced overexpression of *dkk1* in *hs*:dkk1 transgenic fish, led to lower Col XII immunoreactivity in lesioned larvae than in DMSO-treated controls (Fig. 4h, Supplementary Fig. 9b). Hence, strongly reduced levels of Col XII matrix are laid down in the lesion site under conditions of Wnt/β-catenin pathway inhibition.

To analyse the relationship of regenerating axons and Col XII, we used double-immunolabelling of axons (anti-acetylated Tubulin$^+$) and Col XII. This showed little to no Col XII deposition in the lesion site at 0.5 dpl (12 hpl) and no axons that had entered the lesion site at this time point (asterisk in Supplementary Fig. 9c). In contrast, at 1 dpl we detected prominent anti-Col XII immunoreactivity (Supplementary Fig. 9c) and regenerating axons were present in the lesion site in close proximity to Col XII immunoreactivity (*arrowheads* in Fig. 4i, Supplementary Movie 5). The trajectory of axonal fascicles frequently appeared to follow longitudinal fibres of Col XII immunoreactive ECM material (arrowheads in Fig. 4j). We found 31 axonal fascicles of 45 in close apposition with Col XII positive fibres at 1 dpl ($n = 14$ fish). Thus, Col XII deposition correlates well with axonal re-growth in larvae.

In adult zebrafish, lesion site-specific expression of *col12a1a* as well as Col XII deposition was also observed at 7 dpl and 14 dpl (Supplementary Fig. 10a,b). At 14 dpl, anti-acetylated Tubulin$^+$ spinal axons entered the lesion site in close contact with Col XII immunoreactivity, resembling the larval pattern (Supplementary Fig. 10b). Thus, after spinal cord injury, deposition of Col XII matrix in the lesion site is conserved across developmental stages in zebrafish. Taken together, this supports a scenario in which Wnt/β-catenin signaling is necessary for the correct expression and deposition of Col XII in the spinal lesion site, which in turn promotes axon regeneration.

Col XII promotes functional spinal cord regeneration. To determine whether Col XII deposition is required for functional axonal regeneration, we co-injected Vivo-Morpholinos (MO), which act as cell-permeable translation blocking anti-sense molecules for *col12a1a* and *col12a1b*, into the circulation for efficient distribution in 3 dpf larvae (Supplementary Fig. 11a[50]). This approach effectively reduced Col XII immunoreactivity in the lesion site compared to control MO-injected larvae (Fig. 5a,b). In contrast, immunoreactivity for Fibronectin and Collagen I was unaffected (Supplementary Fig. 11b), indicating specificity of the manipulation for *col12a1a/b* expression.

The proportion of larvae with an axonal bridge (determined in *Xla.Tubb*:DsRED transgenic animals) was reduced by 43% in *col12a1a/b* morphants compared to control MO-injected larvae at 2 dpl (Fig. 5c). In lesioned *col12a1a/b* morphants swimming

Fig. 4 Wnt/β-catenin signaling controls *col12a1a/b* transcription and Col XII deposition in a spinal lesion site. **a** Wnt/β-catenin pathway inhibition (IWR-1) results in lower expression of select collagen genes (*red box*) in the lesion site at 1 dpl, determined by in situ hybridization. **b** *col12a1a* and *col12a1b* expression is transiently upregulated in the lesion site during regeneration. **c** Inhibition of Wnt/β-catenin signaling (IWR-1) interferes with *col12a1a/b* expression in the lesion site (*t*-test: $^{***}P < 0.001$). **d** *wnt8* overexpression upregulates *col12a1a/b* expression in the lesion site in *hs*:wnt8 transgenic fish (*t*-test: $^{*}P < 0.05$, $^{**}P < 0.01$). Signal was underdeveloped to optimize detection of differences in signal strength. **e** A subpopulation of *col12a1a* or *col12a1b*-expressing cells (*red*) in the lesion site co-labels with transcripts of the *6xTCF*:dGFP Wnt reporter (*green, arrows*). **f**,**g** Anti-Col XII immunoreactivity is increased in the lesion site (*arrows*) compared to adjacent unlesioned trunk tissue at 1 dpl. Shown is a confocal image of a whole mount (**f**, confocal depth was limited to spinal cord) and a transversal section though the lesion site **g**,**h** Inhibition of Wnt/β-catenin signaling (IWR-1) interferes with Col XII deposition in the lesion site (*t*-test: $^{**}P < 0.01$). Note continuity of tissue in IWR-1-treated animals as shown by re-epithelialization of the lesion site by basal keratinocytes in *krtt1c19e*:EGFP transgenic fish. **i**,**j** Double immunolabelling of axons (anti-acetylated Tubulin$^+$) and Col XII shows Col XII matrix deposition in the lesion site through which regenerating axons grow **i**. Shown is a maximum intensity projection in **i** with *inset* higher magnification; the confocal depth was limited to spinal cord. *Arrowheads* point to regenerating axonal fascicle in close apposition to Col XII immunoreactivity (also see Supplementary Movie 5). Note, that the trajectory of axonal fascicles appear to follow longitudinal fibres of Col XII immunoreactive ECM material in the lesion site (**j**, *arrowheads*). **a**–**j** Views are lateral (**a**–**d**,**f**,**h**–**j**; dorsal is *up*, rostral is *left*) or transversal (**e**,**g**; dorsal is *up*). BF: brightfield. *Scale bars*: 100 µm **a**–**d**,**f**,**h**, 50 µm **e**,**g**,**i**, 25 µm **j**. *Error bars* indicate s.e.m

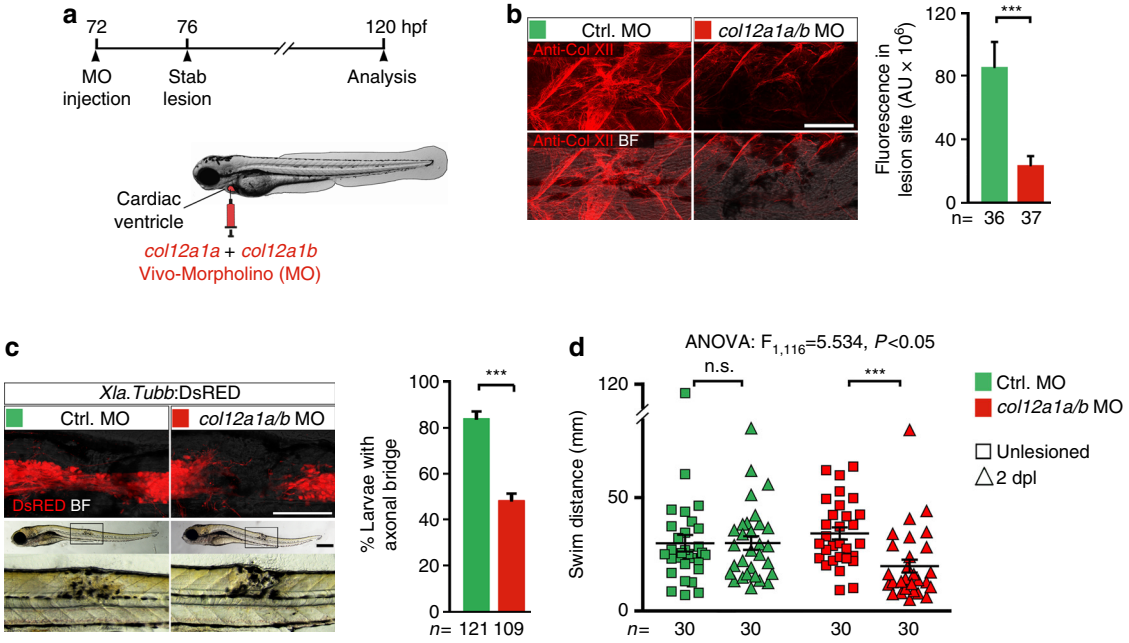

Fig. 5 Knockdown of *col12a1a/b* inhibits functional axon regeneration. **a** Cartoon showing strategy used for systemic delivery of Vivo-Morpholino (MO), which acts as cell-permeable translation blocking anti-sense molecules. MOs against *col12a1a* and *col12a1b* were co-injected into the cardiac ventricle at 3 dpf, 4 h before lesion. **b** *col12a1a/b* MO injection strongly reduces Col XII immunoreactivity in the lesion site compared to control MO injected animals. (*t*-test: ***$P < 0.001$). **c** *col12a1a/b* MO injection inhibits axon regeneration after lesion (Fischer's exact test: ***$P < 0.001$). **d** *col12a1a/b* MO injection interferes with functional recovery after lesion (two-way ANOVA: $F_{1,116} = 5.534$, $p < 0.05$; *t*-test: ***$P < 0.001$). **a**–**d** Lateral views are shown (dorsal is *up*, rostral is *left*). BF: brightfield. n.s.: not significant. *Scale bars*: 200 µm **c** and 100 µm (**b**,**c**). *Error bars* indicate s.e.m

distance was reduced by 58% compared to unlesioned *col12a1a/b* MO-injected larvae (Fig. 5d). Importantly, Vivo-Morpholino treatment was not toxic, since lesioned control MO-injected larvae recovered to the same swimming capacity as unlesioned age-matched control MO-injected larvae at 2 dpl, and *col12a1a/b* MO treatment did not impair swimming in unlesioned animals. Impaired functional regeneration after MO knockdown supports that Col XII is part of the axon-growth promoting ECM in the lesion site.

To independently confirm the function of *col12a1a/b*, we used transient CRISPR/Cas9-mediated gene editing. Injection of small guide-RNA (gRNA) and *cas9* mRNA into the zygote efficiently generates biallelic mutations of targeted genes in a very high proportion of cells, leading to loss-of-function phenotypes[51]. Indeed, targeting of *col12a1a* and *coll12a1b* efficiently disrupted both genes in CRISPR-injected embryos, as shown by loss of targeted endonuclease restriction sites (Fig. 6a, b). Quantitative RT-PCR indicated reduced abundance of transcripts at 1 dpf, likely caused by non-sense mediated RNA decay in CRISPR-manipulated larvae (hereafter referred to as Crispants; Fig. 6c). Similarly, after a spinal lesion in Crispants the abundance of both *col12a1a* and *col12a1b* mRNAs in the lesion site was also reduced, as determined by quantification of fluorescence in situ hybridisation signals (Fig. 6d). Targeting of only *col12a1a* or *col12a1b* did not affect axonal regeneration, possibly due to compensation of the non-targeted paralog (Supplementary Fig. 12a). In contrast, in Crispants in which both *col12a1* genes were targeted, the proportion of larvae with axonal continuity (anti-acetylated Tubulin^{+}) between spinal cord ends was reduced by 31% compared to controls (Fig. 6e). Single larvae analysis showed that lack of axonal bridging in *col12a1a* and *col12a1b*-targeted animals (analysed in *Xla.Tubb*:DsRED transgenic fish) correlated with high gene editing efficiency of both *col12a1* paralogs, supporting specificity of the CRISPR/Cas9 manipulation (Supplementary Fig. 12b). Hence, both MO knockdown and CRISPR manipulation indicate an important contribution of Col XII to functional spinal cord regeneration in zebrafish.

To determine the relevance of Col XII as a downstream effector of Wnt/β-catenin signaling, we asked whether experimentally increasing expression of *col12a1a* was sufficient to rescue the regeneration phenotype induced by inhibition of the Wnt/β-catenin pathway. To this end, we created zebrafish that are transgenic for heat shock-inducible expression of full-length *col12a1a* (*hs*:col12a1a-p2a-Cerulean, short *hs*:col12a1a; Supplementary Fig. 13a). Activation of the transgene in unlesioned animals increased anti-Col XII immunoreactivity in developmental Col XII domains but also in ectopic sites, including the spinal cord (arrow in Supplementary Fig. 13b). To increase Col XII deposition in the lesion site, we applied repetitive heat shocks to *hs*:col12a1a transgenic animals until immediately before the lesion (3 dpf). This treatment increased detectability of transgene mRNA for at least 24 h after the last heat shock (Fig. 7a) and was sufficient to increase Col XII immunoreactivity in the lesion site of larvae in which the Wnt/β-catenin pathway was inhibited (IWR-1 treatment; analyzed at 2 dpl; arrow in Fig. 7b). We found that under these experimental conditions, *col12a1a* overexpression more than doubled the proportion of IWR-1-treated larvae with axonal bridge to 77% of all lesioned larvae, compared to 32% in only IWR-1-treated lesioned larvae (determined in *Xla.Tubb*:DsRED transgenic animals; Fig. 7c). This represents a rescue of the axonal bridging phenotype to near wild type levels (compare Supplementary Fig. 1b). *col12a1a* overexpression also improved functional recovery in IWR-1-treated larvae (+ 55% of the swim distance covered by Wnt/β-catenin pathway-inhibited lesioned animals; Fig. 7d). This identifies Col XII as a major downstream effector of Wnt/β-catenin signaling in the regenerating zebrafish spinal cord.

We next asked whether *col12a1a* overexpression is sufficient to augment axon regeneration. To this end, we assessed

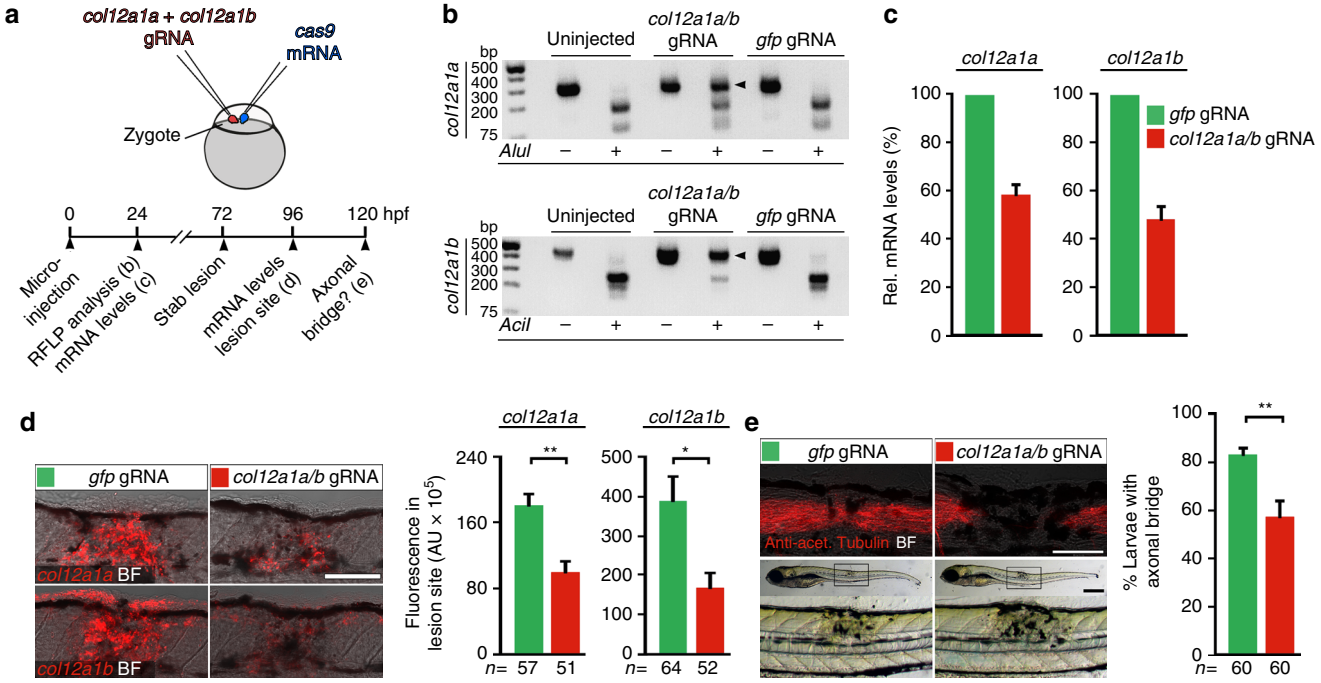

Fig. 6 CRISPR/Cas9-mediated disruption of *col12a1a/b* leads to depletion of mRNA and impaired axonal regeneration. **a** Cartoon showing strategy used for CRISPR/Cas9-mediated *col12a1a/b* gene disruption. *cas9* mRNA and small guide-RNA (gRNA) targeting *col12a1a* and *col12a1b* were co-injected into the zygote. Crispants were analysed for *col12a1a/b* mRNA levels and axonal regeneration as indicated in the timeline. **b** Restriction fragment length polymorphisms (RFLP) analysis reveals efficient somatic mutation in the gRNA target site (indicated by resistance to restriction endonuclease digest; arrowheads) in both *col12a1* paralogs after microinjection. **c** *col12a1a/b* Crispants exhibit reduced developmental *col12a1a* and *col12a1b* mRNA expression, determined by quantitative RT-PCR. Representative plot from three independent experiments for each mRNA are shown. mRNA levels in *gfp* gRNA-injected control animals were set to 100%. **d** *col12a1a/b* Crispants exhibit reduced *col12a1a* and *col12a1b* mRNA levels after lesion, determined by quantification of fluorescent in situ hybridization signal in the lesion site (*t*-test: $^{**}P < 0.01$, $^{*}P < 0.05$). **e** *col12a1a/b* Crispants show reduced axonal bridging events after lesion (*t*-test: $^{**}P < 0.01$). **a**–**e** Views are lateral (dorsal is *up*, rostral is *left*). BF: brightfield. *Scale bars*: 200 µm **e** and 100 µm **d**,**e**. *Error bars* indicate s.e.m

axonal bridging in *hs*:col12a1a transgenic animals and their wild type control siblings at 18 hpl (Fig. 7e). At this early time point, 41% of lesioned control larvae showed axonal continuity (anti-acetylated Tubulin^{+}) between spinal cord ends. Remarkably, *col12a1a* overexpression increased the proportion of larvae with axonal bridge to 63%. Thus, Col XII is sufficient to enhance axon regeneration after a spinal lesion in zebrafish. Taken together, these findings determine Col XII as major pro-regenerative, Wnt/β-catenin-controlled ECM factor in the spinal lesion site.

Discussion

Here, we demonstrate an important role for Wnt/β-catenin signaling in controlling the composition of the spinal lesion ECM, which is essential for functional axon regeneration in zebrafish. Our data support a model (Fig. 8) in which spinal cord transection triggers upregulation of Wnt/β-catenin signaling in non-neural cells. The vast majority of these are fibroblast-like cells accumulating in the lesion site. Wnt/β-catenin signaling regulates *col12a1* transcription and deposition of Col XII by fibroblast-like cells in the spinal lesion ECM. The presence of Col XII in the ECM promotes axon growth across the lesion site and functional recovery.

How does Col XII support axonal regeneration? Col XII is abundant in the spinal lesion site in species of high regenerative capacity, such as in larval and adult zebrafish (this report) and salamanders[6]. Col XII is a member of the FACITs family of collagens, which do not form supramolecular aggregates but are associated with Collagen fibrils[46, 52]. Previously, Col XII was found to interact with Col I fibrils[52]. However, we find that Col I immunoreactivity remained grossly unchanged after interfering with *col12a1a/b* translation. Col XII also interacts with Col VI in forming matrix bridges between developing osteoblasts[53]. Interestingly, we find in our expression screen that *col6a2*, coding for a Col VI α-chain, is co-regulated with *col12a1a/b* by Wnt/β-catenin signaling, which may be related to functional interactions of the proteins. In addition, Col XII binds a variety of other matrix proteins, such as Tenascin-X, Decorin, and Fibromodulin[54, 55]. Hence, Col XII could promote growth of axons indirectly by organising the lesion site ECM. Another possibility is that Col XII could directly interact with axons via specific receptors. This is supported by our observation that overexpression of *col12a1a* alone is sufficient to enhance axonal regeneration. While specific axonal receptors for Col XII have not been identified, potential direct Col XII-axon interactions could be mediated by its integrin-binding site, the NC1 domain, as reported for Col IV[46, 56, 57]. Future studies will need to clarify the precise mechanism by which Col XII promotes axonal re-growth.

While our results identify Col XII as critical factor for axon regeneration, several additional ECM molecules likely contribute to establishing the growth promoting lesion site environment found in zebrafish. For example, Tenascin-C has been shown to be important for spinal cord regeneration in zebrafish, but possible interactions with Col XII are not known[5]. Furthermore, Col I and Fibronectin, which we find to be abundantly present in the lesion site, are also known ECM components that promote axons growth[45, 58, 59].

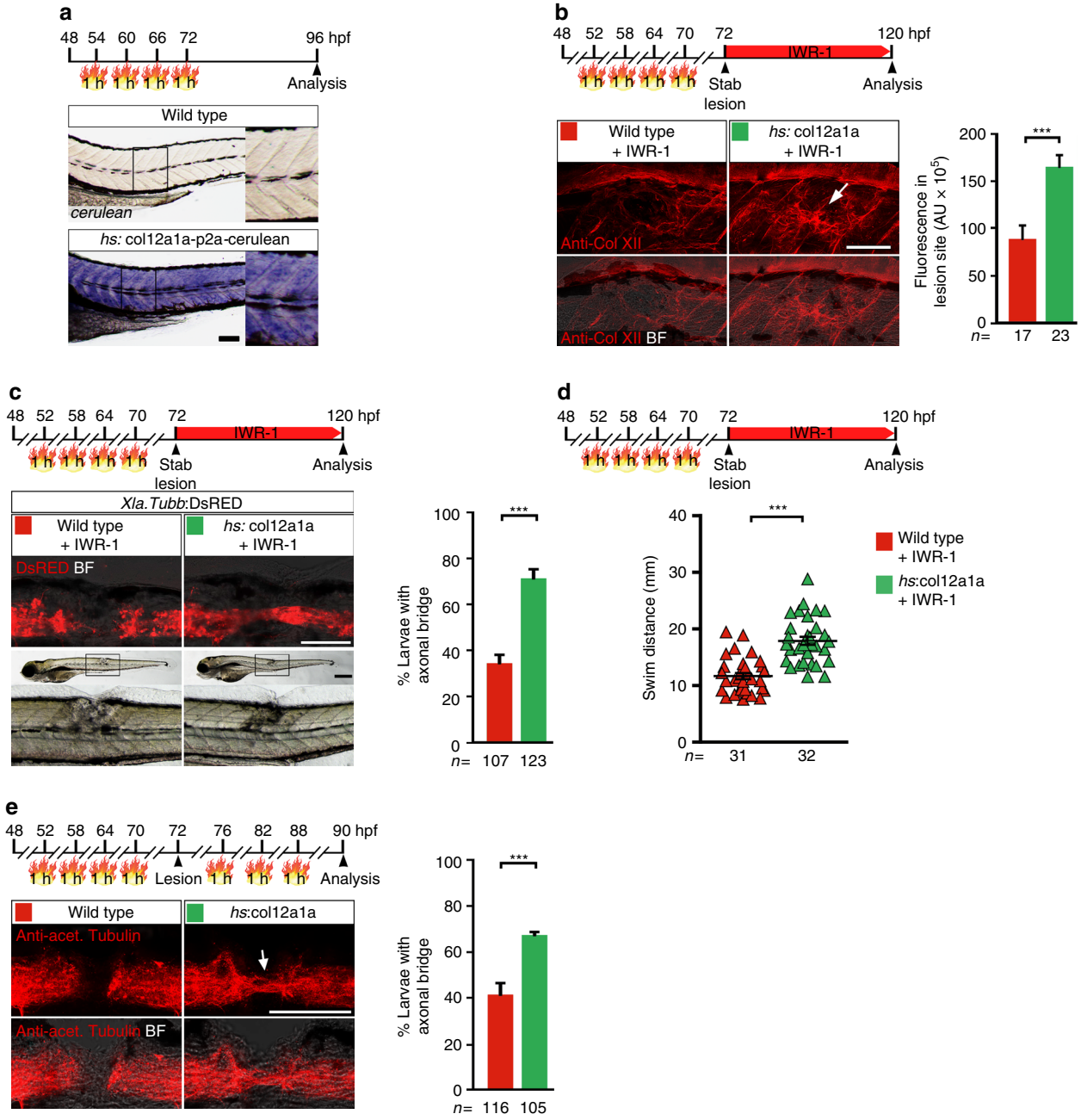

Fig. 7 Overexpression of *col12a1a* promotes axon regeneration in Wnt/β-catenin pathway-inhibited and wild type zebrafish larvae. **a** *cerulean* mRNA is robustly detectable 24 h after the last heat shock in *hs*:col12a1a-p2a-Cerulean transgenic larvae. **b** *col12a1a* overexpression increases anti-Col XII immunoreactivity in the lesion site of Wnt/β-pathway-inhibited (IWR-1 treatment) *hs*:col12a1a transgenic larvae (*arrow*; *t*-test: ***$P < 0.001$). **c** *col12a1a* overexpression rescues axon regeneration in Wnt/β-catenin pathway-inhibited (IWR-1 treatment) *hs*:col12a1a transgenic larvae (Fischer's exact test: ***$P < 0.001$). **d** *col12a1a* overexpression improves functional recovery in Wnt/β-catenin pathway-inhibited (IWR-1 treatment) *hs*:col12a1a transgenic larvae (*t*-test: ***$P < 0.001$). **e** *col12a1a* overexpression is sufficient to augment axon regeneration (Fischer's exact test: *** $P< 0.001$). **a**–**e** Views are lateral (dorsal is *up*, rostral is *left*). BF: brightfield. *Scale bars*: 200 µm **c** and 100 µm **a**–**c**, **e**. *Error bars* indicate s.e.m

How does Wnt/β-catenin signaling act on *col12a1a/b* expression? Wnt-responding cells co-express *col12a1a/b*. Hence, Wnt/β-catenin pathway activity likely acts in the same cells to increase expression of *col12a1a/b* after a lesion. Regulation of Collagens in fibroblasts by Wnt/β-catenin signaling has also been observed in dermal fibroblasts or myofibroblasts in the context of fibrosis[8–10, 60]. However, a sizable population of fibroblast-like cells showed Wnt-dependent *col12a1a/b* upregulation without having detectable Wnt/β-catenin pathway activity. Our results show that the effect of Wnt/β-catenin pathway inhibition on *col12a1a/b* expression is delayed and therefore likely indirect and that Wnt/β-catenin signaling does not need to be sustained for *col12a1a/b* expression and successful regeneration. These observations are consistent with the possibility that Wnt/β-catenin signaling is only transiently active in *col12a1a/b*-expressing cells. Alternatively, secondary signals from Wnt-responding cells could instruct transcriptional regulation of *col12a1a/b* in non-Wnt-responsive cells.

Are astroglia-like cell bridges a necessary substrate for axonal regeneration across a spinal lesion site? Regenerating axons could

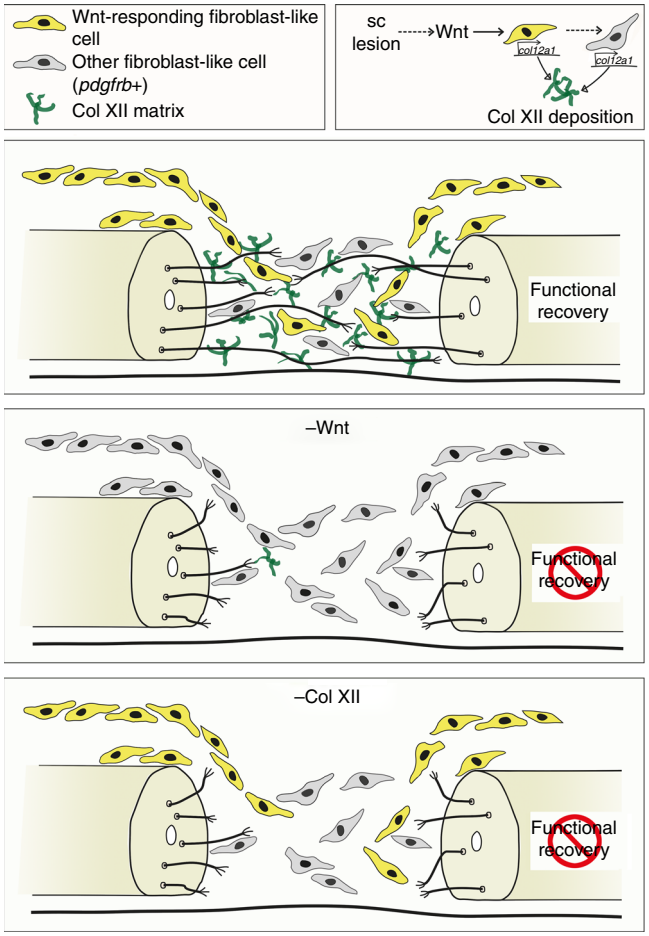

Fig. 8 Model for Wnt/β-catenin function during axonal regeneration in the zebrafish spinal cord. Spinal cord (sc) lesion triggers Wnt/β-catenin pathway activation in fibroblast-like cells. Wnt/β-catenin signaling controls *col12a1a/b* transcription and deposition of Col XII in the lesion site ECM, through which axons regenerate to facilitate functional recovery. Interference with Wnt/β-catenin signaling in fibroblast-like cells or Col XII deposition prevents axon regeneration and functional recovery

directly interact with the lesion site ECM or simply follow glial processes that bridge the lesion site. In histological preparations this is difficult to assess, as axons and glial processes tend to fasciculate[27]. Indeed, at 2 dpl almost all tissue bridges were composed of neuronal and glial processes. However, simultaneous time-lapse video microscopy imaging of axonal and glial processes indicated that the majority of axons highly dynamically enter and cross the lesion site independently of glial processes. Moreover, our data show that re-establishment of axonal continuity of the transected spinal cord precedes that of glial continuity, similar to observations in the lesioned spinal cord of the adult eel[61]. Finally, in contrast to reducing the amount of Col XII protein in the lesion site, massive depletion of glial processes did not reduce the proportion of animals that showed axonal continuity after regeneration. While these observations support the relative importance of the ECM compared to that of glial substrates for axonal regeneration, we cannot exclude that fine glial processes that escaped detection and ablation still served as a substrate for axon re-growth. Moreover, glial processes are likely to support regeneration by physically aligning with regenerating fascicles[27] and producing essential growth-factors[28], which may be more important in a larger lesion site of adult zebrafish.

Is larval regeneration comparable to adult spinal cord regeneration? In both larvae and adult zebrafish, functional regeneration after complete spinal cord transection depends on axons successfully crossing a non-neural lesion site (this report and refs. 11, 13, 28) and forming connections[11, 12]. Both show lesion-specific upregulation of *col12a1a* and axons regenerate in close proximity to Col XII in larval and adult zebrafish (this report). At least some axons grow independently of glia at both developmental stages (this report and ref. 27) and, crucially both larval and adult regeneration depend on Wnt/β-catenin signaling (this report and refs. 14, 15). This suggests that key aspects of regeneration are conserved across developmental stages. However, regeneration times in adults are much longer than in larvae[62], such that timing of signaling processes may differ in adults.

In conclusion, Col XII deposition, controlled by Wnt-responsive fibroblasts, promotes spinal cord regeneration in zebrafish. Interestingly, transplanting Wnt3a-secreting fibroblasts into a spinal lesion site in rats enhances functional recovery[63]. Thus, elucidating the molecular cues that promote axon regeneration in zebrafish could provide strategies in mammals to modulate the composition of the lesion site to tip the balance towards a growth-conducive ECM environment.

Methods

Animals. All fish were kept and bred in our laboratory fish facility according to standard procedures[64], and all experiments have been approved by the British Home Office (project license no.: 70/8805). Details of the transgenic zebrafish lines used can be found in Supplementary Note 1. We used the WIK wild type strain of zebrafish and the following transgenic zebrafish lines: *6xTCF/Lef-miniP*:2dGFP (*6xTCF*:dGFP[24]); *7xTCF-Xla.Siam*:nlsmCherry^{la5} (*7xTCF*:mCherry[23]); *gfap*:Gal4ff^{s995};*UAS-E1b*:Eco.NfsB-mCherry^{c264} (*gfap*:Gal4ff^{s995};*UAS*:NTR-mCherry[31]);*gfap*:GFP^{mi200129}, *her4.3*:EGFP^{y83} (formerly known as *her4.1*:EGFP[30]); *her4.3*:irtTAM2(3F)-p2a-AmCyan^{ulm6} (*her4.3*:TetA AmCyan[25]); *her4.1*:Tet-GBD-p2A-mCherry^{tud6} (*her4.3*:mCherry[41]); *hsp70l*:dkk1-GFP^{w32} (*hs*:dkk1[42]); *hsp70l*:Mmu.Axin1-YFP^{w35} (*hs*:Axin1[34]); *hspl70l*:wnt8a-GFP^{w34}(*hs*:wnt8[47]); *krtt1c19e*:EGFP^{sq1744}, *pdgfrb*:Gal4ff^{mcv24};*UAS*:GFP (*pdgfrb*:GFP[48]) *TetRE*:Mmu.Axin1-YFP^{tud1} (*TetRE*:Axin1-YFP[41]); *Top*:dGFP^{w2522}; *ubiquitin*:irtTAM2(3F)-p2a-AmCyan^{ulm2}(*ubi*:TetA AmCyan[25]);*Xla.Tubb*:DsRED^{zf14826}. The *lef1*:irtTAM2(3F)-p2a-AmCyan^{ulm11} (*lef1*:TetA AmCyan), *Xla.Tubb*:irtTAM2(3F)-p2a-AmCyan^{ue103} (*Xla.Tubb*:TetA AmCyan) and *hsp70l*:col12a1a-p2a-Cerulen^{ue104} (*hsp70l*:col12a1a) transgenic zebrafish lines were established by Tol2-mediated transgenesis[65] using the DNA constructs described below.

DNA constructs. The *lef1*:irtTAM2(3F)-p2A-AmCyan construct was generated by replacing the translation start codon of *lef1* in the BAC clone CH73-164H6 with the previously described irtTAM2(3F)-p2A-AmCyan TetActivator cassette[41, 66] using standard BAC recombination techniques[67]. Additionally, Tol2 inverted repeats were introduced into the BAC backbone. The final BAC was purified using the HiPure Midiprep kit (Invitrogen). The *Xla.Tubb*:irTAM2(3F)-p2A-AmCyan construct was generated by cloning the previously described sequence of the *Xenopus laevis* neural-specific beta tubulin regulatory element (*Xla.Tubb2b)* upstream of the published doxycycline (DOX)-inducible transcriptional activator [irtTAM2(3F)] tagged with p2a and AmCyan[26, 41, 66]. For generation of the *hsp70l*:col12a1a-p2a-Cerulean construct, 3 overlapping fragments spanning the full-length *col12a1a* CDS were amplified from 1 dpl cDNA (primer sequences are given in Supplementary Table 1) and fused via internal restriction sites (BsiWI, BsrGI). The complete *col12a1a* CDS was then subcloned into the *hsp70l*:irtTAM-p2a-Cerulean construct[41] thereby replacing the irtTAM TetActivator CDS.

Reverse transcriptase PCR and quantitative RT-PCR. To assess the effect of IWR-1 treatment on lesion-induced gene expression total RNA from lesion site-enriched trunk tissue was extracted using Trizol (Invitrogen). Twenty larvae were pooled for each experimental condition. To assess the effect of *col12a1a/b* gRNA/*cas9* mRNA microinjection on developmental *col12a1a/b* mRNA levels total RNA from ten 24 hpf embryos was extracted using Trizol. Reverse transcription of 500 ng RNA was performed with the SuperScript III kit (Invitrogen) using a combination of oligo(dT) and random hexamer primer. Standard RT-PCR (58 °C, 30 cycles) was performed using 10 mM of each dNTP and 10 µM of each primer. qRT-PCR was performed at 58 °C using Roche Light Cycler 96 and relative mRNA levels determined using Roche Light Cycler 96 SW1.1 software. Samples were run in triplicate and expression levels were normalized to β-actin control. Primer were designed to span an exon–exon

junction using Primer-BLAST software. Primer sequences are given in Supplementary Table 2.

Spinal cord lesions and behavioral recovery. Zebrafish larvae (3 dpf) were anesthetized in PBS containing 0.02% aminobenzoic acid ethyl methyl ester (MS222; Sigma-Aldrich). For dorsal incision lesions, larvae were transferred to a lid of a plastic Petri dish. Following aspiration of excess water, which placed the larvae in a lateral position, the tip of a sharp 30 G syringe needle was used to inflict a lesion in the dorsal trunk at the level of the anal pore. Survival of larvae was typically > 95%. Larvae that had undergone extensive damage to the notochord showed the formation of a notochord-derived bulgy tissue structure (~ 10%). Those larvae were excluded from further analysis. For less invasive stab lesions, larvae were transferred to an agarose-coated Petri dish and larvae were placed in a lateral position through removal of excess water. The tip of a sharp 30 G syringe needle was pushed through the spinal cord at the level of the anal pore immediately dorsal to the notochord. Kinetics of anatomical/functional spinal cord regeneration were comparable in larvae that underwent dorsal incision lesion or stab lesion. After surgery, larvae were returned to E3 medium for recovery and kept at 28.5 °C. Wherever possible, *Xla.Tubb*:DsRED transgenic larvae were used for experiments to visually verify completeness of spinal cord transection after lesion. Analysis of behavioral recovery was performed as described previously[13]. Behavioral data are shown as distance travelled within 15 s after touch, averaged for triplicate measures per larvae. Adult spinal cord lesions have been described previously[62]. Briefly, fish (≥ 3 month post-fertilization) were anesthetized by immersion in 0.02% MS222 in PBS for 5 min. A longitudinal incision was made at the side of the fish to expose the vertebral column. The spinal cord was completely transected under visual control, 3.5 mm caudal to the brainstem-spinal cord junction.

Drug treatments and heat-shock treatments. Heat shocks and drug treatments were performed according to the schematic timelines shown with each experiment. For heat shocks, larvae were kept in 50 ml conical centrifuge tubes filled with 40 ml E3 embryo medium, which floated in a programmable thermostat-controlled water bath (Lauda, Germany). Heat shocks of transgenic animals and non-transgenic sibling controls were performed for 1 h at 38 °C after which larvae were returned to 28.5 °C. For drug treatments, up to 10 larvae were incubated in 7 ml of E3 embryo medium, containing the drug. Larvae were kept in the dark at 28.5 °C and water was exchanged daily. The Axin1 stabilizer IWR-1 (Sigma-Aldrich) was dissolved in DMSO (6 mM stock) and used at a final concentration of 15 µM. Doxycycline (DOX; Sigma-Aldrich) was dissolved in 50% EtOH (50 mg/ml stock) and used at a final concentration of 40 µg/ml. For targeted cell ablation, the pro-drug Metranidozole (MTZ; Sigma-Adrich) was dissolved in DMSO (200 mM) and used at a final concentration of 2 mM.

Morpholino injection. Knockdown of *col12a1a/b* was performed by injecting Vivo-Morpholinos (MO) to *col12a1a/b*, which act as cell-permeable translation blocking anti-sense molecules, into the circulation for efficient distribution in 3 dpf larvae (Supplementary Fig. 11a[50]). Two translation blocking Vivo-Morpholinos, antisense to the transcriptional start site of *col12a1a* (ENSDART00000154728) and *col12a1b* (ENSDART00000025926), were designed (Gene Tools, Philomath, OR, USA): *col12a1a* MO 5′-CGGCCAAAGA-CAACCTGATCTTCAT-3′; *col12a1b* MO 5′-TGCCAAATGCCTGACCGA-CATCTTC-3′. 100% homology of MO sequences to target sites were confirmed by sequencing. Approximately a total of 27 nl injection mix (9 repetitive injections 3 nl each), containing Cascade Blue Dextran (MW: 3000; Molecular Probes) and 0.25 mM of each Morpholino, was injected directly into the ventricle of 3 dpf larvae as described previously[50]. Larvae that showed strong and ubiquitous fluorescence at 2–3 h post-injection were subsequently lesioned. As control a standard Vivo-Morpholino from Gene Tools was used.

CRISPR-mediated genome editing. CRISPR *col12a1a* and *col12a1b* gRNA were designed using a combination of different webtools: ZiFit (http://zifit.partners.org/ZiFiT), CRISPR Design (http://crispr.mit.edu), and Mojo Hand (http://talendesign.org). gRNA expression vectors were built by ligation of annealed oligonucleotides into pT7-gRNA expression vector (Addgene #46759) as described previously[51]. Capped sense *nls-zCas9-nls* RNA was synthesized using mMESSAGE mMACHINE T3 kit (Ambion) and pT3TS-nCas9n (Addgene # 46757) as template[51]. RNA was purified using RNAeasy Mini Kit (Qiagen). gRNA was in vitro transcribed from gRNA expression vectors using mMESSAGE mMACHINE T7 kit and purified using mirVana miRNA isolation kit (Ambion). All synthesized RNAs were assessed for size and quality by gel electrophoresis. A mix of 75 pg gRNA and 150 pg *nls-zCas9-nls* RNA was microinjected into one-cell-stage embryos to determine efficiency of individual gRNAs to introduce mutations in the target site in pools of 24 hpf embryos using restriction fragment length polymorphisms (RFLP) analysis. For subsequent experiments we used a combination (75 pg each) of *col12a1a* gRNA#1 (target sequence 5′-GGCTGTGGTTCAGTACAGCT-3′; targeting exon 6) and *col12a1b* gRNA#1 (target sequence 5′- GGTCAGGCATTTGGCAGCGG-3′; targeting exon 2) and 150 pg *nls-zCas9-nls* RNA for microinjection. A previously described gRNA targeting GFP (target sequence: 5′GGCGAGGGCGATGC-CACCTA-3) served as control[68]. Efficient mutagenesis of target loci was confirmed after each injection by RFLP analysis as follows. For *col12a1a* gRNA#1, a 308 bp fragment was amplified using primers 5′- TGGAGTGTGGGAAGAGAAAACTT-3′ and 5′- CTAATGAGAATTTGTCGGCAGCG-3′ and digested with AluI. For *col12a1b* gRNA#1, a 400 bp fragment was amplified using primers 5′-TGGAG-CATGTATTTTCCCCTTGA-3′ and 5′-GCTCCAGTCCTTTTGTTCATTCC-3′ and digested with AciI.

Live imaging of zebrafish larvae and time-lapse imaging. For live confocal imaging, zebrafish larvae were anesthetized in PBS containing 0.02% MS222 and mounted in the appropriate orientation in 1%low melting point agarose (Ultra-Pure^{TM}, Invitrogen). During imaging the larvae were covered with 0.01% MS222-containing fish water to keep preparations from drying out. For time-lapse imaging, agarose covering the lesion site was gently removed after gelation. Time-lapse imaging was performed for 19 h starting at 6 hpl. After initial visual inspection, acquired time-lapse images were denoised to improve image quality (enhance detail). Background noise, caused by the low signal to noise ratio, was removed from acquired time-lapse images using the ImageJ plugin CANDLE-J algorithm, which allows to remove the noise compartment while preserving the structural information with high fidelity[69]. We verified that this procedure did not remove signals from processes of low fluorescence intensity by comparing raw movies with CANDLE-J-processed movies, which showed that that edges of features remained conserved after denoising.

Quantifications and statistics. Re-established axonal or glial connections (bridges) were scored in static preparations (fixed immunolabelled samples, live transgenic animals) or in still images of time-lapse movies at time points of interest. Larvae were directly visually evaluated using a compound fluorescence microscope (Zeiss Imager.Z1), or after confocal imaging (Zeiss LSM 710, 880). A larva was scored as having a bridged lesion site when continuity of the neuronal or glial labeling between the rostral and caudal part of the spinal cord was observed. Continuity of labeling was defined as at least one fascicle being continuous between rostral and caudal spinal cord ends irrespective of the fascicle thickness. Larvae in which the lesion site was obscured by melanocytes were excluded from analysis. For all quantifications, the observer was blinded to the experimental treatments. Scores of key experiments were validated by a second independent observer.

Quantification of axonal and glial fascicle composition in static preparations at 1 dpl was performed after confocal imaging (Zeiss LSM 880) of immunolabeled or live animals. Fascicles were identified as fluorescent protrusions from the severed spinal cord that projected into the injury site for at least 20 µm or had crossed it completely. This was done by inspecting single optical sections and 3D renderings of the lesion site. If more than half of the length of a fascicle contained fluorescence for both glial and neuronal markers it was scored as "mixed", otherwise it was scored as purely "axonal" or "glial" depending on the markers used. The threshold of half the length was used to exclude situations in which one type of process followed the other long after that one was established.

For quantification of axonal and glial fascicle composition in time-lapse movies we included only fascicles that grew during the observation period.

Fascicles were classified as purely "axonal" or "glial" when the distal part of a given fascicle was labelled by the respective marker throughout the entire observation period. In "mixed" fascicles, both markers were present in the distal portion of the fascicle.

Fascicles were considered to be in close apposition with ECM in histological preparations when > 50% of an axonal fascicle that had entered or crossed the lesion site was aligned with ECM immunoreactivity. This was assessed in single optical sections and 3D renderings.

Quantification of immunohistochemistry or fluorescent in situ hybridization signal in the lesion site was performed on captured images of whole mount samples using ImageJ software as described in subsection "Image analysis". Samples were imaged using a compound fluorescence microscope (Zeiss Imager.Z1) or confocal microscope (Zeiss LSM 710, 880). Measurements were performed in a blinded fashion.

Quantification of $GFP^+/p63^+$ and $GFP^+/p63^-$ cells in 1 dpl and 2 dpl *6xTCF*:dGFP transgenic larvae was performed on immunolabeled sections of individual animals ($n = 10$).

For non-quantitative data, the number of specimens that showed a given phenotype and the total number of specimens analyzed is given as a ratio in each figure. Phenotypes were scored in a blinded fashion.

All experiments were performed at least three times. Animals were randomly assigned to different experimental groups but no formal method of randomisation was used. Power analysis of pilot experiments informed minimum samples size. All quantitative data were tested for normality and analyzed with parametric and non-parametric tests as appropriate. An F-test was used to check for equal variances. We used one-way ANOVA followed by Dunn's multiple comparison test, two-way ANOVA, followed by Student's *t*-test, or Fischer's exact test, as indicated in the figure legends. $^*P < 0.05$, $^{**}P < 0.01$, $^{***}P < 0.001$, n.s. indicates not significant. Error bars always indicate the standard error of the mean (SEM).

Image analysis. Quantitative analysis of immunohistochemistry or fluorescent ISH signals in the lesion site was performed on captured images. Samples were

imaged using a compound fluorescence microscope (Zeiss Imager.Z1) or confocal microscope (Zeiss LSM 710, 880). Analysis of confocal images were performed on maximum intensity projections that were generated from confocal stacks. Image analysis was based on published protocols for fluorescent signal quantification[70]. For all measurements except in Fig. 7b, ImageJ software was used to determine the number of pixel above an intensity threshold (thresholded pixel area) in the region of interest (ROI) (an example of such a measurement is shown in Supplementary Fig. 14). In brief, a minimum intensity threshold was applied to all raw images from the same dataset, limiting pixels to only those of equal or higher intensity. The intensity threshold was determined for each experimental data set individually, using untreated lesioned control samples as reference. The threshold was set such that the thresholded pixel area included most pixels of the fluorescence signal domain in the lesion site while low background signal in the vicinity of the lesion site was largely excluded (efficient image segmentation). After thresholding, a ROI was additionally defined manually to exclude pixels from analysis that fell within the threshold intensity range but were located outside the lesion site. This was necessary in some samples to exclude autofluorescence (e.g., from blood vessels) or constitutively labelled domains (e.g., myosepta for Col XII). Measurements of immunoreactivity in the lesion site, shown in Fig. 7b, was performed by determining the pixel area in a pre-defined ROI of constant size without prior thresholding. This was necessary due to low signal to noise ratio. In brief, the image was converted to a binary image using the automated binary thresholding function of ImageJ. The ROI was placed in the center of the lesion site. All measurements were performed in a blinded fashion.

In situ hybridization. All incubations were performed at room temperature unless stated otherwise.

For chromogenic and Fast Red fluorescence whole mount in situ hybridization (ISH), larvae were fixed overnight at 4 °C in 4% PFA-PBS. On the following day, larvae were washed twice in PBT (0.1% Tween-20 in PBS) and incubated for 30 min in PBT containing 40 µg/ml Proteinase K (Invitrogen). Thereafter, larvae were washed briefly in PBT and were refixed for 20 min in 4% PFA-PBS followed by five washes in PBT for 5 min each. Thereafter, larvae were incubated at 65 °C for > 1 h in pre-warmed hybridization buffer (5x SSC, 500 µg/ml type VI Torula yeast RNA, 50 µg/ml Heparin, 0.1% Tween 20, 9 mM citric acid [Monohydrate]), 50% deionized formamide, pH 6.0). Hybridization buffer was replaced with digoxigenin (DIG) and/or fluorescein-labelled ISH probes diluted in hybridization buffer and incubated at 65 °C overnight. On the following day, larvae were washed at 65 °C once in hybridization buffer, three times in 50% 2×SSCT/50% deionized formamide, and twice in 2xSSCT for 20 min each, followed by four washes at 65 °C in 0.2x SSCT (30x SSC: 300 mM NaCl, 200 mM Na-Citrate, pH 7; SSCT: 0.1 % Tween 20 in 1xSSC) for 30 min each. Thereafter, larvae were washed twice in PBT and incubated for > 1 h in blocking buffer (5% heat-inactivated sheep serum, 10 mg/ml BSA in PBT) for 5 min each under slow agitation. Subsequently, larvae were incubated overnight at 4 °C in blocking buffer containing pre-absorbed anti-DIG or anti-fluorescein antibody coupled to alkaline phosphatase (1:3000–4000). On the following day, larvae were washed six times in PBT for 20 min each, followed by three washes in staining buffer (50 mM $MgCl_2$, 100 mM NaCl, 100 mM Tris-HCl, 0.1% Tween 20, pH 9.5) for 5 min each. Color reaction was performed by incubating larvae in staining buffer supplemented with NBT/BCIP (Sigma-Aldrich) or SIGMAFAST Fast Red (Sigma-Aldrich) substrate. The staining reaction was terminated by washing larvae in PBT. For chromogenic ISH, background staining was cleared by incubating larvae two times in 100% EtOH for 15 min each and once in 50% EtOH-PBT for 5 min, followed by five washes in PBT for 5 min each.

TSA fluorescence ISH was performed using the TSA Plus System Kit (Perkin Elmer) as described for chromogenic ISH with some modifications. 1) Proteinase K treatment was performed for 20 min (20 µg/ml Proteinase K). 2) Before pre-hybridization, endogenous peroxidase activity was quenched by incubating larvae in 1% H_2O_2 for 20 min. 3) Larvae were blocked in blocking reagent (1% in PBT) provided with the kit. 4) Antibodies used to detect labelled RNA hybrids were anti-digoxigenin or anti-fluorescein antibodies coupled to peroxidase (1:500). 5) Color reaction was performed for 30 min in amplification buffer containing Tyramid substrate (1:500) provided with the Kit, followed by washes in PBT for 20 min each.

Simultaneous detection of two different mRNAs by ISH was performed using two-color TSA fluorescence or combinations of Fast Red and TSA fluorescence. Stained samples (Fast Red and TSA fluorescence) were embedded in 4% Agarose-PBS and sectioned at 50–100 µm using a vibratome. Sections were stained for DAPI (Thermo Scientific) to visualize nuclei, followed by two washes in PBS and mounted in 75% Glycerol-PBS. Larvae were incubated for 30 min in 2% H_2O_2 after the first color reaction to deactivate antibody-conjugated peroxidase.

For Fast Red fluorescent ISH on floating agarose sections of larval zebrafish, larvae were fixed in 4% PFA-PBS at 4 °C overnight. After two brief washes in PBT (0.1% Tween-20 in PBS), larvae were embedded in 4% Agarose-PBS and sectioned at 50–100 µm using a vibratome. Sections were incubated for 20 min in PBT containing 10 µg/ml Proteinase K (Invitrogen) and further processed as described for whole mount preparations.

For Fast Red fluorescent ISH on floating agarose sections of adult zebrafish tissue, zebrafish were transcardially perfused with PBS followed by fixative (4% PFA). The lesion site with surrounding non-neural tissue and spinal cord was dissected in a semi-intact preparation and the tissue was post-fixed in 4% PFA overnight. Tissue was embedded in 4% Agarose-PBS and sectioned at 100–200 µm using a vibratome. Sections were briefly rinsed in PBS, incubated for 30 min in PBT containing 40 µg/ml Proteinase K (Invitrogen) and further processed as described for whole mount preparations.

To detect *gfp* transcripts in *6xTCF*:dGFP;*hs*:Axin1-YFP double transgenic larvae we used a probe against the destabilizing signal (sequence coding for residues 422–461 of mouse ornithine decarboxylase [MODC] as reported previously[25].

To detect *cerulean* transcripts in *hs*:col12a1a-p2a-Cerulean transgenic fish we used a probe against the closely sequence-related *gfp* as described previously[25].

Information on ISH probes, including primer sequences used for molecular cloning, is provided in the Supplementary Data 1. Where possible, probes to detect collagen chains-coding transcripts were designed to include 3′UTR, which in most cases contained sequences with the lowest possible similarity to other collagen genes. During the ISH screen only genes were considered detectably expressed for which probes showed a signal in the lesion site within 8 h after initiation of staining reaction. Functionality of probes that showed no staining in the lesion site was verified by the presence of specific staining domains in non-lesion site tissue, which was true for all probes except *col4a4*, *col8a1b*, and *col16a1*, which did not show constitutive expression domains in 4 dpf larvae. Lesion-induced upregulation of genes in the lesion site was determined by comparing the signal intensity in the lesion site to that in adjacent unlesioned trunk tissue.

Immunofluorescence. All incubations were performed at room temperature unless stated otherwise.

For whole mount acetylated Tubulin/GFAP immunolabeling, larvae were fixed in 2% TCA-PBTx (1% Triton X-100 in PBS) for 3 h, followed by brief washes in PBTx and PBS. Thereafter, larvae were incubated for 30 min in 0.25% Trypsin (Gibco) diluted in PBS, followed by five washes in PBTx for 5 min each. Larvae were blocked in 4% BSA-PBTx for 1 h and incubated with primary antibody (1:300) diluted in blocking buffer at 4 °C overnight. On the following day, larvae were washed six times in PBTx for 20 min each, followed by incubation with secondary antibody of interest diluted in blocking buffer (1:300) at 4 °C overnight. On the following day, larvae were washed six times each in PBTx for 20 min each, followed by mounting in PBS or 75% Glycerol-PBS.

For whole mount GFP/acetylated Tubulin/p63 immunolabelling in *6xTCF*:dGFP transgenic larvae, larvae were fixed in 4% PFA-PBS containing 1% DMSO at 4 °C overnight. On the following day, larvae were washed four times in PBS, followed by two washes in PBTx (0.2% Triton X-100 in PBS) for 5 min each. Thereafter, larvae were permeabilized by incubation in PBS containing 2 mg/ml Collagenase (Sigma-Aldrich) for 25 min. To terminate Collagenase digest, larvae were briefly rinsed in PBTx. Subsequently, larvae were incubated in 50 mM glycine in PBTx for 10 min, followed by a brief rinse in PBTx. Larvae were blocked in blocking buffer (0.7% PBTx, 1% DMSO, 1% normal donkey serum, 1% BSA) for 2 h, and incubated with primary antibody (1:300–1:500) diluted in blocking buffer at 4 °C overnight. On the following day, larvae were washed three times in PBTx for 15 min each, followed by incubation with secondary antibody of interest diluted in blocking buffer (1:300) at 4 °C overnight. On the following day, larvae were washed three times in PBTx and once in PBS for 15 min each, before mounting in 75% Glycerol-PBS.

For whole mount acetylated Tubulin/GFAP immunolabelling, as well as all other combinations of immunolabelling on whole mounts (e.g., acetylated Tubulin/Col XII), larvae were fixed in 4% PFA-PBS for 1 h, followed by brief washes in 0.1% PBT (0.1% Tween-20 in PBS). Thereafter, larvae were stepwise dehydrated by successive incubation in 25% MeOH-PBT, 50% MeOH-PBT, 75% MeOH-PBT, 100% MeOH for 5 min each, and stored at −20 °C until need. When required, head and tail of larvae were removed and lesion site-enriched trunk tissue was incubated in 100% MeOH at −20 °C overnight. On the following day, samples were rehydrated by successive incubations in 75% MeOH-PBT, 50% MeOH-PBT and 25% MeOH-PBT for 5 min each, followed by four washes each in PBT for 5 min each. Larvae were washed twice in distilled H_2O for 5 min each, followed by incubation in 100% Acetone (pre-chilled to −20 °C) at −20 °C for 10 min. Thereafter, larvae were washed twice in distilled H_2O for 5 min each, followed by two 5 min washes in PBT. Subsequently, larvae were incubated in PBT containing 10 µg/ml Proteinase K (Invitrogen) for 15 min, followed by two brief washes in PBT and re-fixation in 4% PFA-PBS for 15 min. Thereafter, larvae were washed tree times in PBTx (1% Triton X-100 in PBS) 10 min each and incubated in blocking buffer (4% BSA in PBTx) for 1 h. Thereafter, larvae were incubated with primary antibody (1:300) diluted in blocking buffer at 4 °C for 2–3 days. Thereafter, larvae were washed eight times in PBTx for 20 min each, followed by incubation with secondary antibody of interest diluted in blocking buffer (1:300) at 4 °C for 1–2 days. Thereafter, larvae were washed six times in PBTx for 20 min each and once in PBS for 15 min before mounting in 75% Glycerol-PBS.

For immunohistochemistry on floating agarose sections of larval zebrafish, larvae were fixed in 4% PFA-PBS containing 1% DMSO at 4 °C overnight. After two brief washes in PBT (0.1% Tween-20 in PBS), larvae were embedded in 4% Agarose-PBS and sectioned at 50–100 µm using a vibratome. Sections were briefly rinsed in PBS and incubated in PBS containing 2 mg/ml Collagenase (Sigma-Aldrich) for 20 min. Thereafter, sections were washed several times in PBTx (0.5% Triton X-100 in PBS) followed by incubation in blocking buffer (0.7% PBTx, 1% DMSO, 1% normal donkey serum, 1% BSA) for 1 h, and incubated with primary antibody (1:50–1:200) diluted in blocking buffer at 4 °C for 2–3 days.

Thereafter, sections were washed eight times in PBTx for 20 min each, followed by incubation with secondary antibody of interest diluted in blocking buffer (1:300) at 4 °C overnight. On the following day, larvae were washed six times in PBTx and twice in PBS for 20 min each. Sections were stained for DAPI (Thermo Scientific) to visualize nuclei, followed by two washes in PBS and mounted in 75% Glycerol-PBS.

For immunohistochemistry on floating agarose sections of adult zebrafish tissue, zebrafish were transcardially perfused with PBS followed by fixative (4% PFA-PBS). The lesion site with surrounding non-neural tissue and spinal cord was dissected in a semi-intact preparation and the tissue was post-fixed in 4% PFA for 1 h. Tissue was embedded in 4% Agarose-PBS and sectioned at 100–200 µm using a vibratome. Sections were briefly rinsed in PBS and washed several times in PBTx (1% Triton X-100 in PBS) for a total of 1 h followed by incubation in blocking buffer (4% BSA in PBTx). Thereafter, sections were incubated with primary antibody (1:250) diluted in blocking buffer at 4 °C for 3 days. Thereafter, sections were washed eighteen times in PBTx for 10 min each, followed by incubation with secondary antibody of interest diluted in blocking buffer (1:250) at 4 °C for 2 days. On the following day, sections were washed twelve times in PBTx and twice in PBS for 20 min each. Sections were mounted in 75% Glycerol-PBS.

All primary antibodies used are given in Supplementary Table 3. Primary antibodies used are specific for zebrafish antigens as shown in the indicated publications. To detect basal keratinocytes, we used anti-p63 immunohistochemistry, which is a commonly used marker for this cell lineage[37]. The antibody used in this study, anti-tp63 antibody (Sigma-Aldrich), replicates selective labelling of monolayered basal keratinocytes found in previous publications with other antibodies to this antigen. Secondary fluorophore-conjugated antibodies were from Jackson Immuno Research.

Data availability. The authors declare that all data supporting the findings of this study are available within the article and its supplementary information files, or from the corresponding authors on reasonable request.

Received: 9 December 2016 Accepted: 2 June 2017
Published online: 25 July 2017

References

1. Burnside, E. R. & Bradbury, E. J. Manipulating the extracellular matrix and its role in brain and spinal cord plasticity and repair. *Neuropathol. Appl. Neurobiol.* **40**, 26–59 (2014).
2. Fawcett, J. W., Schwab, M. E., Montani, L., Brazda, N. & Muller, H. W. Defeating inhibition of regeneration by scar and myelin components. *Handb. Clin. Neurol.* **109**, 503–522 (2012).
3. Diaz Quiroz, J. F. & Echeverri, K. Spinal cord regeneration: where fish, frogs and salamanders lead the way, can we follow? *Biochem. J.* **451**, 353–364 (2013).
4. Takeda, A., Atobe, Y., Kadota, T., Goris, R. C. & Funakoshi, K. Axonal regeneration through the fibrous scar in lesioned goldfish spinal cord. *Neuroscience* **284**, 134–152 (2015).
5. Yu, Y. M. et al. The extracellular matrix glycoprotein tenascin-C promotes locomotor recovery after spinal cord injury in adult zebrafish. *Neuroscience* **183**, 238–250 (2011).
6. Zukor, K. A., Kent, D. T. & Odelberg, S. J. Meningeal cells and glia establish a permissive environment for axon regeneration after spinal cord injury in newts. *Neural. Dev.* **6**, 1 (2011).
7. Chen, D., Jarrell, A., Guo, C., Lang, R. & Atit, R. Dermal beta-catenin activity in response to epidermal Wnt ligands is required for fibroblast proliferation and hair follicle initiation. *Development* **139**, 1522–1533 (2012).
8. Hamburg-Shields, E., DiNuoscio, G. J., Mullin, N. K., Lafyatis, R. & Atit, R. P. Sustained beta-catenin activity in dermal fibroblasts promotes fibrosis by up-regulating expression of extracellular matrix protein-coding genes. *J. Pathol.* **235**, 686–697 (2015).
9. Beyer, C. et al. beta-catenin is a central mediator of pro-fibrotic Wnt signaling in systemic sclerosis. *Ann. Rheum. Dis.* **71**, 761–767 (2012).
10. Kabashima, K. et al. Involvement of Wnt signaling in dermal fibroblasts. *Am. J. Pathol.* **176**, 721–732 (2010).
11. Becker, C. G. et al. L1.1 is involved in spinal cord regeneration in adult zebrafish. *J. Neurosci.* **24**, 7837–7842 (2004).
12. Bhatt, D. H., Otto, S. J., Depoister, B. & Fetcho, J. R. Cyclic AMP-induced repair of zebrafish spinal circuits. *Science* **305**, 254–258 (2004).
13. Ohnmacht, J. et al. Spinal motor neurons are regenerated after mechanical lesion and genetic ablation in larval zebrafish. *Development* **143**, 1464–1474 (2016).
14. Briona, L. K., Poulain, F. E., Mosimann, C. & Dorsky, R. I. Wnt/b-catenin signaling is required for radial glial neurogenesis following spinal cord injury. *Dev. Biol.* **403**, 15–21 (2015).
15. Strand, N. S. et al. Wnt/beta-catenin signaling promotes regeneration after adult zebrafish spinal cord injury. *Biochem. Biophys. Res. Commun.* **477**, 952–956 (2016).
16. MacDonald, B. T., Tamai, K. & He, X. Wnt/beta-catenin signaling: components, mechanisms, and diseases. *Dev. Cell* **17**, 9–26 (2009).
17. Guillon, E., Bretaud, S. & Ruggiero, F. Slow muscle precursors lay down a collagen XV matrix fingerprint to guide motor axon navigation. *J. Neurosci.* **36**, 2663–2676 (2016).
18. Hilario, J. D., Wang, C. & Beattie, C. E. Collagen XIXa1 is crucial for motor axon navigation at intermediate targets. *Development* **137**, 4261–4269 (2010).
19. Isaacman-Beck, J., Schneider, V., Franzini-Armstrong, C. & Granato, M. The lh3 glycosyltransferase directs target-selective peripheral nerve regeneration. *Neuron* **88**, 691–703 (2015).
20. Schneider, V. A. & Granato, M. The myotomal diwanka (lh3) glycosyltransferase and type XVIII collagen are critical for motor growth cone migration. *Neuron* **50**, 683–695 (2006).
21. Briona, L. K. & Dorsky, R. I. Radial glial progenitors repair the zebrafish spinal cord following transection. *Exp. Neurol.* **256**, 81–92 (2014).
22. Dorsky, R. I., Sheldahl, L. C. & Moon, R. T. A transgenic Lef1/beta-catenin-dependent reporter is expressed in spatially restricted domains throughout zebrafish development. *Dev. Biol.* **241**, 229–237 (2002).
23. Moro, E. et al. In vivo Wnt signaling tracing through a transgenic biosensor fish reveals novel activity domains. *Dev. Biol.* **366**, 327–340 (2012).
24. Shimizu, N., Kawakami, K. & Ishitani, T. Visualization and exploration of Tcf/Lef function using a highly responsive Wnt/beta-catenin signaling-reporter transgenic zebrafish. *Dev. Biol.* **370**, 71–85 (2012).
25. Wehner, D. et al. Wnt/beta-catenin signaling defines organizing centers that orchestrate growth and differentiation of the regenerating zebrafish caudal fin. *Cell Rep.* **6**, 467–481 (2014).
26. Peri, F. & Nusslein-Volhard, C. Live imaging of neuronal degradation by microglia reveals a role for v0-ATPase a1 in phagosomal fusion in vivo. *Cell* **133**, 916–927 (2008).
27. Goldshmit, Y. et al. Fgf-dependent glial cell bridges facilitate spinal cord regeneration in zebrafish. *J. Neurosci.* **32**, 7477–7492 (2012).
28. Mokalled, M. H. et al. Injury-induced ctgfa directs glial bridging and spinal cord regeneration in zebrafish. *Science* **354**, 630–634 (2016).
29. Bernardos, R. L. & Raymond, P. A. GFAP transgenic zebrafish. *Gene. Exp. Patterns* **6**, 1007–1013 (2006).
30. Yeo, S. Y., Kim, M., Kim, H. S., Huh, T. L. & Chitnis, A. B. Fluorescent protein expression driven by her4 regulatory elements reveals the spatiotemporal pattern of Notch signaling in the nervous system of zebrafish embryos. *Dev. Biol.* **301**, 555–567 (2007).
31. Matsuoka, R. L. et al. Radial glia regulate vascular patterning around the developing spinal cord. *Elife* **5**, e20253 (2016).
32. Filali, M., Cheng, N., Abbott, D., Leontiev, V. & Engelhardt, J. F. Wnt-3A/beta-catenin signaling induces transcription from the LEF-1 promoter. *J. Biol. Chem.* **277**, 33398–33410 (2002).
33. Jho, E. H. et al. Wnt/beta-catenin/Tcf signaling induces the transcription of Axin2, a negative regulator of the signaling pathway. *Mol. Cell Biol.* **22**, 1172–1183 (2002).
34. Kagermeier-Schenk, B. et al. Waif1/5T4 inhibits Wnt/beta-catenin signaling and activates noncanonical Wnt pathways by modifying LRP6 subcellular localization. *Dev. Cell* **21**, 1129–1143 (2011).
35. Devoto, S. H., Melancon, E., Eisen, J. S. & Westerfield, M. Identification of separate slow and fast muscle precursor cells in vivo, prior to somite formation. *Development* **122**, 3371–3380 (1996).
36. Feng, Y., Santoriello, C., Mione, M., Hurlstone, A. & Martin, P. Live imaging of innate immune cell sensing of transformed cells in zebrafish larvae: parallels between tumor initiation and wound inflammation. *PLoS Biol.* **8**, e1000562 (2010).
37. Guzman, A., Ramos-Balderas, J. L., Carrillo-Rosas, S. & Maldonado, E. A stem cell proliferation burst forms new layers of P63 expressing suprabasal cells during zebrafish postembryonic epidermal development. *Biol Open* **2**, 1179–1186 (2013).
38. Bader, H. L. et al. Zebrafish collagen XII is present in embryonic connective tissue sheaths (fascia) and basement membranes. *Matrix Biol.* **28**, 32–43 (2009).
39. Le Guellec, D., Morvan-Dubois, G. & Sire, J. Y. Skin development in bony fish with particular emphasis on collagen deposition in the dermis of the zebrafish (Danio rerio). *Int. J. Dev. Biol.* **48**, 217–231 (2004).
40. Dervan, A. G. & Roberts, B. L. The meningeal sheath of the regenerating spinal cord of the eel, Anguilla. *Anat. Embryol. (Berl).* **207**, 157–167 (2003).
41. Knopf, F. et al. Dually inducible TetON systems for tissue-specific conditional gene expression in zebrafish. *Proc. Natl Acad. Sci. USA* **107**, 19933–19938 (2010).
42. Stoick-Cooper, C. L. et al. Distinct Wnt signaling pathways have opposing roles in appendage regeneration. *Development* **134**, 479–489 (2007).

43. Pastar, I. et al. Epithelialization in wound healing: a comprehensive review. *Adv. Wound Care (New Rochelle)* **3**, 445–464 (2014).
44. Lee, R. T., Asharani, P. V. & Carney, T. J. Basal keratinocytes contribute to all strata of the adult zebrafish epidermis. *PLoS ONE* **9**, e84858 (2014).
45. Tonge, D. A. et al. Fibronectin supports neurite outgrowth and axonal regeneration of adult brain neurons in vitro. *Brain Res.* **1453**, 8–16 (2012).
46. Chiquet, M., Birk, D. E., Bonnemann, C. G. & Koch, M. Collagen XII: Protecting bone and muscle integrity by organizing collagen fibrils. *Int. J. Biochem. Cell Biol.* **53**, 51–54 (2014).
47. Weidinger, G., Thorpe, C. J., Wuennenberg-Stapleton, K., Ngai, J. & Moon, R. T. The Sp1-related transcription factors sp5 and sp5-like act downstream of Wnt/beta-catenin signaling in mesoderm and neuroectoderm patterning. *Curr. Biol.* **15**, 489–500 (2005).
48. Ando, K. et al. Clarification of mural cell coverage of vascular endothelial cells by live imaging of zebrafish. *Development* **143**, 1328–1339 (2016).
49. Goritz, C. et al. A pericyte origin of spinal cord scar tissue. *Science* **333**, 238–242, doi:10.1126/science.1203165 (2011).
50. Konantz, J. & Antos, C. L. Reverse genetic morpholino approach using cardiac ventricular injection to transfect multiple difficult-to-target tissues in the zebrafish larva. *J. Vis. Exp*. (2014).
51. Jao, L. E., Wente, S. R. & Chen, W. Efficient multiplex biallelic zebrafish genome editing using a CRISPR nuclease system. *Proc. Natl Acad. Sci. USA* **110**, 13904–13909 (2013).
52. Koch, M. et al. Large and small splice variants of collagen XII: differential expression and ligand binding. *J. Cell Biol.* **130**, 1005–1014 (1995).
53. Izu, Y., Ezura, Y., Koch, M., Birk, D. E. & Noda, M. Collagens VI and XII form complexes mediating osteoblast interactions during osteogenesis. *Cell Tissue Res.* **364**, 623–635 (2016).
54. Font, B., Eichenberger, D., Rosenberg, L. M. & van der Rest, M. Characterization of the interactions of type XII collagen with two small proteoglycans from fetal bovine tendon, decorin and fibromodulin. *Matrix Biol.* **15**, 341–348 (1996).
55. Veit, G. et al. Collagen XII interacts with avian tenascin-X through its NC3 domain. *J. Biol. Chem.* **281**, 27461–27470 (2006).
56. Yamagata, M. et al. The complete primary structure of type XII collagen shows a chimeric molecule with reiterated fibronectin type III motifs, von Willebrand factor A motifs, a domain homologous to a noncollagenous region of type IX collagen, and short collagenous domains with an Arg-Gly-Asp site. *J. Cell Biol.* **115**, 209–221 (1991).
57. Lein, P. J., Higgins, D., Turner, D. C., Flier, L. A. & Terranova, V. P. The NC1 domain of type IV collagen promotes axonal growth in sympathetic neurons through interaction with the alpha 1 beta 1 integrin. *J. Cell Biol.* **113**, 417–428 (1991).
58. Cholas, R., Hsu, H. P. & Spector, M. Collagen scaffolds incorporating select therapeutic agents to facilitate a reparative response in a standardized hemiresection defect in the rat spinal cord. *Tissue. Eng. A.* **18**, 2158–2172 (2012).
59. Joosten, E. A., Bar, P. R. & Gispen, W. H. Collagen implants and cortico-spinal axonal growth after mid-thoracic spinal cord lesion in the adult rat. *J. Neurosci. Res.* **41**, 481–490 (1995).
60. He, W. et al. Wnt/beta-catenin signaling promotes renal interstitial fibrosis. *J. Am. Soc. Nephrol.* **20**, 765–776 (2009).
61. Dervan, A. G. & Roberts, B. L. Reaction of spinal cord central canal cells to cord transection and their contribution to cord regeneration. *J. Comp. Neurol.* **458**, 293–306 (2003).
62. Becker, T., Wullimann, M. F., Becker, C. G., Bernhardt, R. R. & Schachner, M. Axonal regrowth after spinal cord transection in adult zebrafish. *J. Comp. Neurol.* **377**, 577–595 (1997).
63. Suh, H. I. et al. Axonal regeneration effects of Wnt3a-secreting fibroblast transplantation in spinal cord-injured rats. *Acta. Neurochir. (Wien).* **153**, 1003–1010 (2011).
64. Westerfield, M. in *The Zebrafish Book: a Guide for the Laboratory Use of Zebrafish (Brachydanio rerio)*. 4th edn, (M. Westerfield, 2000).
65. Suster, M. L., Kikuta, H., Urasaki, A., Asakawa, K. & Kawakami, K. Transgenesis in zebrafish with the tol2 transposon system. *Methods Mol. Biol.* **561**, 41–63 (2009).
66. Wehner, D., Jahn, C. & Weidinger, G. Use of the TetON system to study molecular mechanisms of zebrafish regeneration. *J. Vis. Exp.* **2015**, e52756 (2015).
67. Suster, M. L., Abe, G., Schouw, A. & Kawakami, K. Transposon-mediated BAC transgenesis in zebrafish. *Nat. Protoc.* **6**, 1998–2021 (2011).
68. Auer, T. O., Duroure, K., De Cian, A., Concordet, J. P. & Del Bene, F. Highly efficient CRISPR/Cas9-mediated knock-in in zebrafish by homology-independent DNA repair. *Genome Res.* **24**, 142–153 (2014).
69. Coupe, P., Munz, M., Manjon, J. V., Ruthazer, E. S. & Collins, D. L. A CANDLE for a deeper in vivo insight. *Med. Image. Anal.* **16**, 849–864 (2012).
70. Cartwright, A. N., Griggs, J. & Davis, D. M. The immune synapse clears and excludes molecules above a size threshold. *Nat Commun* **5**, 5479 (2014).

Acknowledgements

We thank Silvere Santos for excellent fish care, Dr. Florence Ruggiero for antibodies, Dr. Bertrand Vernay for technical support, and Drs Didier Stainier, Francesco Argenton, Richard I. Dorsky, Thomas J. Carney, Ajay B. Chitnis, Pamela A. Raymond, Francesca Peri, Tohru Ishitani and Naoki Mochizuki for transgenic fish lines. This research was supported by the Deutsche Forschungsgemeinschaft (Forschungsstipendium WE5736/1-1) to D.W., and the BBSRC (BB/L021498/1) and NC3Rs (NC/l001063/1) to C.G.B. and T.B.

Author contributions

Conceptualization, D.W., C.G.B., and T.B.; Investigation, D.W., T.M.T., and A.M.; Writing: D.W., C.G.B., and T.B.; Resources: C.H., M.M.R., and G.W.

Additional information

Supplementary Information accompanies this paper at doi:10.1038/s41467-017-00143-0.

Competing interests: The authors declare no competing financial interests.

Reprints and permission information is available online at http://npg.nature.com/reprintsandpermissions/

Publisher's note: Springer Nature remains neutral with regard to jurisdictional claims in published maps and institutional affiliations.

nature COMMUNICATIONS

ARTICLE

DOI: 10.1038/s41467-018-07036-w OPEN

Dynamic control of proinflammatory cytokines Il-1β and Tnf-α by macrophages in zebrafish spinal cord regeneration

Themistoklis M. Tsarouchas[1], Daniel Wehner[1,4], Leonardo Cavone[1], Tahimina Munir[1], Marcus Keatinge[1], Marvin Lambertus[1,5], Anna Underhill[1], Thomas Barrett[1], Elias Kassapis[1], Nikolay Ogryzko[2], Yi Feng[2], Tjakko J. van Ham[3], Thomas Becker[1] & Catherina G. Becker[1]

Spinal cord injury leads to a massive response of innate immune cells in non-regenerating mammals, but also in successfully regenerating zebrafish. However, the role of the immune response in successful regeneration is poorly defined. Here we show that inhibiting inflammation reduces and promoting it accelerates axonal regeneration in spinal-lesioned zebrafish larvae. Mutant analyses show that peripheral macrophages, but not neutrophils or microglia, are necessary for repair. Macrophage-less *irf8* mutants show prolonged inflammation with elevated levels of Tnf-α and Il-1β. Inhibiting Tnf-α does not rescue axonal growth in *irf8* mutants, but impairs it in wildtype animals, indicating a pro-regenerative role of Tnf-α. In contrast, decreasing Il-1β levels or number of Il-1β^{+} neutrophils rescue functional regeneration in *irf8* mutants. However, during early regeneration, interference with Il-1β function impairs regeneration in *irf8* and wildtype animals. Hence, inflammation is dynamically controlled by macrophages to promote functional spinal cord regeneration in zebrafish.

[1] Centre for Discovery Brain Sciences, University of Edinburgh, The Chancellor's Building, 49 Little France Crescent, Edinburgh EH16 4SB, UK. [2] MRC Centre for Inflammation Research, Queen's Medical Research Institute, University of Edinburgh, Edinburgh EH16 4TJ, UK. [3] Department of Clinical Genetics, Erasmus University Medical Center, Wytemaweg 80, 3015 CN Rotterdam, The Netherlands. [4] Present address: Technische Universität Dresden, DFG-Center of Regenerative Therapies Dresden, Fetscherstraße 105, Dresden 01307, Germany. [5] Present address: Department of Pharmaceutical Biosciences, School of Pharmacy, University of Oslo, 0316 Oslo, Norway. These authors contributed equally: Thomas Becker, Catherina G. Becker. Correspondence and requests for materials should be addressed to T.B. (email: thomas.becker@ed.ac.uk) or to C.G.B. (email: catherina.becker@ed.ac.uk)

Zebrafish, in contrast to mammals, are capable of functional spinal cord regeneration after injury. Recovery of swimming function critically depends on regeneration of axonal connections across the complex non-neural injury site[1,2]. It is therefore important to determine the factors that allow axons to cross the lesion site in zebrafish.

In mammals, a prolonged immune response, consisting of pro-inflammatory macrophages[3], microglia cells[4] and neutrophils[5] together with cytokines released from other cell types, such as endothelial cells, oligodendrocytes, or fibroblasts[6] contribute to an inhibitory environment for axonal regeneration. However, activated macrophages can also promote axonal regeneration[7–9], suggesting complex roles of the immune response after spinal injury.

In zebrafish, we can dissect the roles of these cell types in successful functional spinal cord repair[10]. Zebrafish possess an innate immune system from early larval stages and develop an adaptive immune system at juvenile stages, similar to those in mammals[11]. Indeed, microglia is activated after spinal cord injury in adult[12,13] and larval zebrafish[14], suggesting functions of innate immune cells in repair. Adaptive immunity is also important for spinal cord regeneration[15].

Larval zebrafish regenerate more rapidly than adults. Axonal and functional regeneration is observed within 48 h after spinal cord injury in 3 day-old larvae[1,2]. At the same time, the larval system presents complex tissue interactions that allow us to analyse how axons cross a non-neural lesion environment. For example, axons encounter Pdgfrb$^+$ fibroblast-like cells that deposit regeneration-promoting Col XII in the lesion site in a Wnt-signalling dependent manner[1]. These cells and molecules are present also in the injury sites of adult zebrafish and mammals[1,6]. How immune cells contribute to this growth-conducive lesion site environment in zebrafish is unclear.

Here we show that peripheral macrophages control axonal regeneration by producing pro-regenerative tumour necrosis factor alpha (Tnf-α) and by reducing levels of interleukin-1 β (Il-1β). While early expression of *il-1β* promotes axonal regeneration, prolonged high levels of Il-1β in the macrophage-less *irf8* mutant are detrimental. Preventing formation of Il-1β producing neutrophils or inhibiting excess *il-1β* directly, largely restored repair in *irf8* mutants. This indicates that regulation of a single immune system-derived factor, Il-1β, is a major determinant of successful spinal cord regeneration.

Results

The immune response coincides with axonal regeneration. We analysed axonal regrowth in larval zebrafish that underwent complete spinal cord transection at 3 days post-fertilisation (dpf) in relation to invasion of the injury site by different cell types. Axons were present in the injury site by 1 day post-lesion (dpl). The thickness of the axonal bundle that connects the injured spinal cord increased up to 2 dpl and thereafter plateaued for up to at least 4 dpl (Supplementary Fig. 1A). The thickness of the connecting axon bundle positively correlated with the recovery of touch-evoked swimming distance for individual animals at 2 dpl (Supplementary Fig. 2A–C). This is consistent with previous results showing continuous axon labelling over the lesion site (axon bridging) in 80% of animals by 2 dpl, which then plateaued. Presence of an axon bridge correlates with functional recovery, as animals without axon bridge showed worse recovery of touch-evoked swimming distance[1] and re-lesioning abolished functional recovery[14]. Hence, a percent score of larvae with bridged injury sites is a quick and reliable measure for anatomical repair[1,14].

After injury, we observed a rapid and massive influx of immune cells, with neutrophils (Mpx$^+$) peaking at 2 h post-lesion (hpl) and macrophages (*mpeg1*:GFP$^+$; 4C4$^-$) and microglia (*mpeg1*:GFP$^+$; 4C4$^+$) accumulating in the lesion site a few hours later and peaking at 2 dpl (Fig. 1a, Supplementary Movie 1). Myelinating cells (*cldnK*:GFP$^+$) and endothelial cells (*fli1*:GFP$^+$) were not abundant in the lesion site during axonal regrowth (Supplementary Fig. 1C, D), in contrast to functionally important *pdgfrb*:GFP$^+$ fibroblasts[1] that were present in the lesion site at 1 dpl, peaking at 2 dpl (Supplementary Fig. 1B). This suggests that myelinating cells and endothelial cells are not essential for axon bridging. However, at later time points after injury, axons were clearly associated with processes of myelinating cells (Supplementary Fig. 1C), which may impact functional repair. In contrast, the spatio-temporal pattern of immune cell invasion of the injury site suggests an early role for the immune system in orchestrating axon growth over the lesion site.

Immune system activation promotes axonal regeneration. To determine the importance of the immune reaction, we inhibited it using the anti-inflammatory synthetic corticosteroid dexamethasone[14]. This reduced the number of microglia[14], macrophages and neutrophils in the injury site (Fig. 1b–d) and the proportion of larvae exhibiting axon bridging (control: 78% of examined animals, dexamethasone: 30%; Fig. 1e). The average thickness of axon bridges was also reduced by dexamethasone treatment and correlated with impaired recovery of touch-evoked swimming distance. (Supplementary Fig. 2A–C). *gfap*:GFP$^+$ astroglia-like processes that cross the injury site slightly later than axons[1] also showed reduced bridging, from 77.6% of examined animals to 48.3% (Supplementary Fig. 2D) under dexamethasone treatment. In addition, depleting the number of immune cells with a well-established morpholino combination against *pu.1* and *gcsfr*[16] reduced the proportion of larvae with axonal bridges from 81% of examined animals to 57% (Supplementary Fig. 3A, B).

For a gain-of-function approach, we used incubation with bacterial lipopolysaccharides (LPS)[17]. This increased the number of neutrophils and macrophages in the lesion site (Fig. 1f–h). To detect a potential accelerating effect on axonal regrowth, we analysed larvae at 18 hpl, when axonal regeneration was incomplete in untreated animals. This showed an increase in the proportion of larvae with axonal bridges from 41% of examined animals in wildtype to 60% in LPS-treated animals (Fig. 1i). Hence, immune system activity is necessary for and promotes axonal regeneration across a spinal lesion site.

Macrophages determine regenerative success. To analyse the role of different immune cell types in repair, we used mutants. In mutants for the macrophage-lineage determining transcription factor *irf8*, macrophages and microglial cells, but not neutrophils are missing during early development[18]. Homozygous mutants are adult viable and show no overt developmental aberrations, except for an increased number of neutrophils[18]. In situ hybridisation for the macrophage and microglia marker *mpeg1* confirmed expression in the ventral trunk of unlesioned larvae and in a spinal lesion site at 2 dpl in wildtype larvae, but complete absence of signal in unlesioned and lesioned *irf8* larvae (Fig. 2a).

Next, we determined axonal regrowth and recovery of parameters of swimming capacity in *irf8* mutants compared to wildtype animals. Wildtype and mutants showed comparable proportions of animals with axon bridges at 1 dpl (wildtype: 44% of examined animals; *irf8* mutant: 43%). At 2 dpl, however, axonal continuity was observed in 80% of wildtype animals but only in 41% of *irf8* mutants (Fig. 2b). At 5 dpl–2.5 times as long as wildtype animals need for maximal axon bridging—the proportion of mutant larvae with bridged lesion sites was increased compared to 2 dpl (55% of examined animals vs. 41%), but

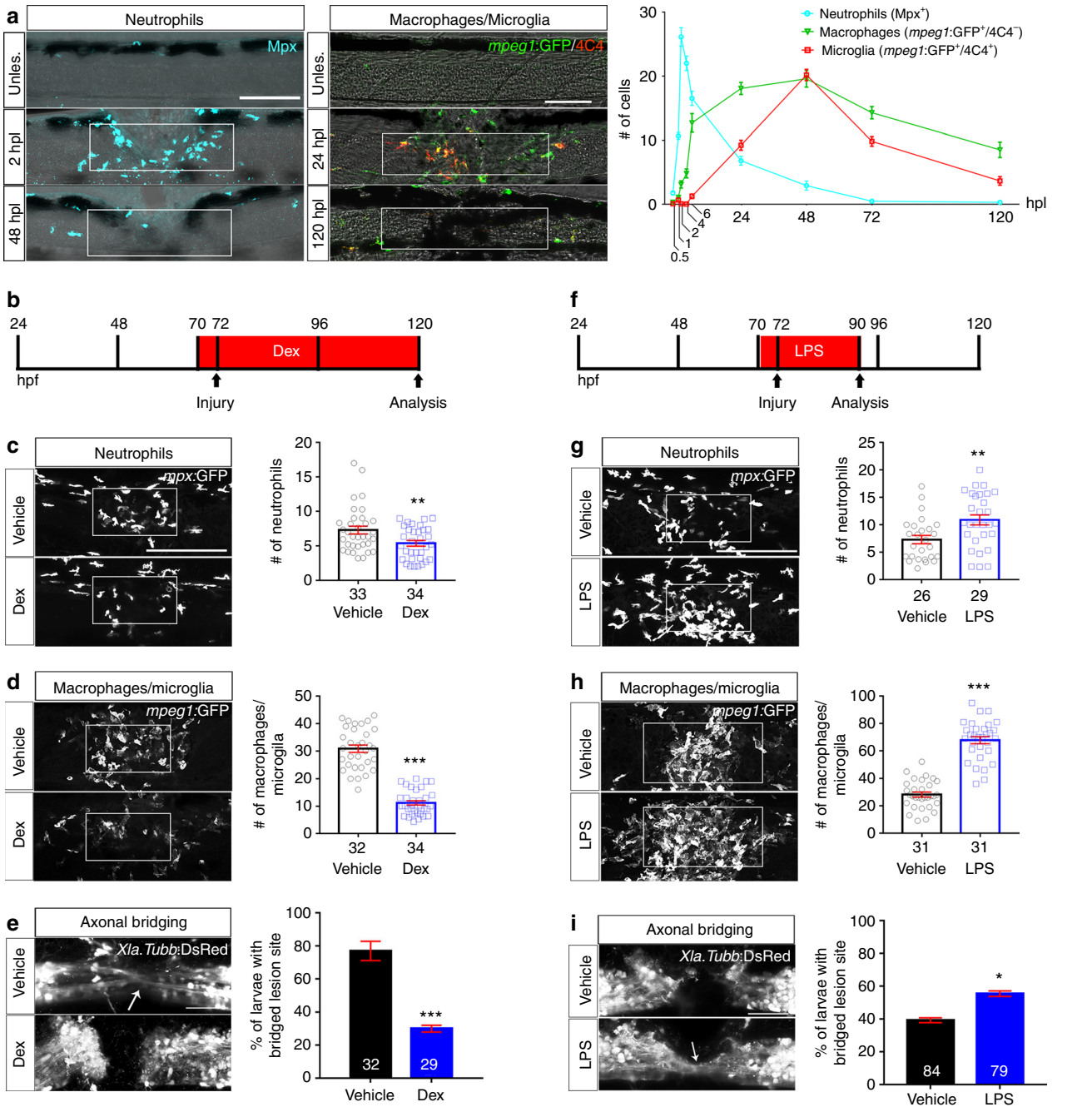

Fig. 1 Spinal injury leads to an inflammatory response that promotes axonal regeneration. **a** Neutrophils, macrophages, and microglial cells show different dynamics after injury. Neutrophils (Mpx$^+$) accumulate in the injury site very early, peaking at 2 hpl. Macrophages (*mpeg1*:GFP$^+$/4C4$^-$) and microglial cell (*mpeg1*:GFP$^+$/4C4$^+$) numbers peak at 48 hpl. Fluorescence images were projected onto transmitted light images. **b**–**e** Incubation with dexamethasone (timeline in **b**) reduces neutrophil and macrophage numbers (**c**, **d**; Mann–Whitney *U*-test: $^{**}P < 0.01$, $^{***}P < 0.001$), as well as the proportion of animals with axonal bridging (**e**; Fisher's exact test: $^{***}P < 0.001$). **f**–**i**, Incubation of animals with LPS during early regeneration (timeline in **f**) increased numbers of neutrophils and macrophages (**g**, **h**; *t*-test: $^{**}P < 0.01$, $^{***}P < 0.001$), as well as the proportion of animals with axonal bridging at 24 hpl (**i** Fisher's exact test: $^{*}P < 0.05$). Lateral views of the injury site are shown; rostral is left. Rectangles indicate region of quantification; arrows indicate axonal bridging. Scale bars: 50 µm; Error bars indicate SEM

regenerative success was still strongly reduced compared to wildtype controls (55% of examined animals vs. 87%; Fig. 2c).

Analysing touch-evoked swimming, we found that wildtype animals swam comparable distances to unlesioned controls at 2 dpl, as previously described[1]. In contrast, recovery of touch-evoked swimming distance in *irf8* larvae plateaued at 2 dpl and did not reach levels of unlesioned animals to at least 5 dpl (Fig. 2c). This indicates that in the absence of macrophages and microglia in *irf8* mutants, initial axonal regeneration is unaffected, but axonal regrowth and functional recovery after spinal cord injury are impaired long-term.

To determine the importance of microglia for regeneration, we analysed *csf1ra/b* double-mutants (see Methods) in which the function of colony-stimulating factor 1 receptor (Csf1r) is

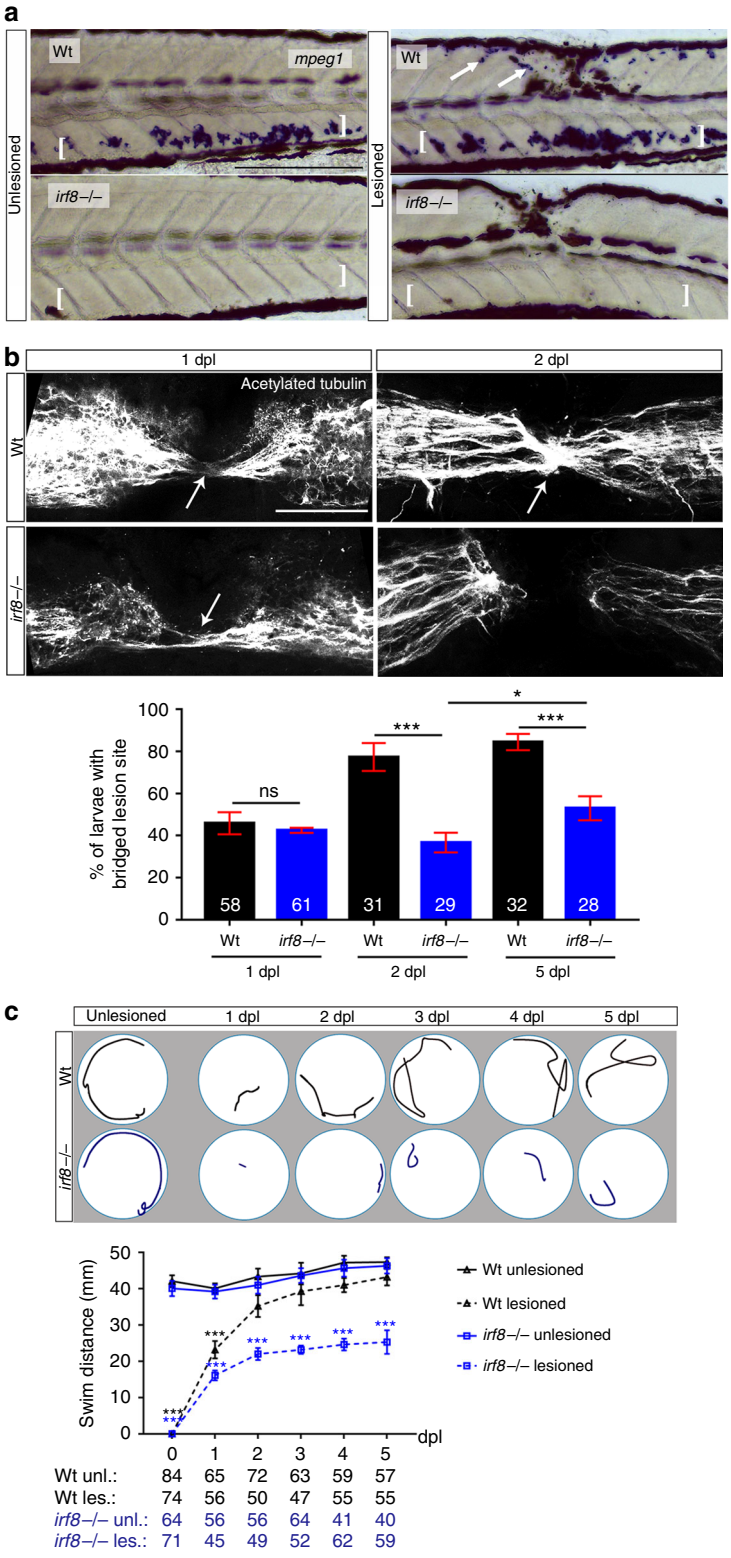

compromised. Csf1r is selectively needed for microglia differentiation[19]. After injury in *csf1ra/b* mutants, we observed a strong reduction in the number of microglial cells (to 17% of wildtype), but an increase in macrophage numbers (by 55% compared to wildtype) in the injury site (Fig. 3a, c). Interestingly, neutrophil numbers were also strongly reduced (to 64.1% of wildtype at 2 hpl and 16% at 1 dpl) (Fig. 3b), perhaps due to feedback regulation from increased macrophage numbers. Whereas microglia cells were reduced in number in the entire fish, neutrophils were still present in the ventral trunk area. In these mutants, axon bridging was unimpaired (Fig. 3d). Hence, microglia are not necessary for axonal regeneration and reduced numbers of neutrophils do not negatively affect axonal regrowth. Combined with results from the *irf8* mutant, this indicates that recruitment of peripheral macrophages is critical for successful spinal cord regeneration.

Fig. 2 In the *irf8* mutant, axonal regeneration and functional recovery after injury show long-term impairment. **a** In situ hybridisation for *mpeg1* confirms the absence of macrophages and microglial cells before and after injury in the *irf8* mutant compared to controls. Arrows indicate labelling around the injury site and brackets indicate the ventral area of the larvae where the macrophages can be found in the circulation. Note that blackish colour is due to melanocytes. **b** Quantification of the proportion of larvae with axonal bridging (anti-acetylated Tubulin) shows that at 1 dpl, axonal bridging is unimpaired in *irf8* mutants, whereas at 2 dpl, *irf8* mutants fail to show full regrowth and even by 5 dpl, the proportion of *irf8* larvae with a bridged lesion site is still lower than in wildtype controls (Fisher's exact test: ***$P < 0.001$, n.s. indicated no significance). **c** *Irf8* mutants never fully recover touch-evoked swimming distance in the observation period, whereas wildtype control animals do. Representative swim tracks are displayed. Note that unlesioned *irf8* larvae show swimming distances that are comparable to those in wildtype controls (Two-way ANOVA: $F_{15,1372} = 11.42$, $P < 0.001$; unles. = unlesioned, les. = lesioned). All lesions are done at 3 dpf. Lateral views of the injury site are shown; rostral is left. Arrows indicate axonal bridging. Scale bars: 200 μm in **a** and 50 μm in **c**. Error bars indicate SEM

Macrophages are not necessary for Col XII deposition. Next, we asked whether macrophages act via a previously reported regeneration-promoting mechanism, comprising Wnt-dependent deposition of Col XII in the lesion site by *pdgfrb*:GFP$^+$ fibroblast-like cells[1]. Inhibition of the immune response with dexamethasone did not inhibit appearance of *pdgfrb*:GFP$^+$ fibroblast-like cells in the lesion site (Supplementary Fig. 4A). By crossing a reporter line for Wnt pathway activity (*6xTCF*:dGFP)[1] into the *irf8* mutant, we found that activation of the pathway was unaltered in the mutant (Supplementary Fig. 4E). Similarly, expression of *col12a1a* and *col12a1b* mRNA in *irf8* mutants was indistinguishable from that in wildtype animals (Supplementary Fig. 4B). Deposition of Col I protein and mRNA expression of 11 other ECM components were also not altered in the *irf8* mutant at 1 and 2 dpl (Supplementary Fig. 4B, C). Moreover, immunolabelling against Tp63 showed that by 2 dpl, the injury site in the *irf8* mutants was completely covered by basal keratinocytes, an additional source of Col XII[1], as in wildtype animals (Supplementary Fig. 4D). In contrast, a PCR screen of 21 potentially macrophage-derived ECM-modifying matrix metalloproteinases[20] (*mmps*) indicated lower mRNA levels for *mmp11a*, *mmp16a/b*, *mmp24*, and *mmp28* in the injury site of *irf8* mutants compared to wildtype animals (Supplementary Fig. 5A, B). This suggests a potential for macrophages to alter the lesion site ECM with Mmps. Overall, macrophages do not overtly regulate Wnt-signalling, deposition of some crucial ECM components or basal keratinocyte coverage of the injury site during regeneration.

Cellular debris is not a major impediment to regeneration. Macrophages could serve as a substrate for axon growth or promote regeneration by removing debris by phagocytosis—a major function of macrophages in peripheral nerve regeneration in zebrafish[21,22]. In time-lapse movies of double transgenic animals in which neurons (*Xla.Tubb*:DsRed) and macrophages (*mpeg1*:GFP) were labelled (Supplementary Fig. 6B and Supplementary Movie 2) we observed axons crossing the spinal lesion site at the same time macrophages migrated in and out of the injury site. However, no obvious physical interactions between these cell types were observed, making it unlikely that macrophages acted as an axon growth substrate.

We frequently observed macrophages ingesting neuronal material and transporting that away from the injury site in time-lapse movies (Supplementary Fig. 6B and Supplementary Movie 2). In agreement with this observation, TUNEL labelling indicated strongly increased levels of dead or dying cells in the late (48 hpl), but not the early (24 hpl) phase of axonal regeneration in the injury site of *irf8* mutants (Supplementary Fig. 6A).

To determine the impact of debris on regeneration, we prevented cell death and consequently debris accumulation in *irf8* larvae using the pan-caspase inhibitor QVD[23], that is functional in zebrafish[24]. This treatment led to lower debris levels that were comparable to those seen in wildtype larvae at 2 dpl (Supplementary Fig. 6C), but failed to increase regenerative success in *irf8* mutants (control, 38% of examined larvae with axon bridges; QVD, 40%. Thickness of axon bridge: control 19.03 +/−2.14 μm; QVD: 18.32+/−2.53 μm; *t*-test: $P > 0.05$. Supplementary Fig. 6E). Conversely, inhibiting debris phagocytosis with the pharmacological inhibitor O-phospho-L-serine (L-SOP)[25] in wildtype animals increased levels of debris in the injury site, but did not impair axonal bridging (Supplementary Fig. 7A–C). This suggests no obvious connection between debris levels and/or phagocytosis and regenerative success.

Pro-and anti-inflammatory phases are altered in *irf8* mutants. To determine a possible role of cytokines in the regenerative failure of *irf8* mutants, we analysed relative levels of pro-and anti-inflammatory cytokines in the lesion site during regeneration in wildtype animals and *irf8* mutants by qRT-PCR. In wildtype animals, expression levels of pro-inflammatory cytokines *il-1β* and *tnf-α* were high during initial regeneration (>25-fold for *il-1β*; >12-fold for *tnf-α* for approximately to 12 hpl) and reduced again during late regeneration (12–48 hpl), although still elevated compared to unlesioned controls (Fig. 4a, b). Anti-inflammatory cytokines, such as *tgf-β1a* and *tgf-β3* were expressed at low levels during initial regeneration, and upregulated during late regeneration (approximately 3-fold for *tgf-β1a* and 2-fold for *tgf-β3*), indicating a bi-phasic immune response within the 48-h time frame of analysis (Fig. 4c, d).

In *irf8* mutants, levels of pro-inflammatory cytokines remained high during the late phase of regeneration (Fig. 4a, b) and anti-inflammatory cytokines were not upregulated (Fig. 4c, d), resulting in a sustained pro-inflammatory environment in *irf8* mutants.

The lack of anti-inflammatory cytokines correlated with the lack of macrophages and microglia in *irf8* mutants. We performed qRT-PCR in fluorescence activated flow sorted *mpeg1*:GFP cells in wildtype animals to determine whether macrophages and microglial cells expressed *tgf-β1a and tgf-β3*. *mpeg1*:GFP$^+$ cells, but also *mpeg1*:GFP$^-$ cells expressed these cytokines (Supplementary Fig. 8A). In situ hybridisation showed wide-spread labelling with some more strongly labelled cells around the injury site in wildtype, but not *irf8* mutants (Supplementary Fig. 8B). This is consistent with expression of *tgf-β1a* and *tgf-β3* in microglia/macrophages and other cell types[26]. Hence, the immune response is bi-phasic with an initial pro-inflammatory phase, followed by an anti-inflammatory phase in wildtype animals. In the absence of macrophages in *irf8* mutants, animals fail to switch to an anti-inflammatory state.

Tnf-α promotes axonal regeneration. To determine whether increased levels of pro-inflammatory cytokines contributed to impaired axon growth in *irf8* mutants, we first inhibited Tnf-α signalling. Pomalidomide, a pharmacological inhibitor of Tnf-α release[27], had no effect on axonal regrowth in *irf8* mutants. In

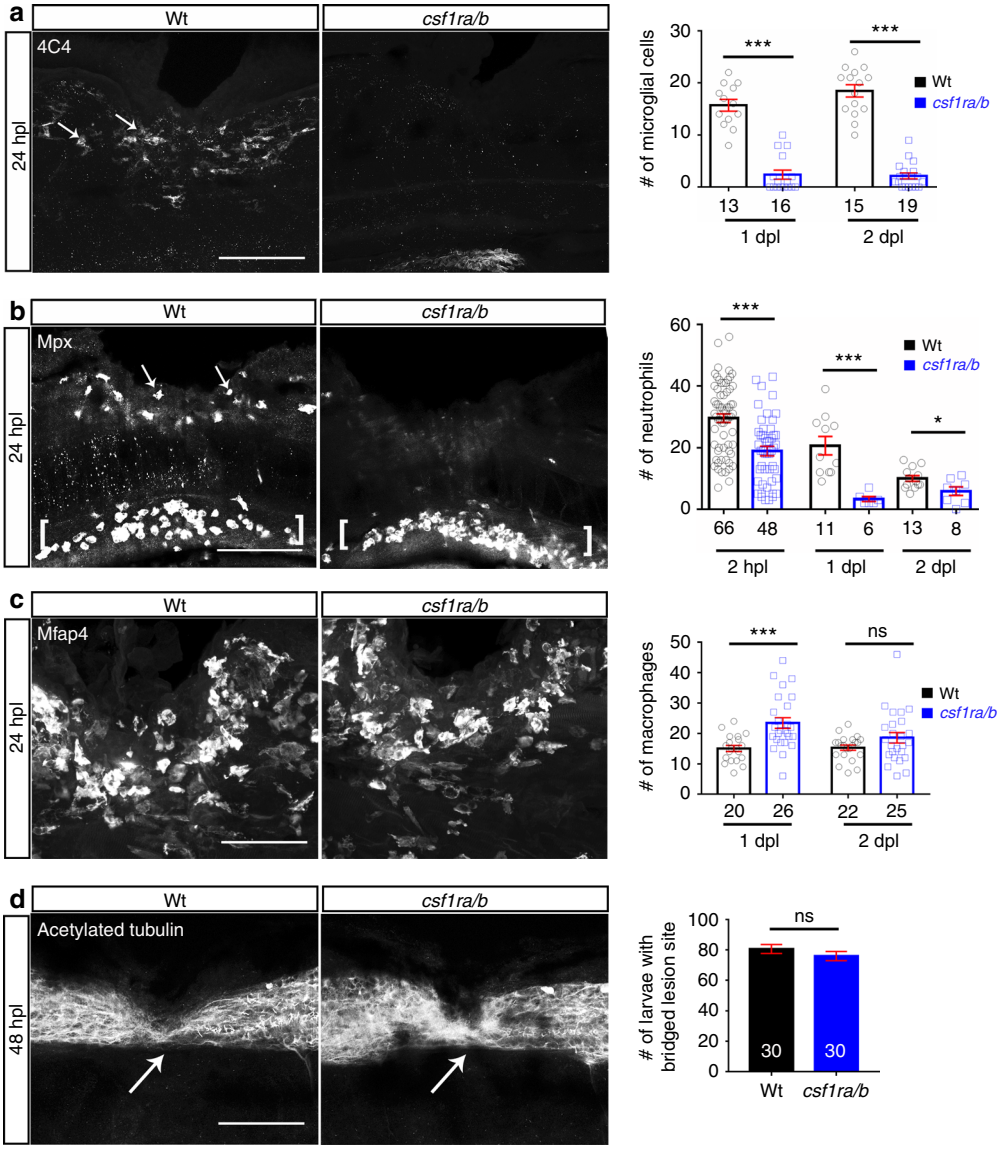

Fig. 3 Absence of microglial cells and reduced neutrophil numbers do not affect axon bridging. **a** Numbers of microglial cells (4C4$^+$; arrows) in the injury site of the *csf1ra/b* mutants are much lower than in wildtype animals (*t*-test: ***$P < 0.001$). **b** Fewer neutrophils (Mpx$^+$) are found in the injury site (arrows) of *csf1ra/b* mutants than in wildtype animals (*t*-test: *$P < 0.05$, ***$P < 0.001$). Note neutrophils ventral to the injury site (brackets). **c** The number of macrophages (Mfap4$^+$) is increased in the injury site in the mutants at 1 dpl, but not at 2 dpl (*t*-test: ***$P < 0.001$, ns indicates no significance). **d** Immunostaining against acetylated tubulin shows that axon bridging (arrows) is not affected in the mutants compared to wildtype animals at 2 dpl (Fisher's exact test: ns indicates no significance). Lateral views of the injury site are shown; rostral is left. Wt = wildtype; Scale bars: 50 µm in **a**, **b**, **d**; 25 µm in **b**. Error bars indicate SEM

contrast, in wildtype animals Pomalidomide strongly inhibited axon bridging at 1 dpl (control: 62% of examined animals showed an axonal bridge; Pomalidomide: 36%) and 2 dpl (control: 75% of examined animals; Pomalidomide: 45%) (Fig. 5a).

To confirm pharmacological results, we targeted *tnf-α* by using CRISPR manipulation with a gene-specific guideRNA (gRNA). Injection of the gRNA into the zygote efficiently mutated the gene as shown by restriction fragment length polymorphism (RFLP) analysis (Fig. 5b) and produced function-disrupting insertion-deletion mutations in a highly conserved domain[28] (Supplementary Table 1). Western blots of 4-day old larvae and immunohistochemistry in the injury site showed robustly reduced Tnf-α protein levels (Supplementary Fig. 9A, B).

Axon bridging was inhibited in wildtype animals by *tnf-α* gRNA injection in a way that was comparable to drug treatment (1 dpl: control: 51% of examined animals showed bridging; gRNA: 27%; 2 dpl: control: 88% of examined animals showed bridging; gRNA: 40%). At 5 dpl, axon bridging was still strongly impaired (control: 84.1% of examined animals showed bridging; gRNA: 38.3%; Fig. 5c), indicating long-term impairment of regeneration. Hence, *tnf-α* dysregulation is not a major cause of regenerative failure in *irf8* mutants, but *tnf-α* is necessary for axonal regeneration in wildtype animals.

To determine which cells expressed *tnf-α* in wildtype animals, we used immunohistochemistry for L-Plastin, labelling all immune cells, in *tnf-α*:GFP transgenic fish (Fig. 6d). Nearly all *tnf-α*:GFP$^+$ cells co-labelled with L-Plastin (96%) at 12 hpl. Thus, expression of *tnf-α* occurred mainly in immune cells (Fig. 6a). Double-labelling *tnf-α*:GFP reporter fish with neutrophil (Mpx), microglia (4C4) and macrophage (Mfap4) markers at 24 hpl, when axons were actively growing, indicated that >95% of *tnf-α*:GFP$^+$ cells in the injury were peripheral macrophages. However

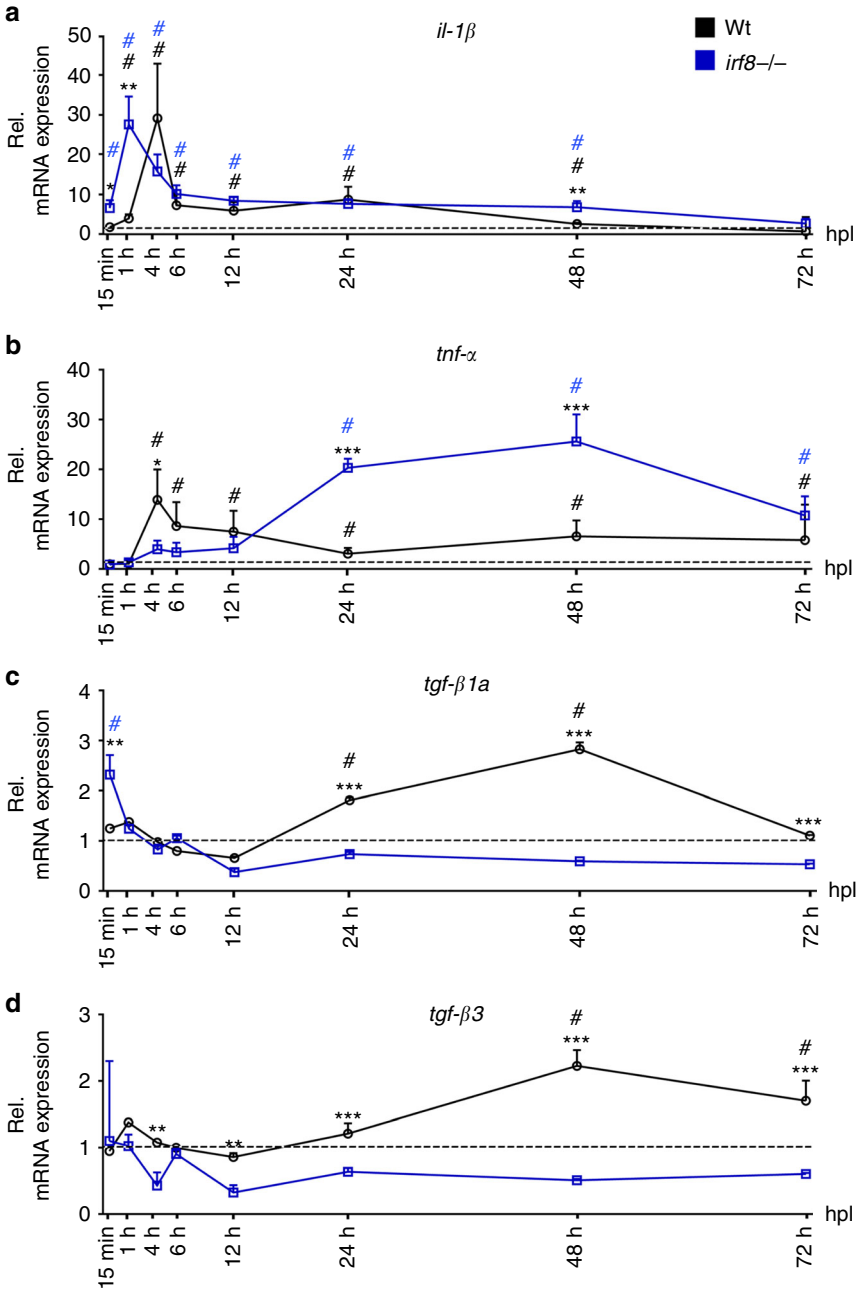

Fig. 4 Inflammation is bi-phasic and dysregulated in *irf8* mutants. **a**, **b** Absence of macrophages in the *irf8* mutant fish leads to increased *il-1β* and *tnf-α* mRNA levels during the late stage of inflammation (>12 hpl). An early peak in *tnf-α* expression is missing in *irf8* mutants. **c**, **d** Expression of anti-inflammatory cytokines, *tgf-β1a* and *tgf-β3*, which peak during late regenerative phases in wildtype animals, is strongly reduced in *irf8* mutants (*t*-tests: $*P < 0.05$, $**P < 0.01$, $***P < 0.001$; wt = wildtype animals). # indicates statistical significance when compared to unlesioned animals. Error bars indicate SEM

other cell types, such as neurons[29], may also express *tnf-α*. More than 72% of macrophages were *tnf-α*:GFP$^+$, whereas for microglia (<6.5%) and neutrophils (<0.7%) the proportion was much smaller. Over time, the proportion of *tnf-α*:GFP$^+$ macrophages was reduced (from 72.5% at 1 dpl to 59% at 2 dpl) (Fig. 6b). Our observations suggest that macrophages promote regeneration by expressing *tnf-α*.

To elucidate effects of *tnf-α* inhibition, we determined numbers of neutrophils and macrophages/microglia at 24 and 48 hpl in *tnf-α* gRNA injected animals. This showed no changes in macrophages, but a 49.7% increase in the number of neutrophils at 1 dpl (Fig. 6c). qRT-PCR indicated that *il-1β* mRNA levels were increased by 108%, whereas *tnf-α*, *tgf-β1a* and *tgf-β3* mRNA levels remained unchanged at 2 dpl (Fig. 6d). This suggests a moderate enhancement of the pro-inflammatory response when Tnf-α is inhibited.

Il-1β inhibits regeneration in *irf8* mutants. To test whether sustained high levels of Il-1β were responsible for regenerative failure in *irf8* mutants, we interfered with *il-1β* function in three different ways. Firstly, we inhibited caspase-1, which is necessary for activation of Il-1β, using the pharmacological inhibitor YVAD that is functional in zebrafish[30] (Fig.7a–e). Secondly, we disrupted *il-1β* RNA splicing with an established morpholino (Supplementary Fig. 10A–D)[31]. Finally, we targeted *il-1β* in a CRISPR approach (Supplementary Fig. 10E–H).

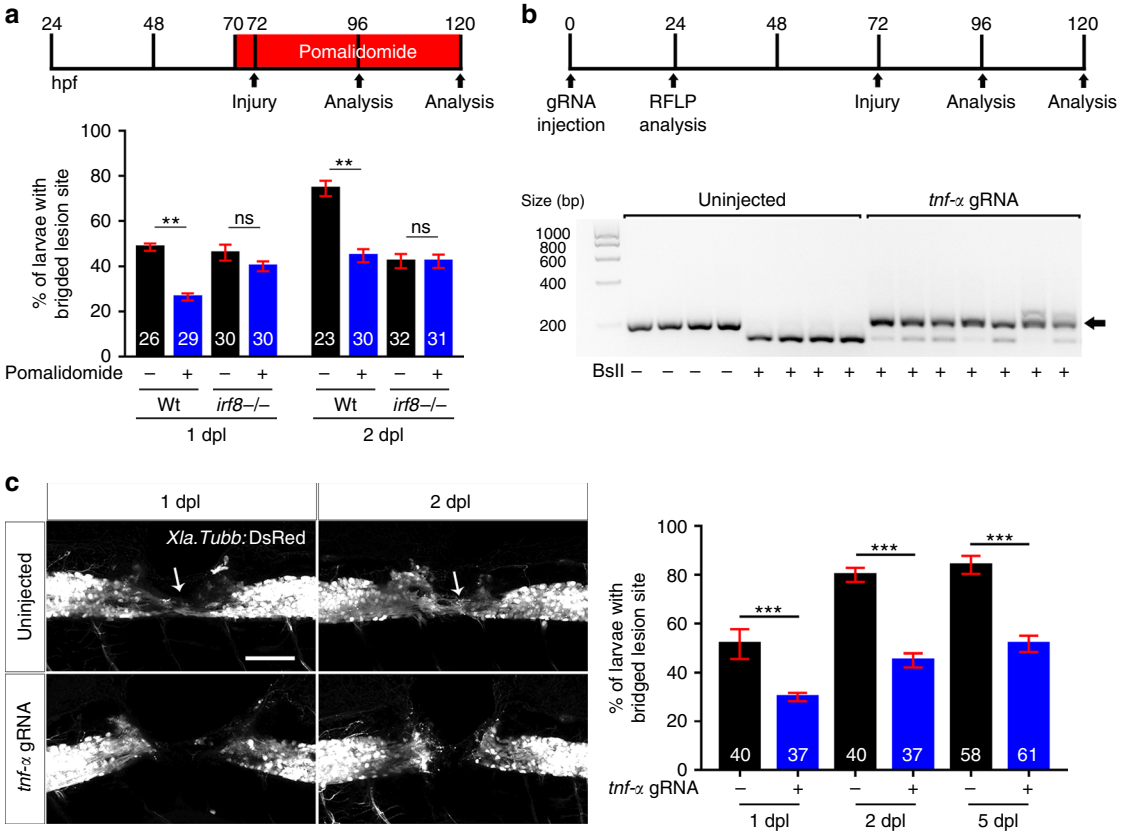

Fig. 5 Tnf-α is essential for axonal regeneration. **a** Tnf-α inhibition by Pomalidomide reduces the proportion of wildtype animals with axon bridging at 1 and 2 dpl. No effect is observed in *irf8* mutants (Two-way ANOVA followed by Bonferroni post-test: $F_{3,16} = 12.16$, $^{**}P < 0.01$, n.s indicates no significance). **b** CRISPR/Cas9-mediated disruption of *tnf-α* is effective as shown by RFLP analysis. This reveals efficient somatic mutation in the gRNA target site, indicated by resistance to restriction endonuclease digestion (arrow). **c** Axonal bridging (arrow; *Xla.Tubb*:DsRed^{+}) is strongly impaired after disruption of the *tnf-α* gene. (Fisher's exact test: $^{***}P < 0.001$) and the impairment persists at 5 dpl. Lateral views of the injury site are shown; rostral is left. Scale bar: 50 µm. Error bars indicate SEM

To determine whether interfering with Il-1β function mitigated inflammation in *irf8* mutants, we quantified immune cells, expression of *il-1β*, *tnf-α*, and dead cells. Indeed, after YVAD treatment we observed a reduction of neutrophil peak numbers (by 38% at 2 hpl; Fig. 7b), as well as strongly reduced levels of *il-1β* and *tnf-α* mRNA expression (at 2 dpl; Fig. 7a) in *irf8* mutants. Moreover, the number of TUNEL^{+} cells was reduced at 2 dpl in the *irf8* mutant, but not to wildtype levels (Fig. 7c). In lesioned wildtype animals, YVAD reduced peak numbers of neutrophils (by 40% at 2 hpl) and macrophages (by 28% at 48 hpl), but no influence on low numbers of TUNEL^{+} cells at 2 dpl was observed. Hence, interfering with Il-1β function reduces inflammation in *irf8* mutants and wildtype animals.

Axon bridging in wildtype animals was not affected by YVAD treatment at 2 dpl (control: 79% of examined animals showed bridging; YVAD: 78%) (Fig. 7d), indicating that high levels of Il-1β were not necessary for axonal regeneration. In contrast, in YVAD-treated *irf8* mutants, we observed a remarkable rescue of axon bridging at 2 dpl (control: 38% of examined animals showed bridging; YVAD: 69%) (Fig. 7d).

Injecting a well-established[31] morpholino targeting *il-1β* into *irf8* mutants at the one-cell-stage inhibited *il-1β* splicing (Supplementary Fig. 10A, D). Morpholino-injected animals showed a rescue of axon bridging at 2 dpl (control: 40% of examined animals showed bridging; YVAD: 60%) (Supplementary Fig. 10B, C).

Finally, injecting a gRNA targeting *il-1β* at the one-cell stage led to somatic mutation in the target site of *il-1β*, indicated by RFLP analysis (Supplementary Fig. 10E, H). This strongly rescued axonal bridging in lesioned *irf8* mutants (control: 40% of examined animals showed bridging; acute *il-1β* gRNA: 70%) (Supplementary Fig. 10F, G). Hence, three independent manipulations show that excessive *il-1β* levels in *irf8* mutants are a key reason for impaired axonal regeneration.

Il-1β promotes axonal regeneration during the early regeneration. To determine whether roles of Il-1β and general inflammation differed for different phases of the inflammation, we separately analysed early (0–1 dpl; Supplementary Fig. 11A) and late (1–2 dpl; Supplementary Fig. 11B) regeneration by drug incubation. During the early phase, YVAD treatment led to a weak inhibition of axonal regeneration in both wildtype (control: 58% of examined animals showed bridging; YVAD: 41%) and *irf8* mutants (control: 41% of examined animals showed bridging; YVAD: 36%). Similarly, dexamethasone treatment inhibited axonal regeneration in both wildtype (control: 57.5% of examined animals showed bridging; dexamethasone: 36.6%) and *irf8* (control: 44.6% of examined animals showed bridging; dexamethasone: 34%). Interestingly, while LPS promoted regeneration in the early phase in wildtype animals (control: 53.2% of examined animals showed bridging; LPS: 68.7%), it was detrimental in *irf8* mutants (control: 39% of examined animals showed bridging; LPS: 25.5%), perhaps because baseline inflammation was already high in the mutant.

During late regeneration, only dexamethasone had an inhibitory effect in wildtype animals (from 82.1% of examined animals that showed bridging to 64.4%). YVAD had no effect in

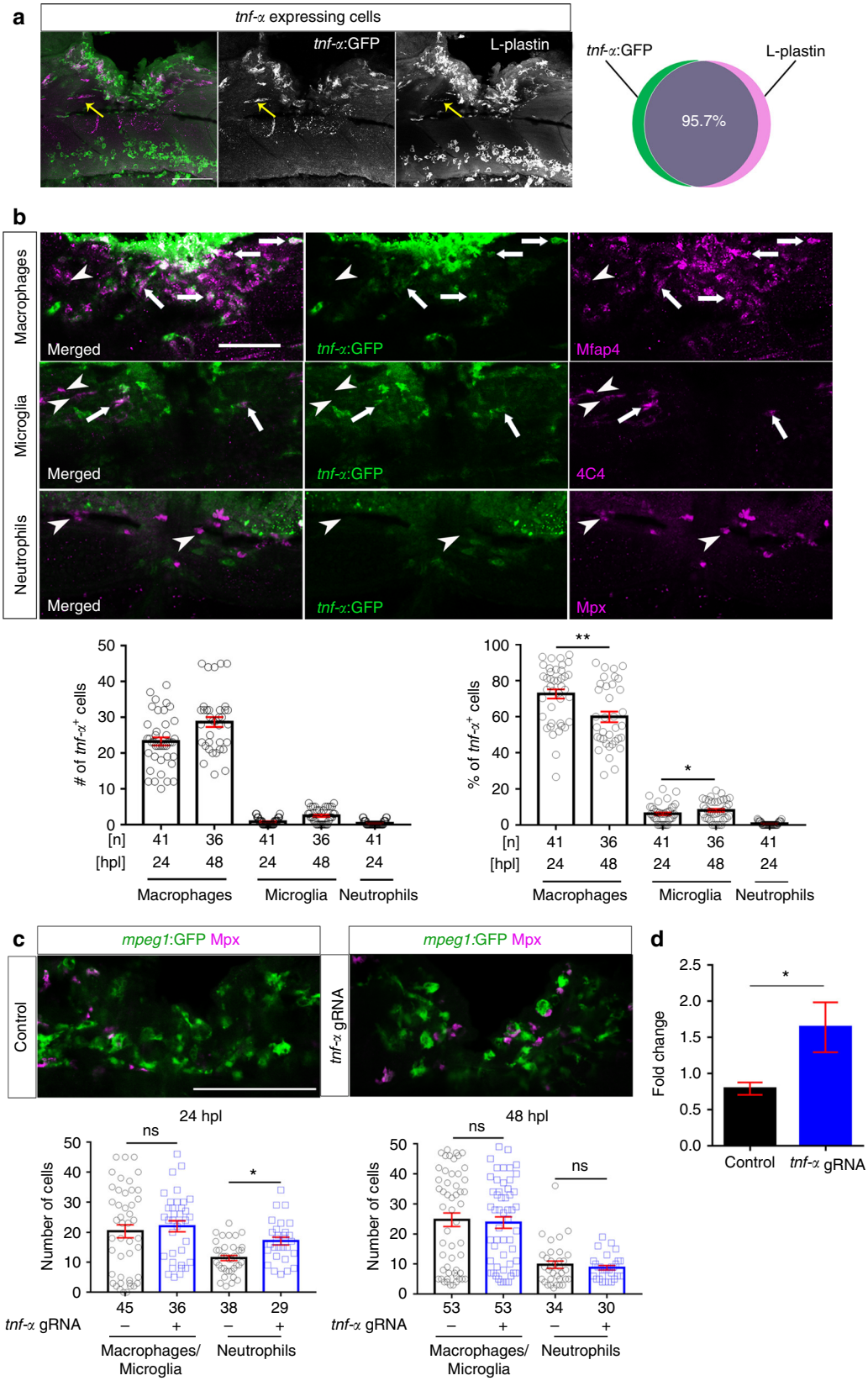

wildtype animals during late regeneration, when *il-1β* was already down-regulated (control: 81% crossing; YVAD: 78% crossing), but a strong rescue effect of YVAD was observed in the *irf8* mutant (control: 37% of examined animals showed bridging; YVAD: 68%). This rescue effect was comparable to that observed when Il-1β was suppressed for the entire 48 h (cf. Fig. 7d). LPS had no effect in wildtype or mutants during late regeneration. Hence, early inflammation and *il-1β* upregulation promote regeneration, but *il-1β* must be down-regulated at later phases of axonal regeneration.

Fig. 6 *Tnf-α* is expressed by macrophages and regulates the immune response. **a** Top row: *tnf-α*:GFP labelling occurs almost exclusively in L-plastin$^+$ immune cells (L-plastin in green; *tnf-α*:GFP in magenta; yellow arrow indicates a rare *tnf- α*:GFP$^+$ microglial cell; 12 hpl) **b** In the injury site, the number and proportion of macrophages (Mfap4$^+$) that are *tnf-α*:GFP$^+$ are much higher than numbers and proportions of microglia (4C4$^+$) and neutrophils (Mpx$^+$), indicating that the main source of Tnf-α is the macrophages. Arrows indicate double-labelled cells and arrowheads indicate immune cells that are *tnf-α*:GFP$^-$. Single optical sections are shown; the proportion of macrophages that are *tnf-α*:GFP$^+$ decreases over time, whereas the proportion of *tnf-α*:GFP$^+$ microglial cells slightly increases (One-way ANOVA followed by Bonferroni post-*test*: $F_{4,195} = 376.3$, $^{**}P < 0.01$, $^{*}P < 0.05$). **c** Quantification of the immune cells after *tnf-α* gRNA injection shows that Tnf-α disruption leads to increased numbers of neutrophils (Mpx$^+$) at 1 dpl but not at 2 dpl, whereas the numbers of macrophages/microglia (*mpeg1*:GFP$^+$) remains unchanged (Mann–Whitney *U*-test: $^{*}P < 0.05$, ns indicates no significance). **d** qRT-PCR indicates that *tnf-α* disruption leads to increased levels of *il-1β* mRNA at 2 dpl (*t*-tests: $^{*}P < 0.05$). Lateral views of the injury site are shown; rostral is left. Scale bars: 50 μm. Error bars indicate SEM

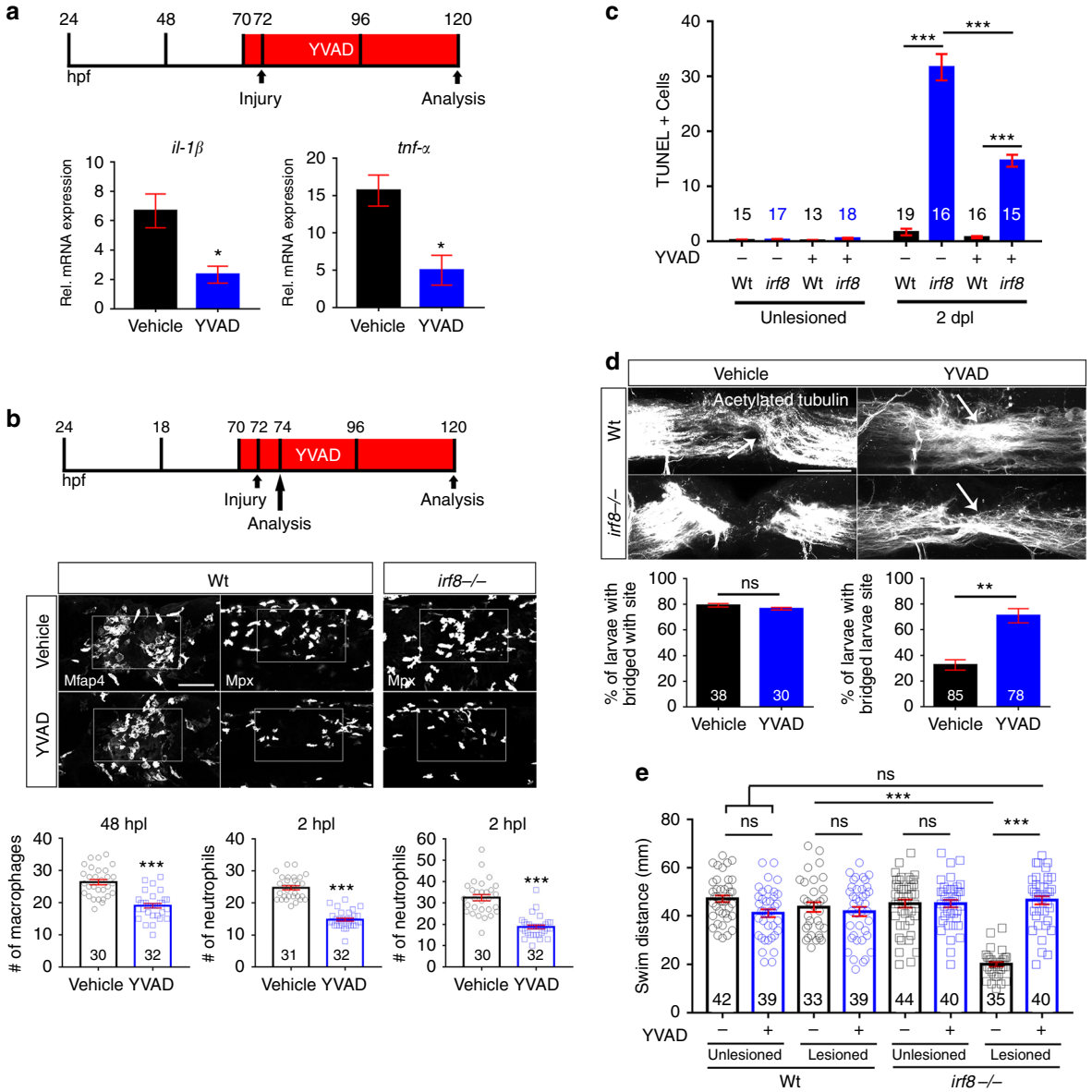

Fig. 7 Inhibition of Il-1β function rescues axonal regeneration in *irf8* mutants. Lateral views of the injury site are shown; rostral is left. **a** YVAD reduces expression levels of *il-1β* and *tnf-α* in *irf8* mutants (two-sample *t*-test: $^{*}P < 0.05$) at 2 dpl. **b** YVAD impairs migration of peripheral macrophages (Mfap4$^+$) and neutrophils (Mpx$^+$) in wildtype animals and *irf8* mutants (only neutrophils quantified, due to absence of macrophages) (*t*-tests: $^{***}P < 0.001$). **c** YVAD moderately reduces the number of TUNEL$^+$ cells in the *irf8* mutants at 2 dpl. (Two-Way ANOVA followed by Bonferroni multiple comparisons: $F_{3,121} = 112.5$, $^{***}P < 0.001$). **d** YVAD does not influence axonal regeneration in wildtype animals but rescues axonal bridging (arrows) in *irf8* mutants (Fisher's exact test: $^{**}P < 0.01$, ns indicates no significance) at 2 dpl. **e** Impaired touch-evoked swimming distance in *irf8* mutants is rescued by YVAD treatment, to levels that are no longer different from lesioned and unlesioned wildtype animals at 2 dpl. YVAD has no influence on swimming distance in lesioned or unlesioned wildtype animals (Two-way ANOVA followed by Bonferroni multiple comparisons: $F_{1,309} = 35.229$, $^{***}P < 0.0001$, ns indicates no significance). Rectangle in **b** denotes quantification area. Scale bar: 50 μm for **b**, **d**. Error bars indicate SEM

Reduction of Il-1β levels rescues swimming in irf8 mutants. To determine whether ll-1β inhibition also rescued recovery of swimming function in *irf8* mutants, we analysed touch-evoked swimming distances. YVAD had no effect in unlesioned mutant or wildtype animals and did not affect recovery in lesioned wildtype animals (Fig. 7e). In contrast, YVAD-treatment rescued the touch-evoked swimming distance in *irf8* mutants to levels that were indistinguishable from wildtype lesioned or unlesioned animals (Fig. 7e). Mean velocity and path shape (meandering) were also rescued (Supplementary Fig. 10I, J). These observations indicate that inhibition of Il-1β alone restores most axonal regeneration and recovery of touch-evoked swimming parameters in the absence of macrophages.

Neutrophils are a major source of il-1β. To understand *il-1β* regulation, we determined the source of Il-1β in wildtype and *irf8* mutants. Using Il-1β immunohistochemistry and a transgenic reporter line (*il-1β*:GFP), we found expression in microglia, macrophages, neutrophils and basal keratinocytes in the injury site (Fig. 8c, d; Supplementary 12A). Neuronal labelling (HuC/D$^+$) did not overlap with *il-1β*:GFP labelling (Supplementary Fig. 12B). While numbers of *il-1β*:GFP$^+$ immune cells did not change significantly between 1 and 2 dpl, the percentage of macrophages (from 50.6 to 34.3%) and neutrophils that were labelled for the *il-1β*:GFP transgene were reduced (from 53.3 to 23.7%), likely reflecting resolution of inflammation (Supplementary Fig. 12A).

In *irf8* mutants, detection of *il-1β* mRNA by qRT-PCR and in situ hybridisation confirmed increased levels at 2 dpl, but not 1 dpl (Fig. 8a, b), despite lack of *il-1β* expressing microglia and macrophages. Instead, we observed increased numbers of Il-1β$^+$ neutrophils (by 97%) and basal keratinocytes (by 58%) compared to wildtype animals at 1 dpl (Fig. 8c, d). Importantly, the proportion of neutrophils that were Il-1β$^+$ was also increased from 33.6% in wildtype animals to 49% in the *irf8* mutant at 1 dpl. This demonstrates that neutrophils are more likely to express *il-1β* in the absence of macrophages.

Increased numbers of Il-1β$^+$ neutrophils in *irf8* mutants could, at least in part, be due to higher overall numbers of neutrophils in the injury site. We found a peak of neutrophil numbers in the lesion site of *irf8* mutants at 2 hpl, as in wildtype animals (Fig. 9a). However, the number of neutrophils was 27% higher than in wildtype, potentially due to the higher abundance of this cell type in the *irf8* mutant[18]. While neutrophil numbers declined over time in wildtype and *irf8* mutants, they did so more slowly in *irf8* mutants. At 24 hpl, twice, and at 48 hpl, three times the number of neutrophils as in wildtype animals remained in the mutant. Hence, macrophages control number of and cytokine expression by neutrophils[32], leading to prolonged presence of Il-1β$^+$ neutrophils in the injury site of *irf8* mutants.

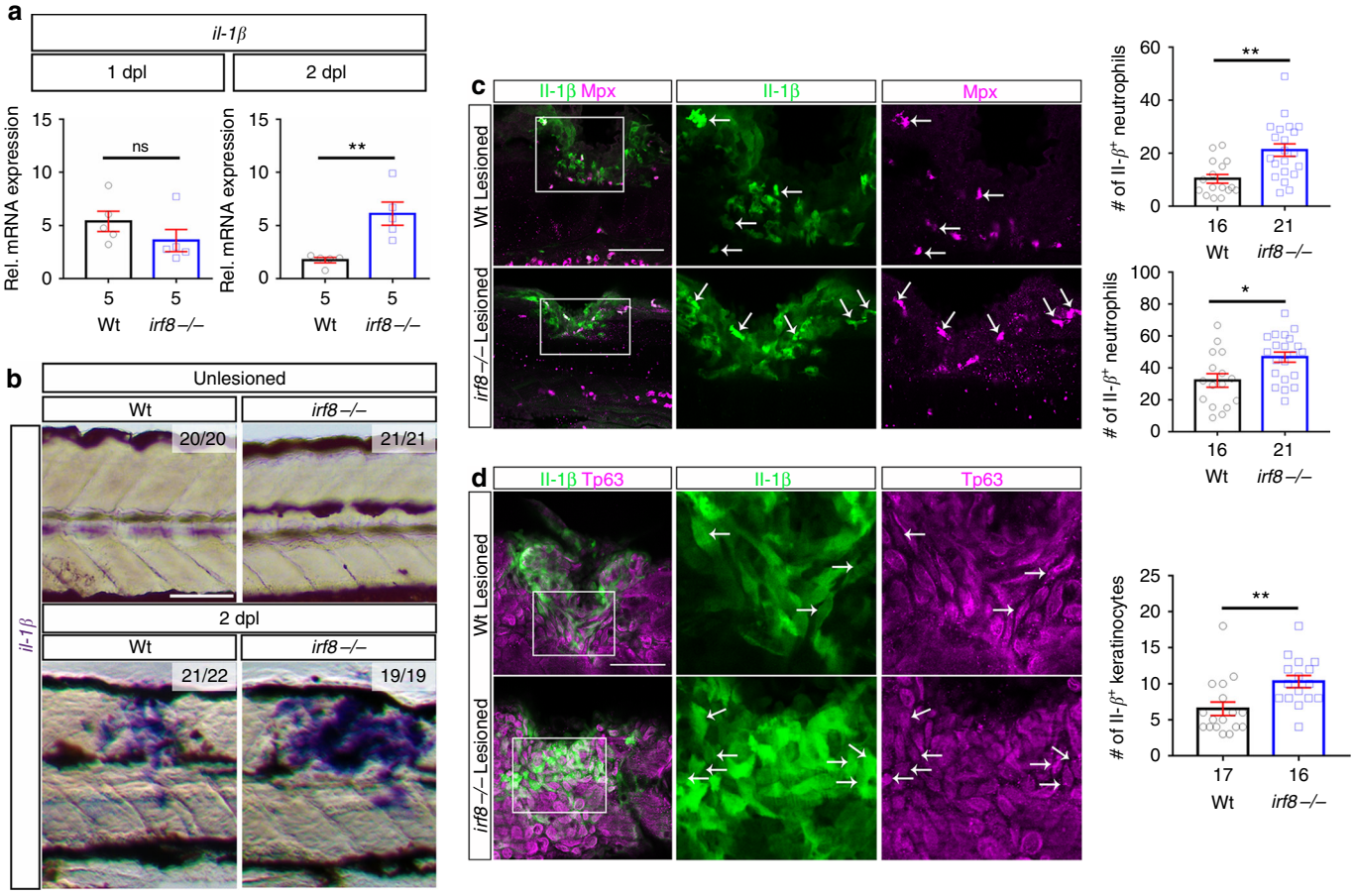

Fig. 8 Levels of *il-1β* expression are increased in the injury site of *irf8* mutants. **a** At 1 dpl, expression levels of *il-1β* are comparable between *irf8* mutants and wildtype (Wt) animals but are higher in the mutant at 2 dpl in qRT-PCR (*t*-test: $^{**}P < 0.01$, ns indicates no significance). **b** In situ hybridisation confirms increased expression of *il-1β* mRNA at 2 dpl. **c** In the injury site, the number and proportion of neutrophils (Mpx$^+$) that are Il-1β immuno-positive (arrows) are increased in *irf8* mutants at 1 dpl compared to wildtype animals. **d** The number of basal keratinocytes (Tp63$^+$) that are Il-1β immuno-positive is increased in *irf8* mutants. Single optical sections are shown; boxed areas are shown in higher magnifications (*t*-test: $^{*}P < 0.05$, $^{**}P < 0.01$). Lateral views of the injury site are shown; rostral is left. Scale bars: 100 µm in **b**, **c**, **d** and 50 µm for higher magnification areas. Error bars indicate SEM

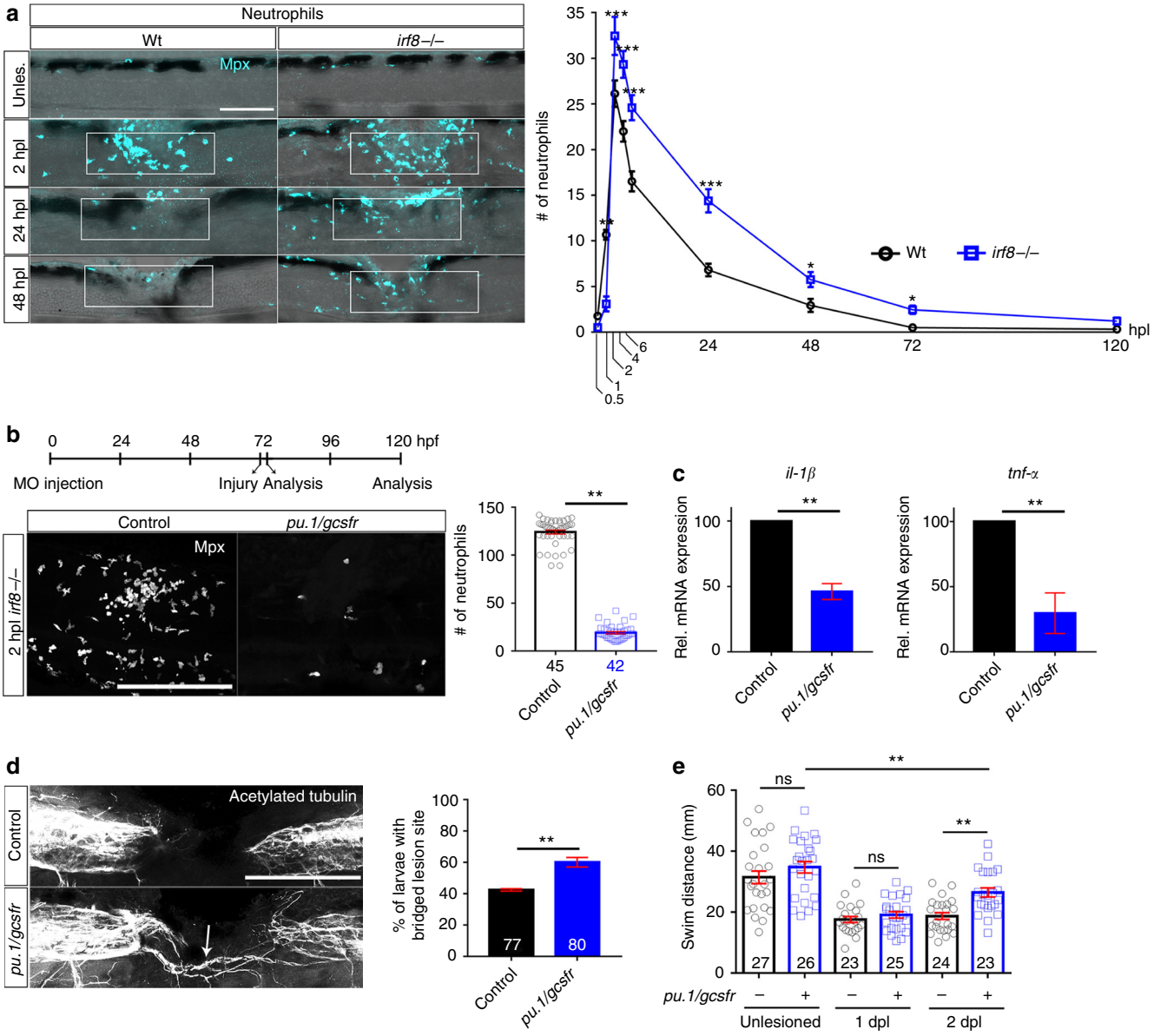

Fig. 9 Preventing neutrophil formation partially rescues functional spinal cord regeneration in the *irf8* mutant. **a** In *irf8* mutants, higher peak numbers of neutrophils (Mpx$^+$) at 2 hpl and slower clearance over the course of regeneration are observed (Two-Way ANOVA followed by Bonferroni multiple comparisons: $F_{8,427} = 13.19$ $^*P < 0.05$, $^{**}P < 0.01$, $^{***}P < 0.001$). Note that wildtype data are the same as shown in Fig. 1a, as counts in *irf8* mutants and wildtype animals were done in the same experiments. **b** Combination treatment with *pu.1* and *gcsfr* morpholinos efficiently prevents neutrophil accumulation in the lesion site (Mann–Whitney *U*-test: $^{***}P < 0.001$). **c** In *pu.1/gcsfr* morpholino injected *irf8* mutant fish, levels of *il-1β* and *tnf-α* mRNA expression are reduced at 2 dpl, as shown by qRT-PCR (*t*-test: $^{***}P < 0.001$). **d**, **e** In *pu.1/gcsfr* morpholino injected *irf8* mutant fish, axonal bridging (arrows, **d** Fisher's exact test: $^{**}P < 0.01$) and behavioural recovery (**e** One-Way ANOVA followed by Bonferroni multiple comparisons: $F_{5,142} = 23.21$, $^{**}P < 0.01$, ns indicates no significance) are partially rescued. Lateral views of the injury site are shown; rostral is left. Scale bars: 100 μm. Error bars indicate SEM

Neutrophils inhibit regeneration in irf8 mutants. To determine the relative importance of the neutrophils for regenerative failure in *irf8* mutants, we reduced their numbers using *pu.1/gcsfr* morpholino treatment. This strongly reduced numbers of neutrophils by 84.6% in the injury site at 2 hpl, when the neutrophil reaction peaked in untreated *irf8* mutants (Fig. 9b). *pu.1/gcsfr* morpholino treatment also reduced *il-1β* mRNA levels by 54% and *tnf-α* mRNA levels by 70% at 2 dpl (Fig. 9c). Remarkably, axon bridging (control: 43% of examined animals showed bridging; *pu.1/gcsfr* morpholino: 60%; Fig. 9d) and recovery of touch-evoked swimming distance were partially rescued in these neutrophil-depleted mutants at 2 dpl (Fig. 9e). This shows that in the absence of macrophages, the prolonged presence of Il-1β$^+$ neutrophils is detrimental to regeneration.

Discussion

We identify a biphasic role of the innate immune response for axonal bridging of the non-neural lesion site in larval zebrafish. Initial inflammation and Il-1β presence promote axon bridging, whereas later, Il-1β levels need to be tightly controlled by peripheral macrophages. Inhibiting Il-1β largely compensated for the absence of macrophages, underscoring the central role of this cytokine. Macrophage-derived Tnf-α promotes regeneration,

partially by reducing neutrophil number and *il-1β* levels (summarised in Supplementary Fig. 13). This indicates important and highly dynamic functions of the immune system for successful spinal cord regeneration.

The function of the immune system changes dramatically over time. Within the first hours after injury, neutrophils and the pro-inflammatory cytokines *il-1β* and *tnf-α* dominate the injury site. Initially, inflammation promotes axonal growth. This is indicated by reducing effects on axon bridging of early Il-1β inhibition and the promoting effect of LPS in wildtype animals. Indeed, it has been reported that Il-1β can promote neurite growth[33,34]. However, from about 12 hpl, macrophages and anti-inflammatory cytokines are in the lesion site and during this late phase of regeneration, Il-1β mediated inflammation in macrophage-less mutants strongly inhibits regeneration.

How does Il-1β inhibit spinal cord regeneration? High Il-1β levels may condition the environment to be inhibitory to axonal regrowth. Blocking excessive Il-1β signalling in *irf8* mutants revealed that Il-1β increases numbers of neutrophils, levels of *il-1β* and *tnf-α* expression, as well as cell death in the lesion environment. Morevover, reduced expression of some metalloproteinases in the *irf8* mutant suggest that the lesion site ECM may be altered. However, several ECM components, including functionally important Col XII[1], were unaltered in expression in the *irf8* mutant. Similar to our observations, an Il-1β deficient mouse showed slightly increased axonal regrowth after spinal injury[35].

Axonal regeneration is promoted by Tnf-α. Even though *il-1β* and *tnf-α* were similarly upregulated in the *irf8* mutant, only reducing Il-1β levels rescued the mutant. Conversely, in wildtype animals, Il-1β had only a relatively small promoting effect on early regeneration, whereas Tnf-α was indispensable for axonal regrowth. Different functions for the two pro-inflammatory cytokines have been reported[36]. They also differ in cell type of origin. Whereas Il-1β is expressed by a substantial proportion of neutrophils, microglia and macrophages, Tnf-α is mainly expressed by macrophages in the injury site. This indicates a clear difference between tissue-resident microglia and peripheral macrophages. In mammals, *tnf-α* is produced by both microglia and macrophages[37].

Tnf-α may exert its positive role for regeneration at least in part by controlling neutrophil numbers and Il-1β levels. Both of these parameters are increased when Tnf-α is inhibited and are inhibitory to regeneration. Anti-inflammatory actions of Tnf-α have been described in the context of auto-immunity[38], but whether this interaction between Tnf-α and Il-1β is direct or indirect, needs to be elucidated. For example, Tnf-α can be neuroprotective after CNS injury[36,39] and thus indirectly reduce inflammation. In the regenerating fin, Tnf-α has an important promoting function for blastema formation[40]. This suggests that Tnf-α may be involved in remodelling repair cells in the lesion site after spinal injury, which then creates an axon growth-promoting environment.

The role of Tnf-α for axonal regeneration in mammals is not clear. Some reports indicate axon growth promoting properties of Tnf-α[41,42], whereas others show inhibition of axon growth[43]. Negative effects of Tnf-α on lesion-induced cell death[44] and functional recovery[37,45] have also been reported. However, knock out of Tnf-α had no reported effect after spinal injury[46].

Preventing neutrophil formation in *irf8* mutants, indicates that *il-1β* expressing neutrophils are major mediators of the inhibitory immune response in the absence of microglia and macrophages. However, the rescue of axon regrowth and swimming function was only partial. This could be explained by the absence of the early regeneration-promoting influence of the inflammation or basal keratinocytes still expressing *il-1β* in neutrophil-depleted *irf8* mutants. In mammals, neutrophils cause secondary cell death[47,48] and depleting neutrophils leads to favourable injury outcomes[5], similar to our observations.

Macrophages control inflammation, as their absence in *irf8* mutants leads to abnormally high expression levels of pro-inflammatory cytokines *il-1β* and *tnf-α*. This is similar to observations in fin regeneration[49]. In the absence of macrophages, positive feedback regulation of *il-1β* takes place, as indicated by more *il-1β* positive neutrophils and basal keratinocytes in the *irf8* mutants and reduced *il-1β* mRNA levels when Il-1β function was inhibited. Moreover, a higher proportion of neutrophils were Il-1β^{+} in *irf8* mutants, showing that without macrophages, neutrophils have a more pro-inflammatory phenotype. We show that macrophages/microglia, together with other tissues, express anti-inflammatory cytokines *tgf-β1a* and *tgf-β3* and could thus be partly responsible for reducing pro-inflammatory phenotypes in wildtype animals.

Macrophages do not promote regeneration primarily by preventing cell death or removing debris. We observed phagocytosing macrophages by time-lapse imaging and debris levels were clearly increased it the absence of macrophages in *irf8* mutants. However, when axon regrowth was rescued in the mutant by Il-1β inhibition, debris levels were still higher than in controls. Preventing cell death did not rescue axon growth and inhibition phagocytosis in wildtype animals did not impair regeneration. Hence, regenerative success does not correlate with debris abundance. Interestingly, in fin regeneration, lack of macrophages also leads to increased cell death. As this leads to death of tissue progenitor cells, fin regeneration is inhibited[49]. In mammalian spinal injury, debris, especially myelin debris, is inhibitory to regeneration[50].

Are macrophages the most important immune cell type for axonal regrowth? Unimpaired axonal regrowth in the *csfr1a/b* mutant, in which microglial cells are absent and neutrophils are strongly reduced in number, indicates that these cells may be dispensable for regeneration. However, the increase in peripheral macrophages in this mutant could have compensated for a possible regeneration-promoting role of microglia. Since some neutrophils are still present in the injury site in *csfr1a/b* mutants, these might contribute to promoting axonal regrowth.

Endothelial cells and myelinating cells are unlikely to be major mediators of early regeneration in larval spinal cord regeneration. Endothelial cells from injured blood vessels were slow to reform blood vessels and were rarely invading the lesion site. In contrast, in mammals endothelial cells accumulate in the injury site, where they may have anti-inflammatory functions[51]. Myelinating cells bridged the lesion site, but were not abundant and only did so, when axons had already crossed the lesion site. Although relatively late, axons become remyelinated, which may contribute to recovery of some swimming parameters after injury. In mammals, transplanted myelinating cells, such as olfactory ensheathing cells and Schwann cells have been shown to improve recovery after spinal injury[52,53].

Astroglia-like processes cross the injury site and this depends on the immune response, as we show here. While these processes cross the injury site independently of and slightly later than axons and axons still cross when these cells are ablated[1], astroglia-like processes produce growth factors that support axonal regeneration[54,55].

Timing of the immune response is crucial for regenerative success after spinal lesion. Macrophages in mammals[3,37] and zebrafish[56] display pro-inflammatory and anti-inflammatory phenotypes and the anti-inflammatory phenotypes are seen as beneficial for regeneration[7–9]. We show that inflammation is rapidly downregulated in zebrafish concurrent with the upregulation of anti-inflammatory cytokines, which does not readily occur in mammals[3].

In summary, we have established an accessible in vivo system to study complex interactions of immune cells and a spinal injury site in successful regeneration. This allows fundamental insight into the role of immune cells that may ultimately inform non-regenerating systems. Here, we demonstrate a pivotal role of macrophages in promoting functional spinal cord regeneration, by producing Tnf-α and controlling Il-1β-mediated inflammation.

Methods

Animals. All zebrafish lines were kept and raised under standard conditions[57] and all experiments were approved by the British Home Office (project license no.: 70/8805). Regeneration proceeds within 48 h of the lesion, therefore most analyses of axonal regrowth, cellular repair, and behavioural recovery can be performed before the fish are protected under the A(SP)A 1986, reducing the number of animals used in regeneration studies following the principles of the 3 rs. Approximately 11,000 larvae of either sex were used for this study, of which 8% were over 5 dpf.

The following lines were used: WIK wild type zebrafish, Tg(*Xla.Tubb*:DsRed)^{zf14826}, abbreviated as *Xla.Tubb*:DsRed[58]; Tg(*mpeg1*:EGFP)^{gl22}, abbreviated as *mpeg1*:GFP[59], and Tg(*mpx*:GFP)^{uwm1}, abbreviated as *mpx*:GFP[60], Tg(*fli1*:EGFP)^{y1}, abbreviated as *fli1*:GFP[61]; *irf8*$^{st95/st95}$, abbreviated as *irf8* mutants[18]; *csf1ra*$^{j4e1/j4e1}$ × csf1rb$^{+/re01}$ incrosses, phenotypically sorted for absence of 4C4^{+} cells in the head, abbreviated as *csfr1a/b* mutants[19]; TgBAC(*pdgfrb*:Gal4FF)^{ncv24}; Tg(*UAS*:GFP), abbreviated as *pdgfrb*:GFP[62],Tg(*6xTCF/LefminiP*:2dGFP), abbreviated as *6xTCF*:dGFP[63], Tg(*claudin k*:Gal4)^{ue101}; Tg(14x*UAS*:GFP) abbreviated as *cldnK*:GFP[64], Tg(*tnfa*:eGFP-F)^{sa43296}, abbreviated as *tnf-α*:GFP[56] and Tg(*il-1β*:eGFP)^{sh445}, abbreviated as *il-1β*:GFP[65].

Drug treatment. Dexamethasone (Dex) (Sigma, Gillingham, UK) was dissolved in DMSO to a stock concentration of 5 mM. The working concentration was 10 µM prepared by dilution from stock solution in fish water. Ac-YVAD-cmk (YVAD) (Sigma) was dissolved in DMSO to a stock concentration of 10 mM. The working concentration was 50 µM prepared by dilution from the stock solution in fish water. Q-VD-OPh (Sigma), abbreviated as QVD in the manuscript, was dissolved in DMSO to a stock concentration of 10 mM. The working concentration was 50 µM. O-Phospho-L-serine (L-SOP) (Sigma) was dissolved in PBS to a stock concentration of 10 mM. The working concentration was 10 µM prepared by dilution from stock solution. Lipopolysaccharides from Escherichia coli O55:B5 (LPS, Sigma) were dissolved in PBS to a stock concentration of 1 mg/ml. The working dilution was 50 µg/ml. Pomalidomide (Cayman Chemicals, Michigan, USA) was diluted in DMSO at a stock concentration of 10 mg/ml. For the treatments, 6.9 µl of the stock where diluted in 1.5 ml of fish water. Larvae were pre-treated for 2 h before the injury and were incubated for 24 and 48 hpl. Larvae were collected from the breeding tanks and were randomly divided into Petri dishes at a density of maximally 30 larvae per dish, but no formal randomisation method was used. For most drug treatments, larvae were incubated with the drug from 3 dpl until 5 dpl, if not indicated differently.

Spinal cord lesions. Zebrafish larvae at 3 dpf were anaesthetised in PBS containing 0.02% aminobenzoic-acid-ethyl methyl-ester (MS222, Sigma), as described[1]. Larvae were transferred to an agarose-coated petri dish. Following removal of excess water, the larvae were placed in a lateral position, and the tip of a sharp 30 ½ G syringe needle was used to inflict a stab injury or a dorsal incision on the dorsal part of the trunk at the level of the 15th myotome.

Behavioural analysis. Behavioural analysis was performed as previously described[14]. Briefly, lesioned and unlesioned larvae were touched caudal to the lesion site using a glass capillary. The swim distance of their escape response, the mean velocity and the meandering were recorded for 15 s after touch and analyzed using a Noldus behaviour analysis setup (EthoVision version 7). Data given is averaged from triplicate measures per fish. Between repeated measures, the larvae were left to recover for 1 min. The observer was blinded to the treatment during the behavioural assay. The assay was performed on five independent clutches in order to assess the behavioural recovery in the *irf8* mutants and three independent clutches after the YVAD treatment.

Fluorescence-activated cell sorting. Macrophages and microglia were isolated from 4 dpf transgenic *mpeg1*:eGFP embryos by FACS. For this purpose, about 500 fish were lesioned by transecting the spinal cord. Trunk-containing lesion site were dissected and collected at 24 hpl and used for cell dissociation[66]. Cells purified after FACS were used for qRT-PCR.

Quantitative RT-PCR. RNA was isolated from the injury sites of the larvae using the RNeasy Mini Kit (Qiagen, Hilden, Germany). Forty larvae were used for each condition. cDNA used as template was created using the iScript™ cDNA Synthesis Kit (Bio-Rad, Munich, Germany). Standard RT-PCR was performed using SYBR Green Master Mix (Bio-Rad). qRT-PCR was performed at 58 °C using Roche Light Cycler 96 (Roche Diagnostics, West Sussex, UK) and relative mRNA levels determined using the Roche Light Cycler 96 SW1 software. Samples were run in duplicates and expression levels were normalised to β-actin control. Primers were designed to span an exon-exon junction using Primer-BLAST. Sequences are given in supplementary Table 2. All experiments were carried out at least as biological triplicates.

In situ hybridisation. For whole mount in situ hybridisation[1], after fixation in 4% PFA, larvae were digested with 40 µg/ml Proteinase K (Invitrogen, Carlsbad, USA). Thereafter, larvae were washed briefly in PBT and were re-fixed for 20 min in 4% PFA followed by washes in PBT. After washes, larvae were incubated at 67 °C for 2 h in pre-warmed hybridisation buffer. Hybridisation buffer was replaced with digoxigenin (DIG) labelled ISH probes diluted in hybridisation buffer and incubated at 67 °C overnight. The next day, larvae were washed thoroughly at 67 °C with hybridisation buffer, 50% 2× SSCT/50% deionized formamide, 2x SSCT and 0.2x SSCT. Larvae were then washed in PBT and incubated for 1 h in blocking buffer under slow agitation. Thereafter, larvae were incubated overnight at 4 °C in blocking buffer containing pre-absorbed anti-DIG antibody. The next day, larvae were washed in PBT, followed by washes in staining buffer. Colour reaction was performed by incubating larvae in staining buffer supplemented with NBT/BCIP (Sigma-Aldrich) substrate. The staining reaction was terminated by washing larvae in PBT.

Immunofluorescence. All incubations were performed at room temperature unless stated otherwise. Antibodies used are listed in supplementary Table 3. For most immunolabelling experiments, the larvae were fixed in 4% PFA-PBS containing 1% DMSO at 4 °C overnight. After washes in PBS, larvae were washed in PBTx. After permeabilization by incubation in PBS containing 2 mg/ml Collagenase (Sigma) for 25 min larvae were washed in PBTx. They were then incubated in blocking buffer for 2 h and incubated with primary antibody (1:50–1:500) diluted in blocking buffer at 4 °C overnight. On the following day, larvae were washed times in PBTx, followed by incubation with secondary antibody diluted in blocking buffer (1:300) at 4 °C overnight. The next day, larvae were washed three times in PBTx and once in PBS for 15 min each, before mounting in glycerol.

For whole mount immunostaining using primary antibodies from the same host species (rabbit anti-Il-1β, rabbit anti-Mpx, rabbit anti-Tp63) the samples were initially incubated with the first primary antibody at 4 °C overnight. After washes with PBTx the samples were incubated with the conjugated first secondary antibody overnight at 4 °C. Subsequently, samples were incubated with blocking buffer for 1 h at RT in order to saturate open binding sites of the first primary antibody. Next, the samples were incubated with unconjugated Fab antibody against the host species of the primary antibody in order to cover the IgG sites of the first primary antibody, so that the second secondary antibody will not bind to it. After this, samples were incubated with the second primary antibody overnight at 4 °C and subsequently with the second conjugated secondary antibody overnight at 4 °C before mounting in glycerol. No signal was detected when the second primary antibody was omitted, indicating specificity of the consecutive immunolabeling protocol.

For whole mount immunostaining of acetylated tubulin[1], larvae were fixed in 4% PFA for 1 h and then were dehydrated and transferred to 100% MeOH and then stored at −20 °C overnight. The next day, head and tail were removed, and the samples were incubated in pre-chilled Acetone. Thereafter, larvae were washed and digested with Proteinase K and re-fixed in 4% PFA. After washes the larvae were incubated with BSA in PBTx for 1 h. Subsequently the larvae were incubated for 2 overnights with primary antibody (acetylated tubulin). After washes and incubation with the secondary antibody the samples were washed in PBS for 15 min each, before mounting in glycerol.

Evaluation of cell death using acridine orange. In order to assess the levels of cell death after injury we used the acridine orange live staining as described by others[67]. Briefly, at 1 and 2 dpl the larvae were incubated in 2.5 µg/ml solution of dye diluted into conditioned water for 20 min. After the staining, the larvae were washed by changing the water and larvae were live-mounted for imaging.

Identification of dying cells after injury. In order to assess the levels of cell death after injury cross sections of larvae were used. Larvae were fixed in 4% PFA overnight at 4 °C. After washes with 0.5% PBSTx, the larvae were transferred to 100% methanol and incubated for 10 min at room temperature. After rehydration, the larvae were washed with PBSTx 0.5%. Following this, larvae were mounted in 4% agarose and 50 µm sections were performed using a vibratome (MICROM HM 650 V, VWR, Leicestershire, UK). The sections were then permeabilized using 14 µg/ml diluted in 0.5% PBSTx. After brief wash with PBSTx the sections were postfixed in 4% PFA for 20 min. Excess PFA was washed out and the samples were incubated with the TUNEL reaction mix according to the In-situ Cell Death Detection Kit TMR red protocol (Roche).

Western blotting. Zebrafish larvae were sacrificed by an overdose of MS-222 at 4 dpf and used for protein extraction. Around 60 fish per condition were homogenised in 250 µl of 1x PBS/1% Triton X-100 (containing protease inhibitor cocktail complete, Roche Diagnostics), using a tissue grinder. After 1 h incubation

at 4 degrees, lysates were centrifuged at 12,000 rpm for 20 mins to remove Triton-X-100-insoluble debris. Protein concentrations were quantified using a BCA assay following manufacturer's instruction and the same amount of protein for each sample was loaded on a denaturating 12% acrylamide gel. After the electrophoretic run, the proteins were transferred on a nitrocellulose membrane (BioRad, Germany) and, after 1 h blocking in PBS/5% non-fat dry milk/0.1% Tween-20, probed with either rabbit anti-TNFα (1:2000, Anaspec; Fremont, CA), rabbit anti IL-1 (1:200, Proteintech, Manchester, UK) or mouse anti-α Tubulin (1:2000, DSHB) O/N at 4 degrees. Goat anti-rabbit (IRdye680LT, LI-COR, Lincoln, Nebraska, USA) and goat anti-mouse (IRdye800CW, LI-COR) secondary antibodies were used and the signal was detected by an Odyssey (LI-COR) imaging system and analysed with the Image Studio Lite software version 5.2.

Morpholino injection. All morpholinos were injected into single cell stage larvae in total volume of 2 nl. Knockdown of *il-1β* was carried out using the antisense morpholino against *il-1β* (5′-CCCACAAACTGCAAAATATCAGCTT-3′), targeting the splice site between intron 2 and exon 3 according to[31]. In order to block neutrophil development, we used the previously described MO combination of *pu.1* (5′-GATATACTGATACTCCATTGGTGGT-3′) which targets the translational start (ATG) of the pu.1 and the splice blocking MO against *gcsfr* (5′-TTTGTCTTTACAGATCCGCCAGTTC-3′)[16]. All morpholinos and standard control (5′-CCTCTTACCTCAGTTACAATTTATA-3′) were obtained from Gene Tools, LLC, Oregon, USA.

CRISPR-mediated genome editing. CRISPR gRNA for *il-1β* was designed using CRISPR Design (http://crispr.mit.edu) and ZiFit (http://zifit.partners.org/ZiFiT) webtools. Vectors were generated by ligating the annealed oligonucleotides into the pT7-gRNA expression vector[1]. The gRNA was transcribed using the mMESSAGE mMACHINE T7 kit (Ambion, ThermoFisher SCIENTIFIC, Loughborough, UK) and assessed for size and quality on an electrophoresis gel. The injection mix consisted of 75 pg *il-1β* gRNA (target sequence: 5′-TGTGGAGCGGAGCCT TCGGCGGG-3′) and 150 pg Cas9 RNA and was injected into single cell stage larvae. The CrRNA for *tnf-α* (target sequence: 5′-CCCGATGATGGCATTTA TTTTGT-3′) and the tracrRNA were ordered from Merck KGaA (Germany, Darmstadt). The injection mix included 1 µl Tracer 250 ng/µl, 1 µl gRNA, 1 µl Cas9 protein, 1 µl RNAse free H_20, 1 µl fluorescent dextran. Larvae injected with GFP gRNA (target sequence: 5′GGCGAGGGCGATGCCACCTA-3) and uninjected larvae were used as controls. The efficiency of the mutagenesis was assessed by RFLP analysis.

Live imaging of zebrafish larvae and time-lapse imaging. For the acquisition of all fluorescent images, LSM 710 and LSM 880 confocal microscopes were used. For live confocal imaging, zebrafish larvae were anesthetized in PBS containing 0.02% MS222 and mounted in 1.5% low melting point agarose (Ultra-PureTM, Invitrogen). During imaging, the larvae were covered with 0.01% MS222-containing fish water to keep preparations from drying out. For time-lapse imaging, agarose covering the lesion site was gently removed after gelation. Time-lapse imaging was performed for 19 h starting at 6 hpl. Acquired time-lapse images were denoised using the ImageJ plugin CANDLE-J algorithm. Comparison of raw movies with CANDLE-J-processed movies showed that edges of features remained conserved after denoising.

Scoring and measurement of spinal cord bridging. Axonal and astroglial bridging was scored in fixed and live mounted samples using fluorescence-equipped stereomicroscope (Leica MDG41) and confocal microscopes (LSM 710, LSM 880) at time points of interest as previously described[1]. Any continuity of labelling between the two spinal cord stumps was scored as "bridged". In some cases, the thickness of the axonal bridge was measured in collapsed confocal image stacks, by determining the length of (a) vertical line(s) that covers the width of crossing fascicles at the centre of the injury site. The observer was blinded to the experimental condition before scoring or measuring and experiments were performed blinded to the experimental condition on at least three independent clutches of larvae.

Cell counting in whole-mounted larvae. A volume of interest was defined centred on the lesion site from confocal images. The dimensions were: width = 200 µm, height = 75 µm (above the notochord), depth = 50 µm. Images were analysed using the Imaris (Bitplane, Belfast, UK) or ImageJ software. The number of cells was quantified manually in 3D view, blinded to the experimental condition on at least three independent clutches of larvae.

Quantification of diffuse signals in whole-mount larvae. For most quantifications of diffuse signal, e.g., acridine orange, image stacks, centred in the lesion site (height: 50 µm) were collapsed and an area of interest defined: width = 100 µm, height = 50 µm (above the notochord). The image was thresholded and the "Analyze Particles" tool in Fiji with default settings was used to calculate the percentage of area taken up by signal.

To quantify Col I and Tnf-α in the injury site (Supplementary Figs 4C and 9A) we used a previously published protocol[1]. Briefly, image stacks were collapsed, thresholded and the area of the signal was measured.

All analyses were performed blinded to the experimental condition on at least three independent clutches of larvae.

Statistical analysis. Power analysis using G*Power[68], was used to calculate power (aim > 0.8) for the experiments and determine the group sizes accordingly. Statistical power was >0.8 for all experiments. All quantitative data were tested for normality and analyzed with parametric and non-parametric tests as appropriate. The statistical analysis was performed using IBM SPSS Statistics 23.0. Shapiro-Wilk's *W*-test was used in order to assess the normality of the data. Quantitative RT-PCR data were analyzed as previously described[69,70]. Kruskal–Wallis test followed by Dunn's multiple comparisons, One-way ANOVA followed by Bonferroni multiple comparisons test, two-way ANOVA, followed by Bonferroni multiple comparisons, *t*-test, Mann–Whitney *U*-test or Fischer's exact test were used, as indicated in the figure legends. $*P < 0.05$, $**P < 0.01$, $***P < 0.001$, n.s. indicates no significance. Error bars indicate the standard error of the mean (SEM). The Figures were prepared with Adobe Photoshop CC and Adobe Illustrator CC. Graphs were generated using GraphPad Prism 7.

Data availability

The authors declare that all data supporting the findings of this study are available within the article and its supplementary information files, or from the corresponding authors on reasonable request.

Received: 19 May 2018 Accepted: 12 October 2018
Published online: 07 November 2018

References

1. Wehner, D. et al. Wnt signaling controls pro-regenerative Collagen XII in functional spinal cord regeneration in zebrafish. *Nat. Commun.* **8**, 126 (2017).
2. Becker, T., Wullimann, M. F., Becker, C. G., Bernhardt, R. R. & Schachner, M. Axonal regrowth after spinal cord transection in adult zebrafish. *J. Comp. Neurol.* **377**, 577–595 (1997).
3. Kigerl, K. A. et al. Identification of two distinct macrophage subsets with divergent effects causing either neurotoxicity or regeneration in the injured mouse spinal cord. *J. Neurosci.* **29**, 13435–13444 (2009).
4. Norden, D. M., Muccigrosso, M. M. & Godbout, J. P. Microglial priming and enhanced reactivity to secondary insult in aging, and traumatic CNS injury, and neurodegenerative disease. *Neuropharmacology* **96**, 29–41 (2015).
5. Taoka, Y. et al. Role of neutrophils in spinal cord injury in the rat. *Neuroscience* **79**, 1177–1182 (1997).
6. Tran, A. P., Warren, P. M. & Silver, J. The biology of regeneration failure and success after spinal cord injury. *Physiol. Rev.* **98**, 881–917 (2018).
7. Gensel, J. C. et al. Macrophages promote axon regeneration with concurrent neurotoxicity. *J. Neurosci.* **29**, 3956–3968 (2009).
8. David, S., Bouchard, C., Tsatas, O. & Giftochristos, N. Macrophages can modify the nonpermissive nature of the adult mammalian central nervous system. *Neuron* **5**, 463–469 (1990).
9. Yin, Y. et al. Oncomodulin is a macrophage-derived signal for axon regeneration in retinal ganglion cells. *Nat. Neurosci.* **9**, 843–852 (2006).
10. Becker, T. & Becker, C. G. Axonal regeneration in zebrafish. *Curr. Opin. Neurobiol.* **27C**, 186–191 (2014).
11. Renshaw, S. A. & Trede, N. S. A model 450 million years in the making: zebrafish and vertebrate immunity. *Dis. Model Mech.* **5**, 38–47 (2012).
12. Becker, T. & Becker, C. G. Regenerating descending axons preferentially reroute to the gray matter in the presence of a general macrophage/microglial reaction caudal to a spinal transection in adult zebrafish. *J. Comp. Neurol.* **433**, 131–147 (2001).
13. Hui, S. P., Dutta, A. & Ghosh, S. Cellular response after crush injury in adult zebrafish spinal cord. *Dev. Dyn.* **239**, 2962–2979 (2010).
14. Ohnmacht, J. et al. Spinal motor neurons are regenerated after mechanical lesion and genetic ablation in larval zebrafish. *Development* **143**, 1464–1474 (2016).
15. Hui, S. P. et al. Zebrafish regulatory T cells mediate organ-specific regenerative programs. *Dev. Cell* **43**, 659–672 e655 (2017).
16. Feng, Y., Renshaw, S. & Martin, P. Live imaging of tumor initiation in zebrafish larvae reveals a trophic role for leukocyte-derived PGE(2). *Curr. Biol.* **22**, 1253–1259 (2012).
17. Novoa, B., Bowman, T. V., Zon, L. & Figueras, A. LPS response and tolerance in the zebrafish (Danio rerio). *Fish. Shellfish. Immunol.* **26**, 326–331 (2009).

18. Shiau, C. E., Kaufman, Z., Meireles, A. M. & Talbot, W. S. Differential requirement for irf8 in formation of embryonic and Adult macrophages in zebrafish. *PLoS One* **10**, e0117513 (2015).
19. Oosterhof, N. et al. Colony-stimulating factor 1 receptor (CSF1R) regulates microglia density and distribution, but not microglia differentiation in vivo. *Cell Rep.* **24**, 1203–1217.e1206 (2018).
20. Newby, A. C. Metalloproteinase expression in monocytes and macrophages and its relationship to atherosclerotic plaque instability. *Arterioscler. Thromb. Vasc. Biol.* **28**, 2108–2114 (2008).
21. Rosenberg, A. F., Wolman, M. A., Franzini-Armstrong, C. & Granato, M. In vivo nerve-macrophage interactions following peripheral nerve injury. *J. Neurosci.* **32**, 3898–3909 (2012).
22. Villegas, R. et al. Dynamics of degeneration and regeneration in developing zebrafish peripheral axons reveals a requirement for extrinsic cell types. *Neural Dev.* **7**, 19 (2012).
23. Keoni, C. L. & Brown, T. L. Inhibition of apoptosis and efficacy of pan caspase iInhibitor, Q-VD-OPh, in models of human disease. *J. Cell Death* **8**, 1–7 (2015).
24. Ogryzko, N. V. et al. Zebrafish tissue injury causes upregulation of interleukin-1 and caspase-dependent amplification of the inflammatory response. *Dis. Model Mech.* **7**, 259–264 (2014).
25. Witting, A., Muller, P., Herrmann, A., Kettenmann, H. & Nolte, C. Phagocytic clearance of apoptotic neurons by Microglia/Brain macrophages in vitro: involvement of lectin-, integrin-, and phosphatidylserine-mediated recognition. *J. Neurochem.* **75**, 1060–1070 (2000).
26. Finnson, K. W., McLean, S., Di Guglielmo, G. M. & Philip, A. Dynamics of transforming growth factor beta signaling in wound healing and scarring. *Adv. Wound Care* **2**, 195–214 (2013).
27. Muller, G. W. et al. Amino-substituted thalidomide analogs: potent inhibitors of TNF-alpha production. *ACS Med. Chem. Lett.* **9**, 1625–1630 (1999).
28. Savan, R., Kono, T., Igawa, D. & Sakai, M. A novel tumor necrosis factor (TNF) gene present in tandem with theTNF-alpha gene on the same chromosome in teleosts. *Immunogenetics* **57**, 140–150 (2005).
29. Kisiswa, L. et al. TNFalpha reverse signaling promotes sympathetic axon growth and target innervation. *Nat. Neurosci.* **16**, 865–873 (2013).
30. Vojtech, L. N., Scharping, N., Woodson, J. C. & Hansen, J. D. Roles of inflammatory caspases during processing of zebrafish interleukin-1beta in Francisella noatunensis infection. *Infect. Immun.* **80**, 2878–2885 (2012).
31. Nguyen-Chi, M. et al. Transient infection of the zebrafish notochord with E. coli induces chronic inflammation. *Dis. Model Mech.* **7**, 871–882 (2014).
32. Tauzin, S., Starnes, T. W., Becker, F. B., Lam, P. Y. & Huttenlocher, A. Redox and Src family kinase signaling control leukocyte wound attraction and neutrophil reverse migration. *J. Cell. Biol.* **207**, 589–598 (2014).
33. Boato, F. et al. Interleukin-1 beta and neurotrophin-3 synergistically promote neurite growth in vitro. *J. Neuroinflamm.* **8**, 183 (2011).
34. Temporin, K. et al. IL-1beta promotes neurite outgrowth by deactivating RhoA via p38 MAPK pathway. *Biochem. Biophys. Res. Commun.* **365**, 375–380 (2008).
35. Boato, F. et al. Absence of IL-1beta positively affects neurological outcome, lesion development and axonal plasticity after spinal cord injury. *J. Neuroinflamm.* **10**, 6 (2013).
36. Turrin, N. P. & Rivest, S. Tumor necrosis factor alpha but not interleukin 1 beta mediates neuroprotection in response to acute nitric oxide excitotoxicity. *J. Neurosci.* **26**, 143–151 (2006).
37. Kroner, A. et al. TNF and increased intracellular iron alter macrophage polarization to a detrimental M1 phenotype in the injured spinal cord. *Neuron* **83**, 1098–1116 (2014).
38. Liu, J. et al. TNF is a potent anti-inflammatory cytokine in autoimmune-mediated demyelination. *Nat. Med.* **4**, 78–83 (1998).
39. Bruce, A. J. et al. Altered neuronal and microglial responses to excitotoxic and ischemic brain injury in mice lacking TNF receptors. *Nat. Med.* **2**, 788–794 (1996).
40. Nguyen-Chi, M. et al. TNF signaling and macrophages govern fin regeneration in zebrafish larvae. *Cell Death Dis.* **8**, e2979 (2017).
41. Schwartz, M. et al. Tumor necrosis factor facilitates regeneration of injured central nervous system axons. *Brain Res.* **545**, 334–338 (1991).
42. Saleh, A. et al. Tumor necrosis factor-alpha elevates neurite outgrowth through an NF-kappaB-dependent pathway in cultured adult sensory neurons: diminished expression in diabetes may contribute to sensory neuropathy. *Brain Res.* **1423**, 87–95 (2011).
43. Kato, K., Liu, H., Kikuchi, S., Myers, R. R. & Shubayev, V. I. Immediate anti-tumor necrosis factor-alpha (etanercept) therapy enhances axonal regeneration after sciatic nerve crush. *J. Neurosci. Res.* **88**, 360–368 (2010).
44. Ferguson, A. R. et al. Cell death after spinal cord injury is exacerbated by rapid TNF alpha-induced trafficking of GluR2-lacking AMPARs to the plasma membrane. *J. Neurosci.* **28**, 11391–11400 (2008).
45. Genovese, T. et al. TNF-alpha blockage in a mouse model of SCI: evidence for improved outcome. *Shock* **29**, 32–41 (2008).
46. Farooque, M., Isaksson, J. & Olsson, Y. Improved recovery after spinal cord injury in neuronal nitric oxide synthase-deficient mice but not in TNF-alpha-deficient mice. *J. Neurotrauma* **18**, 105–114 (2001).
47. Saiwai, H. et al. The LTB4-BLT1 axis mediates neutrophil infiltration and secondary injury in experimental spinal cord injury. *Am. J. Pathol.* **176**, 2352–2366 (2010).
48. Kubota, K. et al. Myeloperoxidase exacerbates secondary injury by generating highly reactive oxygen species and mediating neutrophil recruitment in experimental spinal cord injury. *Spine* **37**, 1363–1369 (2012).
49. Hasegawa, T. et al. Transient inflammatory response mediated by interleukin-1beta is required for proper regeneration in zebrafish fin fold. *eLife* **6**, e22716 (2017).
50. Church, J. S., Milich, L. M., Lerch, J. K., Popovich, P. G. & McTigue, D. M. E6020, a synthetic TLR4 agonist, accelerates myelin debris clearance, Schwann cell infiltration, and remyelination in the rat spinal cord. *Glia* **65**, 883–899 (2017).
51. Cohen, M. et al. Newly formed endothelial cells regulate myeloid cell activity following spinal cord injury via expression of CD200 ligand. *J. Neurosci.* **37**, 972–985 (2017).
52. Nakhjavan-Shahraki, B. et al. Transplantation of olfactory ensheathing cells on functional recovery and neuropathic pain after spinal cord injury; systematic review and meta-analysis. *Sci. Rep.* **8**, 325 (2018).
53. Bunge, M. B. Efficacy of Schwann cell transplantation for spinal cord repair is improved with combinatorial strategies. *J. Physiol.* **594**, 3533–3538 (2016).
54. Mokalled, M. H. et al. Injury-induced ctgfa directs glial bridging and spinal cord regeneration in zebrafish. *Science* **354**, 630–634 (2016).
55. Goldshmit, Y. et al. Fgf-dependent glial cell bridges facilitate spinal cord regeneration in zebrafish. *J. Neurosci.* **32**, 7477–7492 (2012).
56. Nguyen-Chi, M. et al. Identification of polarized macrophage subsets in zebrafish. *eLife* **4**, e07288 (2015).
57. Westerfield, M. *The Zebrafish Book*: *A Guide for the Laboratory use of Zebrafish* (*Danio rerio*). 4th edn. (University of Oregon Press, 2000).
58. Peri, F. & Nusslein-Volhard, C. Live imaging of neuronal degradation by microglia reveals a role for v0-ATPase a1 in phagosomal fusion in vivo. *Cell* **133**, 916–927 (2008).
59. Ellett, F., Pase, L., Hayman, J. W., Andrianopoulos, A. & Lieschke, G. J. mpeg1 promoter transgenes direct macrophage-lineage expression in zebrafish. *Blood* **117**, e49–e56 (2011).
60. Renshaw, S. A. et al. A transgenic zebrafish model of neutrophilic inflammation. *Blood* **108**, 3976–3978 (2006).
61. Lawson, N. D. & Weinstein, B. M. In vivo imaging of embryonic vascular development using transgenic xebrafish. *Dev. Biol.* **248**, 307–318 (2002).
62. Ando, K. et al. Clarification of mural cell coverage of vascular endothelial cells by live imaging of zebrafish. *Development* **143**, 1328–1339 (2016).
63. Shimizu, N., Kawakami, K. & Ishitani, T. Visualization and exploration of Tcf/Lef function using a highly responsive Wnt/beta-catenin signaling-reporter transgenic zebrafish. *Dev. Biol.* **370**, 71–85 (2012).
64. Münzel, E. J. et al. Claudin k is specifically expressed in cells that form myelin during development of the nervous system and regeneration of the optic nerve in adult zebrafish. *Glia* **60**, 253–270 (2012).
65. Ogryzko, N. V. et al. Macrophage Il-1beta protects against mycobacterial infection downstream of Hif-1alpha in zebrafish. *bioRxiv 306506*, https://doi.org/10.1101/306506 (2018).
66. Reimer, M. M. et al. Dopamine from the brain promotes spinal motor neuron generation during development and adult regeneration. *Dev. Cell* **25**, 478–491 (2013).
67. Tucker, B. & Lardelli, M. A rapid apoptosis assay measuring relative acridine orange fluorescence in zebrafish embryos. *Zebrafish* **4**, 113–116 (2007).
68. Faul, F., Erdfelder, E., Buchner, A. & Lang, A. G. Statistical power analyses using G*Power 3.1: tests for correlation and regression analyses. *Behav. Res. Methods* **41**, 1149–1160 (2009).
69. Ganger, M. T., Dietz, G. D. & Ewing, S. J. A common base method for analysis of qPCR data and the application of simple blocking in qPCR experiments. *BMC Bioinform.* **18**, 534 (2017).
70. Livak, K. J. & Schmittgen, T. D. Analysis of relative gene expression data using real-time quantitative PCR and the 2(-Delta Delta C(T)) Method. *Methods* **25**, 402–408 (2001).

Acknowledgements

We thank Dr. William Talbot and Dr. Stephen Renshaw for sharing mutants before publication, Dr. Bertrand Vernay for expert advice on microscopy and Joly Ghanawi for excellent fish facility management. Supported by the BBSRC to C.G.B. and T.B., NC3Rs PhD studentship to C.G.B./T.B. for T.M.T., DFG to D.W., Summer research studentships

to T.M. (Carnegie Trust) and EK (Anatomical Society). N.O. was funded by Biotechnology and Biological Sciences Research Council (BBSRC) project grant (BB/L000830/1). T.M.T. and M.K. are currently being paid by Biogen who did not have any influence on this study.

Author contributions

Conceptualisation–T.M.T., T.Be. and C.G.B.; Investigation–T.M.T., D.W., L.C., T.M., M. K., M.L., A.U., T.Ba. and E.K.; Resources–N.O., S.A.R., Y.F. and T.J.H.; Supervision–D. W., N.O., Y.F., T.Be. and C.G.B.; Writing–T.M.T., T.Be. and C.G.B.; Funding acquisition–T.Be. and C.G.B.

Additional information

Supplementary Information accompanies this paper at https://doi.org/10.1038/s41467-018-07036-w.

Competing interests: The authors declare no competing interests.

Reprints and permission information is available online at http://npg.nature.com/reprintsandpermissions/

Publisher's note: Springer Nature remains neutral with regard to jurisdictional claims in published maps and institutional affiliations.